Solar combi systems

Andersen, Elsa; Furbo, Simon

Publication date:
2007

Document Version
Publisher's PDF, also known as Version of record

Department of Civil Engineering DTU

Elsa Andersen

Solar Combi Systems
Department of Civil Engineering

PHD THESIS

BYG • DTU

Solar Combi Systems

Elsa Andersen

Ph.D. Thesis

Department of Civil Engineering
Technical University of Denmark

2007

Solar Combi System

Printed by DTU-Tryk
Department of Civil Engineering
ISBN number: 9788778772282
ISSN number: 1601-2917

Preface

This thesis is submitted as a fulfilment of the requirement for the Danish Ph.D. degree. The thesis is divided into two parts. The first part introduces the motivation and highlights the major findings and conclusions. The second part is a collection of papers, presenting the research in details.

Ten papers are written, all of them with more than one author. Below is listed the division of labour in preparing the papers:

Paper I. *Thermal performance of Danish solar combi systems in practice and in theory,* Journal of Solar Energy Engineering, Vol. 126, pp. 744 – 749, May 2004.

Elsa Andersen has written the paper. Louise Jivan Shah has carried out the parameter analysis for solar combi systems shown in Figures 8 and 9 and proof-read the paper. Simon Furbo has supervised the Ph.D. study and proof-read the paper.

Paper II. *The influence of weather on the thermal performance of solar heating systems,* submitted to Journal of Solar Energy, May 2007.

Elsa Andersen has written the paper. Simon Furbo has supervised the Ph.D.-study and proof-read the paper.

Paper III. *The influence of the solar radiation model on the calculated solar radiation from a horizontal surface to a tilted surface*, in proceedings of EuroSun 2004 Congress, Freiburg, Germany, 2004.

Elsa Andersen has written the paper. Hans Lund has carried out the weather data measurements and the description of how the data have been collected and treated and proof-read the paper. Simon Furbo has supervised the Ph.D.-study and proof-read the paper.

Paper IV. *Advantages by discharge from different levels in solar storage tanks*, Journal of Solar Energy 79 (5), pp. 431 – 439, 2005.

Simon Furbo, who was the supervisor for the student Karin Dyhr Andersen that carried out the investigations described in the paper, has written the paper. Elsa Andersen has co-supervised the student Karin Dyhr Andersen and assisted with the calculations and proof-read the paper. Alexander Thür has co-supervised the student Karin Dyhr Andersen, assisted with the measurements and proof-read the paper. Louise Jivan Shah has made the figures in the paper and proof-read the paper. Karin Dyhr Andersen has carried out the investigations during her master thesis project.

Paper V. *Theoretical comparison of solar water/space-heating combi systems and stratification design options,* accepted for publication in Journal of Solar Energy Engineering, April 2007.

Elsa Andersen has written the paper. Simon Furbo has supervised the Ph.D. study and proof-read the paper.

Paper VI. *Theoretical and experimental investigations of inlet stratifiers for solar storage tanks*, Applied Thermal Engineering 25, pp. 2086-2099, 2005.

Louise Jivan Shah has written the paper. Elsa Andersen has carried out the measuements and proof-read the paper. Simon Furbo has proof-read the paper.

Paper VII. *Multilayer fabric stratification pipes for solar tanks*, accepted for publication in Journal of Solar Energy, January 2007.

Elsa Andersen has written the paper. Simon Furbo has supervised the Ph.D. study and proof-read the paper. Jianhua Fan has proof-read the paper.

Paper VIII. *Fabric inlet stratifiers for solar tanks with different volume flow rates,* in proceedings of EuroSun 2006 Congress, Glasgow, Scotland, 2006.

Elsa Andersen has written the paper. Simon Furbo has supervised the Ph.D. study and proof-read the paper.

Paper IX. *Investigations on stratification devices for hot water heat stores*, accepted for publication in International Journal of Energy Research, May 2007.

Elsa Andersen has written the paper. Simon Furbo has supervised the Ph.D.-study and proof-read the paper.

Matthias Hampel has carried out the measurements from ITW in Stuttgart, the CFD calculations described in section 3.2.2, and proof-read the paper. Wolfgang Heidemann and Hans Müller-Steinhagen have proof-read the paper.

Paper X. *Heat losses from pipes connected to hot water storage tanks*, will in a shorter version be submitted to the International Solar World Congress ISES 2007.

Elsa Andersen has written the paper. Jianhua Fan has supervised the study and proof-read the paper. Simon Furbo has supervised the Ph.D. study and proof-read the paper.

Acknowledgements

I gratefully acknowledge the support of my supervisor, Assoc. Prof. Simon Furbo, Technical University of Denmark, and Thomas Krause from the German company SOLVIS GmbH & Co KG for lending me a solar combi system for my investigations.

Further, I would like to thank my colleagues from the Technical University of Denmark: Louise Jivan Shah, Alexander Thür and Jinhua Fan for many fruitful discussions regarding the investigations described in the thesis. The assistance in the laboratory of Martin Dandanell, Poul Linnnert Christiansen, Klaus Myndal, Keld Plougmann and Christian Rasmussen is acknowledged. Financial support from BYG.DTU's Research Foundation and Otto Mønsted Foundation for my participation in Solar Energy Congresses, is greatfully acknowledged.

Furthermore, I acknowledge the support of my foreign colleagues in the International Energy Agency Solar Heating and Cooling program Task 26 and Task 32. Also my foreign colleagues in Nordic Research Program REBUS are acknowledged.

Finally, I acknowledge the written permissions from ASME, Elsevier and John Wiley & Sons Limited to reprint the papers:

From Journal of Solar Energy Engineering, 126, Elsa Andersen, Louise Jivan Shah, Simon Furbo, *Thermal performance of Danish solar combi systems in practice and in theory*, pp. 744 – 749, Copyright (2004) with permission from ASME.

From Journal of Solar Energy 79 (5), Simon Furbo, Elsa Andersen, Alexander Thür, Louise Jivan Shah, Karin Dyhr Andersen, *Advantages by discharging from different levels in solar storage tanks*, pp. 431 – 439, Copyright (2005) with permission from Elsevier.

From Journal of Solar Energy, Elsa Andersen, Simon Furbo, Jianhua Fan, *Multilayer fabric stratification pipes for solar tanks*, accepted for publication January 2007, Copyright (2007) with permission from Elsevier.

From Applied Thermal Engineering 25, Louise Jivan Shah, Elsa Andersen, Simon Furbo, *Theoretical and experimental investigations of inlet stratifiers for solar storage tanks*, pp. 2086 – 2099, Copyright (2005) with permission from Elsevier.

From International Journal of Energy Research, Elsa Andersen, Simon Furbo, Matthias Hampel, Wolfgang Heidemann, Hans Müller-Steinhagen, *Investigations on stratification devices for hot water heat stores*, accepted for publication May 2007, Copyright (2007), Copyright John Wiley & Sons Limited. Reproduced with permission.

Elsa Andersen

January 2007

Abstract

The focus in the present Ph.D. thesis is on the active use of solar energy for domestic hot water and space heating in so-called solar combi systems. Most efforts have been put into detailed investigations on the design of solar combi systems and on devices used for building up thermal stratification in hot water storage tanks. A new stratification device has been developed and patented. The device is a two fabric layer stratification inlet pipe.

The strategy used in the thesis is a combination of experimental and theoretical investigations. The experimental investigations are used to study the thermal behaviour of different components, and the theoretical investigations are used to study the influence of the thermal behaviour on the yearly thermal performance of solar combi systems.

The experimental investigations imply detailed temperature measurements and flow visualization with the Particle Image Velocimetry measurement method.

The theoretical investigations are based on the transient simulation program TrnSys and Computational Fluid Dynamics.

The Ph.D. thesis demonstrates the influence on the thermal performance of solar combi systems of a number of different parameters such as the varying weather conditions in Denmark, the domestic hot water consumption, the space heating demand and the size of the space heating system etc. through a detailed parameter sensitivity analysis. Further the calculations show that high thermal performances of solar heating systems are achieved by highly thermal stratified heat storages. Furthermore, it is demonstrated that thermal stratification can be build up in a nearly perfect way by using stratification devices. Different opertation conditions were applied in the experiments that showed that different stratification devices are suitable for different operation conditions. Tests, simulating both the thermal behaviour of a stratifier in a solar collector loop and in a space heating loop, have been carried out. The thermal behaviour of the stratifiers is demonstrated both with forced flow rates in the range from 2 – 10 l/min and with a volume flow rate based on thermosyphoning, the latter with both an external plate heat exchanger and with an imerged heat exchanger spiral.

Resumé

I forhåndenværende Ph.D. afhandling er der fokuseret på aktiv udnyttelse af solenergi til brugsvand og rumvarme i såkaldt kombianlæg. Der er lagt mest arbejde i de detaljerede undersøgelser af hvorledes kombianlæg designes samt hvorledes komponenter til opbygning af temperaturlagdeling i lagertanke fungerer. En ny komponent til opbygning af temperaturlagdeling i lagertanke er udviklet og patenteret. Komponenten er et indløbsrør konstrueret af to lag stof.

Den anvendte strategi er en kombination af eksperimentelle og teoretiske undersøgelser. De eksperimenteller undersøgelser er anvendt til at studere de termiske forhold for forskellige komponenter mens de teoretiske undersøgelser er anvendt til at studere hvorledes de termiske forhold for enkeltkomponenter influerer på den årlige ydelse af kombianlæg.

De eksperimentelle undersøgelser omfatter detaljerede temperaturmålinger og strømningsvisualisering med Particle Image Velocimetry målemetoden.

De teoretiske undersøgelser er baseret på beregninger med det transiente simuleringsprogram TrnSys samt Computational Fluid Dynamics.

Ph.D. afhandlingen demonstrerer gennem en detaljeret parameter følsomhedsanalyse hvorledes forskellige parametre, såsom varierende danske vejrforhold, varmtvands- og rumvarmeforbruget, anlægsstørrelsen m.v. influerer på ydelsen af kombianlæg. Endvidere viser undersøgelserne at høje anlægsydelser opnås med lagertanke med stor temperaturlagdeling. Endelig er det demonstreret at temperaturlagdeling kan opbygges næsten ideelt med temperaturlagdelingsrør. Forskellige temperaturlagdelingsrør er undersøgt eksperimentelt ved forskellige driftsbetingelser og undersøgelserne viser at forskellige temperaturlagdelingsrør er egnede ved forskellige driftsbetingelser. Der er udført eksperimentelle undersøgelser der simulerer hvorledes temperaturlagdelingsrør både i solfangerkredsen og i rumvarmekredsen fungerer. Virkemåden af temperaturlagdelingsrør er demonstreret både med tvungen volumenstrøm i området 2 – 10 l/min og med selvcirkulerende volumenstrøm, sidstnævnte både via en ekstern pladevarmeveksler samt med en indbygget varmevekslerspiral.

Symbols, definitions and abbreviations

Symbols used in figures

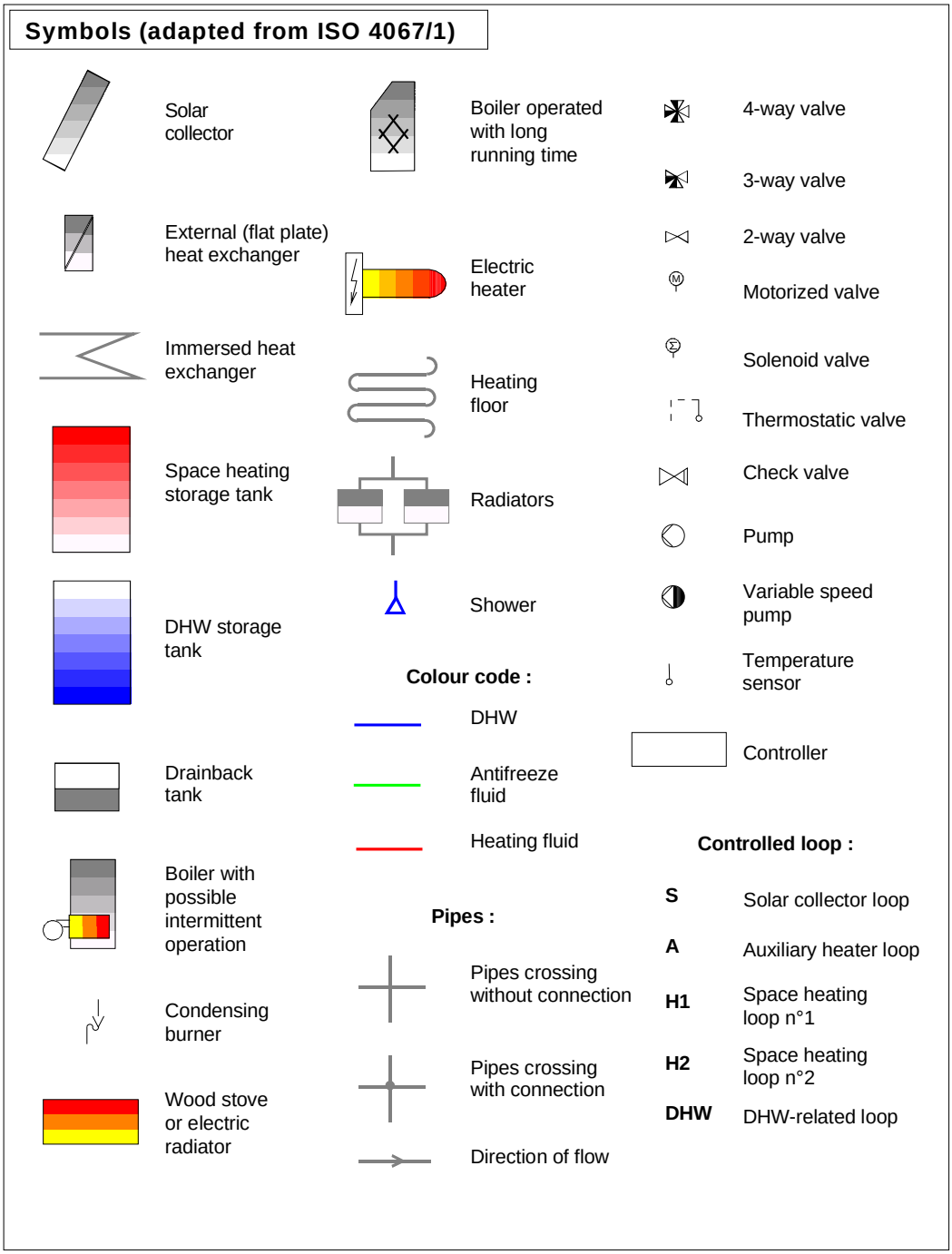

Figure from Suter 2000.

Symbols

R	Result	[same unit as R]
U_R	Uncertainty of the result R	[same unit as R]
ΔT	Temperature difference	[K]
v	Volume flow rate	[m^3/s]
c_p	Specific heat capacity	[J/(kg·K)]
ρ	Density	[kg/m^3]
Q_{COL}	Energy produced by the solar collector	[kWh]
Q_{AUX}	Auxiliary energy consumption	[kWh]
Q_{DHW}	Domestic hot water load	[kWh]
Q_{SH}	Space heating load	[kWh]
Q_{LOSS}	Heat loss from heat storage tank	[kWh]
ΔQ_{TANK}	Internal energy change in heat storage tank	[kWh]

Definitions

Beam radiation	Part of radiation from the sun that passes unscattered through the atmosphere.
Diffuse radiation	Part of radiation from the sun that is scattered in the atmosphere reaching a surface.
Global radiation	Total radiation on horizontal which equals the sum of beam and diffuse radiation.
Total radiation	Total radiation on a tilted surface which equals the sum of beam, diffuse and ground reflected radiation.
Circumsolar radiation	Radiation from the area around the sun disc. The radiation is considered as diffuse radiation.
Horizon brightening	Diffuse radiation from the horizon, an additional diffuse radiation contribution caused by the scattering of solar radiation from the sky dome by the thick layer of particles and dust close to the surface of the earth. Under a clear sky the phenomenon is most significant. The phenomenon does not exist in overcast weather.
Day temperature	Average ambient temperature measured over 24 hours from midnight to midnight.
Net utilized solar energy	Energy charged for domestic hot water and space heating minus auxiliary energy use.

Solar fraction	Net utilized solar energy divided by the energy charged for domestic hot water and space heating.
Performance ratio	Net utilized solar energy divided by the net utilized solar energy of the reference system.
Utilization of solar radiation	Net utilized solar energy divided with the energy of the total solar radiation on the solar collector.
Ideal inlet stratifier	Inlet pipe that leads water of any temperature into a hot water storage tank in the level where the temperature of the water in the storage tank is equal to the temperature of the incoming water
Inlet stratifier	Inlet pipe aiming to work as an ideal inlet stratifier.
Relative height	Height level in the tank divided by the total height of the tank. 0 equals the bottom of the tank and 1 equals the top of the tank.

Abbreviations

spiralHX	Heat exchanger spiral in the solar collector loop.
fixSH	Fixed return inlet height from the space heating system.
strsolar	Inlet stratifier in the solar collector loop.
strSH	Inlet stratifier in the space heating loop.
DHW	Domestic hot water.
SH	Space heating

Table of Contents

PART I

INTRODUCTION AND SUMMARY

1. Introduction

1.1 Background

The sun is an unlimited energy source. The yearly energy of the solar radiation reaching the earth is about 8,500 times higher than the world's total yearly energy consumption. And still the active use of solar energy only covers 0.04% of the total yearly energy consumption (SHC 2006, Risønyt 2006). The potential of solar energy use is huge, but until now the interest in solar heating systems has been very limited. The main reason has been the low fossil fuel energy prices which have been hard to beat with solar heating systems, but also bad reputation and limited public knowledge about solar heating systems has restrained the extension. During the last year however, the prices of fossil fuel have increased to a level where solar heating systems can produce energy at competitive costs.

The fossil fuel reserves are limited. The many ongoing troubles in the oil producing countries raise awareness of our fragility regarding dependence on a constant energy supply, especially at higher latitudes with cold climates.

The climate on earth is changing, it becomes warmer, and it is discussed intensively whether the climate changes are man-created and due to increase of CO_2 and other greenhouse gasses in the atmosphere or natural consequences of changing activity in the magnetic field around the sun and the present location of our solar systems in the universe. The theory about the latter was first put forward ten years ago by Danish researchers who were able to show coincidence between cosmic radiation and the formation of clouds in the sky. According to this theory the level of cosmic radiation is determined by the activity of the sun which on the short term scale changes with a frequency of 11 years but also in the long term scale on the position of our solar system in the galaxy, the Milky Way. The sun travels slowly around the centre of the Milky Way in 240 million years. During this journey it passes through the spiral arms of the galaxy in which the activity e.g. supernova-explosions and formation of stars is higher than between the spiral arms. It is presumed that the main principal source of cosmic radiation is the supernova-explosions. Consequently the cosmic radiation is higher in the spiral arms and the formation of clouds increases and the climate on earth becomes colder (e.g. Ice Age). Between the spiral arms of the galaxy, the cosmic radiation is lower and the climate consequently warmer.

Another theory about the natural course of climate change is related to the fact that the path which the earth follows around the sun varies in time. Also the declination of the earth changes with time and finally, the major axe of the earth is turning around with time. The consequence of the last phenomena is that for instance summer in the northern hemisphere is sometimes when the earth is closest to the sun and sometimes when the earth is farthest away form the sun. The southern hemisphere contains more water than the northern hemisphere and hence has a larger heat capacity. Therefore the mentioned variations have impact on the climate on earth.

Whether the climate changes are caused by the sun and the universe, by eccentricity of the path which the earth follows around the sun or the greenhouse gasses or by a combination of these, the man-created pollution caused by burning fossil fuels is not

healthy for humans, animals or the environment. For this reason alone, the use of non-polluting renewable energy should be strongly enforced in all countries.

There are many good reasons to be interested in solar energy and other renewable energy technologies, among others:

- Limitation of fossil fuels
- Stability in energy supply
- Reduction of air pollution
- Climate changes
- Growth of local industries creating welfare and export

The development of solar heating systems as we know them today started in the late 18th century when it was discovered that window glass could actually trap heat and that the temperature inside a cavity with glass cover could reach above the boiling temperature of water.

The task of a solar combi system is to collect energy from the sun and store the energy in form of heated water in a heat storage tank until it is used either for domestic hot water or for space heating.

The importance of heat storages with small heat losses, highly stratified hot water storage tanks and a good interplay between the solar collectors and the auxiliary energy supply system is well known (Weiss et al. 2003). But how solar combi systems are designed best in order to reach high thermal performances at a low cost is only studied to a limited extent.

Figure 1.1 shows a schematic of a typical Danish solar combi system. The left side of the figure shows the charge side with the energy supply sources, which are the solar collector and the auxiliary energy supply system, in most cases, based on fossil fuels. The middle part shows the hot water storage tank inclusive heat exchangers for heat transfer and the control system. The right side of the figure shows the discharge side that comprises domestic hot water and space heating distribution systems.

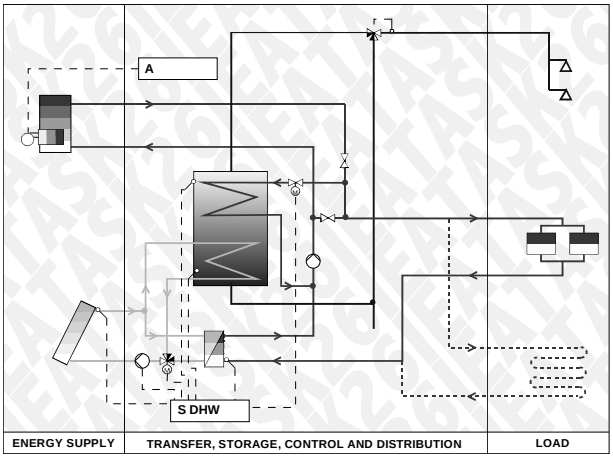

Figure 1.1 Typical Danish solar combi system. (Suter 2000).

The solar combi system shown in Figure 1.1 typically consists of 5 – 20 m^2 solar collectors and 200 – 300 litres storage tank built into a 60 cm by 60 cm unit with all the necessary components such as pumps, valves, expansion vessel, control system etc. Further, solar energy is supplied to the space heating system through a heat exchanger between the solar collector loop and the space heating loop.

Based on measurements carried out in the period 1978 – 1997 of nine solar combi systems (Mikkelsen and Jørgensen 1981), (Andersen 1988) and (Ellehauge 1993, 2000), an overview of the thermal performance of solar combi systems in practice is given. Figure 1.2 shows the measured yearly thermal performances of the solar combi systems. The thermal performances of systems designed as shown in Figure 1.1 are marked with red circles. Apparently, these systems have a high thermal performance and further, there seems to be little correlation between the solar fraction and the yearly thermal performance.

.

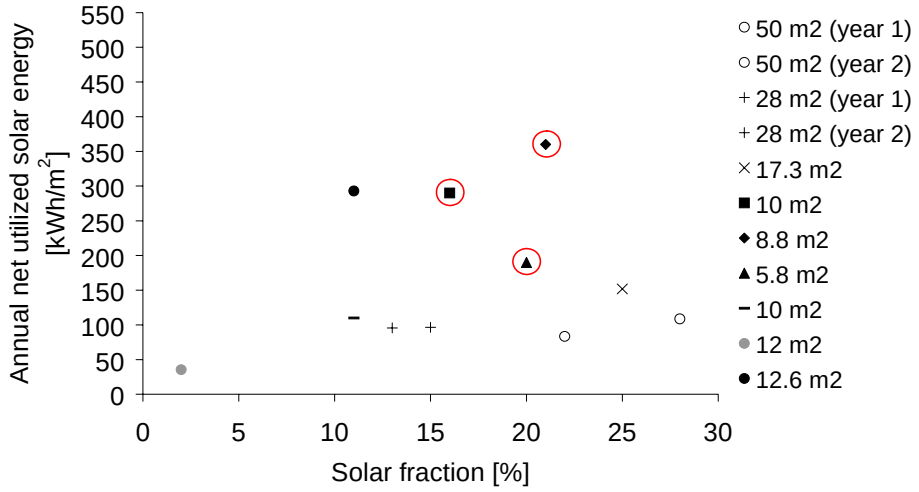

Figure 1.2 Measured yearly thermal performances per. m^2 collector of solar combi systems. Systems designed as shown in Figure 1.1 are marked with red circles.

For further analyses of the measured data, the thermal performances of the systems are compared to theoretically calculated thermal performances. Also the space heating consumption is studied. The results show that all the systems have space heating consumption during summer from May to September and that the higher the space heating consumption is during the summer, the higher is the thermal performance. For the systems with heat exchanger between the solar collector loop and the space heating loop as shown in Figure 1.1, the space heating consumption is only covered by the solar combi system during summer. For the other systems, half of the solar energy utilized for space heating is utilized during the summer period. The other half is utilized during autumn and spring. Some of the systems are large with a high solar fraction and a low net utilized solar energy per m^2 solar collector.

Figure 1.3 shows the two solar combi systems used in the calculations. System no. 1 has a storage tank volume of 300 litres, a small auxiliary volume and a low tank heat loss coefficient. System no. 2 has a storage tank volume of 460 litres with 136 litres

for domestic hot water in the inner tank, a large auxiliary volume and a high heat loss coefficient.

Figure 1.4 shows the measured thermal performances and the calculated thermal performances with and without space heating consumption during summer. The calculations are carried out with different solar collector areas. The solar combi systems have been divided into three groups according to the size of the space heating consumption during the summer The size of the space heating consumption during the summer is determined as the ratio between the space heating consumption during the summer and the space heating consumption for the whole year. For ratios less than 8% the summer space heating consumption is small. For ratios between 8% and 12% the summer space heating consumption is mean, while the summer space heating consumption is high for ratios larger than 12%.

From Figure 1.4 it can be seen that the thermal performance of most of the solar combi systems lies between the calculated thermal performance for a good performing (system no. 1) and poor performing (system no. 2) solar combi system. The poor performing systems situated in the lower left corner all have a low space heating consumption during summer and are all, except for one system, systems with several large tanks and therefore also high heat losses. These systems are situated in the same region as the calculated system no.2 that also has a high heat loss from the storage tank. The systems with a mean summer space heating consumption are situated in the same region, as the calculated system no.1 with a summer space heating demand. The system with the high summer space heating consumption is situated above all other systems. In Figure 1.2 it was difficult to see any correlation between the solar fraction and the annual net utilized solar energy per m^2 solar collector. From Figure 1.4 it becomes obvious that the systems all show a clear correlation between the solar fraction and the annual net utilized solar energy per m^2 solar collector, regardless of the system design, when systems with similar consumption pattern are compared.

Apparently the size of the summer space heating demand is more important for the thermal performance than is the system design. The question that can be asked is: Is there a real space heating demand during the summer, or is the measured space heating consumption during summer just solar energy transferred to the space heating loop to keep the collector from boiling? And how shall solar combi systems without large space heating demands during summer be designed? It would require detailed measurement of the energy consumption in houses before and after installing solar combi systems in order to answer the question concerning space heating demand during summer. Hence, the question is not further addressed in the thesis.

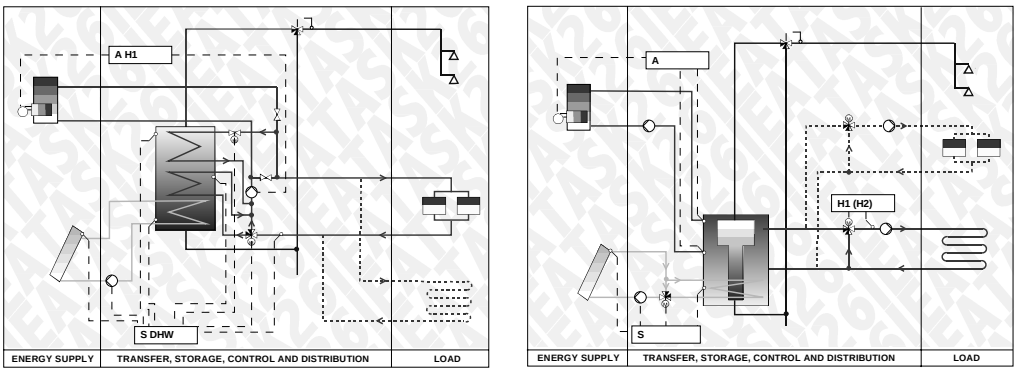

Figure 1.3 Left: Solar combi system based on a hot water tank with three heat exchanger spirals, system no.1. Right: Solar combi system recently introduced on the Danish market, system no.2 (Suter 2000).

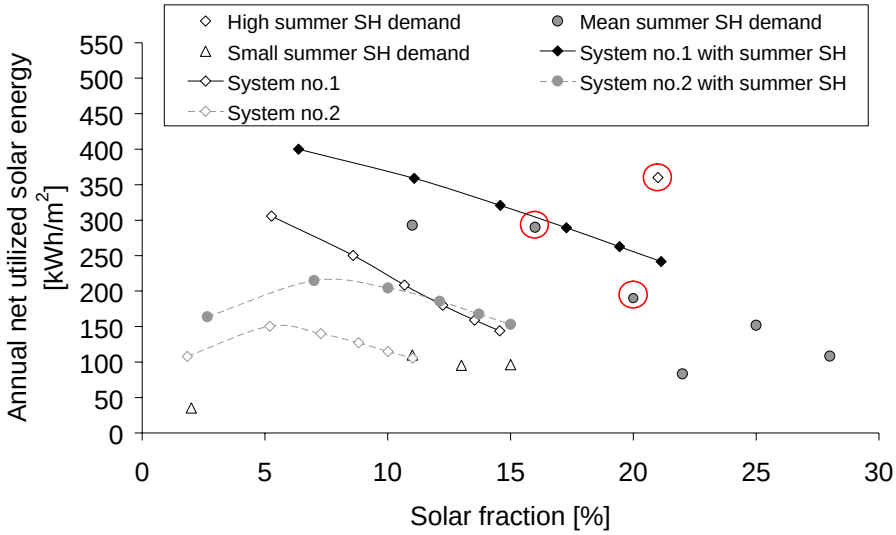

Figure 1.4 Measured and calculated thermal performances. The abbreviation SH refers to space heating. Systems designed as shown in Figure 1.1 are marked with red circles.

Further details in Paper I.

1.2 Aim and related projects

The primary aim of the thesis is to investigate how solar combi systems are designed best in order to reach high solar fractions and in this way, become economical attractive alternatives to traditional energy systems based on fossil fuels.

30% - 50% of the solar heating systems in Denmark for one family houses that are installed today are solar combi systems. The system design shown in Figure 1.1 is used for more than 90% of all solar combi systems in Denmark (Ellehauge and Shah 2000). There is a growing demand for solar heating systems which can provide more than just hot water. The space heating consumption is by far the largest energy

consumption in traditional houses situated at high latitudes, so even if the domestic hot water consumption is covered totally, the yearly savings are limited. Therefore, it makes much sense to develop solar combi systems with high thermal performance at a low cost.

At the beginning of the Ph.D. project, only limited knowledge about solar combi system designs was available. The solar combi systems that were installed in one family houses were individually designed based on the intuitions of the manufacturers, not on detailed research. Real knowledge about the design of solar combi systems, system size and control strategy was not available in Denmark or in other countries. However, internationally there was a large interest in developing attractive solar combi systems with low system costs and high thermal performances.

On this basis, a task force about solar combi systems was formed within the Solar Heating and Cooling program of the International Energy Agency (IEA SHC), Task 26. The work in Task 26 was carried out in the period 1998-2002 with participation of 15 research institutions and universities from 9 different countries. The main focus of the work was establishing an overview of the different solar combi systems on the European market and based on the knowledge of the participants, and preliminary calculations to determine which systems are the most promising. Further, great emphasis was put into establishing reference conditions for different climates representative for the climate in Europe, covering both south and north. Some of the systems were experimentally investigated and validated matematical models were prepared based on experimental data and used in the calculations. Other systems were described by not validated matematical models. The reference conditions were applied to the most promissing solar combi systems and the thermal performances of the investigated systems were compared. Also a cost analysis was performed. Further, attempts were made to find a suitable fast and inexpensive laboratory test method to evaluate the thermal performance of solar combi systems.

Also a method to compare solar combi systems in different climates, with different solar collector area and space heating loads, the so-called Fractional Solar Consumption (FSC) method was developed. The method compares the actual energy savings with the maximum theoretical energy savings with no system losses (Letz 2002).

Finally, a handbook of the work and results from Task 26 was published, (Weiss et al. 2003).

In continuation of the IEA SHC taskforce, Task 26 a new taskforce, Task32 was formed. The work in Task 32 was started in 2004 and will come to an end in 2007. 16 research institutes and universities from 8 different countries participate. The aim of the task is to develop advanced storage concepts for solar houses and low energy buildings. The main goal is to develop storage units for heating or both heating and cooling loads with solar fractions larger than 50 %. The work is concentrated in three subtasks concerning phase change materials (PCM), chemical and sorption storages and advanced water storages. Further, the FSC method for comparing different solar combi systems in different climates, developed in Task 26, has been extended to also include cooling loads.

A state of the art handbook covering the topics was published in 2005 (Hadorn et al. 2005).

In 2003, Nordic Energy Research and in 2006 Nordic Innovation Centre started the projects "Competitive solar heating systems for residential buildings" and "Solar thermal components adapted to common building standards". The project involves research institutes and industrial partners from the Nordic countries Denmark (Technical University of Denmark, Metro Therm A/S, Velux A/S), Norway (University of Oslo, SolarNor) and Sweden (Dalarne University, Lund Institute of Technology, Solentek AB) and the Baltic country Latvia (Riga Technical University, SIA Grandeg). The project will be finished in 2006. The project embrace educational activities and research and demonstration activities where three Ph.D. studies and a post-doc. study concentrate on developing and demonstrating a flexible in size solar combi system suitable for the Nordic market. In Denmark and Norway the research and development focus is on solar heating/natural gas systems, and in Sweden and Latvia the focus is on solar heating/pellet systems. Additionally, Lund Institute of Technology and University of Oslo are studying solar collectors of various types being integrated into the building (Furbo et al. 2006).

The present thesis work is carried out in the same period of time as the above-mentioned projects and is therefore inspired by the findings of the projects. Most effort has been put into the detailed investigations on the design of solar combi systems and on stratification devices, both those already existing on the market and new types.

1.3 Strategy and methods

A combination of experimental and theoretical work forms the basis of the thesis. The best performing solar combi system found in the IEA SHC Task 26 was the SolvisMax from the German company SOLVIS GmbH & Co KG. Consequently the investigations are mainly based on this particular solar combi system.

The SolvisMax has an integrated modulating condensing natural gas boiler built into the heat storage. Inlet stratification pipes are placed in the heat storage for building up thermal stratification in the heat storage during operation, both of the solar collector loop and of the space heating loop. The system has a side arm with a built-in heat exchanger for domestic hot water preparation. A speed controlled pump in the sidearm ensures the hot water comfort by keeping the temperature of the hot water constant. A shunt between the outlet and the inlet of the heat exchanger in the sidearm keeps the temperature that is going into the heat exchanger low. This reduces the risk of lime deposits in the heat exchanger. One control system controls the pump in the solar collector loop and the boiler. Energy from the solar collector is transferred through a very compact immerged heat exchanger. In Figure 1.5 schematic illustrations of the solar combi system and some photos are shown.

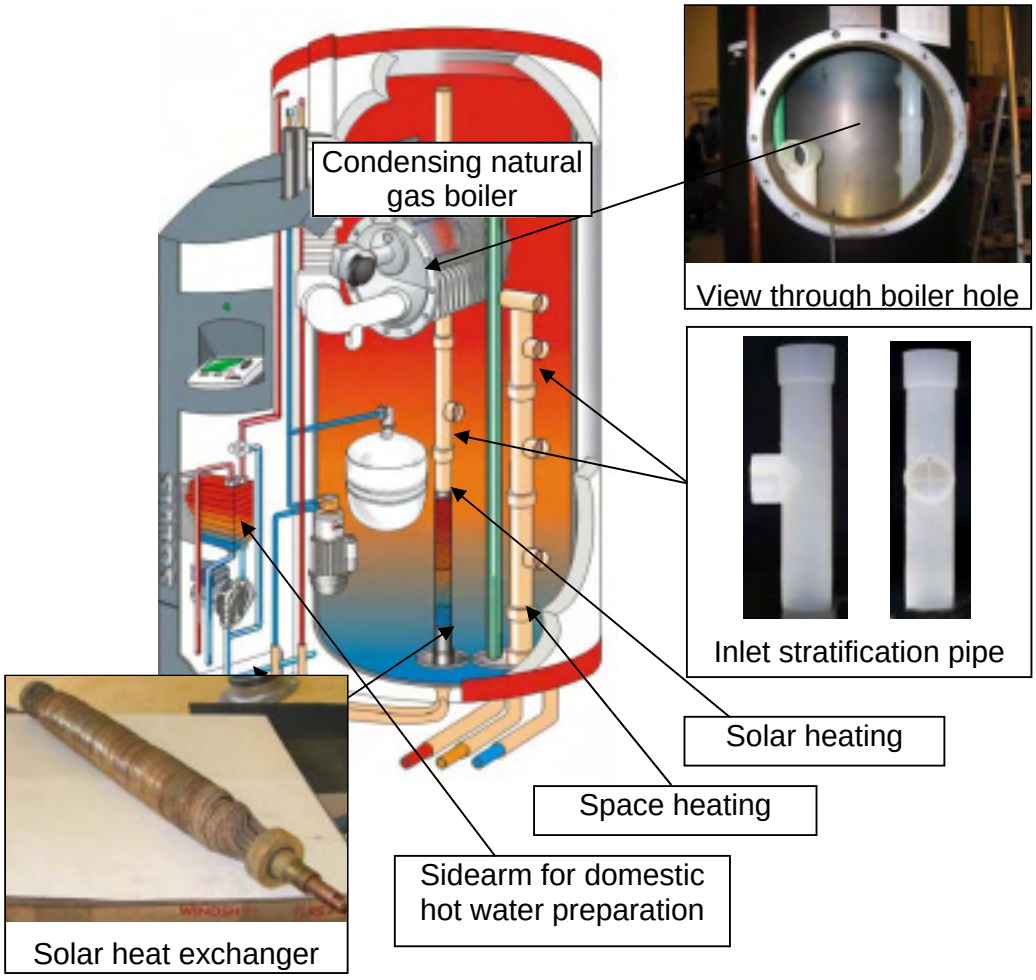

Figure 1.5 The experimentally investigated solar combi system. Picture of tank from Solvis GmbH & Co KG.

The experimental investigations are carried out with temperature sensors and measurement programs. If possible, the temperature sensors are mounted inside the geometry. Otherwise, the temperature sensors are mounted on the outside of the geometry in good thermal contact with the geometry and well insulated from the surroundings.

Also Particle Image Velocimetry (PIV) measurements are carried out (Raffel et al. 1989). The basic principle of PIV is to determine fluid flow velocities indirectly by analysing the motion of seed neutral density particles in the flow (polyamide particles with a diameter of 20 μm). The velocity of each seed particle can be considered to be the same as the fluid velocity. The particles are refractive. When illuminated by a thin laser sheet the particles scatter the laser light as diffuse reflections (randomly distributed) and the scattered light is detected by a camera. With the camera (charge couples device, CCD camera) it is possible to take two pictures with a defined time gap. The velocity vectors are derived by measuring the movement of particles between the two pictures.

Results are similar to computational fluid dynamics (CFD). Therefore, the results can be used to verify the theoretical models. Figure 1.6 shows the principle of PIV measurements.

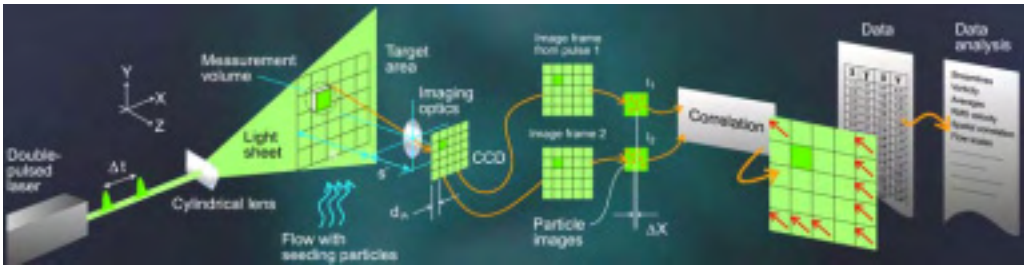

Figure 1.6 Principle of PIV measurements (Dantec Dynamics A/S).

The theoretical investigations are carried out with TrnSys, a transient simulation program (Klein et al. 1996). The program is modular based, which means that a system model is built with modules of every single component that is part of the investigated system. A component module is a mathematical model of the behavior of the component based on parameter information and inputs parameter information, specific for the component, necessary to describe the thermal behavior of the component. TrnSys is an "open source" program which allows users access to all program codes and the possibility to add new components to the program. Altogether, this makes TrnSys a strong and very flexible tool.

Finally, Computational Fluid Dynamics (CFD) is used for theoretical investigations (Fluent 2003). CFD is used to study flow and heat transfer in both fluid and solid regions of a defined geometry in a very detailed way. The goal is to obtain a numerical description of the complete flow field. The pre-processor Gambit is used to define the geometry and the mesh, where the geometry is divided into small control volumes. The solver Fluent is used to solve the mathematical governing equations and for visualization of the results. Fluent uses the finite volume method to solve the governing equations for each control volume. It is required that the mass of fluid is conserved, the rate of change of momentum equals the sum of the forces on a fluid particle (Newton's second law) and the rate of change of energy equals the sum of the rate of heat added to and the rate of work done on a fluid particle (the first law of thermodynamics).

1.4 Accuracy

All types of measurements are subject to some uncertainty. The uncertainty can result from systematic errors and random errors. Systematic errors result from the method used to perform the measurement and can for example be introduced when mounting a temperature sensor on the outside of a hot pipe. The sensor will measure a temperature which is lower than the temperature of the hot water in the pipe. Random errors result from the temperature sensor which will vary if the same temperature is measured many times.

The uncertainty of the measurement equipment is usually given by the manufacturer. The uncertainty is not static, but can change with time. Therefore equipment must be calibrated regularly. The uncertainty of specific measurement equipment can be reduced further than stated by the manufacturer by calibration.

The uncertainties of a temperature measurement U_T with an uncertainty of the temperature sensor called U_{sensor} and an uncertainty of the method used called U_{method} is determined as:

$$U_T = \sqrt{U_{sensor}^2 + U_{method}^2} \tag{1}$$

In case of a compound measurement, e.g. an energy amount calculated based on measurement of a temperature difference, a volume flow rate and the specific heat and density of the fluid, the result (R) of the compound measurement can be written as:

$$R = f\left(\Delta T, v, c_p, \rho\right) \tag{2}$$

When the uncertainties ($U_{\Delta T}, U_v, U_{c_p}, U_\rho$) of the measurements ($\Delta T, v, c_p, \rho$) are known the accuracy of the compound measurement can be calculated as:

$$U_R = \sqrt{\left(\frac{\partial f}{\partial \Delta T}\cdot U_{\Delta T}\right)^2 + \left(\frac{\partial f}{\partial v}\cdot U_v\right)^2 + \left(\frac{\partial f}{\partial c_p}\cdot U_{c_p}\right)^2 + \left(\frac{\partial f}{\partial \rho}\cdot U_\rho\right)^2} \tag{3}$$

Examples of accuracies of measurements are shown in Table 1.

Table 1 Examples of accuracies.

Measurement	Accuracy
Flow meter	0.3%
Temperature sensor Pt100	0.2 K
Temperature difference Pt100	0.05 K
Heat capacity of solar collector fluid	0.5%
Density of solar collector fluid	0.5%
Solar collector area	0.1%

Based on the values from Table 1, the relative accuracy of the compound measurement of the solar collector efficiency for small incidence angles is about 2% while the relative accuracy of the incidence angle modifier is about 3%.

Estimation of the accuracy of the compound measurements that leads to determination of the solar energy from a solar collector is demonstrated in Paper II.

All inputs for computer models are subject to uncertainty both from the uncertainty by determining the input, for example the heat loss coefficient of a heat storage tank, and from simplification of the computer model, for example one tank heat loss coefficient without considering the distribution of the tank heat loss coefficient. The accuracy of a computer model is based on a validation process where measured and calculated temperatures and energy amounts are compared. The model is said to be usable for further investigations when the difference between the measured and calculated energy amounts for different representative test periods (typical summer and winter periods) are lower than for example 5% (Shah 2002). Consequently, a good estimation of the accuracy of the calculated thermal performance of solar heating systems is 5%.

The suitability of the calculations, for example the yearly thermal performance of solar combi systems calculated with for instance a validated Trnsys model, is further evaluated by the energy balance:

$$Q_{COL} + Q_{AUX} - Q_{DHW} - Q_{SH} - Q_{LOSS} - \Delta Q_{TANK} = 0 \quad (4)$$

Non validated computer models may not lead to the best estimation of the yearly thermal performance, but may be suitable for comparison of different system designs and parameter variations since the relative differences are not affected significantly by the actual accuracy of the model.

2. Solar combi system in general

2.1 Design of solar combi systems

It is not obvious how solar combi systems should be designed. In section 2.2 examples of solar combi systems on the European market are shown. In Figure 2.1 the distribution of volumes charged and discharged during operation in the hot water heat storage of a solar combi system are schematically illustrated.

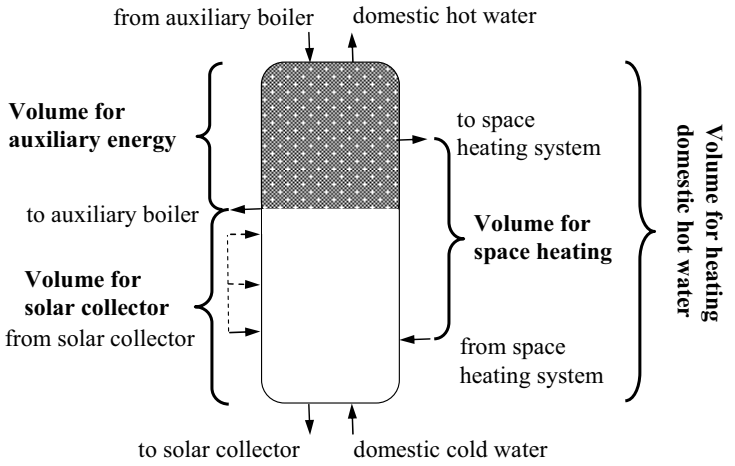

Figure 2.1 Schematical illustration of the storage tank of a solar combi system.

The domestic cold water inlet and domestic hot water outlet are situated at the bottom and the top of the domestic hot water tank, respectively (ref. Figure 2.1). The outlet for domestic hot water can be in different additional levels, also below the auxiliary heated volume. In this way domestic hot water can be discharged with different temperatures. Domestic hot water can also be discharged from the inner tank in a tank-in-tank, with external heat exchangers or immersed heat exchanger spirals as shown in Figure 2.2.

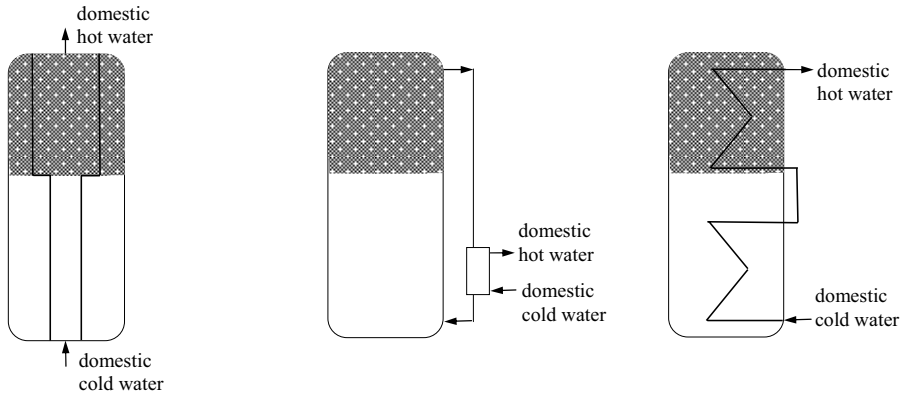

Figure 2.2 Options for domestic hot water discharge. Left: Domestic hot water tank-in-tank. Middle: Sidearm and plate heat exchanger. Right: Immersed heat exchanger spiral.

The outlet for space heating is usually above the lower level of the auxiliary heated volume. Charge and discharge of the storage tank can be done with external heat exchangers or immersed heat exchanger spirals or with direct inlets and outlet.

The storage tank is heated by a solar collector and by an auxiliary energy supply system. It also can be a pre-heating system with a storage tank only heated by a solar collector. The system must be able to supply both domestic hot water and space heating in an effective way. Domestic hot water supply usually requires temperatures higher than 45 ºC, whereas space heating most of the time requires lower temperatures, but the temperature is of course depending on the size of the heating system and the heating demand of the house. Dimensioning flow temperatures and return temperatures of 60ºC / 40ºC or 70ºC / 50ºC with volume flow rates of about 300 l/hr are usually used for traditional radiator heating systems. In floor heating systems, the dimensioning flow temperature is in the range of 35ºC - 40ºC with dimensioning return temperature in the range 30ºC - 35ºC and the volume flow rate is in the range of 1000 l/hr.

The solar collector loop is usually operated with a propylene glycol-water mixture (anti freeze liquid) but can also be operated with water. The latter requires a drain back system where the solar collector is emptied when not in operation. The volume flow rate in the solar collector loop is driven by a pump and is in the range from 0.15 l/min/m^2 – 1.2 l/min/m^2. The low volume flow rate results in high temperature differences between the inlet and the outlet of the solar collector and the high volume flow rate results in low temperature differences.

The energy from the solar collector operated with high volume flow rate in the solar collector loop is usually transferred to the storage tank through a heat exchanger spiral immersed at the bottom of the storage tank (ref. left in Figure 2.3) or through an external heat exchanger with pipe connections to the tank (ref. right in Figure 2.3). In the latter approach, solar energy on the secondary side of the heat exchanger is transferred to the storage tank by a pump.

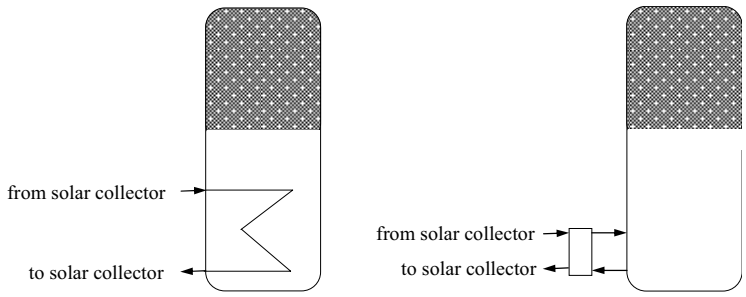

Figure 2.3 Options for transferring energy from the solar collector loop to the heat storage tank with high volume flow rate in the solar collector loop.

Low volume flow rates are used in solar heating systems based on storage tank designs with emphasis on enhancing thermal stratification in the heat storage tank. High volume flow rates are, due to the lower temperature level of the collector outlet, less suitable for this approach.

Low volume flow rate operation in connection with an immersed heat exchanger does normally not provide any thermal advantage. To benefit from a low volume flow rate in the solar collector loop, the solar heat must be transferred to the tank in a level where the temperature of the tank water is close to the temperature produced by the solar collector. Thermal stratification can be achieved, for example by using inlet stratification devices at all inlets to the storage tank. Figure 2.4 show examples of inlet stratification design options in the solar collector loop.

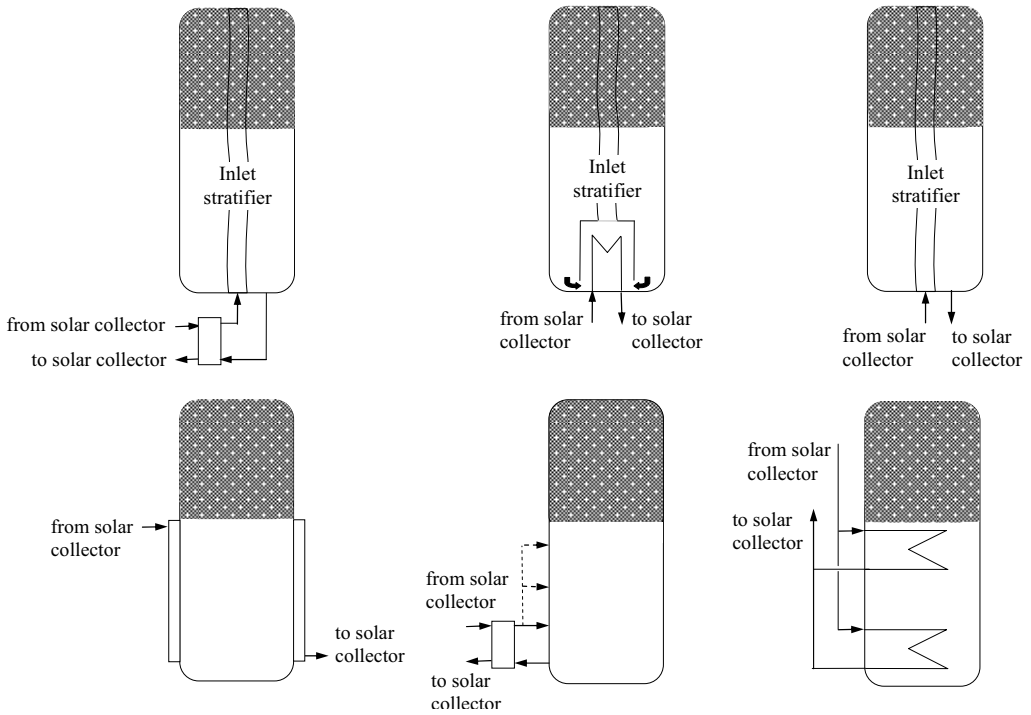

Figure 2.4 Stratification design options schematically illustrated with stratification pipes (fabric inlet stratifiers), mantle tank, external heat exchanger and heat exchanger spirals. Top left: External heat exchanger with either thermosyphoning or pump driven volume flow rate on the secondary side of the heat exchanger. Top middle: Internal heat exchanger with thermosyphoning volume flow rate in the heat storage tank. Top right: Direct inlet (e.g. drain back system). Bottom left: Mantle tank. Bottom middle: External heat exchanger with multiple inlets to the tanks with either thermosyphoning or pump driven volume flow rate on the secondary side of the heat exchanger. Bottom right: Two heat exchanger spirals with inlet to the upper, the lower or both heat exchanger spirals.

Thermal stratification in the storage tank is extremely important in order to achieve high thermal performance of a solar heating system. High temperatures in the top of the storage tank and low temperatures in the bottom of the storage tank lead to the best operation conditions for any solar heating system. High temperatures in the top of the storage tank established by the energy from the solar collector, reduce the use of auxiliary energy. Low temperatures in the bottom of the storage tank improve the operation conditions for the solar collector. The solar collector can easily transfer energy to the storage tank and can be in operation for a longer period leading to a better utilization of the solar collector.

Solar energy can be stored in a domestic hot water tank where domestic hot water is lead directly from the tank to the consumer or in a space heating tank with a heat exchanger between the tank water and the domestic hot water. When storing energy in the domestic water, the retention time of the water in the tank must be considered. Long retention time in the tank in combination with a temperature level in the range 30ºC - 45ºC can create an optimal environment for bacteria growth, e.g. legionella in the tank. Investigations of legionella in storage tanks have showed that legionella

bacteria can not multiply at temperatures below 20 ºC and above 50 ºC and not survive temperatures above 60ºC (Cabeza 2005).

Most solar heating systems are depending on an auxiliary energy supply system. The auxiliary energy supply system can be a gas or an oil boiler, an electrical heater or based on wood or pellet burners. Most auxiliary energy supply systems are connected to the solar heating system as separate units but also solar heating systems with integrated auxiliary energy supply systems exist, for instance solar heating systems with integrated gas boilers (e.g. Solvis). For auxiliary energy supply systems that utilize the energy from the exhaust gas by condensing, it is extremely important that the return temperature to the auxiliary energy supply system is sufficiently low to enable condensing of the exhaust gas. These boilers are more expensive than non-condensing boilers and therefore a bad choice if the condensing feature is not utilized.

Only one control system for controlling the solar collector loop, the auxiliary energy system and the space heating loop should be used. When two independent control systems are used, there is constantly the risk that the auxiliary energy supply system heats up the auxiliary volume during periods when the heating could be easily managed by the solar collector. This results in higher auxiliary energy consumption than necessary and worse operation conditions for the solar collector.

High heat losses from the storage tank reduce the thermal performance of the solar heating system, because the heat losses are partly covered by the auxiliary energy supply system. Heat losses can not be avoided, but kept at a minimum by insulating all parts of the storage tank carefully and in such a way that convection of air between the tank and the insulation material can not take place. Heat losses can be further reduced by keeping all pipe connections in the lower and colder part of the storage tank and by reducing the set point temperature of the auxiliary energy system and the volume for auxiliary energy as much as possible.

It is most common to design small solar combi systems with short term storage with capacity for only a few days, but also large solar combi systems with long term storage are used. In these systems heat collected during summer is stored and used during the heating season.

2.2 Examples of solar combi system types in Europe

In practice, a large number of differently designed solar combi systems for one family houses are on the European market. The size and the design of the systems are specific for different countries and often based on traditions, price level, specific security measures etc. In Germany there is much focus on legionella, hence hot water is not taken directly from the storage tank, but through a heat exchanging device. The systems are rather complicated and much effort is made to enhance thermal stratification in the storage tanks. In the Netherlands, drain back systems are widely used. In France, systems with direct heating from the solar collector into the space heating system are widely used. In Sweden and in Austria, wood or pellet boilers for auxiliary energy supply are popular. The smallest solar combi systems are found on the market in Denmark and the Netherlands. The largest systems are found on the Austrian market. The overall tendency is that the solar combi systems are becoming more advanced with emphasis on thermal stratification in the storage tanks and only one control system for operating both the pump in the solar collector loop and the auxiliary energy supply system.

Figure 2.5 – Figure 2.8 show schematical examples of solar combi system types on the European market.

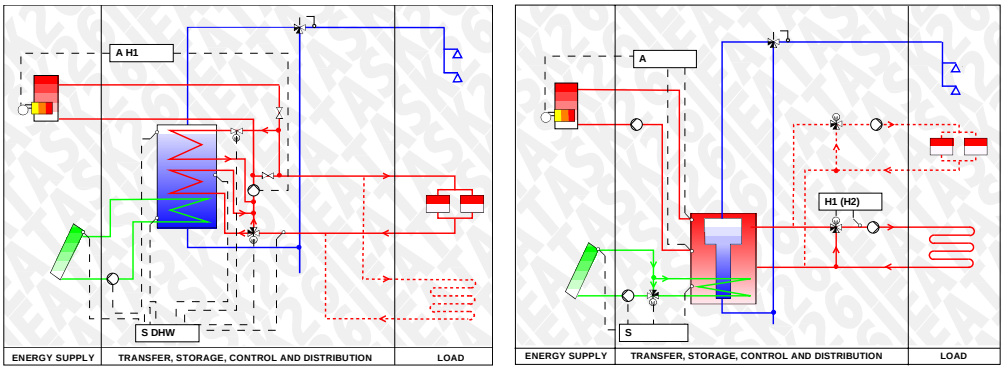

Figure 2.5 Solar combi system types. Left: On the market in Denmark. Right: On the market in Denmark, Switzerland and Austria (Suter 2000).

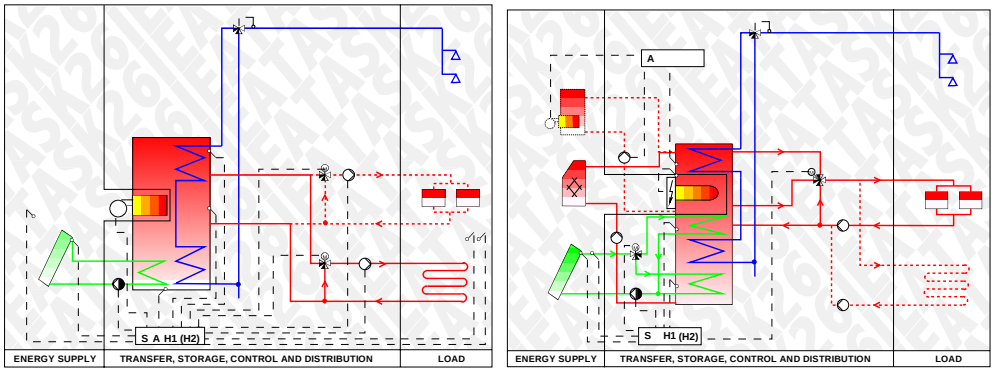

Figure 2.6 Solar combi system types. Left: On the market in Switzerland and Finland. Right: On the market in Sweden and Finland (Suter 2000).

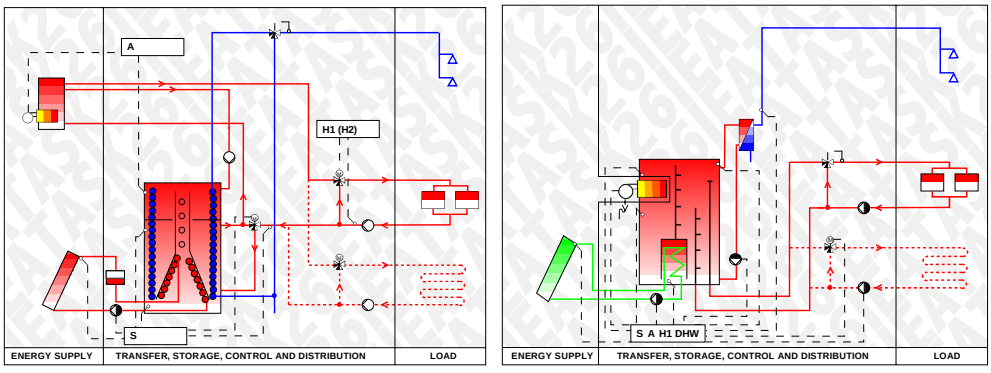

Figure 2.7 Solar combi system types on the market in Germany (Suter 2000).

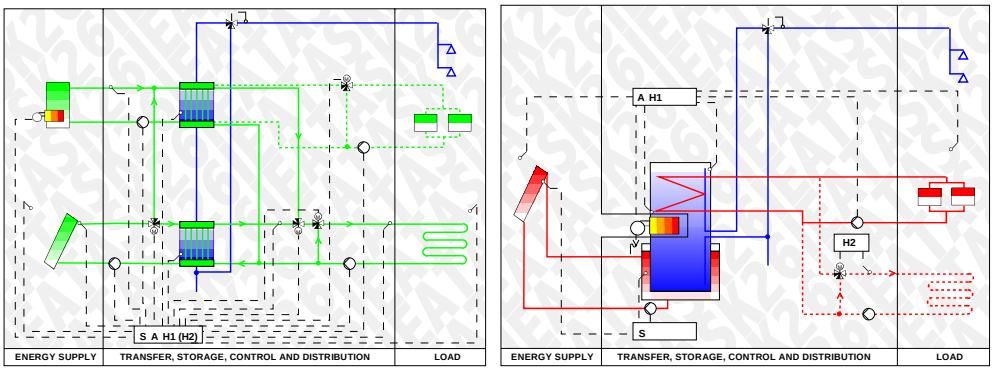

Figure 2.8 Solar combi system types. Left: On the market in France. Right: On the market in the Netherlands (Suter 2000).

2.3 Research on concepts and design of solar combi systems

In IEA SHC, Task 26 Solar CombiSystems, 21 solar combi systems on the European market were evaluated. The evaluation comprised both the system costs and the thermal performance. It was found that most of the systems for one family houses had solar collectors of 10 m^2- 30 m^2 with 0.3 m^3- 3 m^3 tank volumes. The best systems, regarding the performance/cost ratio, were the most advanced systems with inlet stratification pipes, an efficient integrated boiler, and only one control system for both the boiler and the solar collector loop (Weiss et al. 2003).

Streicher and Heimrath (2004) performed a sensitivity analysis of 9 of the investigated Task 26 systems. The influence of climate and heat load and of the solar collector, the storage tank, the boiler and the space heating system, were investigated. It was found that the optimal collector tilt depends on the latitude and the solar fraction. The optimal collector tilt increases with increasing solar fraction in order to better utilize the solar irradiation during the heating season. The thermal performance decreases for increasing volume flow rate in the solar collector loop. The heat exchange capacity rate in the solar collector loop should be about 40 W/K per m^2 solar collector. For heat storages with an internal heat exchanger in the solar collector loop, the temperature sensor of the control system should be placed on a level with the lower 1/3 – 1/2 of the heat exchanger. The optimal storage volume is about 100 l/m^2 solar collector area. Storage insulation thicknesses above 15 cm do not increase the thermal performances. Top insulation is less significant than side insulation because the top area is smaller. The auxiliary volume should be kept small and the set point temperature for the auxiliary energy supply system low. The sensor for the auxiliary heater should be placed below the space heating outlet. No big influence on the position of the return inlet pipe from the space heating loop in the heat storage was found. The thermal performance decreases slightly with increasing position of the outlet height for the space heating loop. Most important for the achieved energy savings is the boiler efficiency.

Streicher (2004) improved 3 of the 9 investigated systems significantly by design changes determined by the sensitivity analysis (Streicher and Heimrath 2004). The strategies used for the improvement were: Keep the boiler efficiency as high as possible, keep the collector inlet as cold as possible, avoid temperature losses through

mixing, keep heat losses as low as possible, and use efficient pumps to decrease the electricity demand. This work showed that optimization can improve the system performance significantly and that, for different system designs, the performance is nearly the same if all aspects of the system are optimized.

Lorenz (2001) showed how the thermal performance of a typical Swedish solar combi system with 20 m^2 solar collectors and a 0.75 m^3 storage tank with three internal heat exchanger spirals could be improved by 10% by small design changes without additional system costs. Further, he showed that the thermal performance can be improved by 25% – 35% by introducing a highly stratified tank instead of a non-stratified tank.

Jordan (2001) investigated the advantage of a stratification inlet pipe instead of a fixed inlet height for transferring solar energy to the storage tank by means of a thermosyphon loop. She found that for a solar combi system with a solar fraction of about 25%, the thermal performance increased by only 1 – 2% by using a stratification manifold instead of a fixed inlet.

Pauschinger et al. (1998) measured similar low performance improvements of about 3% by using low flow and inlet stratifiers for solar combi systems with a solar fraction of about 20%.

Streicher (1998) carried out simulations of solar combi systems. He found that the solar fraction could be roughly estimated by three parameters: The solar collector area, the storage volume and the heat load of the system. The investigations included Austrian, German, Danish and Swedish climates.

Drück and Hahne (1998) compared the thermal performances of four highly advanced and differently designed solar combi systems. They found that the most important parameters for a well performing solar combi system are low heat losses and a small auxiliary volume in the heat storage with a low set point temperature. All pipe connections for the auxiliary and space heating loop should be at appropriate positions. Only then additional thermal performance is achieved with stratification devices.

Common for the mentioned investigations is that the thermal performance can be improved by enhancing stratification in the heat storage tank. Only, the magnitudes of improvements vary. As it will be shown in the thesis, the thermal advantage of stratified heat storage tanks is, among others, strongly depending on the solar fraction of the system and the reference system used for the comparison.

3. Weather

3.1 Weather variations and the influence of weather variations

The weather is unique for different locations around the world. But, the weather also varies for specific locations. Both the ambient temperature and the solar radiation can vary much from one year to another and also the distribution of temperature and solar radiation varies during different years. With measured weather data from the Solar Radiation Measurement station placed on the top of building 119 at the Technical University of Denmark the weather variations in the period from 1990 to 2002 are studied. As a reference to the measured weather data, the Danish Design Reference Year, DRY data file is used (Skertveit et al. 1994). The file contains measured weather data at climate stations in Tåstrup and Værløse from the period 1975 to 1989, which is a time period just prior to the weather data period investigated. Usually the annual thermal performance of a solar heating system is estimated with DRY weather data and fixed consumption and consumption pattern. The consumption and the consumption pattern have a great influence of the thermal performance of solar heating systems, and so has the weather. In years with weather different from DRY weather data, measurements of the thermal performance of solar heating systems in practice will most likely be different from the estimated thermal performance with DRY weather data.

Figure 3.1 shows the measured yearly global and diffuse solar radiation on horizontal from the period 1990 – 2002 and DRY. It is clear, that there are large variations from one year to another.

In Figure 3.2, the monthly average global radiations from the period 1990 – 2002 and from DRY data file are shown. Also the measured monthly radiation variations are shown. It is clear, that the average global radiation from 1990 – 2002 is similar to the global radiation from DRY data file and that the largest radiation variations take place in the summer period April – September.

In Figure 3.3, the monthly average day temperatures from the period 1990 – 2002 and from DRY data file are shown. Also the measured monthly temperature variations are shown. It is clear, that the average day temperature from 1990 – 2002 is higher than in DRY data file, especially in the period January – April and in July and August. The temperature variations are in average ± 3 K, except in February where the temperature variations are larger and in April where they are smaller. In Denmark, February can be a gray and rainy month with rather high temperatures or a beautiful and cold winter month with snow. In April, the weather is mostly cloudy and rainy which prevents large temperature variations.

Solar irradiance data are usually measured on horizontal. The total irradiance on a tilted surface is then calculated from the horizontal irradiance by means of solar radiation processing models. Figure 3.4 show the relative yearly total solar radiation on a south facing 45°-tilted surface as a function of the relative yearly global radiation. The relative values are relative to the same values from DRY weather data. The dotted line indicates a linear relationship between the relative total global radiation and the relative total radiation on the 45°-tilted surface. Years situated above

the dotted line have more solar radiation during spring/fall than DRY weather data while years situated below the dotted line have less solar radiation during spring/fall than DRY weather data. The figure shows that there is no linear relationship.

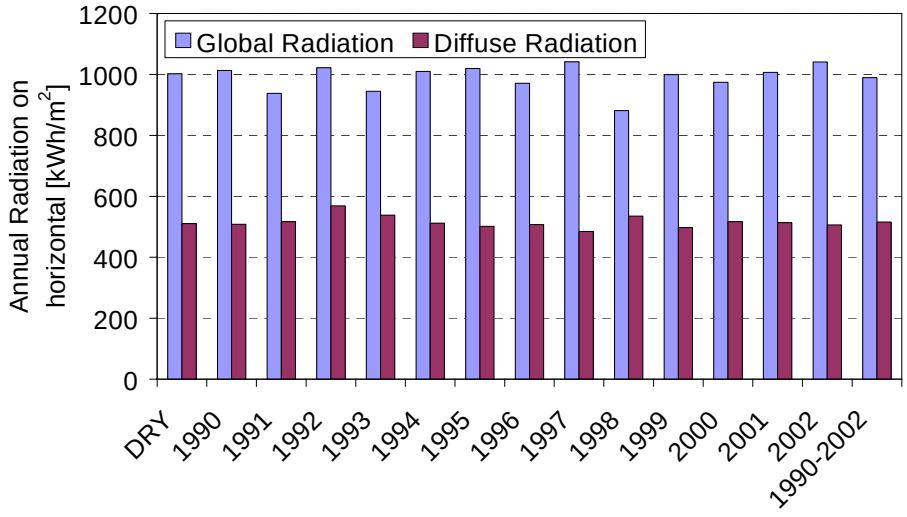

Figure 3.1 Global and diffuse solar radiation on horizontal.

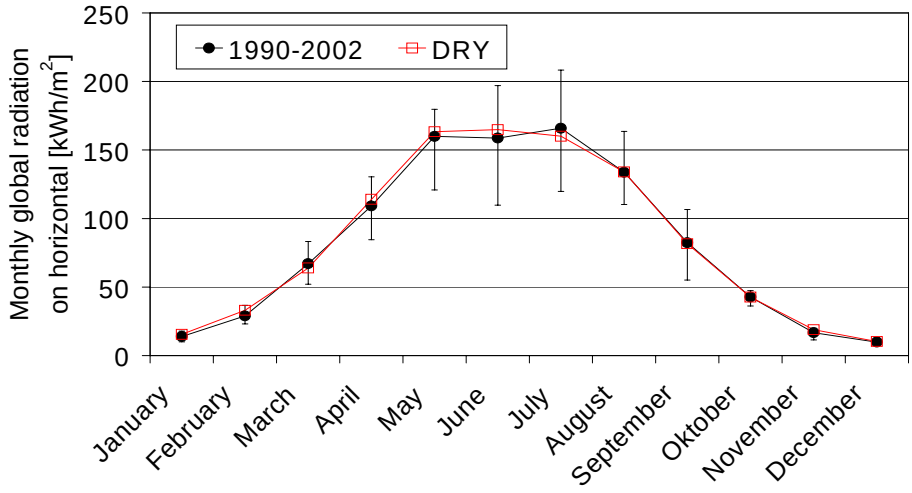

Figure 3.2 Monthly average global radiation and the deviation interval from the average global radiation from the period 1990 – 2002 and DRY weather data.

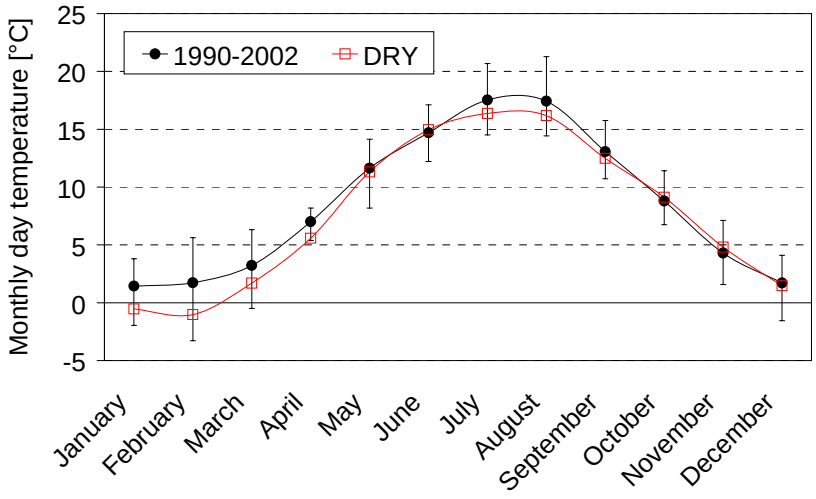

Figure 3.3 Monthly average day temperature and the deviation from the average day temperature from the period 1990 – 2002 and DRY weather data.

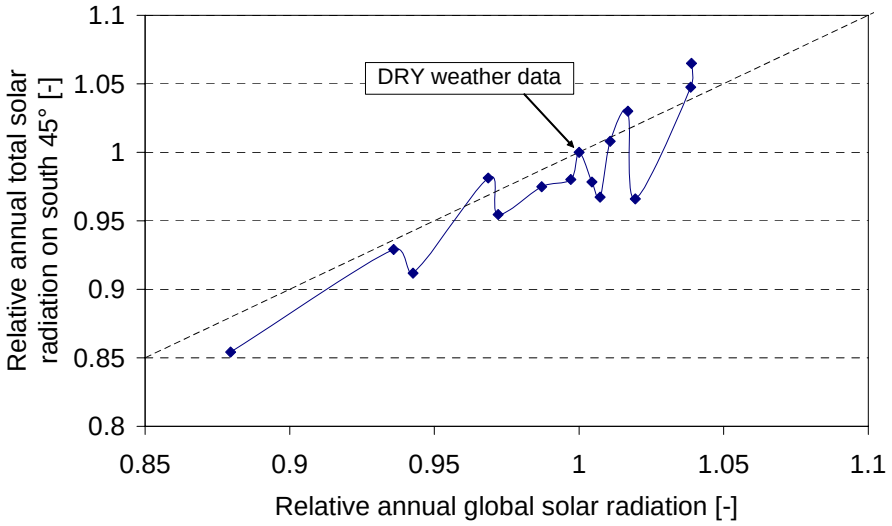

Figure 3.4 The relative annual total solar radiation on a south facing 45°-tilted surface as a function of the relative annual global radiation. The relative values are relative to the same values in DRY weather data file.

The investigations on the influence of weather variations on the thermal performance of solar heating systems are based on the measured weather data from 1990 – 2002 and DRY data file. Solar collectors as well as solar combi systems are included in the investigations.

The annual thermal performance of solar collectors and of solar combi systems increases for increasing annual solar radiation.

The relationship between the yearly thermal performance and the yearly solar radiation can for all types of solar collectors be fitted to a linear relationship, with a good approximation for the yearly radiation on the solar collectors and with a reasonable approximation for the yearly global radiation.

It is not possible to fit the relationship between the yearly thermal performance of solar combi systems and the yearly global solar radiation or the yearly solar radiation on the collector to a linear equation.

The annual utilization of the solar radiation for all types of solar collectors is increasing for increasing annual solar radiation on the collector.

The annual utilization of solar radiation for solar combi systems is not significantly influenced by the annual solar radiation on the collector, regardless of the collector efficiency, the heating demand and the size of the solar heating system. However, the annual utilization of solar radiation is higher and varies more for solar combi systems with high efficient solar collectors than for systems with low efficient solar collectors

Finally the investigations show that the investigated evacuated tubular solar collector utilizes less sunny years with large parts of diffuse radiation relatively better than the flat plate solar collectors.

Further details in Paper II.

3.2 Solar radiation processing models

Measured solar irradiance data are normally available as global irradiance, which is the solar irradiance on horizontal. Solar radiation processing models are used to calculate the solar radiation from horizontal to a certain collector tilt and orientation. The transformation of beam radiation incident on horizontal to a tilted surface can be done exactly whereas the transformation of diffuse radiation incident on horizontal to a tilted surface depends on the assumptions of the distribution of the diffuse radiation. Transient simulation programmes such as TrnSys offer the possibility of four different solar radiation processing models. The different models offered are the isotropic diffuse model (Liu and Jordan 1963) that assume that the diffuse radiation is uniformly distributed over the entire sky dome, the anisotropic diffuse model (Hay and Davis 1980) that divide the diffuse radiation into contribution from uniformly distributed radiation and circumsolar radiation from the area around the sun disc and two models (Reindl et al. 1990b) and (Perez et al. 1987, 1988) that apart from the isotropic and circumsolar contribution also uses horizon brightening.

A comparison between measured solar radiation on differently tilted and orientated surfaces and solar radiation calculated with the four different models show that the anisotropic models are best suited for predicting the solar radiation on tilted surfaces.

Also the influence on the energy from a solar collector calculated with the four different solar radiation processing models is investigated. The results show that the energy output from a collector using the isotropic model is lower than the energy output using the anisotropic models. However, the calculated energy output from the collector, regardless of the solar radiation model used lies within the accuracy of the calculation.

Further details in Paper III.

4. Detailed investigations

4.1 Theoretical investigations of solar combi system types

Two Danish solar combi systems (Figure 2.5) and the best solar combi system from the Task 26 investigations (right in Figure 2.7) are theoretically investigated. Different solar combi system designs have previously been investigated among others by (Dahm et al. 1998), (Drück and Hahne 1998), (Lorenz et al. 1998), (Lorenz et al. 2000), (Lorenz 2001). However not with strong emphasis on the advantage by using highly thermally stratified storage tanks as is the focus in this investigation.

Figure 4.1 shows schematic illustrations of the investigated solar combi system types. The investigation is based on three basically different system models, one model is based on a space heating storage with an external heat exchanger mounted in a side arm for domestic hot water preparation, one model is based on a domestic hot water tank with an internal heat exchanger spiral connected to the space heating system, and one model is based on a hot water tank in tank storage. The three system models are referred to as models 1, 2 and 3, respectively. Further, the models are improved by introducing stratifiers in the solar collector loop and in the space heating loop, and in both the solar collector loop and the space heating loop. The variations in each model are numbered successively (ref. Figure 4.1). The advantage of using stratifiers is that incoming water of any temperature is led into the tank in a level where the temperature of the incoming water matches the temperature of the water in the tank. In this way, thermal stratification in the tank is enhanced without destroying the already existing thermal stratification in the tank. The thermal stratification is assumed to be built up in a perfect way without any mixing by the inlet stratifier. In this way, the investigations show the maximum potential of ideally working inlet stratifiers.

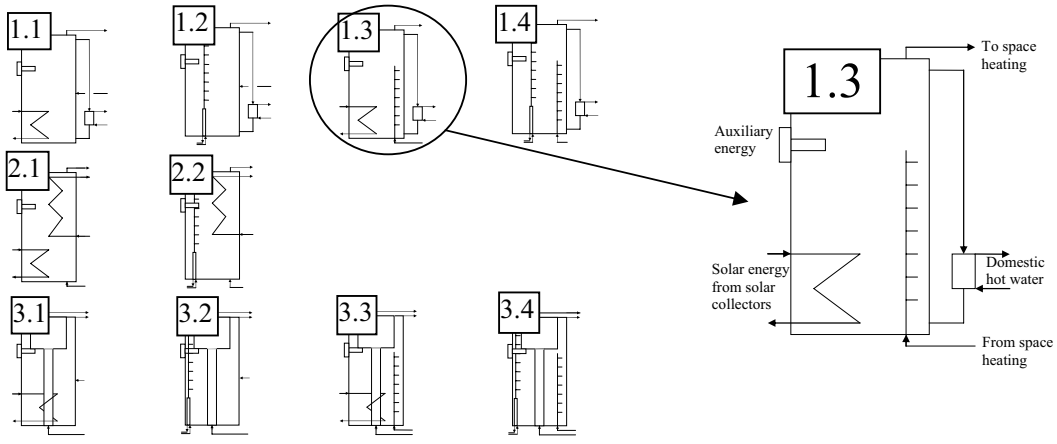

Figure 4.1 Schematics of the three system models: Model 1 (top), model 2 (middle) and model 3 (bottom), and the successively numbered variations of the system models.

The investigations are carried out for systems with 1000 litres storage tanks and 20 m^2 solar collectors. The reference conditions, degree of insulation, position of inlets and outlets etc. are the same for all the system types. The thermal performances of the systems are calculated for different domestic hot water consumptions and space heating demands. Also, it is investigated how the design of the space heating system and the control system in the solar collector loop influences the thermal performance of the solar combi systems. Finally, different sizes of solar combi systems are investigated. The systems have 500 litres, 1000 litres and 1500 litres storage tanks with solar collector areas from 5 m^2 to 60 m^2.

The calculations show that the thermal performance can be significantly improved by using inlet stratification pipes in both the solar collector loop and in the space heating loop instead of heat exchanger spirals in the solar collector loop and fixed inlets for the space heating loop.

Regardless of the solar combi system type and size, the thermal performance increases by 5 – 10% if stratifiers are used only in the solar collector loop and by 2 – 6% if stratifiers are used only in the space heating loop. The thermal performance increases by 7 – 14% if stratifiers are used both in the solar collector loop and in the space heating loop.

Figure 4.2 show examples of the annual net utilized solar energy and the performance ratio as a function of the annual space heating consumption for the system with 20 m^2 solar collectors and 1000 litres storage tank.

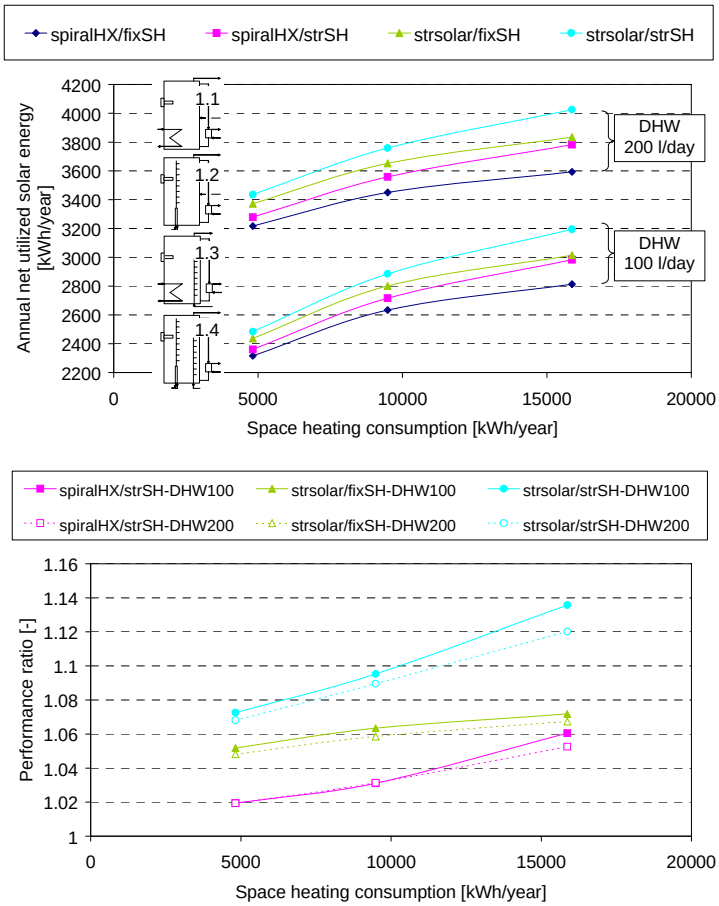

Figure 4.2 Top: The annual net utilized solar energy as a function of the space heating demand and the domestic hot water consumption for model 1 and the step by step improvement of the models. Bottom: The performance ratio relative to the thermal performance of the least advanced model, model 1.1.

Further, the calculations show that the thermal performance is strongly increased for increasing size of the space heating system and that the optimal settings of the control system in the solar collector loop is much more sensitive for systems with a heat exchanger spiral than with an inlet stratification pipe in the solar collector loop.

The best performing solar combi system is based on a tank in tank storage with stratifiers both in the solar collector loop and the space heating loop, system model 3.4.

The optimum design of solar combi systems is influenced by the heat demand and the heating system. This is especially the case if heat exchanger spirals and direct inlets are used, while the use of inlet stratifiers will decrease the influence to a minimum. In practice the knowledge of the heat demand and heating system is limited. Therefore the solar combi systems can not be designed individually for each house. Consequently there is an advantage in practice by using inlet stratifiers instead of heat exchanger spirals and direct inlets.

The potential of highly stratified hot water storage tanks with ideally working inlet stratifiers is shown in Figure 4.3 - Figure 4.5. The calculations are carried out with differently sized solar combi systems (system model 1) with a domestic hot water consumption of 100 l/day corresponding to 1700 kWh/year and a space heating consumption of 9500 kWh/year.

From Figure 4.3 it can be seen that the extra annual net utilized solar energy by using an inlet stratifier in the space heating loop increases with increasing system size. The figure also shows that there is an optimum ratio between the volume of the hot water storage tank and the solar collector loop of 50 l/m^2 collector area for systems with storage tanks of 500 litres and 1000 litres and 30 l/m^2 collector area for the system with 1500 litres storage tank.

Figure 4.4 and Figure 4.5 show that the performance ratio, that is the thermal advantage of inlet stratifiers, decreases with increasing system size and increasing solar fraction. The thermal advantage of inlet stratifiers depends strongly on the solar fraction, the system design, the heating system and the performance of the inlet stratifiers.

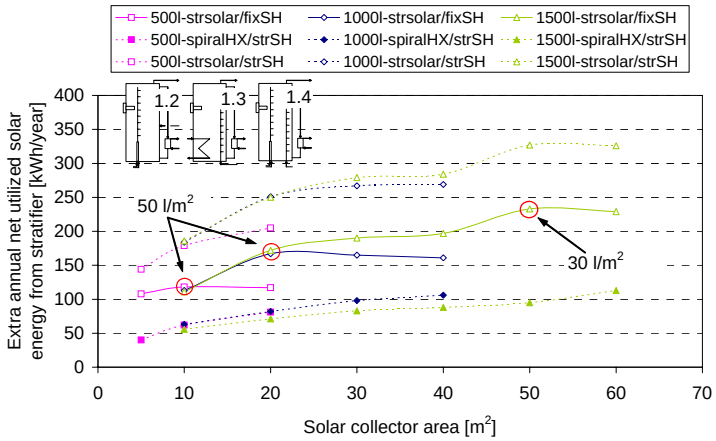

Figure 4.3 Extra annual net utilized solar energy as a function of the system size. The reference system is the similar system model 1.1.

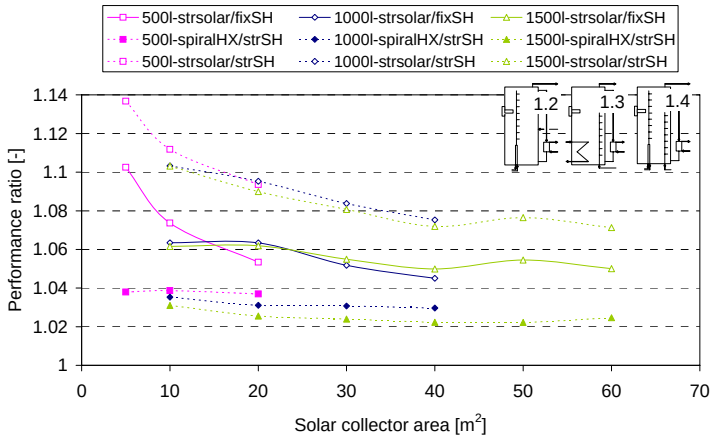

Figure 4.4 The performance ratio as a function of the system size. The reference system is the similar system model 1.1.

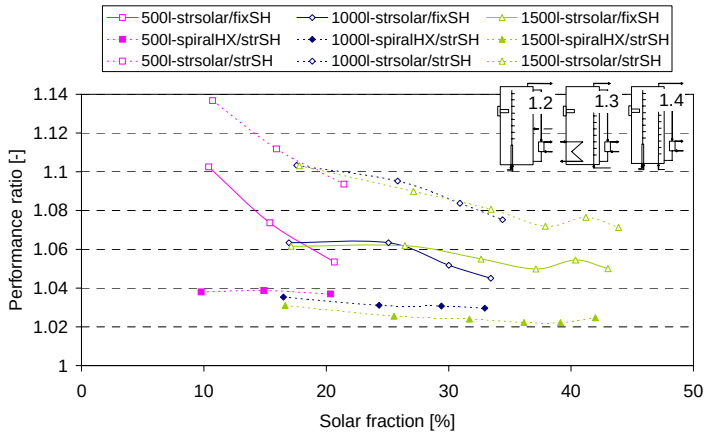

Figure 4.5 The performance ratio as a function of the solar fraction. The reference system is the similar system model 1.1.

Further details in Paper V.

4.2 Tank heat loss

Insufficient insulation and poor insulation work can reduce the thermal performance of solar heating systems significantly. Figure 4.6 show the calculated annual net utilized solar energy and the performance ratio of a solar domestic hot water system as a function of differently sized thermal bridges in the top of the hot water tank. The calculations are based on a marketed mantle tank with a volume of 0.189 m^3 and a marketed flat plate solar collector with an area of 2.19 m^2. The auxiliary volume is constantly heated to 50.5ºC.

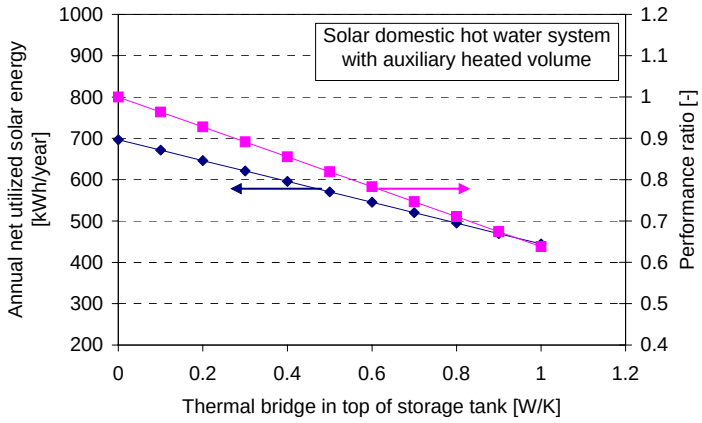

Figure 4.6 Annual net utilized solar energy and performance ratio as function of the thermal bridge in the top of the tank.

The calculations show that the yearly thermal performance of solar domestic hot water systems is strongly reduced if the hot water tank has a thermal bridge located at the top of the tank.

By means of parallel theoretical CFD calculations and experimental tests in a heat storage test facility the heat loss from a hot water tapping pipe connected to the top of a hot water tank is studied. The investigations show how the heat loss is due to heat loss to the surroundings through the boundaries and that heat is transferred to the pipe due to a natural convection flow in the pipe. The heat loss coefficient of a pipe connected to the top of a hot water tank is high, but can be reduced significantly by a heat trap.

Further details in Paper X.

4.3 Space heating systems

In practice, the size of a space heating system should match the insulation degree of a house in such a way that the water returning from the space heating loop is cooled sufficiently. This is crucial for instance for a condensing gas boiler where the efficiency of the boiler depends on the capability of condensing. The return temperature from a space heating loop that enters the storage tank of a solar combi system can significantly decrease the thermal performance of the system if the temperature is too high. Solar combi systems are mostly designed and installed without consideration of the size of the space heating system.

For a fixed space heating demand, three different space heating systems are investigated. Figure 4.7 shows the solar combi systems used for the calculations.

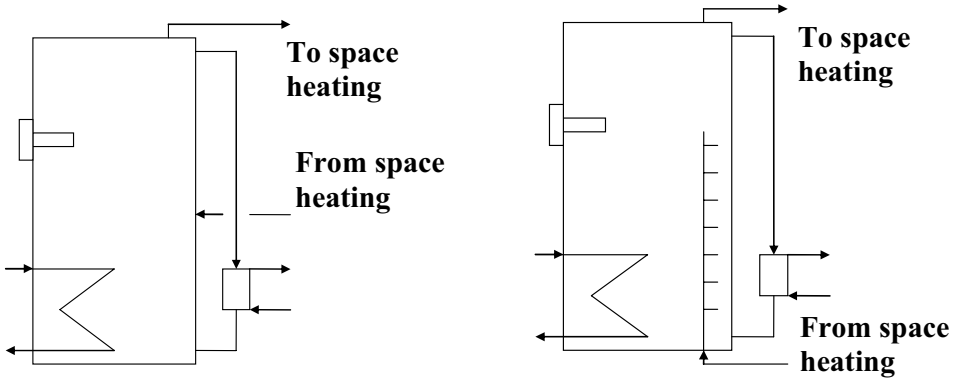

Figure 4.7 Solar combi systems used in the calculations.

The space heating load is 9500 kWh/year. The investigations are carried out for a small space heating system with high flow temperatures and return temperatures, a standard space heating system and a large space heating system with low flow temperatures and return temperatures. Figure 4.8 shows the flow and return temperatures used in the calculations.

Figure 4.9 and Figure 4.10 show the calculated yearly thermal performances and the performance ratios as functions of the relative return inlet height from the space heating loop. The reference system is the system with the standard space heating system with optimal inlet height from the space heating loop. The benefit of a stratifier in the space heating loop is also shown. The return water from the space heating loop enters the stratifier at the bottom of the tank and the inlet from the stratifier to the tank varies with the temperature conditions. To highlight the benefit of a stratifier in the space heating loop, the performance with a stratifier is marked at the optimal relative inlet height with a fixed inlet from the space heating loop.

It can be seen that the thermal performances are highest for large space heating systems and lowest for small space heating systems. Also, it can be seen that the advantage of a stratifier in the space heating loop is largest for small space heating systems. This is because the return inlet temperature from the space heating system is highest and hence, varies the most. For large, standard and small space heating systems, the thermal performance increases by 2%, 3% and 5%, respectively if a stratifier is used in the space heating loop instead of a fixed return inlet.

It is clearly an advantage to use a stratifier instead of a fixed return inlet position from the space heating loop, especially because the size of the space heating system is usually not known in advance when the storage tanks are designed. Therefore the optimum fixed position of the return inlet from the space heating loop, which depends on the size of the space heating system, is not known.

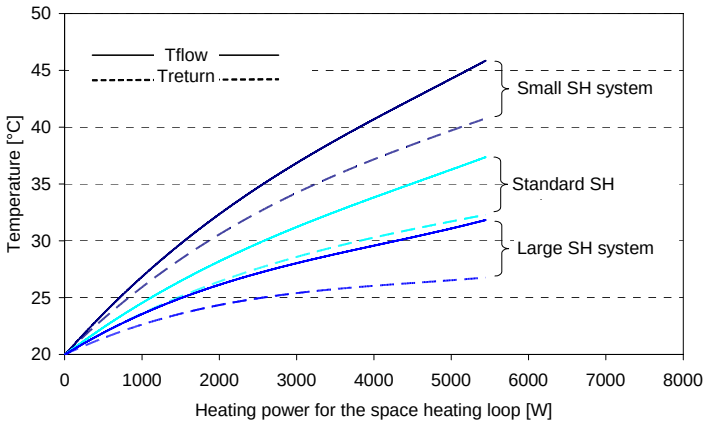

Figure 4.8 The flow and return temperatures for the space heating systems as a function of the heating power demand.

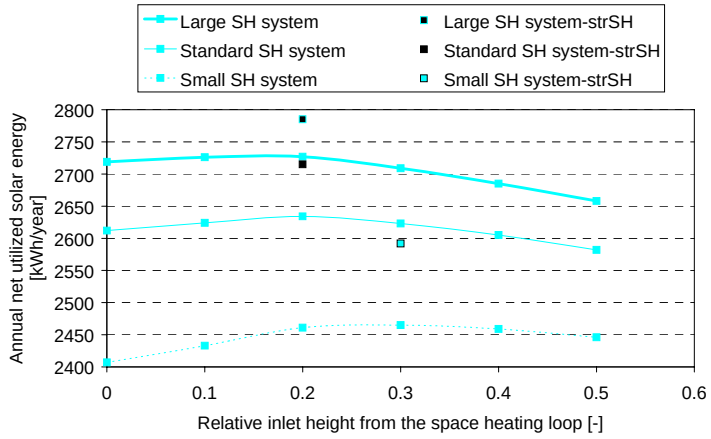

Figure 4.9 The annual net utilized energy as a function of the relative inlet height from the space heating loop. The abbreviations SH and strSH in the legend represent space heating and stratifier in the space heating loop, respectively.

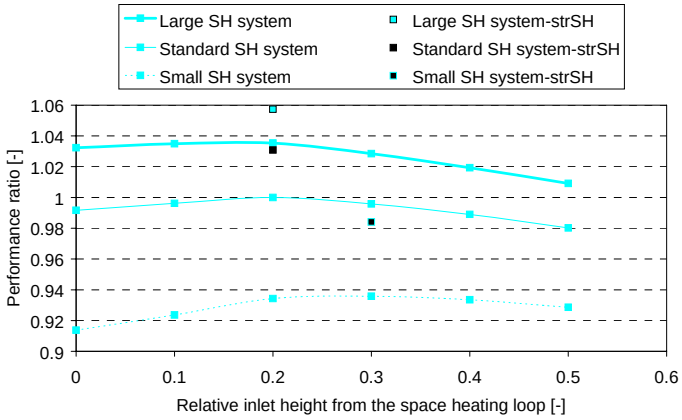

Figure 4.10 The performance ratio as a function of the relative inlet height from the space heating loop. The performance ratio is relative to the performance of the standard space heating system with optimal position of the inlet from the space heating loop.

Further details in Paper V.

4.4 Draw off from different levels

The temperature level in the top of a hot water tank can be much higher than the required hot water temperature. In order to reduce the temperature of the water going to the consumer to the required hot water temperature, cold water is mixed with the hot water from the tank. In this way a smaller volume of water is taken from the storage tank than would be the case if the water taken from the tank could be sent directly to the consumer. For the same reason, a smaller volume of cold water is lead into the bottom of the tank. The cooling of the lower part of the tank is crucial for creating the best operation conditions for the solar collector. An alternative operation strategy is to draw domestic hot water from a lower level in the tank and thereby a lower temperature level. In this way a larger volume of sufficiently hot water is taken from the tank and larger amounts of cold water are lead into the bottom of the tank, cooling the lower part of the tank.

Experimental and theoretical investigations have been carried out with this operation strategy. Two solar domestic hot water systems are experimentally investigated and one solar combi system is theoretically investigated. The investigations showed that it is possible to increase the thermal performance of both solar domestic hot water systems and solar combi systems by using two draw-off levels from the solar tanks instead of one draw-off level at a fixed position. One of the draw-offs was in all cases placed at the top of the tank.

The best position of the second draw-off level is for all the investigated systems in the middle or just above the middle of the tank. For the investigated solar domestic hot water system the extra thermal performance of using a second draw-off level from the hot water tank is strongly influenced by the difference between the set point temperature of the auxiliary energy supply system and the required draw-off temperature. For increasing temperature difference the thermal advantage of the second draw-off level increases. For realistic draw off hot water temperatures of 40°C

and 45°C and an auxiliary volume temperature of 50.5°C the increase of the thermal performance by the second draw-off level is about 6%.

Figure 4.11 shows a schematical illustration of the investigated solar combi system.

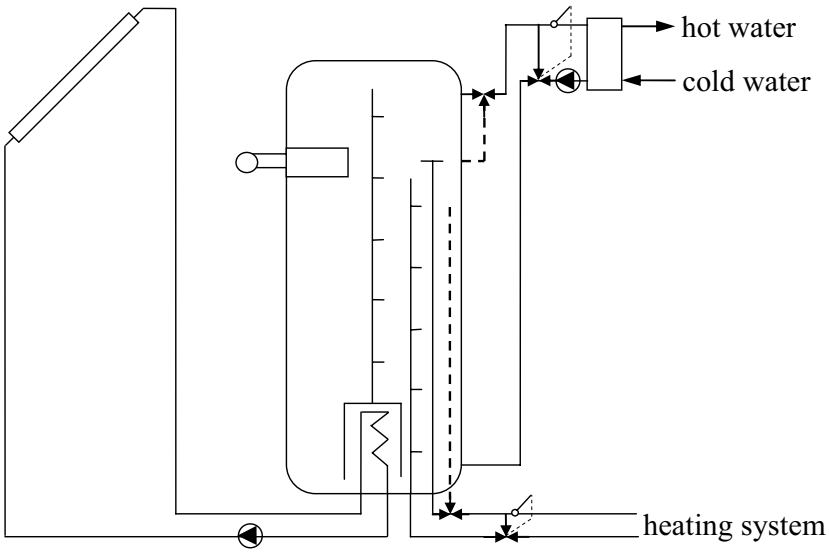

Figure 4.11 Schematical illustration of the investigated solar combi system.

For the investigated solar combi system the extra thermal performance by using one extra draw-off level, either for the domestic hot water heat exchanger or for the heating system, is about 3%, while an improvement of about 5% is possible by using a second draw-off level both for the domestic hot water heat exchanger and for the heating system.

Further details in Paper IV.

4.5 Stratifiers

A well stratified storage tank improves the thermal performance of a solar heating system significantly. The benefit of stratified storage tanks for all solar heating systems has been studied intensively by numerous scientists, see e.g. (Lavan and Thompson 1977), (van Koppen et al. 1979), (Sharp and Loehrke 1979), (Furbo 1984), (Furbo and Mikkelsen 1987), (Furbo and Berg 1990), (Carlsson 1993), (Furbo 1995), (Jordan et al. 1999), (Andersen and Furbo 1999), (Jordan 2001), (Knudsen 2002), (Shah and Furbo 2003), (Furbo 2004), (Knudsen and Furbo 2004), (Furbo et al. 2004), (Furbo and Knudsen 2004), (Jordan and Furbo 2004). The question is how best to build up and maintain thermal stratification during all operation conditions in a simple and cost efficient way. This topic has also been studied intensively, see e.g. (Loehrke et al. 1979), (Gari and Loehrke 1982), (Abu-Hamdan et al. 1992), (Davidson et al. 1992), (Davidson and Adams 1994), (Davidson et al. 1994), (Essert 1995), (Krause and Kühl 2001), (Shah 2002), (Jordan and Vajen 2002). One way of enhancing thermal stratification is by using mantle tanks. Due to limitations in the heat transfer area between the mantle and the tank, mantle tanks are only suitable for tank volumes up to about 1 m^3. Thermal stratification is also enhanced in tanks with several inlet possibilities with valves that open and close depending on the temperature level of the solar heated water and the temperature in the storage tank. Such systems require

advanced control systems. Finally, stratification inlet pipes are used to build up thermal stratification in storage tanks.

Experimental and theoretical investigations are carried out with marketed inlet stratification pipes but also new types are investigated.

In Figure 4.12 the investigated inlet stratification pipes are shown. In the left side of the figure, a rigid inlet stratification pipe with circular openings is depicted. The device is made of 2 mm thick synthetic material resistant to temperature and deformation and is built up by a variable number of "hats" connected by 3 thread rods forming an inner flow channel of 24 mm with an outer diameter of 100 mm. Free convection induced fluid flow can leave the stratification pipe through all circular openings which have a height of 18 mm. The device is patented and marketed by the German company Sailer GmbH & Co KG and was tested at ITW, Stuttgart University. In the middle of the figure, a two layer fabric inlet stratification pipe is shown. The investigated samples consist of pipes with an inner/outer diameter of 40 mm/70 mm and 25 mm/45mm. The pipes are closed at the top. The fabric pipe is invented during the Ph.D. project period and patented. In the right side of the figure, a rigid inlet stratification pipe with lockable openings acting as "non-return" valves is shown. The pipe is made of polypropylene (PP) with an outer diameter of 60 mm and a thickness of 3 mm (Krause 2001) and (Shah 2002). The distance between the centres of each opening is about 292 mm. The pipe is patented and marketed by the German company Solvis GmbH & Co KG.

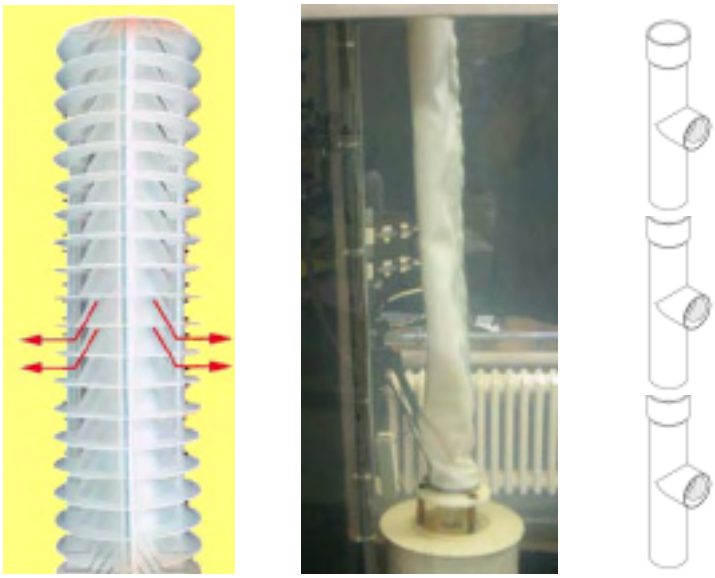

Figure 4.12 Investigated inlet stratification pipes. Left: Rigid stratifier with circular openings. Middle: Fabric stratifier with two fabric layers. Right: Rigid stratifier with lockable openings acting as "non-return" valves.

The experimental investigations are carried out in laboratory tanks with forced volume flow rates in the range 2 l/min – 10 l/min both as heating tests and cooling tests: heating tests to simulate the thermal behavior of the stratifiers used for solar heat transfer to the tank and cooling tests to simulate the thermal behaviour of the stratifiers used for returning water from the space heating loop. The thermal behaviour is also investigated with natural convection flow.

Further, PIV measurements are carried out and compared to CFD calculations.

Figure 4.13 shows an example of PIV measurements with the rigid Solvis stratifier with openings without (left) and with (right) the “non-return” valves mounted in the openings during a heating test with identical operation conditions. The inlet temperature is relatively high compared to the tank temperatures. From the figure it can be seen that with the stratifier with “non-return” valves the lowest opening is closed preventing water from flowing into the stratifier while the water flows into the lowest opening of the stratifier without the “non-return” valves. The cold water entering the pipe mixes with the hot water in the pipe. Hence, the stratifier without “non-return” valves acts more like a mixing device than a stratification device.

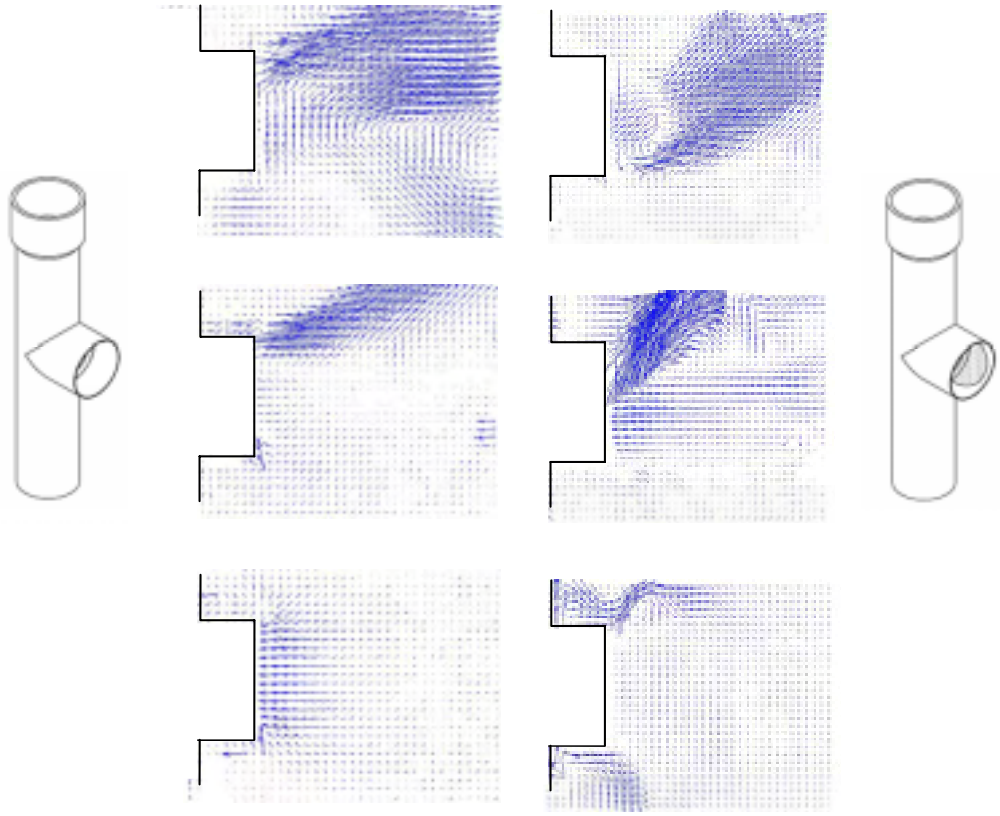

Figure 4.13 Measured velocity vectors for the stratifier without “non-return valves” (left) and with “non-return valves” (right).

Whether water tries to flow into a stratification device or not is depending on the difference between the pressure in the stratification device and the pressure surrounding the stratification device in the same level. The pressure is described by the static pressure which is a function of the height and the temperature of the water placed above the level in question and the dynamic pressure which is a function of the velocity. The “non-return” valves prevent the inflow in spite of the pressure difference. If nothing physically prevents an inflow, the pressure difference, in the heating case, will create an inflow of colder water into the hot stratifier resulting in a temperature decrease for the water flowing upwards inside the pipe. This unwanted inflow can be registered by a fluctuating temperature inside the stratifier.

The fabric stratifier has a dynamic behaviour. The fabric stratifier eliminates the pressure difference by reducing the cross sectional area whereby the velocity and the dynamic pressure inside the pipe are increased until the pressure difference is eliminated. Therefore cold water will not enter into the fabric stratifier. The investigations revealed that thermal stratification can be build up in a nearly perfect way with a well performing stratifier.

The advantages of the fabric stratification pipe are:

- Water is not restricted to leave through fixed holes but can leave the pipe in all levels
- The diameter of the pipe can easily be adjusted to all volume flow rates
- It is cheap to produce

The disadvantage of the fabric stratification pipe is that the long time durability has not yet been investigated. In order to make the fabric stratifier an attractive alternative to other stratifiers on the market, the long time durability must be demonstrated. Therefore long time durability tests will be performed at the Technical University of Denmark in 2007.

Further details in Paper VI, Paper VII, Paper VIII and Paper IX.

5. Summary and outlook

Different separate investigations have contributed to the understanding of how solar combi systems work and which parameters have influences on the thermal performance and the magnitude of the influence.

It is my hope that research and development within the field of solar combi systems in the future will make use of the findings in the thesis. Especially the fabric stratifier appears very promising. Before the fabric stratifier can be directly applicable as a commercial product, the long term durability must be established. Also the possible applications of the fabric stratifier should be established. The design of the stratifier should be optimized for all types of applications and the performance and benefits of the stratifier should be demonstrated in laboratory as well as in practice.

Further the investigations have shown that there is a need for research on:

- Space heating demand in practice, especially in the summer period.
- How do space heating systems work in practice
- How is the space heating demand influenced by the space heating system
- Development of low temperature space heating systems suitable for solar heating systems
- Optimum design of tank-in-tank heat storage
- Is it better to use an auxiliary energy supply system which is build into the heat storage tank than a separate auxiliary energy supply system unit
- How will the warmer climate affect the yearly energy demand, the thermal performance of solar combi systems and the interplay between the energy demand and solar combi systems
- How high solar fractions can be achieved in new low energy houses build according to the building codes when solar combi systems with high efficient evacuated tubular solar collectors are used.
- What are the real energy savings by using solar heating systems

Solar energy and other renewable energy technologies must form the energy supply system in the future. Therefore it is most important that promising renewable energy technologies such as systems for one family houses with seasonal storage based on e.g. phase change materials or off-shore wave energy systems are developed from theoretical possible technologies into final products that can be installed and used as intended. Most important is the task to find good ways to store solar energy from the summer season to the winter season in so called seasonal heat storages. Eventually, seasonal heat storages can be heated once or twice during the heating season by means of excess energy from e.g. wind and wave energy production. In this way seasonal heat storages can be much smaller and consequently cheaper.

The interplay between solar heating systems and wind and wave energy will require development of advanced control systems based on weather forecasts.

References

Abu-Hamdan, M.G., Zurigat, Y.H., Ghajar, A.J., 1992. An Experimental Study of a Stratified Thermal Storage under Variable Inlet Temperature of different Designs. International Journal of Heat and Mass Transfer, Vol. 35, No. 8, pp. 1927-1934.

Andersen, N.B., 1988. "Solvarmeanlæg til rumopvarmning og varmt brugsvand, demonstrationsanlægget i Ejby," Report no. 189, Thermal Insulation Laboratory, Technical University of Denmark.

Andersen, E., Furbo, S., 1999. Thermal destratification in small standard solar tanks due to mixing during tapping. In: Proceedings of ISES Solar World Congress, Jerusalem, Israel, Vol III, pp. 111-119.

Cabeza, L.F., 2005. Legionella in combisystem tanks. A Report of IEA SHC – Task 32.

Carlsson, P.F., 1993. Heat storage for large low flow solar heating systems. In: Proceedings of ISES Solar World Congress, Budapest, Hungary.

Dahm, J., Bales, C., Lorenz, K., Dalenbäck, J.-O., 1998. Evaluation of Storage Configurations with Internal Heat Exchangers, Solar Energy, Vol. 62, No. 6, pp. 407-417.

Dantec Dynamics A/S, www.dantecdynamics.com

Davidson, J.H., Carlson, W.T., Duff, W.S., 1992. Impact of Component selection and operation on thermal rating of drain-back solar water heaters. Journal of Fluids Engineering, Vol. 116, pp. 130-136.

Davidson, J.H., Adams, D.A., 1994. Fabric Stratification Manifolds for Solar Water Heating. Journal of Solar Energy Engineering, Vol. 130, pp. 130-136.

Davidson, J.H., Adams, D.A., Miller, J.A., 1994. A Coefficient to Characterize Mixing in Solar Water Storage Tanks. Journal of Solar Energy Engineering, Vol. 116, pp. 94-99.

Drück H., Hahne, E., 1998. Test and comparison of Hot Water Stores for Solar Combisysteme. In: Proceedings of EuroSun 1998 Congress, Goetzberger A. (Eds.), Vol. 2, III.3.3, Portoroz, Slovenia.

Ellehauge, K., 1993, "Målinger på solvarmeanlæg til kombineret brugsvands- og rumopvarmning – 5 markedsførte solvarmeanlæg installeret hos anlægsejerne," Report no. 255, Thermal Insulation Laboratory, Technical University of Denmark.

Ellehauge, K., et al., 2000, "Erfaringer fra målinger på kombinerede solvarme- og biobrændselsanlæg," Technological Institute, Denmark.

Ellehauge, K., Shah, L.J., 2000. Solar combisystems in Denmark – the most common system design. In: Proceedings of EuroSun 2000 Congress, Copenhagen, Denmark.

Essert, H., 1995. Aufbau und Inbetriebnahme eines Speicherversuchsstandes. Diploma Thesis, Graz University, Austria.

Fluent 6.1 User's Guide, 2003. Fluent Inc. Centerra Resource Park 10 Cavendish Court Lebanon, NH 03766.

Furbo, S., 1984. Varmelagring til solvarmeanlæg. Ph.D. Thesis, report no. 162, Thermal Insulation Laboratory, Technical University of Denmark.

Furbo, S., Mikkelsen, S. E., 1987. Is low flow operation an advantage for solar heating systems? In: Bloss, W.H., Pfistere, F. (Eds.), Advances in Solar Energy Technology, Vol. 1., Pergamon Press, Oxford, pp. 962-966.

Furbo, S., Berg, P., 1990. Calculation of the thermal performance of small hot water solar heating systems using low flow operation. In: North Sun'90 Proceedings, Reading, England.

Furbo, S., 1995. Loeflow/Highflow test. Chapter 8 in "Advanced Solar Domestic Hot Water Systems". Final Report of the Task 14 Advanced Solar DHW Working Group. W.S. Duff (ed.), Colorado State University.

Furbo, S., 2004. Low flow Solar Heating Systems. Department of Civil Engineering, Technical University of Denmark, note U-067.

Furbo, S., Knudsen, S., 2004. Low flow SDHW systems based on mantle tanks – recent findings. In: EuroSun 2004 Proceedings, Freiburg, Germany, Vol. 1, pp. 272-281.

Furbo, S., Vejen, N.K., Shah, L.J., 2005. Thermal performance of a large low flow solar heating system with a highly thermally stratified tank. Journal of Solar Energy Engineering, 127 (1), pp. 15-20.

Furbo, S., et al., 2006. Nordic Energy Research Cooperation on Solar Combisystems. In: Proceedings of EuroSun 2006 Congress, Glasgow, Scotland.

Gari, H.N., Loehrke, R.I., 1982. A controlled buoyant jet for enhancing stratification in a liquid storage tank. Journal of Fluids Engineering, Vol. 104, pp. 475-481.

Hadorn, J-C., et al., 2005. Thermal energy storage for solar and low energy buildings, State of the art by IEA Solar Heating and Cooling Task 32. Typeset by Servei de Publicacions (UdL). ISBN 84-8409-877-X.

Jordan, U., Vajen, K., Knopf, B., Spieler, A., Hilmer, F., 1999. Modelling of a thermosyphonally driven discharge unit of a storage tank. In: Proceedings of ISES Solar World Congress, Jerusalem, Israel, pp. 197-202. ISBN 0-080-438954.

Jordan, U., 2001. Untersuchungen eines Solarspeichers zur kombinierten Trinkwassererwärmung und Heizungsunterstützung. Dissertation, Universität Marburg.

Jordan, U., Vajen, K., 2002. Einfluss verschiedener Beladeeinrichtungen auf den Solarertrag eines typischen Kombisysteme. In: Proceedings of 12. Symposium Thermische Solarenergie, Kloster Banz, Bad Staffelstein.

Jordan, U., Furbo, S., 2003. Investigations of the flow into a storage tank by means of advanced experimental and numerical methods. In: Proceedings of ISES Solar World Congress, Göteborg, Sweden.

Jordan, U., Furbo, S., 2004. Impact of inlet devices on the thermal stratification of a storage tank. In: EuroSun 2004 Proceedings, Freiburg, Germany.

Klein, S.A., et al., 1996. TrnSys 14.1, User Manual, University of Wisconsin Solar Energy Laboratory.

Knudsen, S., 2002. Consumers' influence on the thermal performance of small SDHW systems – theoretical investigations. Solar Energy Vol. 73, No. 1, pp. 33-42.

Knudsen, S., Furbo, S., 2004. Thermal stratification in vertical mantle heat exchangers with application to solar domestic hot water systems. Applied Energy, Vol 78/3, pp. 257-272.

Krause, T., Kühl, L., 2001. Solares Heizen: Konzepte, Auslegung und Praxiserfahrungen. TU Braunschweig, Institut für Gebäude und Solartechnik.

Lavan, Z., Thompson, J., 1977. Experimental study of thermally stratified hot water storage tanks. Solar Energy 19, pp. 519-524.

Letz, T., 2002. Validation and background information on the FSC procedure. A Report of IEA SHC – Task 26.

Loehrke, R.I., Holtzer, J.C., Gari, H.N., Sharp, M.K., 1979. Stratification Enhancement in Liquid Thermal Storage Tanks. Journal of Energy, Vol. 3, No. 3, pp. 129-130.

Lorenz, K., Bales, C., Persson, T., Tepr, R., 1998. Variation of System Performance with Design and Climate for Combisystems in Sweden. In: Proceedings of EuroSun 1998 Congress, Portoroz, Slovenia.

Lorenz, K., Bales, C., Persson, T., 2000. Evaluation of Solar Thermal Combisystems for the Swedish Climate. In: CD-Rom of the EuroSun 2000 Congress, Copenhagen, Denmark.

Lorenz, K., 2001. Kombisolvärmesystem – Utvärdering av möjliga systemförbättringar. Ph.D Thesis, Institutionen för Installationsteknik, Chalmers Tekniska Högskola, Göteborg.

Mikkelsen, S. E., and Jørgensen, L. S., 1981, "Solvarmeanlæg til rumopvarmning, en udredning baseret på 2 års målinger på anlæg i Greve og Gentofte," Report no. 112, Thermal Insulation Laboratory, Technical University of Denmark.

Pauschinger, T., Drück, H., Hahne, E., 1998. Comparison test of solar heating systems for domestic hot water preparation and space heating, Proceedings of Second International ISES Solar Congress.

Raffel, M. Willert, C., Kompenhans, J., 1989. Particle Image Velocimetry. A Practical Guide. Springer Berlin. ISBN 3-504-63683-8.

Risønyt, 2006. Risønyt december 2006 Nº2. Forskningscenter Risø, Frederiksborgvej 399, Postbox 49, 4000 Roskilde, Denmark.

Shah, L.J., 2001. Undersøgelse af et solvarmeanlæg til kombineret rum- og brugsvandsopvarmning. Technical University of Denmark. BYG.DTU SR-01-19.

Shah, L.J., 2002. Stratifikationsindløbsrør. Report SR-02-23. Technical University of Denmark. ISSN 1393-402x.

Shah, L., Furbo, S., 2003. Entrance effets in solar storage tanks. Journal of Solar Energy 75, pp. 337-348.

Sharp, M.K., Loehrke, R.I., 1979. Stratified Thermal Storage in Residential Solar Energy Applications. Journal of Energy 3, pp. 106-113.

SHC, 2006. The time for solar is now. SHC Solar Heating & Cooling Programme, International Energy Agency.

Solvis GmbH & Co KG, www.solvis.de

Streicher W., 1998. Simple estimation of the solar fraction of combisystems and centralized big solar plants, Proceedings of Second International ISES Solar Congress.

Streicher W., 2004. Elements and Examples of “Dream Systems” of Solar Combisystems. A Report of IEA SHC – Task 26.

Streicher W., Heimrath R., 2004. Analysis of System Reports of Task 26 for Sensitivity of Parameters, Technical Report for Subtask C, IEA SHC-Task 26.

Suter, J-M., 2000, “Solar Combisystems – Overview 2000,” IEA SHC – Task 26.

van Koppen, C.W.J., Thomas, J.P.X., Veltkamp, W.B., 1979. The actual Benefits of Thermally Stratified Storage in Small and Medium Size Solar Systems. In: Proceedings of ISES Solar World Congress, Atlanta, USA, pp. 579-580.

Weiss, W., et al., 2003. Solar Heating Systems for Houses, a Design Handbook for Solar Combisystems. Published by James & James Ltd, UK. ISBN 1 902916 46 8.

PART II

PAPERS

Paper I

Thermal Performance of Danish Solar Combi Systems in Practice and in Theory

Journal of Solar Energy Engineering, Vol. 126, pp. 744 – 749, May 2004

Thermal performance of Danish solar combi systems in practice and in theory

Elsa Andersen, Louise Jivan Shah and Simon Furbo

Department of Civil Engineering Technical University of Denmark

DK-2800 Kgs. Lyngby, Denmark, e-mail: ean@byg.dtu.dk

Journal of Solar Energy Engineering, Vol. 126, pp. 744 – 749, May 2004

Abstract

An overview of measured thermal performances of Danish solar combi systems in practice is given. The thermal performance varies greatly from system to system. Measured and calculated thermal performances of different solar combi systems are compared and the main reasons for the different thermal performances are given. Further, a parametric study on two solar combi system types is performed.

Based on the investigation it can be concluded that the thermal performance first of all is influenced by the space heating consumption during the summer period and that the systems in practice perform as theoretically expected.

1 Introduction

A solar combi system is a system where the solar energy gained in the solar collectors is used both for domestic hot water (DHW) supply and for space heating (SH). Such systems can be designed and operated in different ways. Most of the solar combi systems that are installed in Denmark correspond to the system illustrated in Figure 1. In this system the control system operates the three-way valve in the solar collector loop so solar heat is supplied either to the hot water tank or to the heat exchanger between the collector loop and the space heating loop. [1].

How solar combi systems should be designed and operated best has not been very well elucidated. Consequently many different system designs are installed in practice.

The thermal performance and the solar fraction of solar combi systems can be defined in different ways. Here the following definitions of the net utilized solar energy and the solar fraction are used:

$$Q_{NET} = Q_{DHW} + Q_{SH} - Q_{AUX} \quad (1)$$

$$SF = Q_{NET} / (Q_{DHW} + Q_{SH}) \cdot 100\% \quad (2)$$

To facilitate a comparison of the thermal performance of different solar combi systems, the effect of both the total energy consumption and the solar collector area must be eliminated. This is done here by presenting the net utilized solar energy per solar collector area as a function of the solar fraction.

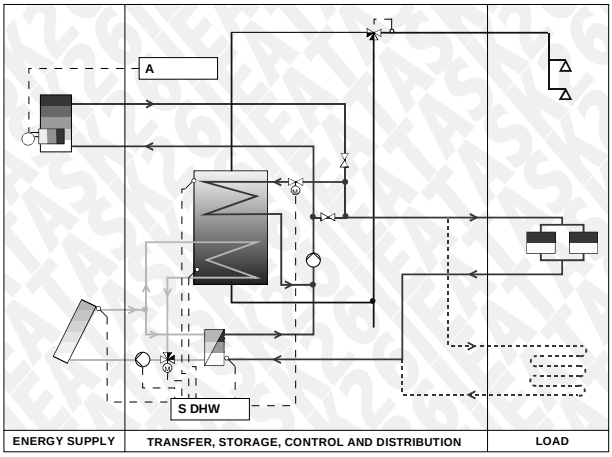

Figure 1: Typical Danish solar combi system. [7].

2 Measurements in practice

In the 1950s the first solar houses with heat supplied from solar combi systems designed to cover the space heating load totally or partly were built in the United States of America, [2-5]. The solar combi systems differed in the way they were designed to collect and store the solar energy where both air and water was used as solar collector fluid while the heat storage could be rock bed storage, water storage, heat of fusion storage or soil storage. The solar combi systems were designed for high solar fractions and the cost/performance ratio of the systems was considered less. Much later, in 1975 the first solar house called the Zero Energy House was built in Denmark at the Technical University of Denmark [6]. This house was based on a solar combi system with water as the solar collector fluid and a water heat storage.

With regard to the cost/performance ratio new Danish solar combi systems for one family houses are, compared to the systems of the 1950s and 1970s, relatively small with typical solar fractions less than 30%. The systems are today based on collectors with glycol/water mixtures as solar collector fluid and with water heat storages.

The thermal performance of a number of Danish solar combi systems has been measured in practice [8-10,18]. The systems are build and installed in the period from 1978 until 1997. The important energy amounts for each solar combi system are measured so that it is possible to determine the annual net utilized solar energy according to Eq. (1). In Table 1 data of the systems are listed along with the most important measured energy amounts and in Figure 2 the measured yearly thermal performance as a function of the yearly solar fraction of the systems are shown.

Table 1: Data of the systems in practice.

Collector area [m^2]	System type	Annual domestic hot water demand [MJ]	Annual space heating demand [MJ]	Space heating during summer [MJ]	Annual net utilized solar energy [MJ/m^2]	Solar fraction [%]
50 (year 1)	Preheating tanks of 5450 l and 130 l and auxiliary heated domestic hot water tank of 80 l [18]	8460	59850	6000	300	22
50 (year 2)		10900	58020	6610	390	28
28 (year 1)	Preheating tanks of 2000 l and 200 l and auxiliary heated domestic hot water tank of 200 l [18]	10050	67940	2910	350	13
28 (year 2)		10860	56610	1500	350	15
17.3	Drain back system with 735 l tank in tank. Upper part is auxiliary heated. Solar energy can additionally be utilized for space heating through a separate "solar radiator" independent of the space heating return temperature [8]	5440	32490	3410	550	25
10	250 l tank with a heat exchanger between the solar collector loop and the space heating loop. In summer the upper 80 l of the tank is auxiliary heated. In winter it is a preheating tank. The system corresponds to the system illustrated in Figure 1 [10]	10730	54400	5290	1040	16
8.8	300 l tank with a heat exchanger between the solar collector loop and the space heating loop. The upper 80 l of the tank is auxiliary heated. The system corresponds to the system illustrated in Figure 1 [10]	7520	48200	9760	1300	21
5.8	275 l tank with a heat exchanger between the solar collector loop and the space heating loop. The upper 90 l of the tank is auxiliary heated. The system corresponds to the system illustrated in Figure 1 [10]	5940	14110 [1)]	4540	680	20
10	265 l tank. Solar energy is only utilized for space heating (floor heating) during summer when the auxiliary energy system is turned off. The upper 74 l of the tank is auxiliary heated [10]	8780	27540	1190	400	11
12	750 l tank in tank + 1000 l tank in connection with a bio mass burner. The solar collectors are not in operation during winter [9]	12110	72830	1840	130	2
12.6	500 l preheating tank with a built in drain back tank + 160 l domestic hot water tank. The auxiliary energy is based on a bio mass burner [9]	13440	106650	9930	1050	11

[1)] The energy for space heating delivered from a wood burning stove is not included in the measurement.

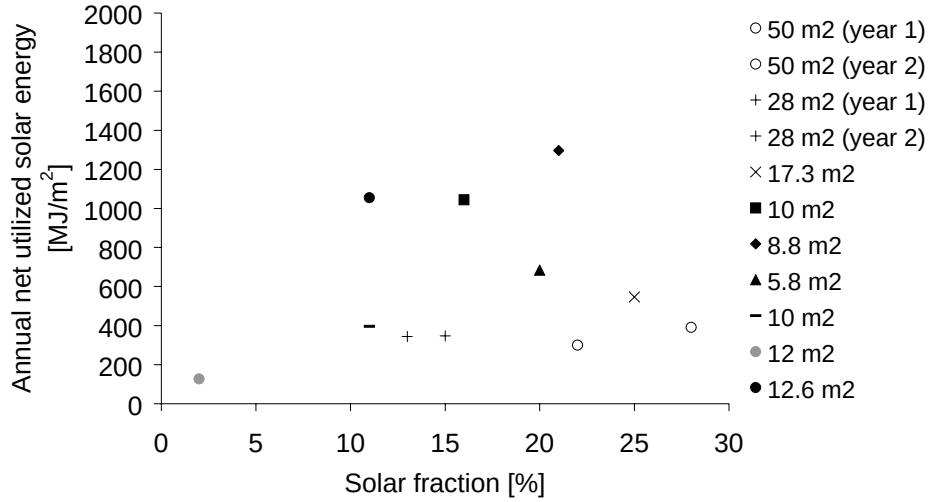

Figure 2: Measured thermal performance of the solar combi systems.

The annual net utilized solar energy varies from 130 to 1300 MJ/m^2, and the annual solar fraction varies from 2 % to 28 %. The mean annual net utilized solar energy of the systems is 590 MJ/m^2 and the mean solar fraction is 17 %. The mean daily hot water consumption is 18 l/m^2 with maximum and minimum values of 31 l/m^2 and 5 l/m^2 respectively. Further, all the systems have a space heating demand during the summer months from the middle of May to the middle of September.

Variations in the yearly thermal performances are expected due to the fact that the systems have different solar collectors, solar collector orientations and tilts and due to the fact that the systems are located in different places in Denmark with different yearly solar radiations and that the measurements are obtained in different years with different yearly solar radiations [11].

As can be seen in Figure 2, there apparently is little correlation between the solar fraction and the yearly net utilized solar energy per m^2 collector for these Danish systems. The main reasons for this are that there are large variations in the space heating demand during the summer months from system to system and that there are large variations in the heat loss from the heat storage of the systems. The measured results will be analysed further in section 4.

3 Theoretical investigation and parametric study of two solar combi systems

3.1 Assumptions for calculations

Two different solar combi systems for single family-houses are investigated: System no.1, which corresponds to the system illustrated in Figure 3 and system no.2, which corresponds to the system illustrated in Figure 4. System no.2 is recently introduced on the Danish market.

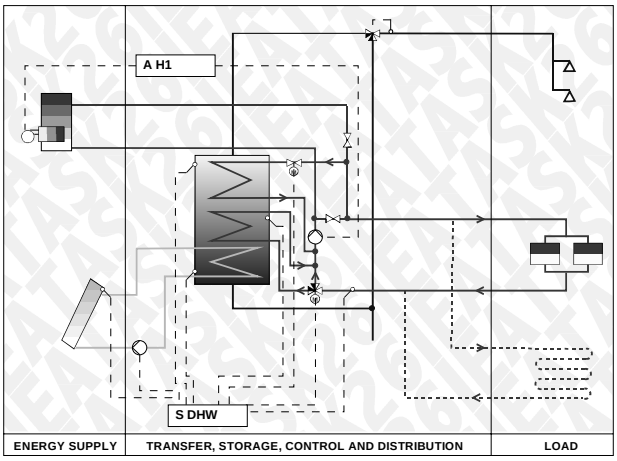

Figure 3: Solar combi system based on a hot water tank with three heat exchanger spirals, system no.1. [7].

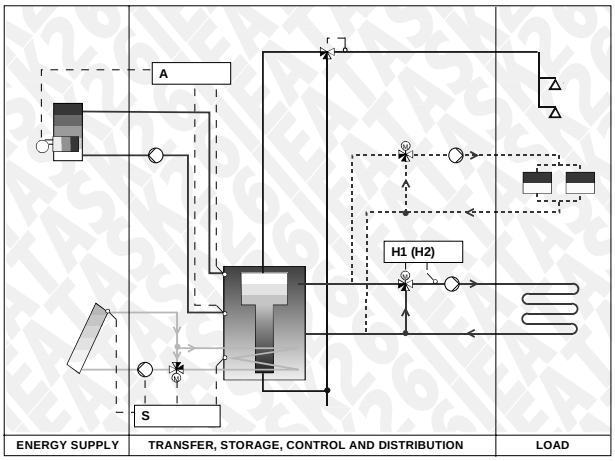

Figure 4: Solar combi system recently introduced on the Danish market, system no.2. [7].

Both combi systems are modelled in the simulation program TRNSYS [12]. The storage tank is modelled with the type 140 [13], which is a multiport store model. The solar collector efficiency expression for small incidence angles is given in Table 2. The collector efficiency expression is valid for all incidence angles by multiplying the first coefficient of the solar collector efficiency expression with the incidence angle modifier for beam radiation. The power of the solar collector (Q) is calculated with the type 132 [14] that has a correction term for diffuse radiation and for the heat capacity of the solar collector including the solar collector fluid. The diffuse radiation uses a separate incidence angle modifier that equals the incidence angle modifier for beam radiation at an incidence angle of 60°:

$$Q = A\cdot[\eta_0\cdot k_\theta(\theta)\cdot E_b + \eta_0\cdot k_\theta(60°)\cdot E_d - a_1\cdot(T_m-T_a) - a_2\cdot(T_m-T_a)^2 - C\cdot dT_m/dt] \quad (3)$$

The SH demand is calculated for a one family houses of 140 m^2 with an annual SH demand of about 360 MJ/m^2. The house has a heat distribution system with a design

temperature of 60°C and a design temperature difference over the heat distribution system of 10 K [15]. The indoor design temperature is 20 °C and the outdoor design temperature is -12 °C. The model of System no.1 is not validated with measurements while the model of system no.2 is validated with measured temperatures and energy quantities from a laboratory test of a marketed system [16]. The weather data of the Danish Design Reference Year, DRY [17] is used in the calculations. The systems used in the calculations are identical except for the storage tanks. The data of the systems used in the calculations are given in Table 2. The data of the storage tanks are given in Table 3.

Table 2: Data for the systems used in the calculations.

Solar collector	
Start efficiency, η_0	0.756
Heat loss coefficient, a_1	4.37 W/m^{2}K
Heat loss coefficient, a_2	0.01 W/m^{2}K^2
Incidence angle modifier coefficient, p	4.2
Efficiency for small incidence angles, η	$\eta_0 - a_1 \cdot (T_m - T_a)/E - a_2 \cdot (T_m - T_a)^2/E$
Incidence angle modifier for beam radiation, k_θ	$1\text{-}\tan^p(\theta/2)$
Heat capacity including the solar collector fluid, C	5000 J/Km^2
Tilt	45°
Orientation	South
Solar collector loop	
Outer/inner pipe diameter	12/10 mm
Length of pipe from solar collector to storage, outdoor	3 m
Length of pipe from storage to solar collector, outdoor	5 m
Length of pipe from solar collector to storage, indoor	3 m
Length of pipe from storage to solar collector, indoor	5 m
Heat loss coefficient of pipe	0.12 W/mK
Solar collector fluid	40% (weight) propylene glycol/water mixture
Volume flow rate in solar collector loop	1.2 l/min/m^2
Power of circulation pump	100 W
Heat exchanger spiral	
Heat transfer coefficient	50 W/K per m^2
Control system	
Differential thermostat control with one sensor in the solar collector and one at the bottom of the tank	
Start/Stop difference	10 K/1 K

Table 3: Data for the storages used in the calculations.

Name	System no.1	System no.2
Type	Spiral tank - corresponding to Fig. 3	Tank in tank storage - corresponding to Fig. 4
Tank material	Steel St 37-2	Steel St 37-2
Hot-water combi storage		
Volume	300 l	460 l (136 l DHW tank)
Height/diameter	1.225/0.559 m	1.490/0.662 m
Material thickness	3 mm	5 mm
Heat loss coefficient	3.4 W/K	5.2 W/K
Auxiliary energy supply system	Upper 75 l of the storage is heated to 50ºC by the auxiliary energy supply system	Upper 262 l of the storage is heated to 55ºC by the auxiliary energy supply system. The DHW volume in the auxiliary heated part is 108 l.
Efficiency of auxiliary energy supply system	100 %	100 %

Different daily quantities of hot water consumption are assumed. The water is heated from 10 ºC to 50 ºC and hot water is tapped in three equal portions at 7 am, noon and 7 pm. The calculations are carried out with solar collector areas from 3 – 18 m^2, daily hot water consumption from 50 – 200 liters and a space heating demand from the middle of September until the middle of May of 54000 MJ and no space heating demand during summer. Also the calculations are carried out with an additional space heating demand in the summer period of 4320 MJ as the measurements show a space heating demand in the summer period. The space heating demand used in the calculations corresponds to the average measured summer space heating demand. Figure 5 shows the space heating load used in the calculations.

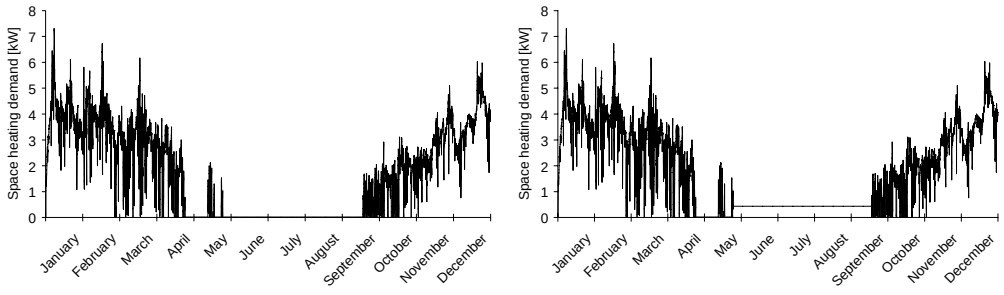

Figure 5: Space heating load used in the calculations. Left figure shows the space heating load without space heating demand during the summer period and right figure shows the space heating load with space heating demand during summer.

Further, calculations without space heating demand during the summer are carried out with the solar combi systems as preheating systems, with heat stores only heated by the solar collectors. In this case the auxiliary energy supply system is assumed built into the hot water pipe from the tank and the auxiliary energy supply system heats up the water instantaneously to the required temperature. Further the auxiliary energy supply system heats up the fluid entering the heating system to the required temperature. In this way the thermal performance of the solar combi system is maximized since the operation temperature of the solar collector is reduced to a minimum and the heat loss from the storage is minimized because the upper part is not kept at a constant high temperature level.

3.2 Calculated results

Figure 6 shows the calculated yearly net utilized solar energy as a function of the yearly solar fraction. Also, the measured net utilized solar energies for the systems in practice are shown in Figure 6.

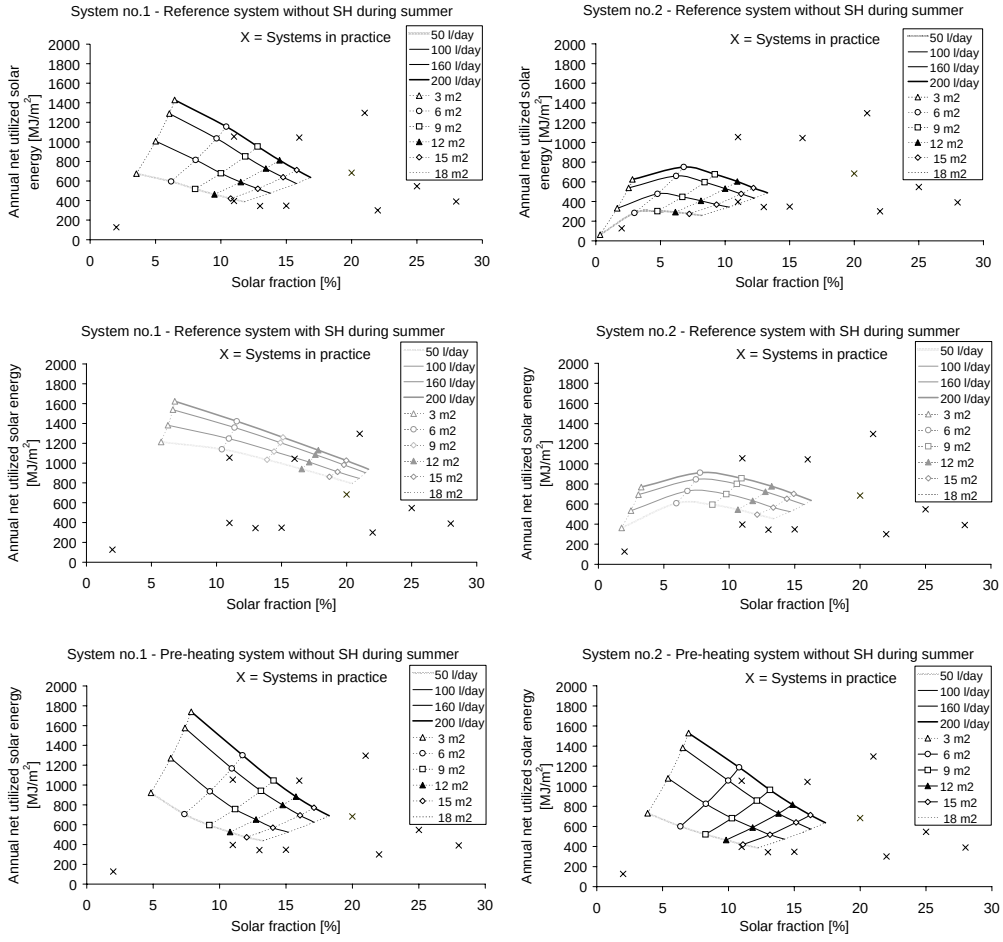

Figure 6: Annual net utilized solar energy as a function of the solar fraction for different solar collector areas and different hot water consumptions.

As shown in the two first graphs of Figure 6, the thermal performance of the solar combi systems is strongly influenced by the hot water consumption when there is no

space heating demand during the summer. In the two middle graphs of Figure 6 it is seen that the thermal performance increases and that the influence from the hot water consumption decreases when there is a space heating demand during the summer. The last two graphs of Figure 6 show the thermal performance of the systems when they are operated as pre-heating systems. The thermal performance of system no.1 is improved only a little while the thermal performance of system no.2 is improved significantly when the systems are operated as pre-heating systems. The significant improvement of system no.2 is due to reduced heat loss, since the large auxiliary volume is no longer constantly heated to a high temperature.

In the calculations it is assumed that the efficiency of the auxiliary energy supply system is 100%. This is not the case in practice where the efficiency varies through the year. In the winter when the auxiliary energy demand is high the efficiency is normally close to 100% but in periods with low auxiliary energy demand the efficiency is much lower. Assuming a more realistic efficiency of the auxiliary energy supply system will lead to energy savings much higher than the net utilized solar energy. However, the variations in efficiencies are not considered in the calculations.

System no.1 performs much better than system no.2. One reason for this is the way the space heating loop is designed and operated. In system no.1 the return water is only lead through the tank when the space heating return temperature is lower than the temperature in the tank. In this way the return water never heats up the lower part of the tank and the temperature stratification in the tank is not destroyed. In system no.2 the return water is always lead into the tank regardless of the temperature and the thermal stratification is destroyed. Another reason is that the auxiliary heated volume in system no.1 is much smaller than in system no.2. Also the temperature of the auxiliary volume is lower in system no.1 than in system no.2. The size and the temperature level of the auxiliary volume have an enormous impact on the thermal performance. The highest thermal performance is reached when both the size and the temperature level of the auxiliary volume are kept at a minimum. Finally the heat storage heat loss coefficient for system no.1 is lower than the heat storage heat loss coefficient for system no.2.

3.3 Parametric study

The systems are designed as described in Table 2 and Table 3 with only one parameter changed at the time. The daily hot water consumption is 160 l and hot water is tapped at 7 am, noon and 7 pm. The SH demand is 54000 MJ/year and there is no SH demand in the summer. The solar collector area is 6 m^2 for system no.1 and 9 m^2 for system no.2.

Figure 7 shows three different temperature conditions in the SH loop through the year corresponding to the different heating systems used in the calculations. Figure 8 and 9 show the calculated net utilized solar energies of the systems with different storage design and operation conditions. Also the figures show the net utilized solar energy of the systems when all the best parameters are used in the calculations at the same time.

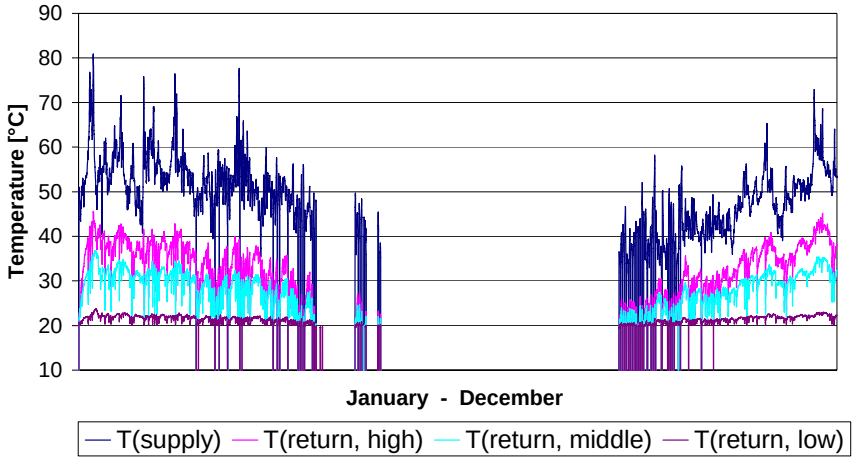

Figure 7: Three different temperature operation conditions in the SH loop which are used in the calculations.

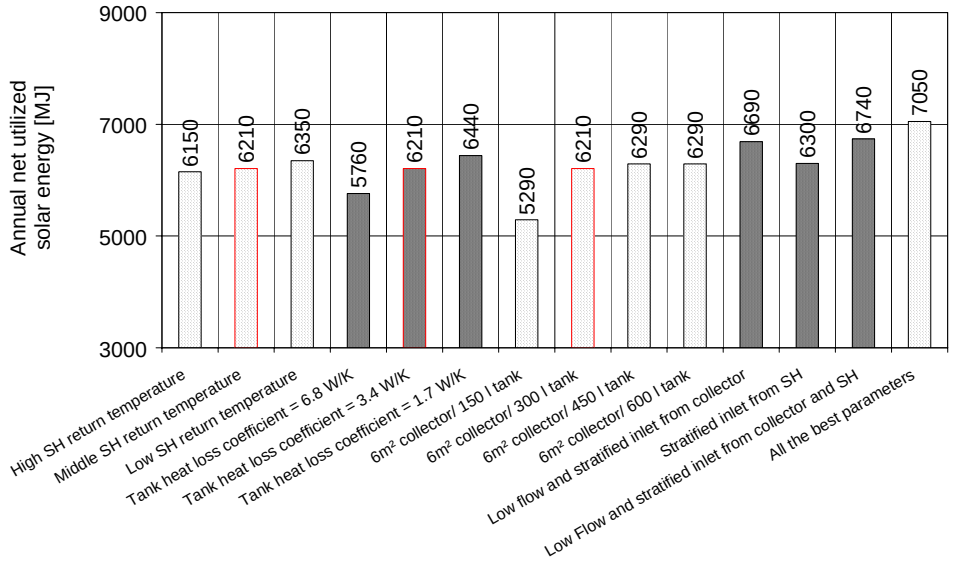

Figure 8: Calculated net utilized solar energies of system no.1 with different storage designs and operation conditions.

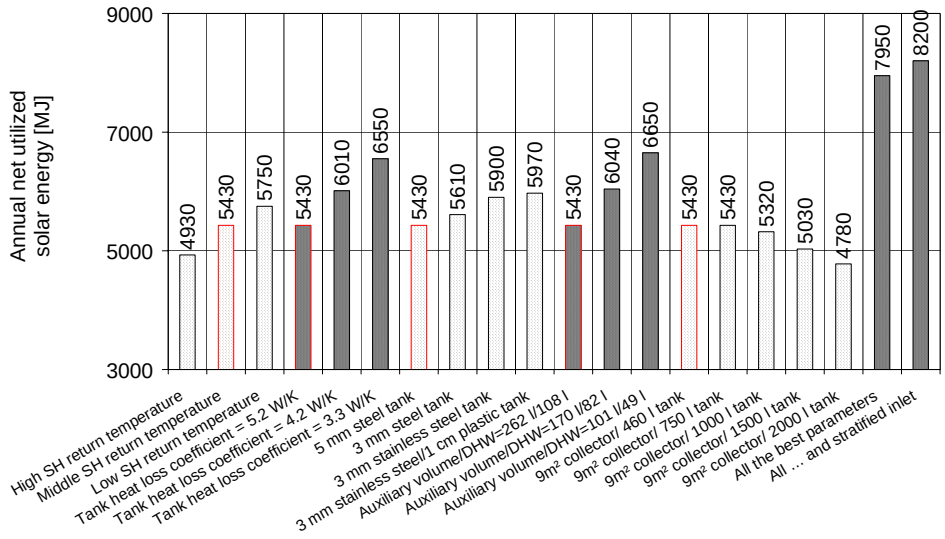

Figure 9: Calculated net utilized solar energies of system no.2 with different storage designs and operation conditions.

From Figure 8, which shows the results for system no.1, it is obvious that both the return temperature from the space heating loop and the tank heat loss coefficient should be low. Further, the thermal performance will not improve if the storage volume is increased. This indicates that the tank volume should not exceed 50 l per m^2 solar collector. Finally the calculations show that the performance will improve by using a stratified inlet both from the solar collector and from the space heating loop. The calculations show that it is possible to improve the annual net utilized solar energy from 6210 MJ to 7050 MJ corresponding to an increase of 13.5 % when all the best design parameters are implemented at the same time.

From Figure 9, which shows the results for system no.2, it is obvious that both the return temperature from the space heating loop and the tank heat loss coefficient should be low. The tank material thickness should be small and the thermal conductivity of the tank material should be low. Further, the thermal performance will not improve if the storage volume is increased. This indicates, like before, that the tank volume should not exceed 50 l per m^2 solar collector. Finally, the thermal performance will improve by reducing the auxiliary heated volume in the top of the tank. It is possible to improve the annual net utilized solar energy from 5430 MJ to 8200 MJ corresponding to an increase of 51 % when all the best parameters are used in the calculations at the same time.

4 Comparison of measurements and calculations

Figure 10 shows the measured thermal performance. The solar combi systems have been divided into three groups according to the size of the space heating demand during the summer. The size of the space heating demand during the summer is determined as the ratio between the space heating demand during the summer and the space heating demand for the whole year. For ratios less than 8 % the summer space heating demand is small. For ratios between 8 % and 12 % the summer space heating

demand is mean, while the summer space heating demand is high for ratios larger than 12 %.

Figure 10 also shows the average of the calculated thermal performance with the different hot water consumptions and the different solar collector areas with and without space heating demand during the summer period. In the calculations with space heating demand during summer, the ratio between the space heating demand during summer and the space heating demand for the whole year is 8 %, which corresponds to the measured mean summer SH demand.

Further the combi systems are divided into two system types. One group includes solar domestic hot water systems with an external heat exchanger between the solar collector loop and the space heating loop, Figure 1. The other one includes the more complicated systems. The two types are referred to as ”a” and ”b” respectively.

For the systems with an external heat exchanger between the solar collector loop and the space heating loop the measurements show, that the space heating demand during the summer equals the total annual energy amount transferred from the solar collector loop to the space heating loop. Hence it can be questioned whether the space heating demand measured during the summer is real or just solar energy transferred to the space heating loop to keep the collector from boiling. With this type of solar combi systems, solar energy is not utilized for space heating except during the summer period.

For the more complicated systems, half of the solar energy utilized for space heating is utilized during the summer period. The other half is utilized during fall and spring. Some of the advanced systems are greatly oversized with a high solar fraction and a low net utilized solar energy per m^2 solar collector. Again it can be questioned whether the space heating demand during the summer is a real space heating demand or just solar energy transferred to the space heating loop to keep the collector from boiling.

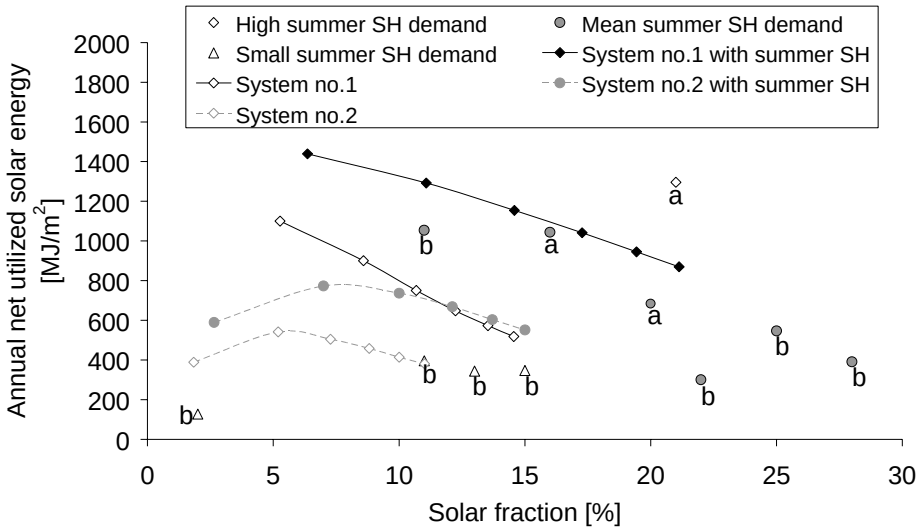

Figure 10: Measured and calculated thermal performances. The letter “a” refer to solar combi systems with an external heat exchanger between the solar collector loop and the space heating loop (see Figure 1), while “b” refer to all other system types.

From Figure 10 it can be seen that the thermal performance of most of the operating solar combi systems lies between the calculated thermal performance for a good performing and poor performing solar combi system. The poor performing systems situated in the lower left corner all have a low space heating demand during summer and are all, except for one system, systems with several large tanks and therefore also high heat losses. These systems are situated in the same region as the calculated system no.2 that also has a high heat loss from the storage tank. The systems with a mean summer space heating demand are situated in the same region, as the calculated system no.1 with a mean summer space heating demand. The system with the high summer space heating demand is situated above all other systems. In Figure 2 it was difficult to see any correlation between the solar fraction and the annual net utilized solar energy per m^2 solar collector. From Figure 10 it becomes obvious that the systems all show a clear correlation between the solar fraction and the annual net utilized solar energy per m^2 solar collector, regardless of the system design, when systems with similar consumption pattern are compared.

From Figure 10 it can be seen that the size of the summer consumption is more important for the thermal performance than the system design.

5 Discussion and conclusion

An investigation has been made of the thermal performance of Danish solar combi systems in single-family houses. The systems are both systems with small tanks and small solar collector areas and systems with large tanks and large solar collector areas. Measurements show that some of the systems are performing well while others have low thermal performance and that all the systems have a space heating demand during the summer period. Also the measurements show that the thermal performance first of all is influenced by the space heating demand during the summer. The higher the space heating demand the higher the thermal performance. The summer period is from the middle of May to the middle of September.

A theoretical investigation of two combi systems for single-family houses has been made. The systems are identical except for the tanks. The first system is based on a 300 l tank with three internal heat exchanger spirals: One in the solar collector loop, one in the space heating loop and one for the auxiliary energy. The second system is based on a 460 l tank in tank storage with an internal heat exchanger spiral in the solar collector loop and direct in- and outlet for the space heating loop and the auxiliary loop. Calculations show that the thermal performance is strongly influenced by the hot water consumption when there is no space heating demand during the summer period. The calculations show that the thermal performance increases when there is a space heating demand during the summer period. Further the calculations show that the influence of the hot water consumption on the thermal performance is decreased when there is a space heating demand during the summer period.

A comparison between measured thermal performances of solar combi systems in practice and calculated thermal performances shows that the solar combi systems in practice perform as expected.

A parametric study of both systems used in the calculations is performed. For the study of the 300 l system, 6 m^2 solar collector is used and for the 460 l system, 9 m^2 solar collector is used. Calculations show that both systems can be improved by design changes. The 300 l system, which is a good performing system, can be

improved with 14 % while the 460 l system, which is a poor performing system, can be improved with 51 %.

The investigation shows that solar combi system can be improved significantly by maintaining high temperature stratification in the storage tank, by keeping the return temperature from the space-heating loop low, by keeping the auxiliary heated volume as small as possible, by keeping the temperature of the auxiliary volume as low as possible and by making sure that the tank is well insulated.

Nomenclature

A	Solar collector area (m^2)
C	Heat capacity of solar collector including the solar collector fluid (J/m^2K)
E	Total solar irradiance (W/m^2)
E_b	Beam solar irradiation (W/m^2)
E_d	Diffuse solar irradiation (W/m^2)
Q_{AUX}	Auxiliary energy consumption (J)
Q_{DHW}	Domestic hot water load (J)
Q_{NET}	Net utilized solar energy (J)
Q_{SH}	Space heating load (J)
Q	Power (W)
SF	Solar fraction (%)
T_a	Ambient temperature (°C)
T_m	Mean solar collector temperature (°C)
a_1	Heat loss coefficient (W/m^2K)
a_2	Heat loss coefficient (W/m^2K^2)
k_θ	Incidence angle modifier for beam radiation (-)
p	Incidence angle modifier coefficient (-)
dT_m	Mean solar collector temperature difference between the present and the previous time step (K)
dt	Time step in the calculation (s)
η	Solar collector efficiency (-)
η_0	Start efficiency of the solar collector (-)
θ	Incidence angle (°)

References

[1] Ellehauge, K., Shah, L. J., 2000, ”Solar Combisystems in Denmark - The Most

Common System Designs," Proc. EuroSun 2000, Copenhagen, Denmark.

[2] Bliss, R.W., 1955, "Design and Performance of the Nation's only Fully Solar-Heated House," Air Conditioning, Heating and Ventilating, 52 (10), p. 92.

[3] Engebretson, C.D., 1964, "The Use of Solar Energy for Space Heating – M.I.T.: Solar House IV." Proc. of the UN Conference on New Sources of Energy, 5, 159.

[4] Löf, G.O.G., El-Wakil, M. M., and Chiou, J. P., 1963, "Residential Heating with Solar Heated Air – the Colorado Solar House," Trans. ASHRAE, 77.

[5] Löf, G.O.G., El-Wakil, M. M., and Chiou, J. P., 1964, "Design and Performance of Domestic Heating Systems Employing Solar Heated Air – the Colorado House," Proc. Inst. Mech. Eng., Part J: J. Eng. Tribol., 5, 185.

[6] Esbensen, and Korsgaard, 1977, "Performance of the Zero Energy House in Denmark," Report no. 64, Thermal Insulation Laboratory, Technical University of Denmark.

[7] Suter, J-M., 2000, "Solar Combisystems – Overview 2000," IEA SHC – Task 26.

[8] Andersen, N. B., 1988, "Solvarmeanlæg til rumopvarmning og varmt brugsvand, demonstrationsanlægget i Ejby," Report no. 189, Thermal Insulation Laboratory, Technical University of Denmark.

[9] Ellehauge, K., et al., 2000, "Erfaringer fra målinger på kombinerede solvarme- og biobrændselsanlæg," Technological Institute, Denmark.

[10] Ellehauge, K., 1993, "Målinger på solvarmeanlæg til kombineret brugsvands- og rumopvarmning – 5 markedsførte solvarmeanlæg installeret hos anlægsejerne," Report no. 255, Thermal Insulation Laboratory, Technical University of Denmark.

[11] Andersen, E., Furbo, S., Shah, L. J., 2003, "The Influence of Weather on the Thermal Performance of Solar Heating Systems," Proc. ISES 2003, Göteborg, Sweeden.

[12] Klein, S. A., et al., 1996, TRNSYS 14.1, User Manual, University of Wisconsin Solar Energy Laboratory.

[13] Drück, H., 2000, "MULTIPORT Store – Model, Type 140 for TrnSys," Institut für Thermodynamik und Wärmetechnik, Universität Stuttgart.

[14] Perers, B., 2000, "A Solar Collector Model and Emulator for IEA Task 26, Description for Solar Thermal System Testing. Based on the CEN 12975 and the TRNSYS Type 132 Collector Model," Vattenfall Utveckling AB.

[15] Streicher, W., et al., 2002, "Solar Combisystems," Milestone report C 0.2, IEA SHC-Task 26.

[16] Shah, L. J., 2001, "Undersøgelse af et solvarmeanlæg til kombineret rum- og brugsvandsopvarmning," SR-01-19, Department of Civil Engineering, Technical University of Denmark.

[17] Skertveit, A., Lund, H., and Olseth, J. A., 1994, "Design Reference Year," Report no. 1194 Klima, Det Norske Institutt.

[18] Mikkelsen, S. E., and Jørgensen, L. S., 1981, ”Solvarmeanlæg til rumopvarmning, en udredning baseret på 2 års målinger på anlæg i Greve og Gentofte,” Report no. 112, Thermal Insulation Laboratory, Technical University of Denmark.

Paper II

The Influence of Weather on the Thermal Performance of Solar Heating Systems

Paper submitted to Journal of Solar Energy, May 2007

The Influence of Weather on the Thermal Performance of Solar Heating Systems

Elsa Andersen and Simon Furbo

Department of Civil Engineering Technical University of Denmark

DK-2800 Kgs. Lyngby, Denmark, e-mail: ean@byg.dtu.dk

Paper submitted to Journal of Solar Energy, May 2007

Abstract

The influence of weather on the thermal performance of solar combi systems and solar collectors is investigated. The investigation is based on weather data from the Danish Design Reference Year, DRY data file, and weather data measured for a period from 1990 to 2002 in Denmark. The investigation is based on calculations with validated models. Solar heating systems with different solar collector types, heat storage volumes and solar fractions are included in the investigation. The yearly solar radiation varies by approximately 23% in the period from 1990 until 2002. The calculations show that the yearly thermal performance of the investigated solar combi systems increases with increasing solar radiation and that the utilized part of the solar radiation primary is influenced by the month by month variations of solar radiation and not by the annual total solar radiation on the solar collector.

The calculations also show that the yearly thermal performance of solar collectors and the utilized part of the solar radiation increases for increasing annual total solar radiation on the solar collector Both the thermal performance and the utilization of solar radiation can with good approximation be fitted to a linear function of the total solar radiation on the collector. Finally the calculations show that evacuated tubular solar collector utilizes less sunny years with large parts of diffuse radiation relatively better than the flat plate solar collectors.

Keywords Measured weather data, solar radiation variations, solar heating systems, solar collectors, thermal performance, utilized part of solar radiation

1 Introduction

Throughout the world, design reference years have been developed for different locations. The weather data in the design reference years are derived from measured weather data for periods of 15–20 years, and common for all locations is that the weather varies from one year to another. Although the results in this study are based on measured Danish weather data, the results are not specific for Danish conditions, but show how the thermal performances of solar heating systems and solar collectors are generally influenced by weather variations.

Hourly weather data have been measured at the Technical University of Denmark (55.8°N), DTU in the period from 1990 to 2002. The weather data varies from year to year and from the weather data represented by the Danish Design Reference Year (Sketeveit et al., 1984). The Danish Design Reference Year represents a typical year based on measured weather data from the period 1975 to 1989. The thermal performance prediction for solar heating systems is normally based on calculations using weather data from the Design Reference Year. The thermal performance of solar heating systems can both directly and indirectly be influenced by the weather: The efficiency and energy production of a solar collector is directly influenced by the weather, first of all the solar irradiance on the collector and the ambient temperature. The space heating demand of buildings is influenced by the weather, first of all the ambient temperature and the solar radiation on the windows. The thermal performance of solar combi systems is therefore both directly and indirectly influenced by the weather.

Cavalcanti (1991) analysed measured global solar radiation data from Rio de Janeiro (22.9°S) for a period from 1979 to 1983 and showed that the global radiation varied 13.9% from the least sunny year to the sunniest year.

Salem et al. (1993) analysed measured global solar radiation data from El-Kharga in Egypt (25°N) from the period 1984 to 1988 and found that the global solar radiation varied 2.9% from the least sunny year to the sunniest year.

Siebers and Viskanta (1977) compared the long term flat plate solar collector performance calculations based on hourly meteorological weather data and averaged meteorological weather data. Weather data from three locations: Sterling, Virginia (39.0°N); Lafayette, Indiana (38.4°N); and Phoenix, Arizona (34.4°N) with various types of climates were used in the investigations. It was concluded that averaged meteorological data only correlate well with performance calculations based on hourly meteorological data, if the variations in weather are small.

Adsten et al. (2001) investigated the influence of climate and location on solar collector performances. Three different locations in Sweden were investigated with weather data from 1983 to 1998. The locations were Lund (55.7°N), Stockholm (59.3°N) and Luleå (65.6°N). The variations in total solar radiation on a south facing 45°-tilted surface from the least sunny year to the sunniest year are 19%, 23% and 26%, respectively. The investigation included a flat plate collector and an evacuated tubular collector. The authors found that the solar radiation variations are larger the further away from equator the location is and that the collector output is strongly influenced by the solar irradiance and less influenced by the ambient temperature during operation. Further they found that the relation between the global radiation and the solar collector output could be fitted to a linear equation.

This study presents the results of an investigation of the influence of weather variations on the thermal performance of solar combi systems and solar collectors. The investigation is based on measured weather, weather data from the Danish Design Reference Year and differently designed solar heating systems, including three solar combi systems, four marketed flat plate solar collectors and one marketed evacuated tubular solar collector. Further, the investigation of solar combi systems is based on different houses.

2 Weather data and solar radiation processing model

The weather data are obtained by a weather station placed on the roof of a building at Department of Civil Engineering, DTU. The measurements are recorded every 2 minutes. From these 2 minutes, hourly data values are created. The measurements include hourly global and diffuse irradiance on horizontal and the ambient temperature. The global and diffuse irradiance is measured with Kipp and Zonen pyranometers CM11 and CM5, respectively. Further, the diffuse irradiance is measured with a shadow ring with a width of 57 mm and a radius of 325 mm. The temperature is measured with a PT1000 sensor.

For an isotropic model, the fraction of the diffuse radiation screened off by the shadow ring is given by (U.S. Department of Energy, 1980):

$$\Delta G_d = \frac{2w}{\pi r}\cos^3\delta(\gamma_{ss}\sin\Phi\sin\delta + \cos\Phi\cos\delta\sin\gamma_{ss}) \quad (1)$$

The correction factor to be applied to the measured diffuse radiation is:

$$k_d = \frac{1}{(1-\Delta G_d)} \quad (2)$$

Figure 1 shows the measured yearly global and diffuse radiation on horizontal. The mean value of the global radiation in the period from 1990 to 2002 is 1.3% lower than the global radiation in DRY. The annual global radiation varies between 881 kWh/m^2/year in 1998 and 1041 kWh/m^2/year in 1997 with an average radiation of 989 kWh/m^2/year, corresponding to a global solar radiation variation from the least sunny year to the sunniest year of about 16%. Further, the average day, day time and night time temperatures are shown. Day time is defined as the period from sunrise to sunset and night time as the period from sunset to sunrise. The average day temperature is 0.9 K higher in the period from 1990 to 2002 than in DRY, and the average day, day time and night time temperatures vary 2.9 K, 2.7 K and 3.0 K, respectively, from the

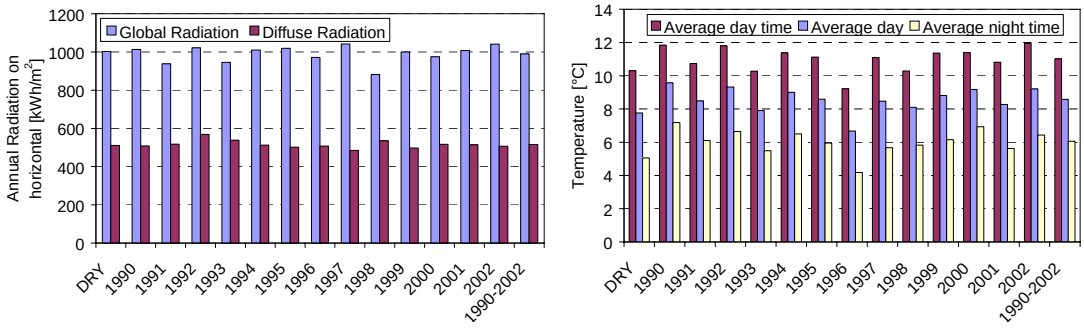

coldest to the hottest year.

Figure 1: Right: The global and diffuse radiation on horizontal. Left: The average daytime, night time and day temperatures.

The isotropic diffuse model (Liu and Jordan, 1963) is used to calculate the total radiation on a tilted surface. The isotropic sky model assumes that the diffuse radiation is uniformly distributed over the entire sky dome. The isotropic model

slightly underestimates the diffuse solar radiation on a tilted surface, mostly because the circumsolar diffuse solar radiation close to the sun disc is not used in the calculation. It is estimated that this underestimation will not influence the calculated thermal performance of solar collectors and solar heating systems significantly.

Figure 2 shows the calculated total and diffuse radiation on a south facing 45°-tilted surface. The mean value of the total radiation on a south facing 45°-tilted surface is 1.7% lower than the same value in DRY. The annual total radiation varies between 991 kWh/m^2/year in 1998 and 1251 kWh/m^2/year in 1997 with an average radiation of 1132 kWh/m^2/year, corresponding to a radiation variation from the least sunny year to the sunniest year of about 23%. The figure also shows the relative annual total radiation on the tilted surface as a function of the relative annual global radiation. The radiation is relative to the radiation in DRY. The dotted line indicates a linear relationship between the relative total global radiation and the relative total radiation on the 45°-tilted surface. The figure shows that a linear relationship is not reasonable. For instance, 1992 is placed below the dotted line, while 1996 is placed above the dotted line. The yearly radiation on the 45º-tilted surface is almost the same for the two years.

Figure 3 shows the monthly total and diffuse radiation on horizontal and on a south facing 45°-tilted surface for the years DRY, 1992 and 1996. From the figure it can be seen that in 1992 the solar radiation is higher in the summer months with high solar altitudes and relatively low in the spring and autumn with low solar altitudes. In 1996, the picture is the opposite. Consequently, the monthly distribution of the solar radiation influences the ratio between the relative yearly total solar radiation on a tilted surface and the relative yearly global radiation.

Figure 4 shows the relative monthly total radiation on the tilted surface as a function of the relative monthly global radiation for the months June and November from the period 1990-2002. The radiation is relative to the radiation in DRY. The dotted line indicates a linear relationship between the relative total global and the relative total radiation on the 45°-tilted surface. It is clear that there is a linear relationship in June and not in November. Similar graphs for all months show that there is only linear relationship during the period May–August while the relationship in the other months of the year is unpredictable. Consequently, it is not possible to predict the yearly total radiation on a tilted surface based on the yearly global radiation due to unpredictable spring, autumn and winter months.

Figure 5 shows the monthly total radiation from DRY and the monthly average total radiation from the period from 1990-2002 on horizontal and on a south facing 45°-tilted surface. Further, the deviation interval from the average yearly total radiation in the period from 1990-2002 is shown. The figure shows that the largest radiation variations take place from March to October and that during the period from October to March there are only very small radiation variations on horizontal. The radiation variations on a south facing 45°-tilted surface and on horizontal are almost the same in the summer months, while the variations in the winter months are much larger on a south facing 45°-tilted surface than on horizontal due to low solar altitudes in the winter.

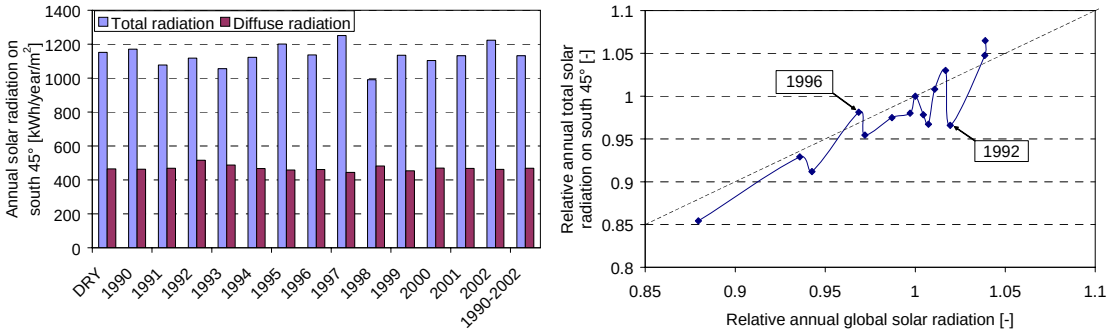

Figure 2: Left: The total and diffuse radiation on a south facing 45°-tilted surface. Right: The relative yearly total solar radiation on a south facing 45°-tilted surface as a function of the relative yearly global radiation. The relative values are relative to the same values in DRY.

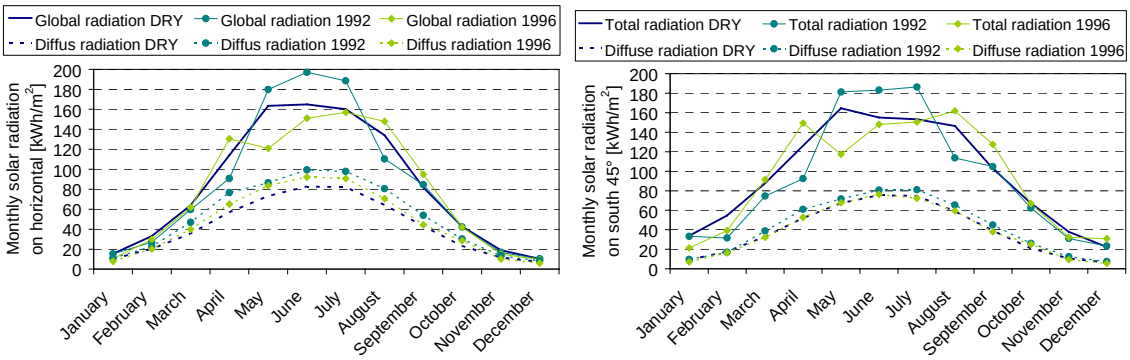

Figure 3: Left: The monthly global radiation and diffuse radiation on horizontal. Right: The monthly total radiation and the diffuse radiation on a south facing 45°-tilted surface. The values are from the years DRY, 1992 and 1996.

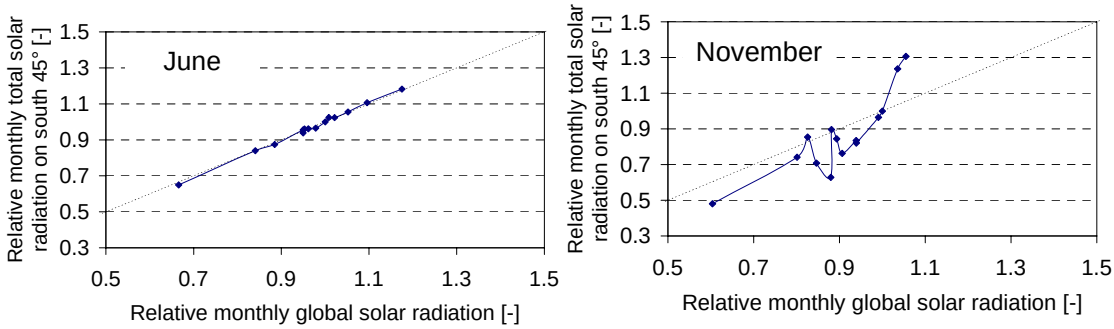

Figure 4: The relative monthly total solar radiation on a south facing 45°-tilted surface as a function of the relative monthly global solar radiation. The values are relative to the same values in DRY.

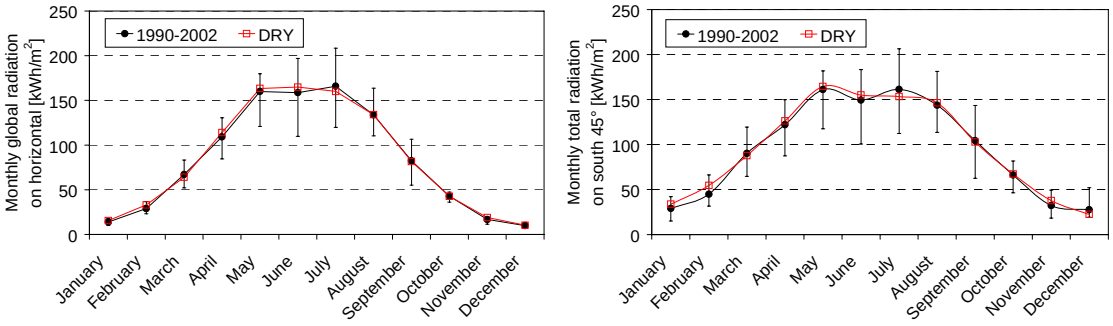

Figure 5: Left: Monthly average global radiation and the deviation interval from the average global radiation. Right: Monthly average total radiation on a south facing 45°-tilted surface and the deviation interval from the average monthly radiation.

3 Solar heating system models and loads

3.1 System models

The calculation of the thermal performance of the solar combi systems is based on TrnSys (Klein et al., 1996). The calculations include two different spiral tanks with volumes of 0.3 m^3 and 0.6 m^3 (Drück, 2000). Two marketed flat plate solar collectors (ST-N(A) and LF3) and one marketed evacuated tubular collector (SLU-1500/12) are used in the calculation. The calculations are carried out with flat plate solar collector areas of 6 m^2 and 12 m^2, and evacuated tubular solar collectors with cross section areas of the tubes that are 70% of the flat plate solar collector areas corresponding to 4.2 m^2 and 8.4 m^2, respectively. Figure 6 shows the evacuated tubular solar collector schematically.

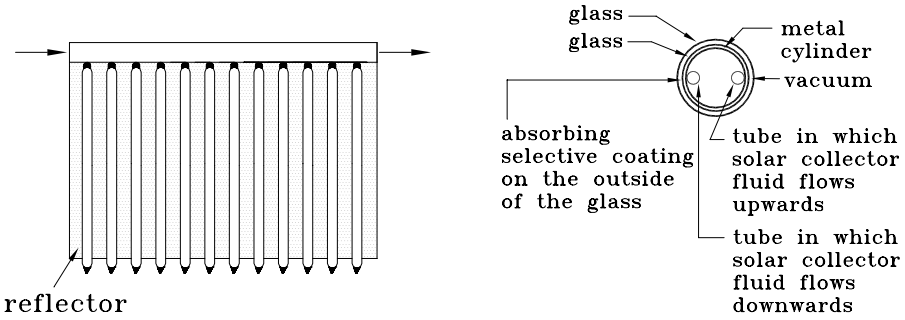

Figure 6: The evacuated tubular solar collector used in the calculations and a cross sectional view of a collector tube. Figure from Qin and Furbo (1999).

The calculation of the thermal performance of the solar collectors is based on a program developed at DTU (Jensen et al, 2001) and includes two marketed flat plate collectors (HT-N(A) and BA120T) and one marketed evacuated tubular collector (SLU-1500/12). The cross section area of the evacuated tubes is again 70% of the area of the flat plate solar collector.

The solar collectors are facing south and tilted 45°. The solar collectors and the tanks used in the calculations are described in Table 1 and Table 2. The relative height is

defined as: the height in question calculated from the bottom of the tank / the total height of the tank. The relative heights of 0 and 1 correspond to the bottom respectively the top of the tank.

In Figure 7 the efficiency curves and the incidence angle modifiers for the solar collectors are shown. The solar collector coefficients for the flat plate collectors given in Table 1 are used to describe the solar collector efficiency η for all incidence angles with the equation:

$$\eta = k_\Theta \eta_0 - a_1 \frac{(T_m - T_a)}{G_t} - a_2 \frac{(T_m - T_a)^2}{G_t} \tag{3}$$

where k_Θ is the incidence angle modifier given by:

$$k_\Theta = 1 - tg^p(\Theta/2) \tag{4}$$

The power of the solar collector Q is calculated with a model that has a correction term for diffuse radiation, (Perers B., 2000). The diffuse radiation uses a separate incidence angle modifier that equals the incidence angle modifier for beam radiation at an incidence angle of 60°:

$$Q = \eta_0 \cdot k_\Theta(\Theta) \cdot G_b + \eta_0 \cdot k_\Theta(60^\circ) \cdot G_d - a_1 \cdot (T_m - T_a) - a_2 \cdot (T_m - T_a)^2 \tag{5}$$

The evacuated tubular collector has two incidence angle modifiers, one longitudinal $k_{\Theta,long}$ and one transverse $k_{\Theta,trans}$. The longitudinal incidence angle modifier equals the incidence angle modifier for a flat plate collector described by eq. (4) while the transverse incidence angle modifier is described by the curve shown in Figure 7. All incidence angle modifiers are determined by means of collector tests. The power Q of the evacuated tubular solar collector is calculated as:

$$\begin{aligned} Q = {} & \eta_0 \cdot k_{\Theta,trans}(\Theta_{b,trans}) \cdot k_{\Theta,long}(\Theta_{b,long}) \cdot G_b + \eta_0 \cdot k_{\Theta,long,d} \cdot k_{\Theta,trans,d} \cdot G_d \\ & - a_1 \cdot (T_m - T_a) - a_2 \cdot (T_m - T_a)^2 \end{aligned} \tag{6}$$

The incidence angle modifiers for diffuse radiation $k_{\Theta,long,d}$ and $k_{\Theta,trans,d}$ are constants determined by integration of the incidence angle modifier curves for beam radiation.

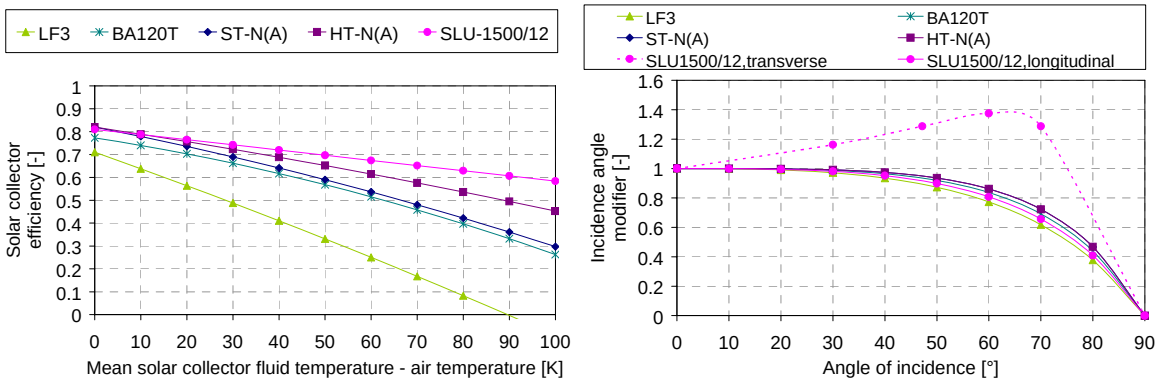

Figure 7: Left: Efficiencies at an incidence angles of 0° and a solar irradiance of 800 W/m^2. Right: Incidence angle modifiers for the solar collectors.

Table 1: Data of the solar collectors.

Collector	ST-N(A)	LF3	SLU-1500/12	HT-N(A)	BA120T
Manufacturer	ARCON Solvarme A/S, Demnark	Aidt Miljø A/S, Denmark	Tsinghua Solar Co., China	ARCON Solvarme A/S, Denmark	BATEC A/S, Denmark
Start efficiency, η_0	0.82	0.71	0.81	0.82	0.773
Heat loss coefficient, a_1 [W/m^2K]	3.18	5.71	1.81	2.44	2.48
Heat loss coefficient, a_2 [W/m^2K^2]	0.01	0.007	0	0.005	0.016
Incidence angle modifier coefficient, p	3.6	2.7	See Figure 7	3.6	3.3
Used to calculate the thermal performance of:	Solar combi systems	Solar combi systems	Solar combi systems and solar collectors	Solar collectors	Solar collectors

Table 2: Data of the tanks.

Tank	Combi tank with three internal heat exchanger spirals for solar collector loop, space heating loop and boiler loop	Combi tank with three internal heat exchanger spirals for solar collector loop, space heating loop and boiler loop
Volume [m^3]	0.300	0.600
Height/diameter [m]	1.225/0.558	1.825/0.647
Auxiliary energy supply system	Upper 0.075 m^3 of the tank is heated to 50.5°C	Upper 0.075 m^3 of the tank is heated to 50.5°C
Relative height inlet / outlet, solar heat exchanger	0.30 / 0.02	0.30 / 0.02
Heat transfer capacity rate, solar heat exchanger [W/(K·m^2 collector)]	50	50
Relative height inlet / outlet, space heating heat exchanger	0.35 / 0.70	0.35 / 0.83
Heat transfer capacity rate, space heating heat exchanger [W/K]	300	300
Tank heat loss coefficient [W/K]	2.5	3.4

3.2 Domestic hot water consumption and space heating demand

The solar combi systems are calculated with a daily hot water consumption of 160 litres. The water is tapped in three equal portions at 7 am, noon and 7 pm. The water is heated from 10°C to 50°C corresponding to a daily hot water consumption of 7.4 kWh.

The space heating consumption is calculated for two geometrically identical one family houses of 150 m^2. The houses have a south facing window area of 12 m^2, east and west facing window areas of 4 m^2 and north facing window area of 3 m^2. One house has a high annual space heating demand of about 100 kWh/(m^2·year) and one has a low annual space heating demand of about 30 kWh/(m^2·year). In the figures, the space heating demands are referred to as SH100 and SH30, respectively. The house with the high space heating demand has a heat distribution system with a design temperature of 60°C and a design temperature difference over the heat distribution system of 10 K, while the house with the low space heating demand has a design temperature for the heat distribution system of 35°C and a design temperature difference over the heat distribution system of 5 K (Streicher et al., 2002). The indoor design temperature is 20 °C and the outdoor design temperature is -12 °C.

4 Simulation results

The net utilized solar energy, the utilization of solar radiation and the performance ratio are defined as:

$$Q_{NET} = Q_{DHW} + Q_{SH} - Q_{AUX} \text{ (Solar combi system)} \quad (7)$$

$$Q_{NET} = Q_{COL} \text{ (Solar collector, assuming constant operation temperature)} \quad (8)$$

$$USR = \frac{Q_{NET}}{Q_{SOL}} \cdot 100\% \quad (9)$$

$$PR = \frac{Q_{NET}}{Q_{NET,REF}} \tag{10}$$

4.1 Solar combi systems

Figure 8 shows the space heating consumption for two one family houses for the different years and the space heating consumption relative to the space heating consumption with DRY as a function of the relative total radiation on a south facing 45°-tilted surface. The high space heating consumption varies between 12900 kWh/year and 18150 kWh/year, while the low space heating consumption varies between 3750 kWh/year and 5560 kWh/year, corresponding to a space heating consumption variation relative to DRY from the coldest to the warmest year of 33% respectively 37%. The average high and low space heating consumption in the period 1990-2002 is respectively 4.9% and 5.7% lower than the space heating consumption with weather data from DRY.

From Figure 8 it can be seen that the annual space heating consumption is low when the average day temperature is high and high when the average day temperature is low. In this case, there is no correlation between the space heating consumption and the solar radiation. The space heating consumption is strongly correlated to the ambient temperature.

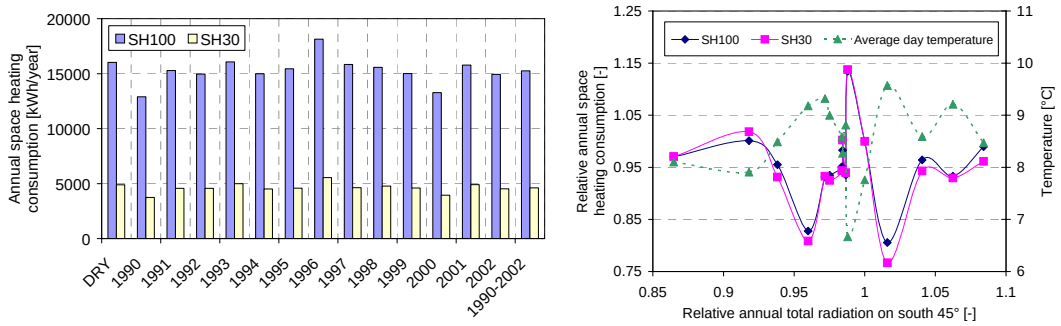

Figure 8: Left: Annual space heating consumption for the different years. Right: Relative space heating consumption and average day temperature as a function of the relative total solar radiation on a south oriented 45°-tilted surface. The values are relative to the same values with DRY as weather data.

Figure 9 shows the annual net utilized solar energy of the solar combi systems and the annual utilization of solar radiation as a function of the different years sorted by increasing total solar radiation on a south facing 45°-tilted surface.

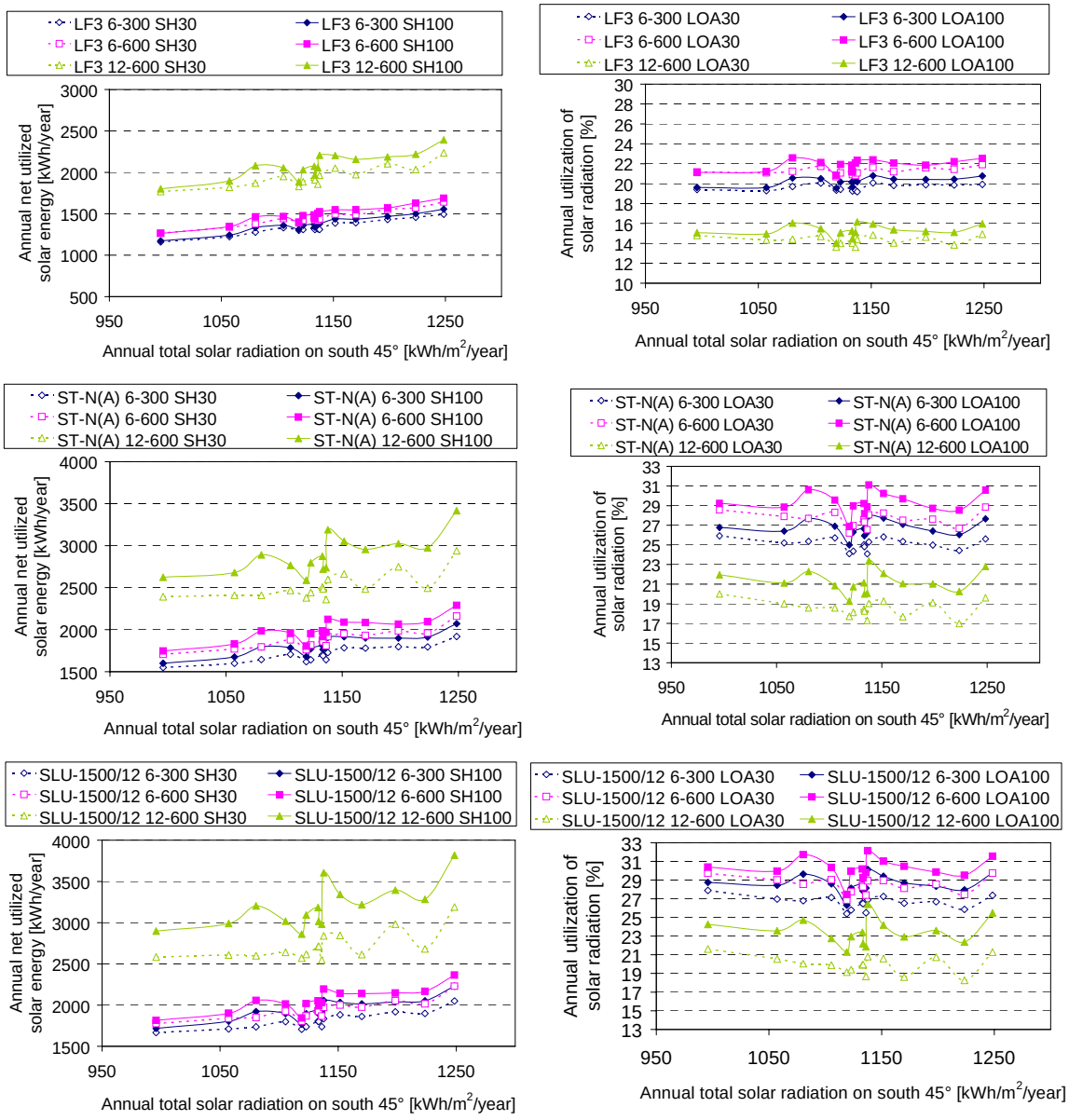

Figure 9: Left: The annual net utilized solar energy of solar combi systems as a function of the different years sorted by increasing total solar radiation on a south oriented 45°-tilted surface. Right: The annual utilization of solar radiation as a function of the annual total solar radiation on a south oriented 45°-tilted surface. The abbreviations in the legend refer to the solar collector type, the solar collector area [m^2], the storage volume [litre] and the space heating demand.

From Figure 9 it can be seen that the net utilized solar energy for solar combi systems increases for increasing solar radiation on the collector. Also it can be seen that the net utilized solar energy increases for increasing space heating demand. The yearly net utilized solar energy is not a linear function of the solar radiation on the collector. Further, the figure shows that the annual utilization of solar radiation is not significantly influenced by the annual total solar radiation. Furthermore, the utilization of solar radiation is lower for low efficient solar collectors than for high efficient solar collectors. Also the variations in the utilization of solar radiation are

lower for low efficient solar collectors. The utilization of solar radiation is highest for the systems with the high ratio between the storage volume and the solar collector area.

The largest variations in the net utilized solar energy and the utilization of solar radiation take place in the region where the total solar radiation is close to the average solar radiation from the period 1990-2002 and DRY where the monthly distribution of the solar radiation influences the results most.

Figure 10 shows the performance ratio for solar combi systems with different solar collectors as a function of the total solar radiation on a south facing 45°-tilted surface. The reference system is the corresponding system with the low efficient solar collector type LF3. In this way the figure shows how much better systems with the solar collectors type ST-N(A) and type SLU-1500/12 perform than a system with the solar collector type LF3.

From the figure it can be seen that the performance ratio is higher for systems with high space heating demands than systems with low space heating demands and that the performance ratio increases with increasing efficiency of the solar collector. Also, the performance ratio increases with the size of the solar combi system. It is an advantage to use a high efficient solar collector instead of a low efficient solar collector. The highest performance ratios are reached for solar combi systems with high efficient solar collectors and the low ratio between the storage volume and the solar collector area. The thermal performance ratio is not significantly influenced by the yearly solar radiation.

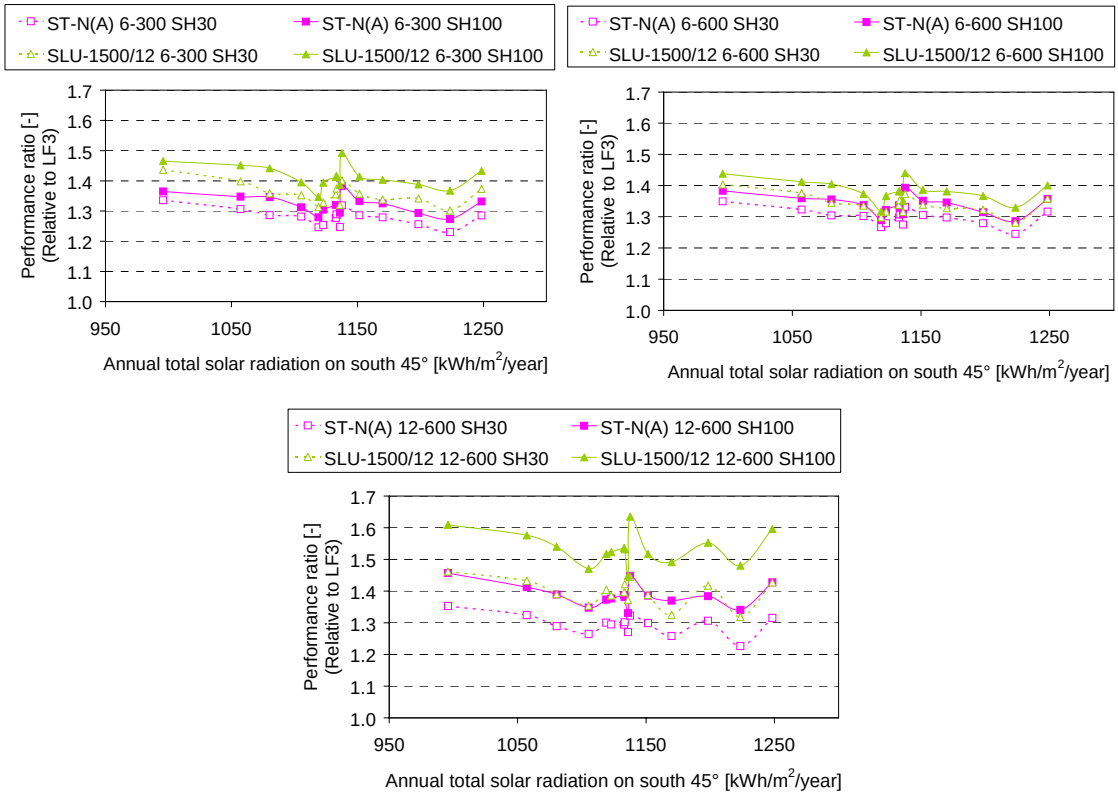

Figure 10: The performance ratio as a function of the annual total solar radiation on a south facing 45°-tilted surface. The reference systems are the corresponding systems with high and low space heating demands and the solar collector type LF3. The abbreviations in the legend refer to the solar collector type, the collector area [m^2], the storage volume [litre] and the space heating demand.

4.2 Solar collectors

Figure 11 shows the yearly thermal performance and the yearly utilization of solar radiation for different solar collectors at different constant operation temperatures as a function of the yearly total solar radiation on a south facing 45°-tilted surface.

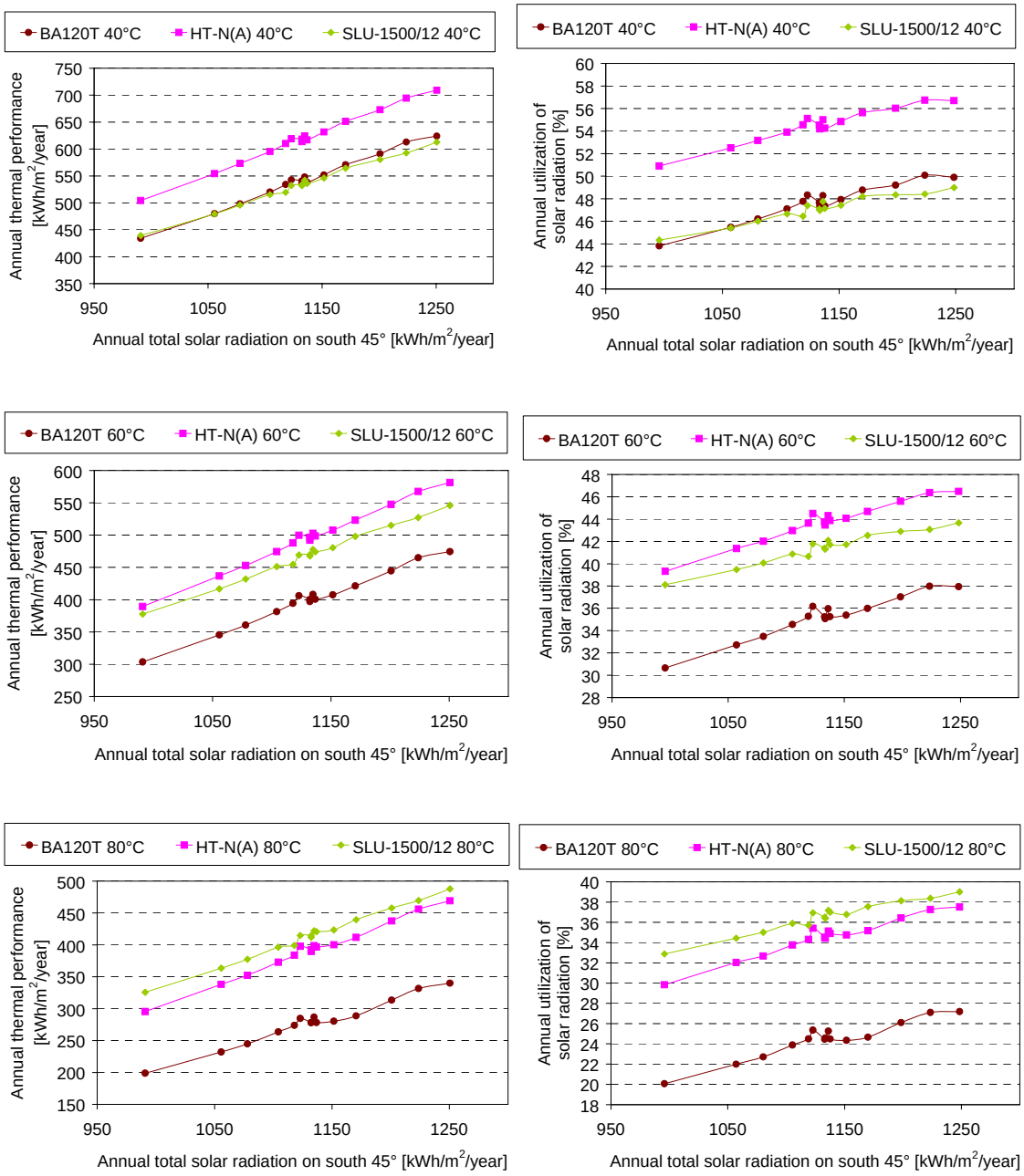

Figure 11: Left: The annual thermal performance of solar collectors as a function of the different years sorted by increasing total solar radiation on a south oriented 45°-tilted surface. Right: The annual utilized solar energy as a function of the annual solar radiation on a south oriented 45°-tilted surface. The abbreviations in the legend refer to the solar collector type and the collector mean fluid temperature.

The figure shows that the annual thermal performance decreases for increasing mean collector fluid temperature and increases for increasing annual total radiation on the solar collector. Further, the evacuated tubular collector utilizes less sunny years with large parts of diffuse radiation relatively better than the flat plate collectors. This can be seen from the inclination of the curve for the evacuated tubular collector which is lower than the inclination of the curves for the flat plate collectors.

The utilization of the yearly solar radiation is with a good approximation a linear function of the yearly solar radiation on the collector.

The thermal performances of solar collectors are strongly influenced by the weather and the collector mean fluid temperature. The high efficient solar collectors, especially the evacuated tubular solar collector, have a large advantage when the mean fluid collector temperature is high due to a very low heat loss coefficient, especially in less sunny years.

4.3 Influence of the global radiation on the thermal performance

Figure 12 shows examples of the annual thermal performance of solar collectors with a constant operating temperature of 60ºC as a function of the annual global solar radiation and Figure 13 shows examples of the net utilized solar energy for solar combi systems as a function of the annual global solar radiation.

Adsten M. et al, (2001) found that the relationship between the global solar radiation and the thermal performance of solar collectors could be fitted with reasonable approximation to a linear equation with R-squared values in the range 0.95 to 0.98 by linear regression. Figure 12 shows that a linear relationship between the global solar radiation and the thermal performance of solar collectors is possible with reasonable approximation. Linear regression gives R-squared values in the range 0.81 to 0.86.

Figure 13 shows that this linear relationship is impossible to achieve for solar combi systems. For solar combi systems with low efficient solar collectors, linear regression gives R-squared values in the range 0.4 to 0.7. For solar combi systems with high efficient solar collectors, linear regression gives R-squared values in the range 0.2 to 0.5. Solar combi systems with high efficient solar collectors utilize less sunny periods relatively better than systems with low efficient solar collectors, especially if there is coincidence between solar radiation and heating demand. Hence, solar combi systems with high efficient solar collectors are more influenced by the weather variations than solar combi systems with low efficient solar collectors.

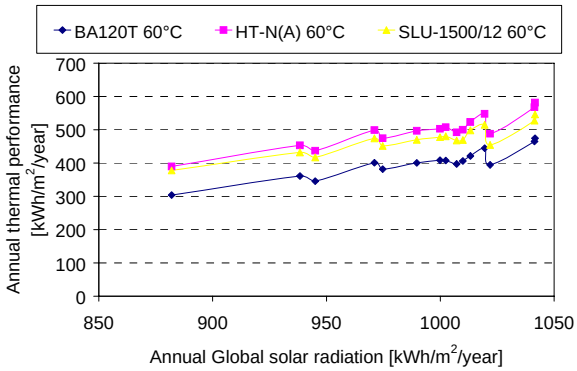

Figure 12: The annual thermal performance of solar collectors as a function of the annual global solar radiation.

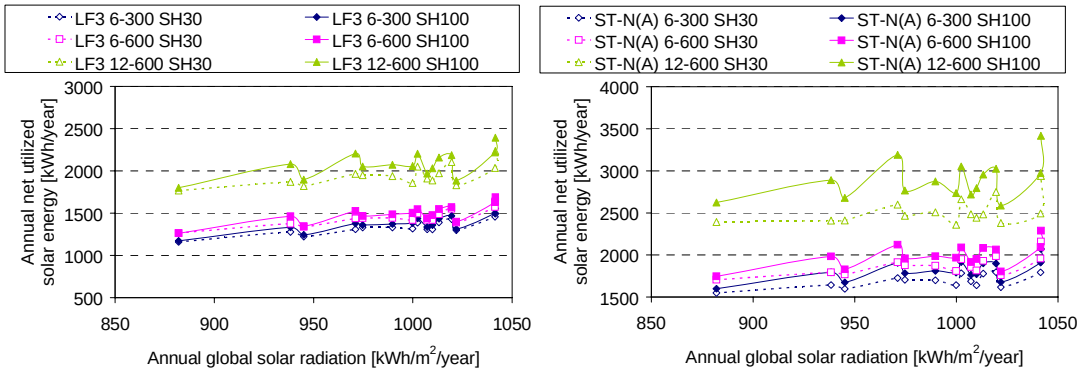

Figure 13: The annual net utilized solar energy for solar combi systems as a function of the annual global solar radiation.

5 Conclusions

The influence of the weather on the thermal performances of solar combi systems and solar collectors with different solar fractions is investigated theoretically.

Differently designed solar heating systems with different solar fractions including three solar combi systems, four marketed flat plate solar collectors and one marketed evacuated tubular solar collector are investigated.

The investigation is based on calculations with weather data from the Danish Design Reference Year and measured Danish weather data from 1990 to 2002. Although the results in the study are based on weather data from Denmark, the results are not specific for Danish conditions, but show how the thermal performances of solar heating systems are generally influenced by weather variations.

The investigations show that there is no reasonable linear relationship between the yearly global radiation and the yearly total solar radiation on a south facing 45º-tilted surface.

The annual thermal performance of solar collectors and of solar combi systems increases for increasing annual solar radiation.

The relationship between the yearly thermal performance and the yearly solar radiation can for all types of solar collectors be fitted to a linear relationship, with a good approximation for the yearly radiation on the solar collectors and with a reasonable approximation for the yearly global radiation.

It is not possible to fit the relationship between the yearly thermal performance of solar combi systems and the yearly global solar radiation or the yearly solar radiation on the collector to a linear equation.

The annual utilization of the solar radiation for all types of solar collectors is increasing for increasing annual solar radiation on the collector.

The annual utilization of solar radiation for solar combi systems is not significantly influenced by the annual solar radiation on the collector, regardless of the collector efficiency, the heating demand and the size of the solar heating system. However, the annual utilization of solar radiation is higher and varies more for solar combi systems with high efficient solar collectors than for systems with low efficient solar collectors.

Nomenclature

w	Width of shadow ring	[m]
r	Radius of shadow ring	[m]
Φ	Latitude of the installation	[°]
δ	Solar declination	[°]
γ_{ss}	Azimuth angle of the sun at sunset	[°]
ΔG_d	Fraction of diffuse radiation screened off by the shadow ring	[-]
k_d	Factor to correct the diffuse radiation for shadow ring	[-]
$k_{\Theta,long}$	Longitudinal incidence angle modifier for beam radiation	[-]
$k_{\Theta,trans}$	Transverse incidence angle modifier for beam radiation	[-]
$k_{\Theta,long,d}$	Longitudinal incidence angle modifier for diffuse radiation	[-]
$k_{\Theta,trans,d}$	Transverse incidence angle modifier for diffuse radiation	[-]
k_{Θ}	Incidence angle modifier	[-]
p	Incidence angle modifier coefficient	[-]
Θ	Incidence angle for beam radiation on tilted surface	[°]
$\Theta_{b,long}$	Longitudinal incidence angle for beam radiation on evacuated tubular solar collector	[°]
$\Theta_{b,trans}$	Transverse incidence angle for beam radiation on evacuated tubular solar collector	[°]
η	Solar collector efficiency	[-]
η_0	Optical efficiency of incident radiation	[-]
a_1	Solar collector heat loss coefficient	[W/m^{2}K]
a_2	Solar collector heat loss coefficient	[W/m^{2}K^2]
T_m	Mean temperature in the solar collector	[°C]
T_a	Ambient temperature	[°C]
Q	Useful solar collector power	[W/m^2]
G_b	Beam irradiance	[W/m^2]
G_d	Diffuse irradiance	[W/m^2]
G_t	Total irradiance	[W/m^2]
Q_{AUX}	Auxiliary energy consumption	[kWh]
Q_{DHW}	Domestic hot water load	[kWh]

Q_{NET}	Net utilized solar energy	[kWh]
$Q_{NET,REF}$	Net utilized solar energy of reference system	[kWh]
Q_{SH}	Space heating load	[kWh]
Q_{COL}	Energy produced by the solar collector	[kWh]
Q_{SOL}	Energy of the total solar radiation on the solar collector	[kWh]
USR	Utilization of solar radiation	[%]
PR	Performance ratio	[-]

References

Adsten M, Peres B and Wäckelgård E. 2001. The influence of climate and location on collector performance. Renewable Energy 25: 499-509.

Andersen E, Shah L J and Furbo S. 2004. Thermal performance of Danish solar combi systems in practice and in theory. Journal of Solar Energy Engineering: 744-749.

Cavalcanti E S C. 1991. Analysis of experimental solar radiation data for Rio de Janeiro, Brazil. Solar Energy 47, 3: 231-235.

Drück H. 2000. MULTIPORT Store – Model, Type 140 for TrnSys. Institut für Thermodynamik und Wärmetechnik. Universität Stuttgart.

Jensen K L, Nielsen T and Andersen K R. 2001. Solfangerydelser i solvarmecentraler ved forskellige temperaturniveauer. Student project at Department of Civil Engineering, Technical University of Denmark.

Klein S A et al. 1996. TRNSYS 14.1, User Manual. University of Wisconsin Solar Energy Laboratory

Qin L. and Furbo S. 1999. Evacuated Tubular Solar Collectors for Solar Heating Systems, Products from Chinese companies. Technical University of Denmark, report R-031, ISBN 87-7877-032-7.

Liu B Y H and Jordan R C. 1963. The Long-Term Average Performance of Flat-Plate Solar Energy Collectors. Solar Energy, 7, 53.

Perers B. 2000. A Solar Collector Model and Emulator for IEA Task 26, Description for Solar Thermal System Testing. Based on the CEN 12975 and the TRNSYS Type 132 Collector Model. Vattenfall Utveckling AB.

Salem A I, Gabr M, Saleem S and Bassyouni A H. 1993. Analysis of solar radiation measurements at El-Kharga (25ºN, 30ºE), Egypt. Mausam 44, 1: 39-44.

Siebers D L and Viskanta R. 1977. Comparison of Long-term flat-plate solar collector performance calculations based on averaged meteorological data. Solar Energy 19: 163-169.

Skertveit A, Lund H, Olseth J A. 1994. Design Reference Year. Det Norske Institutt. Report no. 1194 Klima. 12/1994.

Streicher W et al. 2002. SHC-Task 26: Solar Combisystems. Milestone report C 0.2.

U S Department of Energy. 1980. SHC-task 4. An introduction to meteorological measurements and data handling for solar energy applications. DOE/ER-0084.

Paper III

The Influence of the Solar Radiation model on the Calculated Solar Radiation from a Horizontal Surface to a Tilted Surface

Paper in proceedings: EuroSun 2004 Congress, Freiburg, Germany, 2004

The Influence of the Solar Radiation Model on the Calculated Solar Radiation from a Horizontal Surface to a Tilted Surface

Elsa Andersen, Hans Lund and Simon Furbo

Department of Civil Engineering Technical University of Denmark

DK-2800 Kgs. Lyngby, Denmark, e-mail: ean@byg.dtu.dk

Paper in proceedings: EuroSun 2004 Congress, Freiburg, Germany, 2004

Introduction

Measured solar radiation data are most commonly available as total solar radiation on a horizontal surface. When using solar radiation measured on horizontal to calculate the solar radiation on tilted surfaces and thereby the thermal performance of different applications such as buildings and solar heating systems, different solar radiation models can be used. The calculation of beam radiation from a horizontal surface to a tilted surface can be done exactly whereas different solar radiation models can calculate the sky diffuse radiation. The sky diffuse radiation can either be assumed evenly distributed over the entire sky dome and calculated as pure isotropic radiation or by anisotropic radiation models that also uses contribution from circumsolar radiation in the calculation or by anisotropic radiation models that apart from the isotropic and circumsolar contribution uses horizon brightening in the calculation.

The weather data are measured at the solar radiation measurement station, SMS at the Department of Civil Engineering at the Technical University of Denmark. In this study the weather data are combined with solar collector calculations based on solar collector test carried out at Solar Energy Center, SEC, Denmark.

With measured solar radiation on horizontal and the different solar radiation processing models the total radiation is calculated on differently tilted and oriented surfaces and compared with the measured solar radiation on the different surfaces. Further, the impact on the yearly thermal performances of a solar collector using the different solar radiation processing models is investigated. The study shows that the isotropic diffuse radiation model is underestimating the diffuse radiation from south and overestimating the diffuse radiation from north, while the anisotropic models give a better estimate on the diffuse radiation from all directions.

1 Measurements

The weather data are obtained by a solar radiation measurement station placed on the roof of a building at Department of Civil Engineering, DTU, Kgs. Lyngby, Denmark,

(Lund, 1994). The latitude of the station is 55.8°N and the longitude is 12.5°E. Towards south the neighbour building causes a horizontal screening of up to 3.5°. Figure 1 shows the 360° view from the weather station.

Figure 1: 360° view from weather station.

The measurements are recorded every 2 minutes either integrated over 2 minutes or instantaneous. From these 2 minutes data half hourly and hourly values are created. This study uses both half hourly and hourly values**.** The half hourly measurements include global and diffuse irradiance on horizontal, total radiation on a vertical surface facing south, east and north, total radiation on a 45° tilted south facing surface and the ambient temperature. The ground reflected diffuse radiation is excluded by an artificial horizon from the measurement on the vertical surfaces facing south and east. The half hourly weather data are from the year 2002 and include the months January, March, June, August, October, November and December.

The hourly data include the global irradiance, the diffuse irradiance on horizontal and the ambient temperature. The hourly weather data are from the period 1990 through 2002.

The irradiance is measured with Kipp and Zonen pyranometers CM11 and CM5. The half hourly diffuse irradiance on horizontal is measured with a disk that tracks the sun and blocks the beam radiation from the sun. The hourly diffuse irradiance on horizontal is measured with a shadow ring, width of 57 mm and radius of 325 mm. The temperature is measured with a PT1000 sensor.

For an isotropic model, the fraction of the diffuse radiation screened off by the shadow ring is given by (U.S. Department of Energy, 1980):

$$\Delta G_d = \frac{2 \cdot w}{\pi \cdot r} \cos^3 \delta \cdot \left(\gamma_{ss} \cdot \sin \Phi \cdot \sin \delta + \cos \Phi \cdot \cos \delta \cdot \sin \gamma_{ss} \right) \quad (1)$$

The correction factor to be applied to the hourly measured diffuse radiation is:

$$K_d = \frac{1}{\left(1 - \Delta G_d\right)} \quad (2)$$

Figure 2 shows the half hourly measured total radiation on a 45° tilted south facing surface and the total radiation on the vertical surfaces facing south, east and north. Figure 3 shows the hourly measured global radiation and the diffuse radiation on horizontal from the period 1990-2002. Further the global radiation and the diffuse radiation on horizontal from the Danish Design Reference Year, DRY (Skartveit, 1994) is shown. DRY is normally used to calculate the thermal performance of Danish solar heating systems.

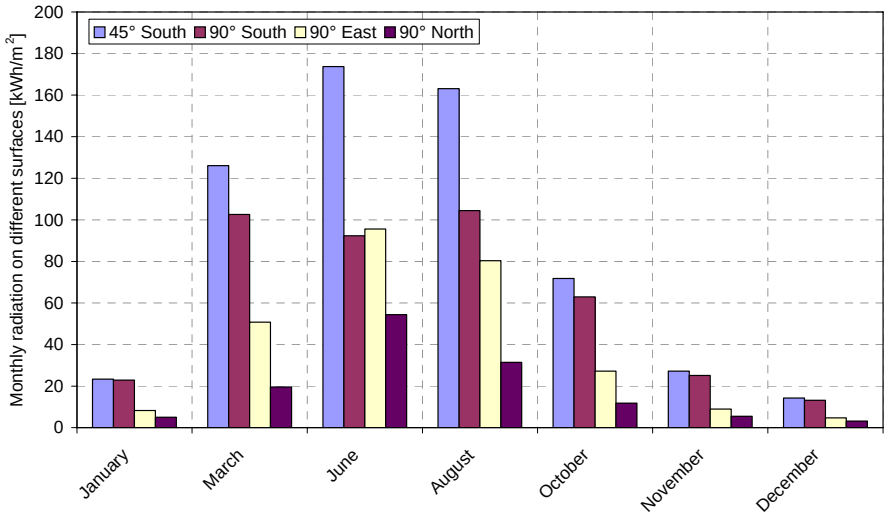

Figure 2: Measured monthly radiation from 2002.

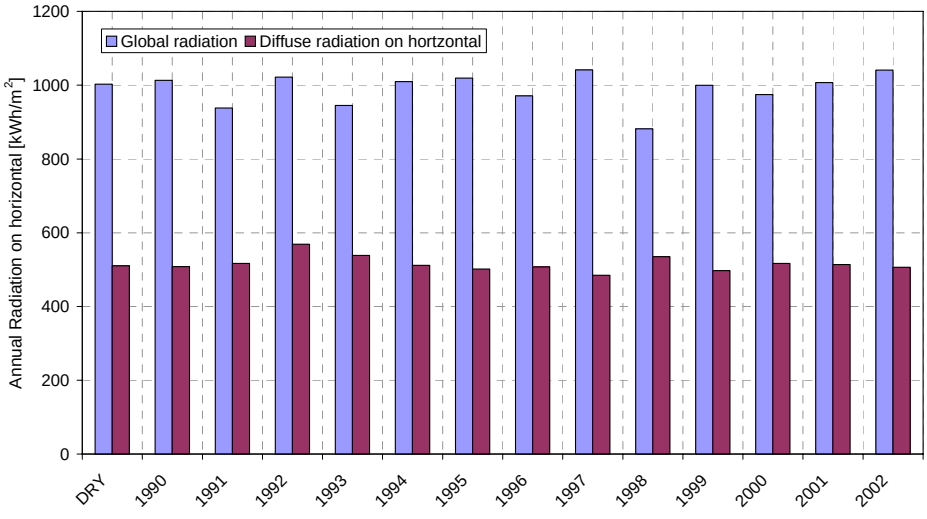

Figure 3: Measured yearly radiation from 1990-2002 and from DRY.

2 Accuracy analysis

The measured data is used to calculate the thermal performance of solar collectors. It is therefore relevant to calculate the accuracy of the compound measurements that leads to determination of the solar energy (Q) from the collectors.

The solar collector efficiency expression for all incidence angles is given by:

$$\eta = \eta_0 \cdot K_\Theta(\Theta) - a \cdot \left(\frac{T_m - T_a}{G} \right) \tag{3}$$

Where the incidence angle modifier for beam radiation is given by:

$$K_{\Theta}\left(\Theta\right) = 1 - \tan^{p}\left(\frac{\Theta}{2}\right) \tag{4}$$

The energy from the solar collector (Q) is calculated with a model developed by (Perers, 2000) that has a correction term for diffuse radiation. The diffuse radiation uses a separate incidence angle modifier that equals the incidence angle modifier for beam radiation at an incidence angle of 60°:

$$Q = A \cdot \left[\eta_0 \cdot k_{\Theta}(\Theta) \cdot G_b + \eta_0 \cdot k_{\Theta}(60^{\circ}) \cdot G_d - a_1 \cdot \left(T_m - T_a\right)\right] \tag{5}$$

The solar collector efficiency and the energy from the solar collector is the result of compound measurements and the result can be written as:

$$R = f\left(x, y, z...\right) \tag{6}$$

When the accuracies ($U_x, U_y, U_z...$) of the measurements are known the accuracy of the compound measurement can be calculated as:

$$U_R = \sqrt{\left(\frac{\partial f}{\partial x} \cdot U_x\right)^2 + \left(\frac{\partial f}{\partial y} \cdot U_y\right)^2 + ...} \tag{7}$$

The solar collector efficiency is measured according to the international standard (International organization of standardization, 1992). With a constant mass flow rate and high irradiance the instant solar collector efficiency (η) for incidence angles less than about 30° is measured for different reduced temperature differences (T^*). The solar collector efficiency equation is finally determined by linear regression:

$$\eta = \frac{\dot{m} \cdot c_p \cdot \Delta T}{A \cdot G} \tag{8}$$

$$T^* = \frac{T_i + \frac{\Delta T}{2} - T_a}{G} \tag{9}$$

The solar collector heat loss coefficient (a) is derived from the declination of the linear regression: $-\left(\frac{\eta_0 - \eta}{T^*(\eta_0) - T^*(\eta)}\right)$

Further the instant solar collector efficiency (η) for different large incidence angles is measured. These measurements are carried out for a solar collector mean temperature equal to the ambient temperature. The incidence angle modifier is then determined as:

$$K_{\Theta}\left(\Theta\right) = \frac{\eta}{\eta_0} \tag{10}$$

To calculate the accuracy of the energy from the solar collector (U_Q), the accuracy of the corrected temperature (U_{T^*}), the solar collector efficiency (U_{η}), the incidence angle modifier ($U_{K_{\Theta}(\Theta)}$) and the solar collector heat loss coefficient (U_a) are calculated:

$$\frac{U_{T^*}}{T^*} = \frac{1}{T^* G}\sqrt{\left(U_{T_i}\right)^2 + \left(\frac{U_{\Delta T}}{2}\right)^2 + \left(U_{T_a}\right)^2 + \left(T^* \cdot G \cdot \frac{U_G}{G}\right)^2} \tag{11}$$

$$\frac{U_\eta}{\eta} = \sqrt{\left(\frac{U_{\dot{m}}}{\dot{m}}\right)^2 + \left(\frac{U_{c_p}}{c_p}\right)^2 + \left(\frac{U_{\Delta T}}{\Delta T}\right)^2 + \left(\frac{U_A}{A}\right)^2 + \left(\frac{U_G}{G}\right)^2} \tag{12}$$

$$\frac{U_{K_\Theta(\Theta)}}{K_\Theta(\Theta)} = \sqrt{\left(\frac{U_\eta}{\eta}\right)^2 + \left(\frac{U_{\eta_0}}{\eta_0}\right)^2} \tag{13}$$

$$\frac{U_a}{a} = \sqrt{\left(\frac{\eta_0}{aT^*(\eta)} \cdot \frac{U_{\eta_0}}{\eta_0}\right)^2 + \left(\frac{\eta}{aT^*(\eta)} \cdot \frac{U_\eta}{\eta}\right)^2 + \left(\frac{U_{T^*(\eta)}}{T^*(\eta)}\right)^2} \tag{14}$$

The accuracy for the calculation with the isotropic model is found by:

$$\frac{U_Q}{Q} = \frac{A}{Q}\sqrt{\begin{aligned}&\left(\left(\eta_0 K_\Theta(\Theta) G_b + \eta_0 K_\Theta(60^\circ) G_d - a(T_m - T_a)\right)\frac{U_A}{A}\right)^2 \\ &+\left(\left(K_\Theta(\Theta) G_b + K_\Theta(60^\circ) G_d\right)\frac{U_{\eta_0}}{\eta_0}\eta_0\right)^2 + \left(\eta_0 G_b \frac{U_{K_\Theta(\Theta)}}{K_\Theta(\Theta)} K_\Theta(\Theta)\right)^2 \\ &+\left(\eta_0 G_d \frac{U_{K_\Theta(60^\circ)}}{K_\Theta(60^\circ)} K_\Theta(60^\circ)\right)^2 + \left(\eta_0 K_\Theta(\Theta)\frac{U_{G_b}}{G_b} G_b\right)^2 \\ &+\left(\eta_0 K_\Theta(60^\circ)\frac{U_{G_d}}{G_d} \cdot G_d\right)^2 + \left((T_m - T_a)\frac{U_a}{a} a\right)^2 + \left(aU_{T_m}\right)^2 + \left(aU_{T_a}\right)^2\end{aligned}} \tag{15}$$

The accuracy for the calculation with the anisotropic models uses a radiation term where the diffuse radiation is divided into isotropic diffuse and circumsolar diffuse where the latter is treated as beam radiation and hence uses the incidence angle modifier for beam radiation.

The energy from the solar collector is calculated from the global irradiance and the diffuse irradiance measured on horizontal. The accuracy of the different solar radiation models used to calculate the total radiations on the solar collector are neglected in the calculation of the accuracy of the energy from the solar collector.

Table 1 shows the measuring equipment and accuracy of the measuring equipment both for the solar radiation measurement station and the test facility for solar collector testing. Further, the accuracies of the compound measurements are shown.

Measurement / Symbol		Equipment / Accuracy
Solar irradiance (measured at SMS)	Global irradiance / G	Pyranometer CM11 / 1 %
	Diffuse irradiance on horizontal / G_d	Pyranometer CM11 / 1 %
	Total irradiance on 45° south / G_t	Pyranometer CM5 / 4 %
	Total irradiance on vertical south / G_t	Pyranometer CM11 /2 %
	Total irradiance on vertical east / G_t	Pyranometer CM5 / 4 %
	Total irradiance on vertical north / G_t	Pyranometer CM5 / 5 %
	Ambient temperature / T_a	Pt1000 / 0.5 K
Solar collector efficiendy (measured at SEC)	Solar collector inlet temperature / T_i	Pt100 / 0.1 K
	Temperature difference between solar collector inlet and outlet / ΔT	Pt100 / 0.05 K
	Ambient temperature / T_a	Pt100 / 0.2 K
	Solar collector mass flow / $\dot{m}$	Mass flow meter / 0.3 %
	Solar collector area / A	/ 0.1 %
	Heat capacity of solar collector fluid / c_p	/ 0.5 %
	Total irradiance in collector plane / G	Pyranometer PSP / 2 %
	Reduced temperature difference / T^*	/ 2.3 %
	Solar collector efficiency / η	/ 2.2 %
	Heat loss coefficient / a	/ 5.9 %
	Incidence angle modifier / $K_\Theta(\Theta)$	/ 3.1 %

Table 4: Data of measuring equipment and accuracy.

3 Solar radiation processing models

Four different models are used to calculate the total radiation on a tilted surface. The models are the isotropic diffuse model (Liu and Jordan, 1963) that assumes that the diffuse radiation is uniformly distributed over the entire sky dome, the anisotropic diffuse model (Hay and Davis, 1980) that also uses contribution from circumsolar radiation in the calculation and the anisotropic models (Reindl et al., 1990b) and (Perez et al., 1987, 1988) that apart from the isotropic and circumsolar contribution uses horizon brightening in the calculation. These models are also the solar radiation processing models used in the simulation program TrnSys (Klein et al., 1996) that is widely used for calculating the thermal performance of solar heating systems.

The total radiation on a tilted surface is calculated as the sum of the beam radiation (G_{bt}), the diffuse radiation (G_{dt}) and the ground reflected diffuse radiation (G_{gt}):

$$G_t = G_{bt} + G_{dt} + G_{gt} \tag{16}$$

The beam radiation on a tilted surface (G_{bt}) is calculated evenly for all the models by applying the geometric factor (R_b) to the measured beam radiation (G_b), (Hottel, 1942). The geometric factor is given by the ratio between the incidence angle on the tilted surface (Θ) and the incidence angle on horizontal, which is also the zenith angle (Θ_z):

$$G_{bT} = G_b \cdot R_b \tag{17}$$

$$R_b = \frac{\cos\Theta}{\cos\Theta_z} \tag{18}$$

$$\cos\Theta = \cos(\Phi - \beta)\cdot\cos\delta\cdot\cos\varpi + \sin(\Phi - \beta)\cdot\sin\delta \tag{19}$$

$$\cos\Theta_z = \cos\Phi\cdot\cos\delta\cdot\cos\varpi + \sin\Phi\cdot\sin\delta \tag{20}$$

The isotropic diffuse radiation model (Liu and Jordan, 1963) calculates the isotropic diffuse radiation (G_{dt}) by applying the view factor to the sky (R_d) to the measured diffuse radiation (G_d). The view factor is given by the ratio of diffuse radiation on the tilted surface to that on a horizontal surface:

$$G_{dt} = G_d \cdot R_d \tag{21}$$

$$R_d = \frac{(1+\cos\beta)}{2} \tag{22}$$

Under clear sky conditions there is an increased intensity of diffuse radiation in the area around the sun, called circumsolar radiation, and from the horizon, called horizon brightening. The anisotropic diffuse radiation models (Hay and Davis, 1980) and (Reindel et al., 1990b) weight the amount of circumsolar diffuse radiation by an anisotropic index (A_i). The circumsolar diffuse radiation is considered to be incident as beam radiation and hence multiplied with the geometric factor (R_b). The remaining part of the diffuse radiation is treated as isotropic diffuse radiation. The model (Reindl et al., 1990b) includes the horizontal brightening as a supplementary to the isotropic diffuse radiation.

The anisotropic diffuse radiation model (Hay and Davis, 1980) calculates the diffuse radiation (G_{dt}) as isotropic diffuse and circumsolar diffuse:

$$G_{dt} = G_d \cdot \left((1 - A_i)\cdot R_d + A_i \cdot R_b\right) \tag{23}$$

$$A_i = \frac{G_{bn}}{G_{on}} \tag{24}$$

The anisotropic diffuse radiation model (Reindl et al., 1990b) calculates the diffuse radiation (G_{dt}) by adding a term for the horizon brightening to the model (Hay and Davis, 1980). The horizon brightening term was proposed by (Klucher, 1979). Hence the model is referred to as HDKR:

$$G_{dt} = G_d \cdot \left((1 - A_i) \cdot R_d \cdot \left(1 + f \cdot \sin^3\left(\frac{\beta}{2}\right)\right) + A_i \cdot R_b \right) \tag{25}$$

$$f = \sqrt{\frac{G_b}{G}} \tag{26}$$

The anisotropic diffuse radiation model (Perez et al., 1987, 1988) calculates the diffuse radiation (G_{dt}) by calculating the circumsolar coefficient (F_1) and the horizon brightening coefficient (F_2). The brightness coefficients are calculated as linear combination of the brightness index (Δ) and the zenith angle (Θ_z) and for different intervals of the clearness index (ε) different coefficients ($f_{11}, f_{12}, f_{13}, f_{21}, f_{22}, f_{23}$) are derived. The coefficients used are the coefficients from the simulation program TrnSys (Klein et al., 1996). The clearness and brightness index describe the characteristics of the atmosphere in terms of cloudiness and optical depth:

$$G_{dt} = G_d \cdot \left((1 - F_1) \cdot R_d + F_1 \cdot \frac{a}{b} + F_2 \cdot \sin(\beta) \right) \tag{27}$$

$$a = \max[0, \cos(\Theta)] \tag{28}$$

$$b = \max[\cos(85^\circ), \cos(\Theta_z)] \tag{29}$$

$$F_1 = \max\left[0, \left(f_{11} + f_{12} \cdot \Delta + \frac{\pi \cdot \Theta_z}{180} \cdot f_{13} \right) \right] \tag{30}$$

$$F_2 = \left(f_{21} + f_{22} \cdot \Delta + \frac{\pi \cdot \Theta_z}{180} \cdot f_{23} \right) \tag{31}$$

$$\varepsilon = \frac{\frac{G_d + G_n}{G_d} + 5.535 \cdot 10^{-6} \cdot \Theta_z^3}{1 + 5.535 \cdot 10^{-6} \cdot \Theta_z^3} \tag{32}$$

$$\Delta = m \frac{G_d}{G_{on}} \tag{33}$$

The reflected radiation on the tilted surface (G_{gt}) is calculated by applying the reflectance of the total solar radiation from the surroundings (ρ_g) and the view factor to the ground (R_r) to the measured global radiation (G). The view factor is given by the ratio of reflected radiation on the tilted surface to the global radiation:

$$G_{gt} = G \cdot \rho_g \cdot R_r \tag{34}$$

$$R_r = \frac{(1 - \cos\beta)}{2} \tag{35}$$

The reflected radiation on the tilted surface is considered as diffuse radiation.

4 Comparison of measured and calculated solar radiation

Figure 4-Figure 7 show the total solar radiation calculated with the four different solar radiation models and the measured total solar radiation from the half hourly measurements from 2002. Also the accuracy of the measured solar radiation is shown.

From the figures, it can be seen that there is a good degree of similarity between the solar radiation calculations with the anisotropic models and the measured solar radiation for all surfaces and periods with the exception of vertical surfaces facing south and east in the summer time. The anisotropic diffuse radiation models weights a part of the diffuse radiation as circumsolar diffuse and the remaining part as isotropic radiation. Therefore the calculated radiation with the anisotropic models on south facing surfaces is higher than the calculated radiation with the isotropic model. For the north facing surface, which receives almost only diffuse radiation the calculated radiation is higher with the isotropic diffuse radiation model because this model calculates all the diffuse radiation as isotropic. The isotropic model was the first developed model and the anisotropic models are all further developments of the first model and are, as show in the figures, better suited for calculating radiation from a horizontal surface to a tilted surfaces.

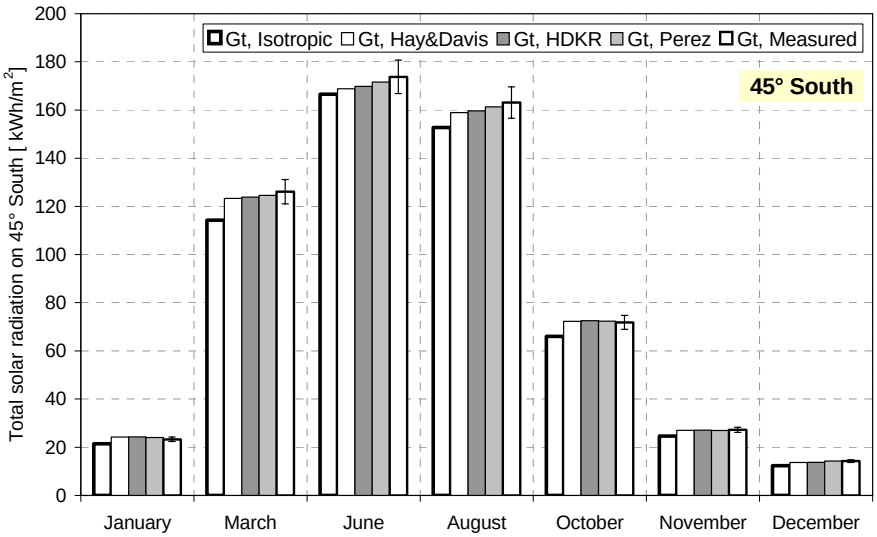

Figure 4: Measured and calculated total radiation on a south oriented 45º tilted surface with the half hourly measured weather data from 2002.

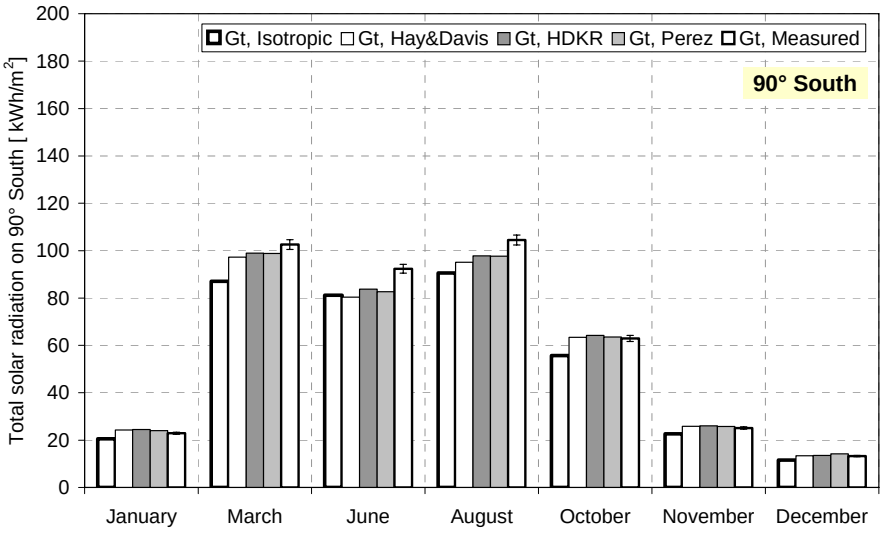

Figure 5: Measured and calculated total radiation on a south oriented 90º tilted surface with the half hourly measured weather data from 2002.

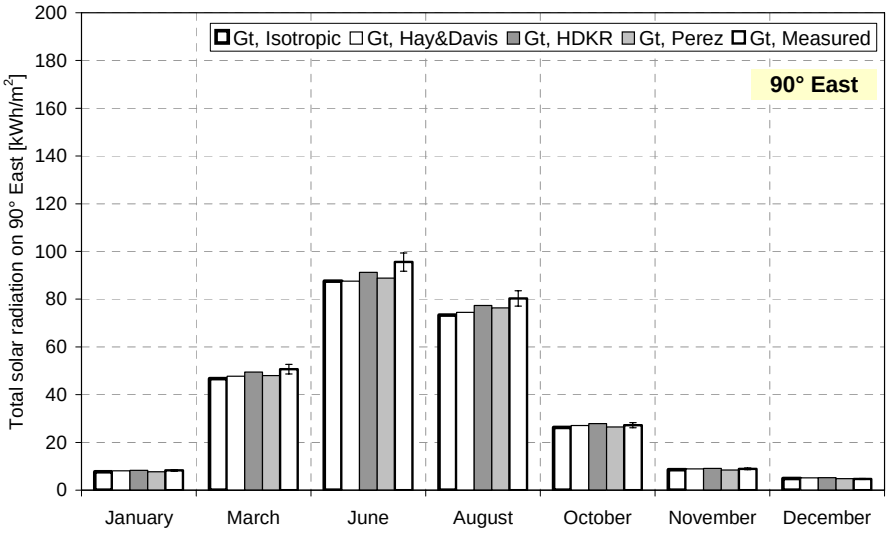

Figure 6: Measured and calculated total radiation on a east oriented 90º tilted surface with the half hourly measured weather data from 2002.

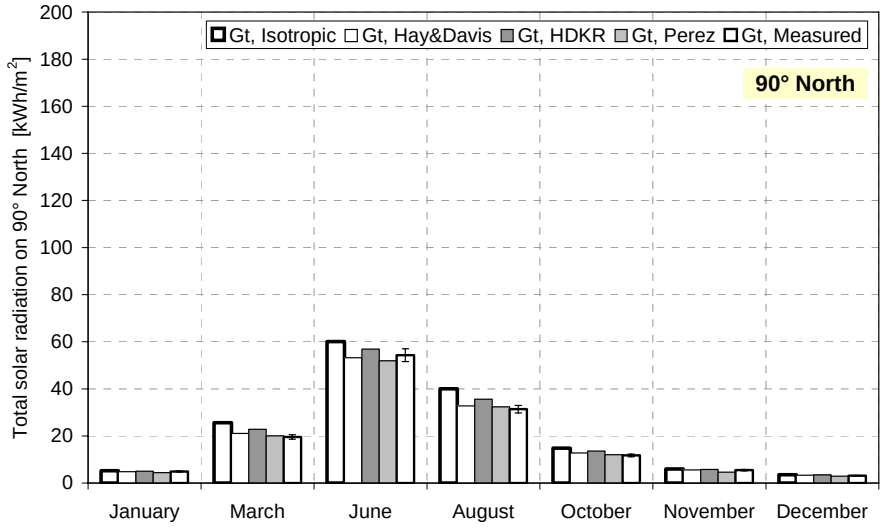

Figure 7: Measured and calculated total radiation on a north oriented 90º tilted surface with the half hourly measured weather data from 2002.

5 Calculated thermal performance of a solar collector based on different solar radiation processing models

The calculations are carried out with the hourly measured weather data from the period 1990-2002 and DRY. The four solar radiation processing models are used to calculate the total solar radiation on the collector surface from measured global and diffuse radiation on horizontal.

The calculation is based on a marketed solar collector from the Danish company Arcon Solvarme A/S. The linear solar collector efficiency expression for all incidence angles is:

$$\eta = 0.82 \cdot K_{\Theta}(\Theta) - 2.64 \cdot \frac{(T_m - T_a)}{G}$$

$$K_{\Theta}(\Theta) = 1 - \tan^{3.6}\left(\frac{\Theta}{2}\right)$$

Figure 8-Figure 13 show the calculated energy from the solar collector at a constant solar collector fluid temperature of 40°C throughout the year with a collector tilt of 45° and 90°. Calculations are carried out for the solar collector facing south, east and west. Further, the accuracy of the calculation is shown.

The calculated energy using the isotropic solar radiation model is lower than the calculated energy using the anisotropic models. The calculations that use the anisotropic models are very similar. Also the figure shows that the variation in the calculated energy from the solar collector from one year to another varies much more than the calculated energy output from one year using different solar radiation models.

Table 2 shows the calculated mean value of the energy from the solar collector from 1990-2002.

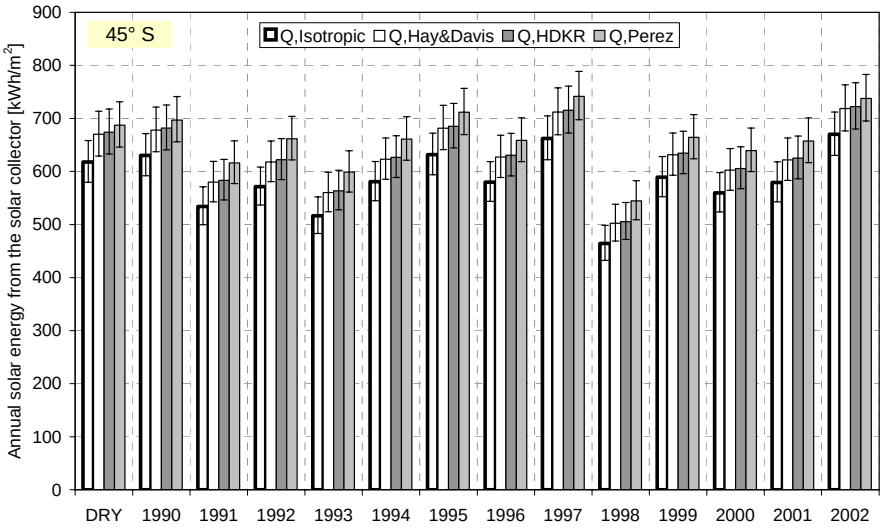

Figure 8: Calculated energy from a south facing 45º tilted solar collector with the hourly measured weather data from 1990-2002 and DRY.

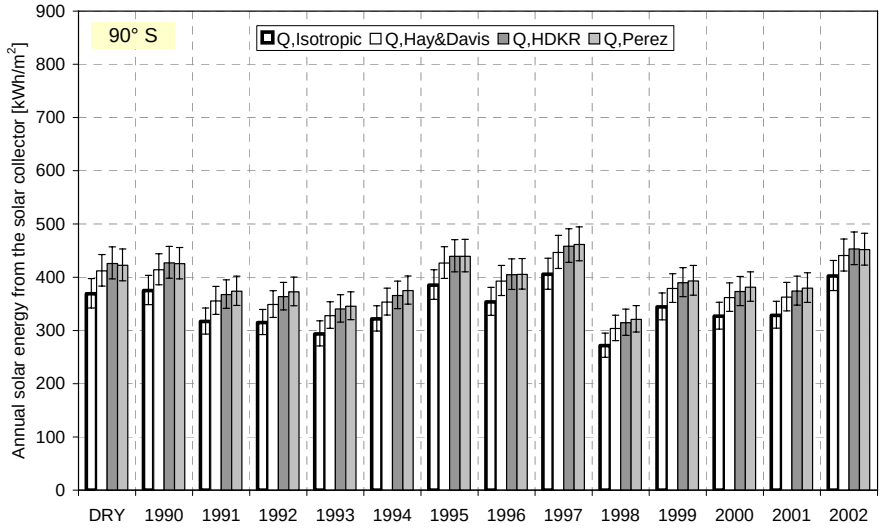

Figure 9: Calculated energy from a south facing 90º tilted solar collector with the hourly measured weather data from 1990-2002 and DRY.

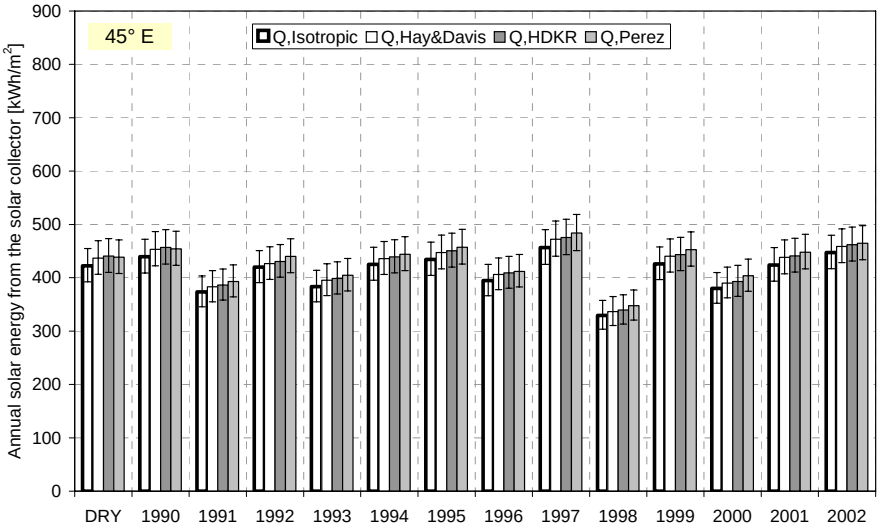

Figure 10: Calculated energy from a east facing 45º tilted solar collector with the hourly measured weather data from 1990-2002 and DRY.

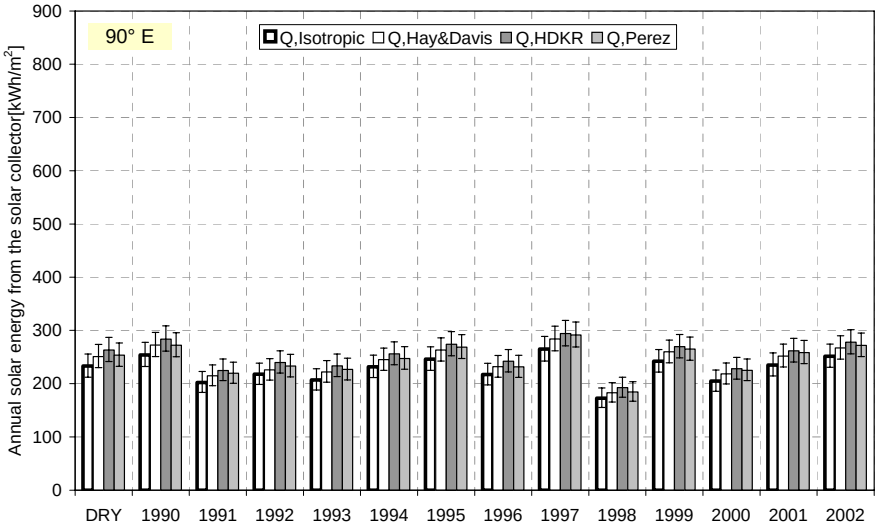

Figure 11: Calculated energy from a east facing 90º tilted solar collector with the hourly measured weather data from 1990-2002 and DRY.

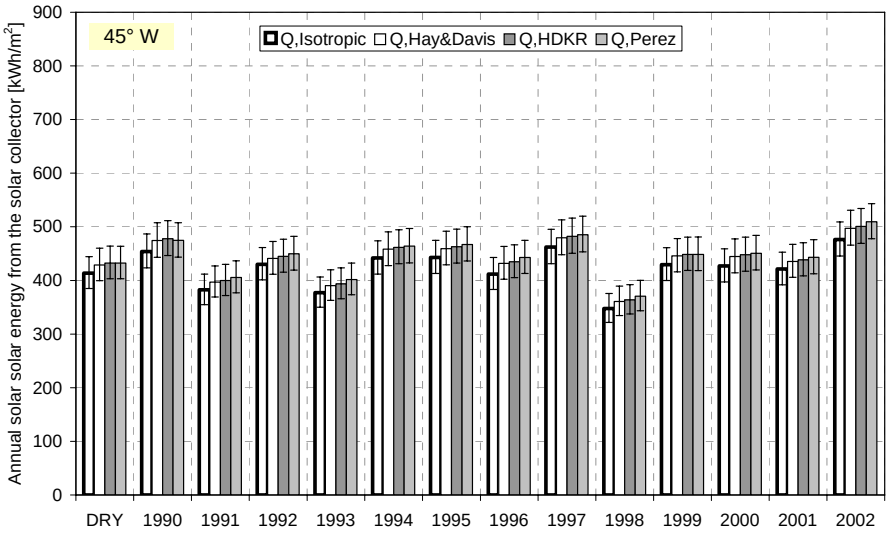

Figure 12: Calculated energy from a west facing 45º tilted solar collector with the hourly measured weather data from 1990-2002 and DRY.

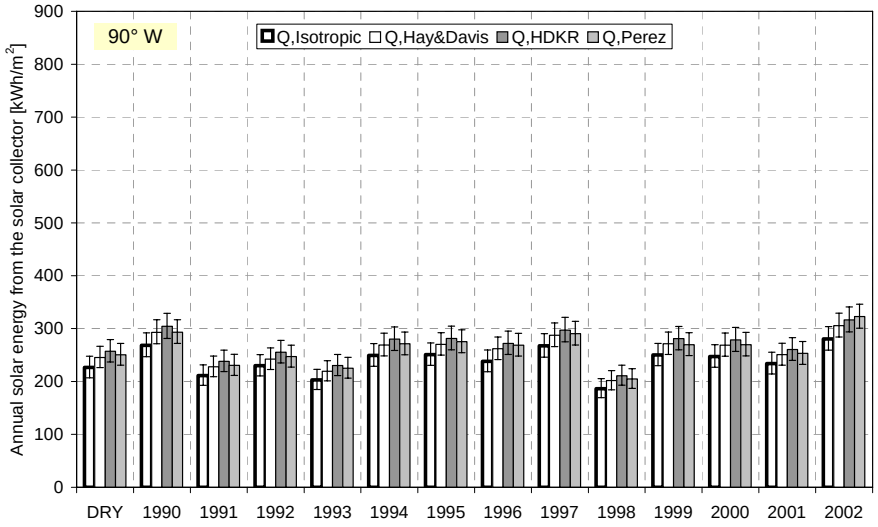

Figure 13: Calculated energy from a west facing 90º tilted solar collector with the hourly measured weather data from 1990-2002 and DRY.

	Q, Isotropic (1990-2002)	Q, Hay&Davis (1990-2002)	Q, HDKR (1990-2002)	Q, Perez (1990-2002)
45° South	582	627	631	661
90° South	341	378	390	394
45° West	423	440	443	447
90° West	240	259	270	263
45° East	410	422	425	431
90° East	227	241	252	246

Table 2: Mean value of the calculated energy from the solar collector from 1990-2002.

6 Conclusion

The influence of the solar radiation model on the calculated solar radiation from a horizontal surface to differently tilted and oriented surfaces is investigated. Four different models are used to calculate the total radiation on tilted surfaces from measured horizontal radiation. The solar radiation models used are the isotropic model (Liu and Jordan, 1963) and the anisotropic models (Hay and Davis, 1980), (Reindl et al., 1990b) and (Perez et al., 1987, 1988). The calculated radiation on the different surfaces is compared to measured radiation. The investigation shows that the anisotropic models are better suited for calculating the radiation from horizontal to tilted surfaces than the isotropic model. Further the investigation shows that there is a good degree of similarity between the solar radiation calculations with the anisotropic models and the measured solar radiation for all surfaces and periods with the exception of vertical surfaces facing south and east in the summer time.

Also the influence on the energy from a solar collector calculated with the four different solar radiation processing models is investigated. Measured horizontal radiation from 1990 through 2002 is used in the calculations. The investigation shows that the calculated energy from the solar collector using the isotropic solar radiation model is lower than the calculated energy using the anisotropic models. The calculations that use the anisotropic models are very similar. From this investigation it can be concluded that the anisotropic models by (Reindl et al., 1990b) and (Perez et al., 1987, 1988) are best suited for processing solar radiation from horizontal to tilted surfaces. Also the investigation shows that the variation in the calculated energy from the solar collector from one year to another varies much more than the calculated energy output from one year using different solar radiation models.

Nomenclature

w, r	width and radius of shadow ring	[m]
Φ	latitude of the installation	[°]
δ	solar declination	[°]

γ_{ss}	azimuth angle of the sun at sunset	[°]
ΔG_d	fraction of diffuse radiation screened off by the shadow ring	[-]
K_d	factor to correct the diffuse radiation for shadow ring	[-]
$K_\Theta(\Theta)$	incidence angle modifier	[-]
p	incidence angle modifier coefficient	[-]
Θ	incidence angle for beam radiation on tilted surface	[°]
Θ_z	zenith angle	[°]
η	solar collector efficiency	[-]
η_0	start efficiency of the solar collector	[-]
a	solar collector heat loss coefficient	[W/m^{2}K]
T_m	mean temperature in the solar collector	[°C]
T_a	ambient temperature	[°C]
ΔT	temperature difference	[K]
Q	useful solar collector energy	[kWh]
A	Solar collector area	[m^2]
T^*	reduced temperature difference	[Km^2/W]
$\dot{m}$	mass flow rate	[kg/s]
c_p	specific heat capacity	[J/kgK]
ϖ	hour angle	[°]
ε, Δ	clearness index and brightness index	[-]
m	air mass	[-]
A_i	anisotropic index	[-]
β	slope	[°]
F_1, F_2	brightness coefficients	[-]
$f_{11} \ldots f_{23}$	brightness coefficients	[-]
G	global irradiance	[W/m^2]
G_{bn}, G_{on}	normal incident beam and extraterrestrial irradiance	[W/m^2]
G_t, G_b, G_d	total, beam and diffuse irradiance on horizontal	[W/m^2]
G_{bt}, G_{dt}, G_{gt}	beam, diffuse and ground reflected irradiance on tilted surface	[W/m^2]
R_b	geometric factor	[-]

R_d	ratio of diffuse irradiance on a tilted surface to that on a horizontal surface	[-]
R_r	ratio of reflected irradiance on a tilted surface to the global radiation	[-]
ρ_g	ground reflectance	[-]
U_z	accuracy	[same unit as z]

Reference

Hay J.E. and Davis J.A. (1980). Calculation of the Solar Radiation Incident on an Inclined Surface. Proc. First Canadian Solar Radiation Data Workshop (Hay J.E. and Won T.K., eds.), Ministry of Supply and Services Canada, 59.

Hottel H.C. and Woertz B.B. (1942). Performance of Flat-Plate Solar Heat Collectors. Trans. ASME, 64, 91.

International organization of standardization (1992). Draft international standard ISO/DS 9806-1.2. Thermal performance tests for solar collectors, Part 1.

Klein S.A et al. (1996). TRNSYS 14.1, User Manual. University of Wisconsin Solar Energy Laboratory

Klucher T.M. (1979). Evaluating Models to Predict Insolation on Tilted Surfaces. Solar Energy, 23, 111.

Liu B.Y.H. and R.C Jordan, (1963). The Long-Term Average Performance of Flat-Plate Solar Energy Collectors. Solar Energy, 7, 53.

Lund H. (1994). Solar measurement station. Thermal Insulation Laboratory. Technical University of Denmark. Report 94-18.

Perers B. (2000). A Solar Collector Model and Emulator for IEA Task 26, Description for Solar Thermal System Testing. Based on the CEN 12975 and the TRNSYS Type 132 Collector Model. Vattenfall Utveckling AB.

Perez R., Seals P., Ineichen P., Stewart R. and Menicucci (1987). A new Simplified Version of the Perez Diffusion Irradiation Model for Tilted Surfaces. Solar Energy, 39, 221.

Perez R., Stewart R., Seals P. and Guertin T. (1988). The Development and Verification of the Perez Diffuse Radiation Model. Sandia National Laboratories Contractor Report SAND88-7030.

Reindl D.T., Beckman W.A. and Duffie J.A. (1990b). Evaluation of Hourly Tilted Surface Radiation Models. Solar Energy, 45, 9.

U.S. Department of Energy (1980). SHC-task 4. An introduction to meteorological measurements and data handling for solar energy applications. DOE/ER-0084.

Skartveit A., Lund H., Olseth J.A (1994). Design Reference Year. Det Norske Institutt. Report no. 1194 Klima. 12/1994.

Paper IV

Advantages by discharge from different levels in solar storage tanks

Journal of Solar Energy 79 (5), pp. 431 – 439, 2005

Advantages by discharge from different levels in solar storage tanks

Simon Furbo, Elsa Andersen, Alexander Thür, Louise Jivan Shah and Karin Dyhr Andersen

Department of Civil Engineering, Technical University of Denmark, Building 118, DK-2800 Kgs. Lyngby, Denmark

Journal of Solar Energy 79 (5), pp. 431 – 439, 2005

Abstract

The thermal advantages by utilizing discharge from different levels in solar storage tanks are investigated, both for a small SDHW system and for a solar combisystem.

The investigations showed that it is possible to increase the thermal performance of both types of systems by using two draw-off levels from the solar tanks instead of one draw-off level at a fixed position.

The best position of the second draw-off level is in the middle or just above the middle of the tank.

For the investigated small SDHW system with a realistic draw off hot water temperature of 40°C and 45°C and an auxiliary volume temperature of 50.5°C the increase of the thermal performance by the second draw-off level is about 6%.

For the investigated solar combisystem the extra thermal performance by using one extra draw-off level, either for the domestic hot water heat exchanger or for the heating system, is about 3%, while an improvement of about 5% is possible by using a second draw-off level both for the domestic hot water heat exchanger and for the heating system.

Keywords SDHW systems, solar combisystems, heat storage tanks, thermal stratification, advanced discharge strategies

1 Introduction

The thermal performance of solar heating systems is strongly influenced by the thermal stratification in the heat storage tank. Investigations by van Koppen et al. (1979) showed that the thermal performance is increasing for increasing thermal stratification in the heat storage.

Thermal stratification in solar storage tanks is normally established in two ways:

- During charge periods, where heat from the auxiliary energy supply system or from the solar collectors is transferred to the "right" level of the tank. That is, the heat from the auxiliary energy supply system is normally transferred to the top of the tank and the solar heat is transferred to the level in the storage tank, where the tank temperature is close to the temperature of the incoming fluid transferring the solar heat to the tank. Furbo and Mikkelsen (1987), Shah and Furbo (1998) and Knudsen and Furbo (2004) showed that for small SDHW systems this is with advantage done by means of a vertical mantle heat exchanger. For large SDHW systems and for solar combisystems this is with advantage done by means of inlet stratifiers as shown by Weiss (2003), Furbo et al. (2004) and Andersen et al. (2004).

- During discharge periods where heat is discharged from a fixed level of the tank, for instance from the top of the tank for SDHW systems or from a level just above the lower level of the auxiliary volume in a storage tank for solar combisystems. Thermal stratification is best established during discharge if cold water enters the bottom of the tank in SDHW systems during draw-offs, and if the returning water from the heating system enters the tank through inlet stratifiers in solar combisystems as described by Weiss (2003).

Thermal stratification can be built up to a greater extent than normally if the solar tank is discharged from more than one level, as proposed by Furbo (1984) and Lorenz (2001). For instance, a hot water tank for SDHW systems can be equipped with two draw-off pipes, one at the very top of the tank and one at the middle of the tank. In periods where the temperature at the top of the tank is higher than the required hot water temperature, a part of the hot water can with advantage be tapped at a lower temperature through the lower draw-off pipe. In this way the volume of the cold water entering the tank during draw-off is increased, resulting in increased solar collector efficiency, decreased tank heat loss, decreased auxiliary energy supply and consequently increased thermal performance of the SDHW system.

Solar combisystems making use of two draw-off levels in the solar tanks are marketed by Jenni Energietechnik AG (2004).

This paper presents the results of theoretical as well as experimental investigations of the thermal advantage of discharge from different levels in solar storage tanks, both for SDHW systems and for solar combisystems.

2 Solar domstic hot water systems

2.1 Experiments

2.1.1 System design

Two small low flow SDHW systems were tested side-by-side in a laboratory test facility for solar heating systems. With the exception of the solar tank the systems were identical.

Figure 1 shows schematic illustrations of the two tanks. Both tanks are standard mantle tanks suitable for low flow systems. In both tanks the auxiliary energy is supplied by electric heating elements. One tank is equipped with a PEX pipe for hot water draw-off from the very top of the tank.

The other tank is equipped with two PEX pipes for hot water draw-off from the very top of the tank and from the middle of the tank.

A three way valve, type RAVI from Danfoss A/S, ensures that the temperature of the tapped water from the tank during draw-offs is equal to the required hot water temperature. If this is not possible due to high tank temperatures, the valve ensures that the difference between the tapped water temperature and the required hot water temperature is as low as possible. That is, the three way valve ensures that the right part of the hot water is tapped from the top and from the middle of the tank.

The most important data of the tested systems are given in Table 1.

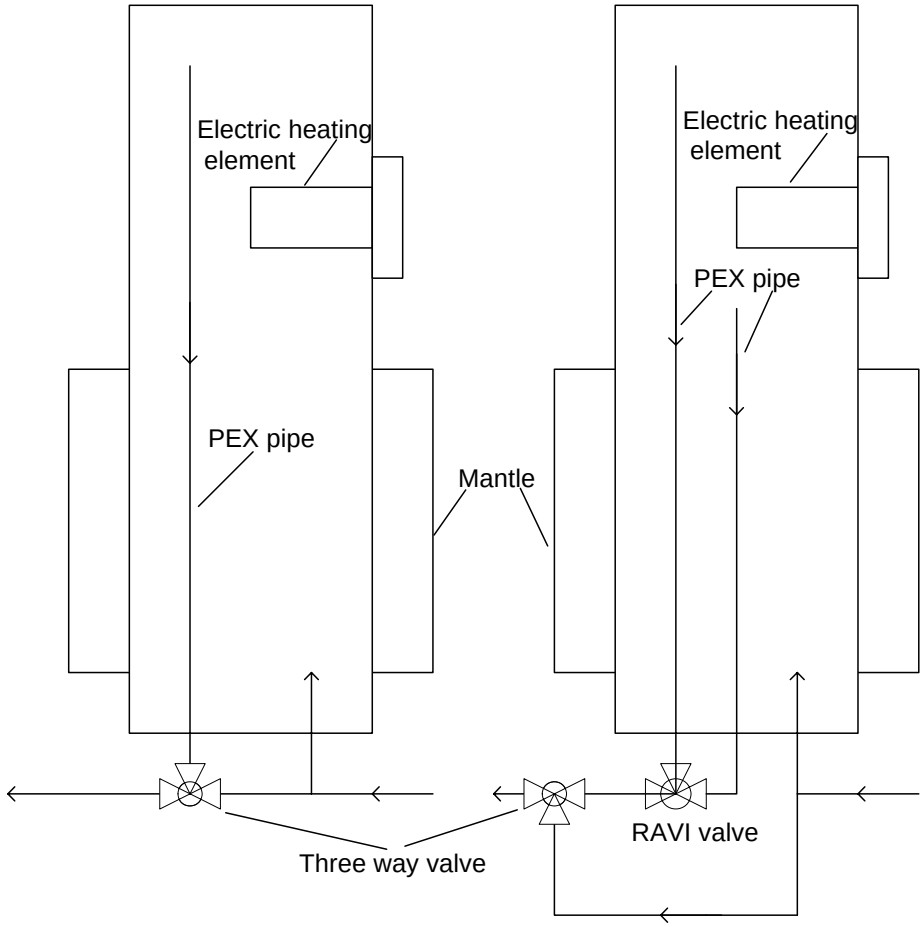

Figure 1: Schematic illustration of the two investigated solar tanks.

Table 1: Data for the two SDHW systems in the side-by-side laboratory test.

Tank design – Nilan A/S	
Hot-water tank volume, [m³]	0.175
Inner height / inner diameter [m]	1.45 / 0.394
Tank wall thickness, [m]	0.003
Auxiliary volume, [m³]	0.063
Draw-off level(s)	1.44 m/1.44 m and 0.87 m from bottom of tank
Power of electric heating element, [W]	1200

Mantle volume, [m³]	0.0319
Mantle height / mantle gap, [m]	0.7 / 0.0335
Position of mantle inlet	Top
Inside diameter of mantle inlet, [m]	0.0189
Material	Mineral wool
Insulation top, [m]	0.13
Insulation side above/below mantle, [m]	0.06
Insulation side mantle, [m]	0.06
Insulation bottom, [m]	0.0
Solar collector – Type: ST-NA, Arcon Solvarme A/S	
Area, [m²]	2.51
Start efficiency, [-]	0.81
1st order heat loss coefficient, [W/m²·K]	3.21
2nd order heat loss coefficient, [W/m²·K²]	0.013
Incident angle modifier (tangens equation)	a = 3.6
Heat capacity, [J/m²·K]	5339
Tilt, [º]	45
Orientation	South
Solar collector loop	
Flow rate, [l/min]	0.5
Pipe material	Copper
Outer / inner diameter, [m]	0.010 / 0.008
Insulation thickness (PUR foam), [m]	0.01
Length of pipe from storage to collector, indoor, [m]	4.6
Length of pipe from storage to collector, outdoor, [m]	13.3
Length of pipe from collector to storage, indoor, [m]	5.1
Length of pipe from collector to storage, outdoor, [m]	10.0
Solar collector fluid (propylene glycol / water mixture), [%]	40
Power of circulation pump, [W]	50
Control system - Danotek	
Type: DTP 2200 Differential temperature controller with one temperature sensor in the top of the collector and one temperature sensor at the bottom of the mantle	
Start / stop temperature difference, [K]	10 / 2

2.1.2 Operating conditions

The electric heating elements heat up the top volume to 53°C during all hours.

The solar irradiance on the collectors and the daily hot water consumption are the same for both systems. An energy quantity of 1.53 kWh, corresponding to 33 l of hot water heated from 10°C to 50°C or 36 l of hot water heated from 10°C to 47°C is tapped from each system three times each day: 7 am, 12 am and 7 pm.

2.1.3 Measured results

Measured energy quantities for 6 weeks with a draw-off temperature of 50°C are given in Table 2 and measured energy quantities for 7 weeks with a draw-off temperature of 47°C are given in Table 3. The net utilized solar energy is the tapped energy from the solar tank minus the energy supply to the electric heating elements.

For the 6 weeks test period with a hot water draw-off temperature of 50°C the net utilized solar energy for the solar heating system with two draw-off levels is 8 kWh higher than the net utilized solar energy for the standard system. For the 7 weeks test period with a hot water draw-off temperature of 47°C the net utilized solar energy for the solar heating system with two draw-off levels is 18 kWh higher than the net utilized solar energy for the standard system.

The thermal performance of the systems is small, since the tests were carried out in the winter. The thermal advantage of two draw-off levels is higher for a draw-off temperature of 47°C than for a draw-off temperature of 50°C.

Table 2: Measured thermal performance for the two tested systems with a hot water draw-off temperature of 50°C.

	Standard system			System with two draw-off levels		
Period	Tapped energy	Auxiliary energy	Net utilized solar energy	Tapped energy	Auxiliary energy	Net utilized solar energy
15-21/10-03	32 kWh	25 kWh	7 kWh	32 kWh	23 kWh	9 kWh
22-28/10-03	32 kWh	25 kWh	7 kWh	32 kWh	23 kWh	9 kWh
29/10-4/11-03	32 kWh	33 kWh	-1 kWh	32 kWh	32 kWh	0 kWh
5-11/11-03	32 kWh	35 kWh	-3 kWh	32 kWh	33 kWh	-1 kWh
1-7/12-03	32 kWh	35 kWh	-3 kWh	32 kWh	35 kWh	-3 kWh
17-23/12-03	32 kWh	33 kWh	-1 kWh	32 kWh	32 kWh	0 kWh
6 weeks	192 kWh	186 kWh	6 kWh	192 kWh	178 kWh	14 kWh

Table 3: Measured thermal performance for two tested systems with a hot water draw-off temperature of 47°C.

	Standard system			System with two draw-off levels		
Period	Tapped energy	Auxiliary energy	Net utilized solar energy	Tapped energy	Auxiliary energy	Net utilized solar energy
9-15/2-04	32 kWh	28 kWh	4 kWh	32 kWh	27 kWh	5 kWh
16-22/2-04	32 kWh	17 kWh	15 kWh	32 kWh	14 kWh	18 kWh
23-29/2-04	32 kWh	26 kWh	6 kWh	32 kWh	23 kWh	9 kWh
1-7/3-04	32 kWh	17 kWh	15 kWh	32 kWh	13 kWh	19 kWh
11-17/3-04	32 kWh	20 kWh	12 kWh	32 kWh	17 kWh	15 kWh
18-24/3-04	32 kWh	18 kWh	14 kWh	32 kWh	16 kWh	16 kWh
25-31/3-04	32 kWh	21 kWh	11 kWh	32 kWh	19 kWh	13 kWh
7 weeks	224 kWh	147 kWh	77 kWh	224 kWh	129 kWh	95 kWh

2.2 Calculation

2.2.1 Simulation model

Calculations were carried out with the simulation model Mantlsim developed at the Technical University of Denmark by Furbo and Berg (1990), Shah and Furbo (1998), Knudsen and Furbo (2004) and Furbo and Knudsen (2004). The two tested low flow systems with the data given in Table 1 are taken into calculation. Weather data of the Danish Test Reference Year developed by Statens Byggeforskningsinstitut (1982) is used in the calculations.

The daily hot water consumption is 4.6 kWh, corresponding to 100 l water heated from 10°C to 50°C. Hot water is tapped with an energy quantity of 1.53 kWh three times each day: 7 am, 12 am and 7 pm. The required hot water draw-off temperature is 50°C.

The thermal performance of the system with the two draw-off levels was calculated with one draw-off pipe at the very top of the tank and with different positions of the second draw-off level.

2.2.2 Simulation results

Figure 2 shows the calculated yearly net utilized solar energy of the system as a function of the relative position of the second draw-off level and as a function of the auxiliary set point temperature.

Figure 3 shows the calculated yearly percentage increase of the net utilized solar energy by using a second draw-off pipe as functions of the relative position of the second draw-off level and the set point temperature for the auxiliary energy system. If

the relative position of the second draw-off level is at the top of the tank, the system is identical to the standard system with only one draw-off level at the very top of the tank. The thermal advantage of using a second draw-off pipe is strongly influenced by the auxiliary set point temperature. The higher the set point temperature the larger the advantage. If the auxiliary set point temperature is only 0.5 K higher than the required draw-off hot water temperature, the extra thermal performance by using a second draw-off level is about 1%. If the auxiliary set point temperature is 15 K higher than the required hot water temperature, the extra thermal performance by using a second draw-off level is about 13%. The second draw-off level is best placed in the middle of the tank.

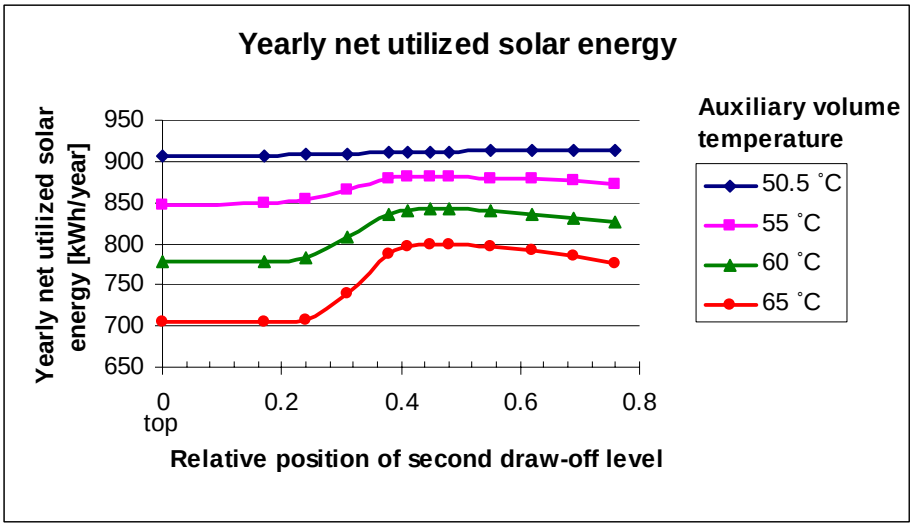

Figure 2: Calculated net utilized solar energy of the SDHW system as functions of the position of the second draw-off level and of the auxiliary set point temperature.

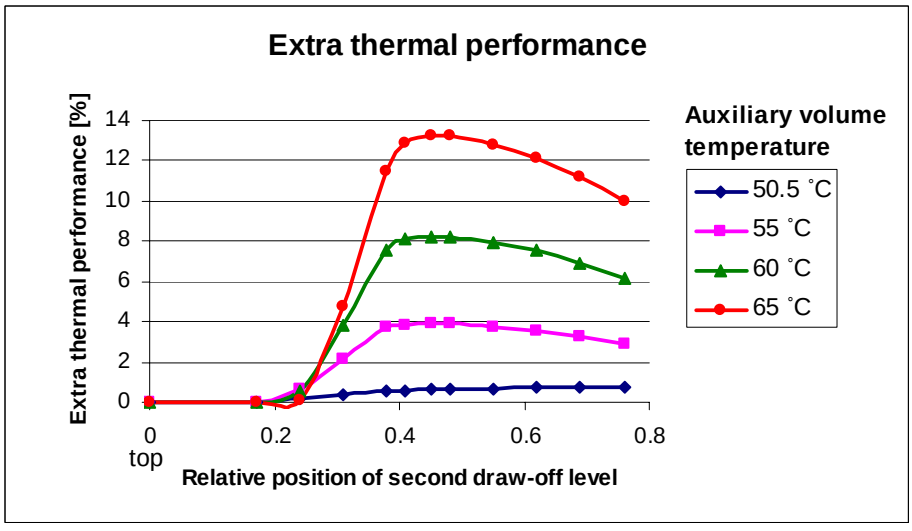

Figure 3: Calculated extra percentage net utilized solar energy of the system by using two draw-off levels as functions of the position of the second draw-off level and of the auxiliary set point temperature.

Figure 4 and Figure 5 show the calculated yearly net utilized solar energy of the system and the calculated extra percentage net utilized solar energy of the system by using two draw-off levels as a function of the position of the second draw-off level for four different daily hot water consumptions: 50, 100, 160 and 180 l. Hot water is tapped by means of three daily draw-offs with the same draw-off volume: At 7 am, 12 am and 7 pm. Hot water is tapped at 45°C at 7 am and at 7 pm, while hot water is tapped at 40°C at 12 am. During all hours the top auxiliary volume is heated to 50.5°C. The draw-off temperatures are realistic, since hot water is not used at the same temperature level in practice. Further, in practice the set point of the auxiliary energy supply system is often 5-10 K higher than the required hot water draw-off temperature. The figures show that the net utilized solar energy is increased by about 6% by using two draw-off levels. Again, the second draw-off level is best placed in the middle of the tank. It should be mentioned, that there is a need for development of an advanced control system before solar tanks in practice can supply the consumers with different draw-off temperatures.

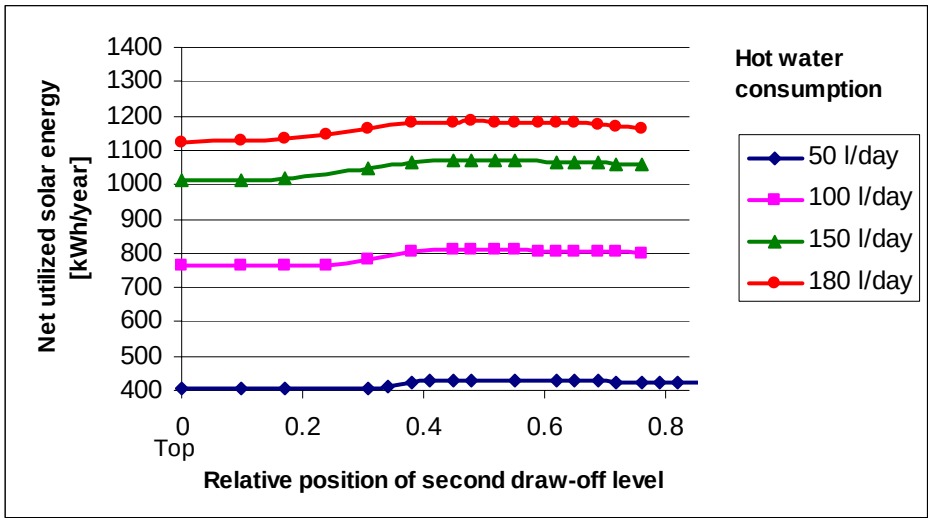

Figure 4: Calculated yearly net utilized solar energy of the SDHW system as a function of the position of the second draw-off level for different daily hot water consumptions.

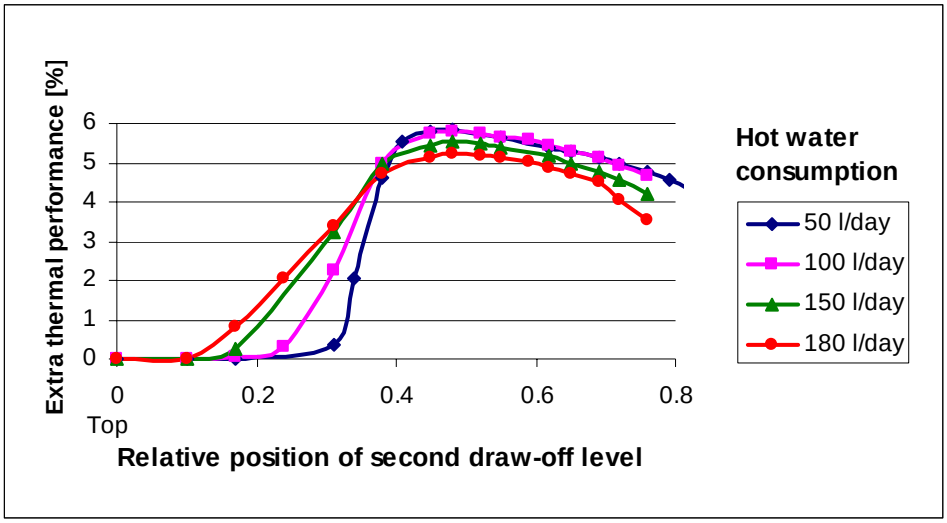

Figure 5: Calculated extra percentage net utilized solar energy of the SDHW system by using two draw-off levels as a function of the position of the second draw-off level.

3 Solar combisystems

Calculations of the yearly net utilized solar energy of a solar combisystem are carried out by means of TRNSYS developed by Klein et al. (1996) and Drück (2000). The solar combisystem taken into calculation is schematically shown in Figure 6.

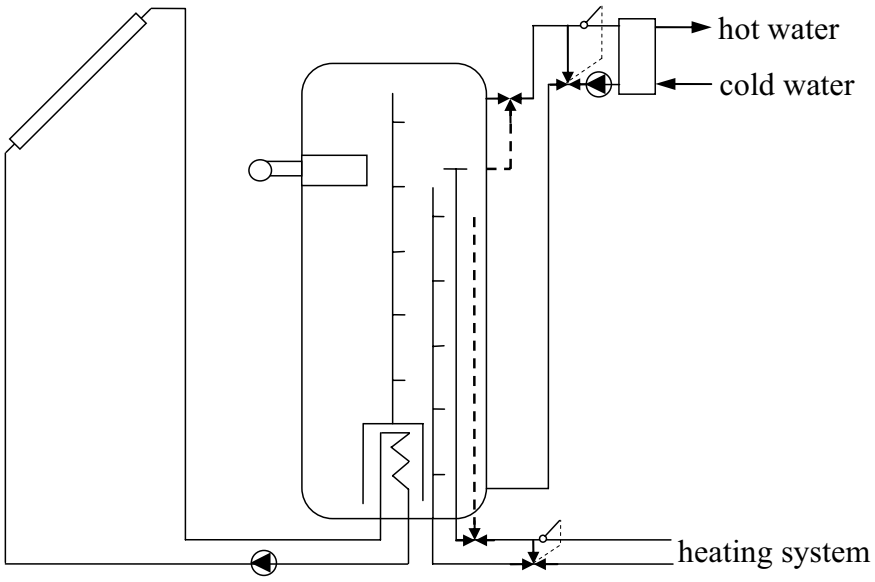

Figure 6: Schematic illustration of solar combi system taken into calculation.

The solar heating system, which is a marketed system by SOLVIS Solar Systeme GmbH, was the best system investigated by Weiss (2003). The system has a compact heat storage unit with the following components integrated: A water tank with an auxiliary condensing natural gas burner, a domestic hot water flat plate heat

exchanger with a pump, a solar collector loop and a solar heat exchanger. Thermal stratification is built up in the heat storage in a good way, since SOLVIS inlet stratifiers ensure that the solar heat is transferred to the "right" level in the tank and that the water returning from the heating system enters the tank in the right level.

The volume of the tank is 650 l and the auxiliary volume heated by the natural gas burner is 136 l. The natural gas burner heats up the auxiliary volume to 57°C. The solar collectors described in the previous section are also used in the calculations on the thermal performance of the solar combisystem. The solar collector area is 12.55 m².

The water to the heating system is tapped from a level just above the lower level of the auxiliary volume.

The space heating demand of the house taken into calculation is 14970 kWh/year. The heating system is a traditional radiator system which, at an indoor temperature of 20°C and an outdoor temperature of -12°C, can supply the required heating power of the house with an inlet water temperature of 60°C and an outlet water temperature of 50°C. A daily hot water consumption of 150 l heated from 10°C to 51°C is assumed. Weather data of the Danish Test Reference Year is used in the calculations. The draw-off level for the domestic hot water heat exchanger is placed at a relative position of 0.05 from the very top of the tank and the draw-off level for the space heating system is placed at a relative position of 0.23 from the very top of the tank.

Calculations of the yearly net utilized solar energy of the system are carried out for the standard system, for the system with two draw-off levels for the domestic hot water heat exchanger with different positions of the second draw-off level, for the system with two draw-off levels for the space heating system with different positions of the second draw-off level and for a system with two draw-off levels, both for the domestic hot water heat exchanger and for the space heating system.

Figure 7 shows the calculated yearly net utilized solar energy of the system with two draw-off levels to the domestic hot water heat exchanger and the standard draw-off level to the heating system, as well as the yearly net utilized solar energy of the system with two draw-off levels to the heating system and the standard draw-off level to the domestic hot water heat exchanger as functions of the position of the second draw-off level.

Figure 8 shows the extra percentage net utilized solar energy for the solar combisystem by utilizing two draw-off levels to the domestic hot water heat exchanger as well as the extra percentage net utilized solar energy for the solar combisystem by utilizing two draw-off levels to the heating system as a function of the position of the second draw-off level. It is possible to increase the yearly thermal performance of the system by about 3%, either by using two draw-off pipes for the domestic hot water heat exchanger instead of one or by using two draw-off pipes for the heating system instead of one. The best position of the second draw-off level for the domestic hot water heat exchanger is in the middle of the tank, and the best position of the second draw-off level for the heating system is just above the middle of the tank.

Further calculations showed that by using a second draw-off level, both to the domestic hot water heat exchanger and to the heating system, the yearly net utilized solar energy of the solar combisystem is increased by about 5% compared to the standard system. Also for this design, the second draw-off pipe for the domestic hot

water heat exchanger is best placed in the middle of the tank, while the second draw-off pipe for the heating system is best placed just above the middle of the tank.

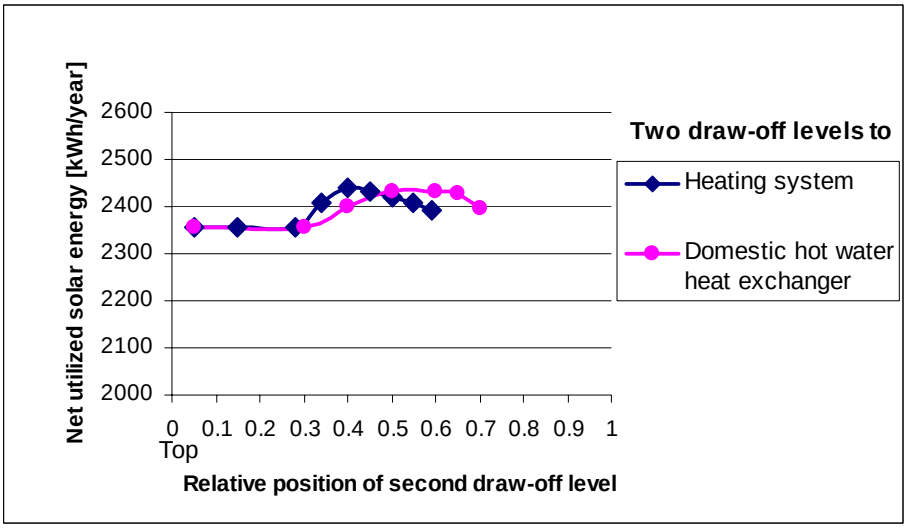

Figure 7: Calculated yearly net utilized solar energy for the solar combisystem as a function of the position of the second draw-off level.

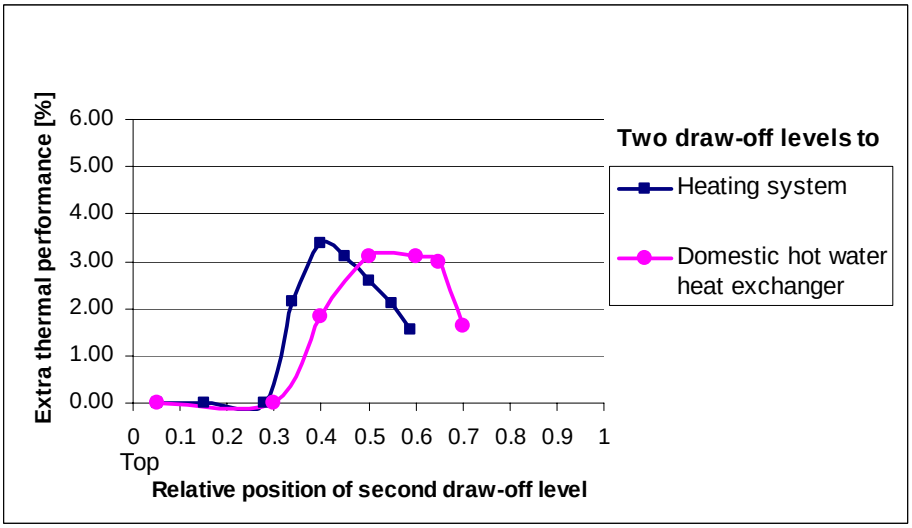

Figure 8: Extra net utilized solar energy for the solar combi system by using two draw-off levels for the domestic hot water heat exchanger instead of one draw-off level and by using two draw-off levels for the heating system instead of one draw-off level as a function of the position of the second draw-off level.

4 Conclusions

The investigations showed that it is possible to increase the thermal performance of both SDHW systems and solar combisystems by using two draw-off levels from the solar tanks instead of one draw-off level at a fixed position.

The best position of the second draw-off level is for all the investigated systems in the middle or just above the middle of the tank. For the investigated SDHW system the extra thermal performance of using a second draw-off level from the hot water tank is strongly influenced by the difference between the set point temperature of the auxiliary energy supply system and the required draw-off temperature. For increasing temperature difference the thermal advantage of the second draw-off level increases. For a realistic draw off hot water temperature of 40°C and 45°C and an auxiliary volume temperature of 50.5°C the increase of the thermal performance by the second draw-off level is about 6%.

For the investigated solar combisystem the extra thermal performance by using one extra draw-off level, either for the domestic hot water heat exchanger or for the heating system, is about 3%, while an improvement of about 5% is possible by using a second draw-off level both for the domestic hot water heat exchanger and for the heating system.

References

Andersen, E., Jordan, U., Shah, L.J., Furbo, S., 2004. Investigations of the SOLVIS stratification inlet pipe for solar tanks. In: EuroSun 2004 Proceedings, Freiburg, Germany, Vol. 1, 076-085.

Drück, H., 2000. SOLVISMAX – Model for TRNSYS, Type 147. Institut für Thermodynamik und Wärmetechnik. Universität Stuttgart.

Furbo, S., 1984. Varmelagring til solvarmeanlæg. Ph.D. Thesis, report no. 162. Thermal Insulation Laboratory, Technical University of Denmark.

Furbo, S., Mikkelsen, S.E., 1987. Is low flow operation an advantage for solar heating systems? In: Bloss, W.H., Pfisterer, F. (Eds.), Advances in Solar Energy Technology, Vol. 1., Pergamon Press, Oxford, 962-966.

Furbo, S., Berg, P., 1990. Calculation of the thermal performance of small hot water solar heating systems using low flow operation. In: North Sun'90 Proceedings, Reading, England.

Furbo, S., Knudsen, S., 2004. Low flow SDHW systems based on mantle tanks – recent findings. In: EuroSun 2004 Proceedings, Freiburg, Germany, Vol. 1, 272-281.

Furbo, S., Vejen, N.K., Shah, L.J., 2004. Thermal performance of a large low flow solar heating system with a highly thermally stratified tank. Journal of Solar Energy Engineering, in press.

Jenni Energietechnik AG, 2004. www.jenni.ch/html/Produkte/Armaturen/Heizungsgruppe%20zweistufig.htm

Klein, S.A. et al. (1996). TRNSYS 14.1, User Manual. University of Wisconsin, Solar Energy Laboratory.

Knudsen, S., Furbo, S., 2004. Thermal stratification in vertical mantle heat exchangers with application to solar domestic hot water systems. Applied Energy, Vol 78/3, 257-272.

Lorenz, K., 2001. Kombisolvärmesystem. Utvärdering av möjliga systemförbättringar". Report D59:2001. Institutionen för Installationsteknik, Chalmers Tekniska Högskola, Sweden.

Shah, L.J., Furbo, S., 1998. Correlation of Experimental and Theoretical Heat Transfer in Mantle Tanks used in Low Flow SDHW Systems". Solar Energy, Vol. 64 (4-6), 245-256.

Statens Byggeforskningsinstitut, 1982. Vejrdata for VVS og energi. Dansk referenceår TRY.

van Koppen, C.W.J., Thomas, J.P.X., Veltkamp, W.B., 1979. The Actual Benefits of Thermally Stratified Storage in a Small and Medium Size Solar System. In: Proceedings of ISES Solar World Congress, Atlanta, USA, 579-80.

Weiss, W. (Ed.), 2003. Solar Heating Systems for Houses. A design Handbook for Solar Combisystems. James & James Ltd. Solar Heating and Cooling Executive Committee of International Energy Agency (IEA).

Paper V

Theoretical comparison of solar water/space-heating combi systems and stratification design options

Accepted for publication in Journal of Solar Energy Engineering, April 2007

Theoretical comparison of solar water/space-heating combi systems and stratification design options

E. Andersen and S. Furbo

Department of Civil Engineering. Technical University of Denmark

Building 118, DK-2800 Kgs. Lyngby, Denmark

e-mail : ean@byg.dtu.dk

Accepted for publication in Journal of Solar Energy Engineering, April 2007

Abstract

A theoretical analysis of differently designed solar combi systems is performed with weather data from the Danish Design Reference Year (55ºN). Three solar combi system designs found on the market are investigated. The investigation focuses on the influence of stratification on the thermal performance under different operation conditions with different domestic hot water and space heating demands. The solar combi systems are initially equipped with heat exchanger spirals and direct inlets to the tank. A step-by-step investigation is performed demonstrating the influence on the thermal performance of using inlet stratification pipes at the different inlets. Also, it is investigated how the design of the space heating system, the control system of the solar collectors, and the system size influence the thermal performance of solar combi systems.

The work is carried out within the Solar Heating and Cooling Programme of the International Energy Agency (IEA SHC), Task 32.

Keywords Solar combi system design; solar combi system size; space heating system; inlet stratifier; net utilized solar energy; solar fraction.

1 Introduction

In the period 1998-2002, the IEA SHC, Task 26 Solar CombiSystems evaluated 21 solar combi systems on the European market. The evaluation comprised both the system costs and the thermal performance. It was found that most of the systems for one family houses had solar collectors of 10 m^2- 30 m^2 with 0.3 m^3- 3 m^3 tank volumes. The best systems, regarding the performance/cost ratio, were the most advanced systems with inlet stratification pipes, an efficient integrated boiler, and only one control system for both the boiler and the solar collector loop [1].

Further, a sensitivity analysis of 9 of the investigated Task 26 systems was performed [2]. The influence of climate and heat load and of the solar collector, the storage tank, the boiler and the space heating system were investigated. It was found that the optimal collector tilt depends on the latitude and the solar fraction. The optimal

collector tilt increases with increasing solar fraction in order to better utilize the solar irradiation during the heating season. The thermal performance decreases for increasing volume flow rate in the solar collector loop. The heat exchange capacity rate in the solar collector loop should be about 40 W/K per m^2 solar collector. For heat storages with an internal heat exchanger in the solar collector loop, the temperature sensor of the control system should be placed on a level with the lower 1/3 – 1/2 of the heat exchanger. The optimal storage volume is about 100 l/m^2 solar collector area. Storage insulation thicknesses above 15 cm do not increase the thermal performances. Top insulation is less significant than side insulation because the top area is smaller. The auxiliary volume should be kept small and the set point temperature for the auxiliary energy supply system low. The sensor for the auxiliary heater should be placed below the space heating outlet. No big influence on the position of the return inlet pipe from the space heating loop in the heat storage was found. The thermal performance decreases slightly with increasing position of the outlet height for the space heating loop. Most important for the achieved energy savings is the boiler efficiency.

Finally, 3 of the 9 investigated systems were improved significantly by design changes determined by the sensitivity analysis [3]. The strategies used for the improvement were: Keep the boiler efficiency as high as possible, keep the collector inlet as cold as possible, avoid temperature losses through mixing, keep heat losses as low as possible, and use efficient pumps to decrease the electricity demand. This work showed that optimization can improve the system performance significantly and that, for different system designs, the performance is nearly the same if all aspects of the system are optimized.

In [4] it was shown how the thermal performance of a typical Swedish solar combi system with 20 m^2 solar collectors and a 0.75 m^3 storage tank with three internal heat exchanger spirals could be improved by 10% by small design changes without additional system costs. Further, it was shown that the thermal performance can be improved by 25% – 35% by introducing a highly stratified tank.

The advantage of a stratification inlet pipe instead of a fixed inlet height for transferring solar energy to the storage tank by means of a thermosyphon loop was investigated [5]. It was found that for a solar combi system with a solar fraction of about 25%, the thermal performance increased by only 1 – 2% by using a stratification manifold instead of a fixed inlet.

Similar low performance improvements of about 3% by using low flow and inlet stratifiers were measured for solar combi systems with a solar fraction of about 20% [6].

Simulations of solar combi systems were carried out, and it was found that the solar fraction could be roughly estimated by three parameters: The solar collector area, the storage volume and the heat load of the system. The investigations included Austrian, German, Danish and Swedish climates [7].

The thermal performances of four highly advanced and differently designed solar combi systems were compared [8]. The authors found that the most important parameters for a well performing solar combi system are low heat losses and a small auxiliary volume in the heat storage with a low set point temperature. All pipe connections for the auxiliary and space heating loop should be at appropriate

positions. Only then additional thermal performance is achieved with stratification devices.

A number of stratification inlet pipes, so-called stratifiers, were investigated [9]. It was found that in practice thermal stratification can be built up in a nearly perfect way with certain stratifiers, among others with multilayer fabric stratifiers and with rigid stratifiers with holes with flaps that work as non-return valves.

Some of the investigations mentioned above show large thermal advantages by using inlet stratifiers, some show small advantages. The thermal advantage of inlet stratifiers depends strongly on the solar fraction of the solar combi system, the system design, the heating system and the performance of the inlet stratifiers. Further the advantage depends on the reference system used for the comparison. Some of the reference systems in the above mentioned investigations have partially stratified storage tanks. This study focuses on the thermal advantage by using storage tanks with ideally working inlet stratifiers instead of storage tanks without inlet stratifiers for different sizes and designs of solar heating and space heating systems with the same reference conditions. Also, it is investigated how the control system in the solar collector loop influences the thermal performance of solar combi systems. The investigation is carried out by means of the simulation program Trnsys [10] and the multiport store model [11]. The differently designed systems have 1000 litre storage tanks and 20 m^2 solar collectors. The differently sized solar combi systems are based on one system design with storage tanks of 500 litres, 1000 litres and 1500 litres, and solar collector areas from 5 m^2 to 60 m^2.

2 Investigations of differently designed solar combi systems

Figure 1 shows schematic illustrations of the investigated solar combi system types. The first system model is based on a space heating storage with an external heat exchanger mounted in a side arm for domestic hot water preparation. The second system model is based on a domestic hot water tank with an internal heat exchanger spiral connected to the space heating system. The third system model is based on a hot water tank-in-tank storage.

The three system models are referred to as models 1, 2 and 3, respectively. Further, the models are improved by introducing stratifiers in the solar collector loop and in the space heating loop, and in both the solar collector loop and the space heating loop. The variations in each model are numbered successively (Figure 1). The advantage of using stratifiers is that incoming water of any temperature is led into the tank in a level where the temperature of the incoming water matches the temperature of the water in the tank. In this way, thermal stratification in the tank is enhanced without destroying the already existing thermal stratification in the tank. In the present investigation, the thermal stratification is assumed to be built up in a perfect way without any mixing by the inlet stratifier. In this way the investigations show the maximum potential of inlet stratifiers.

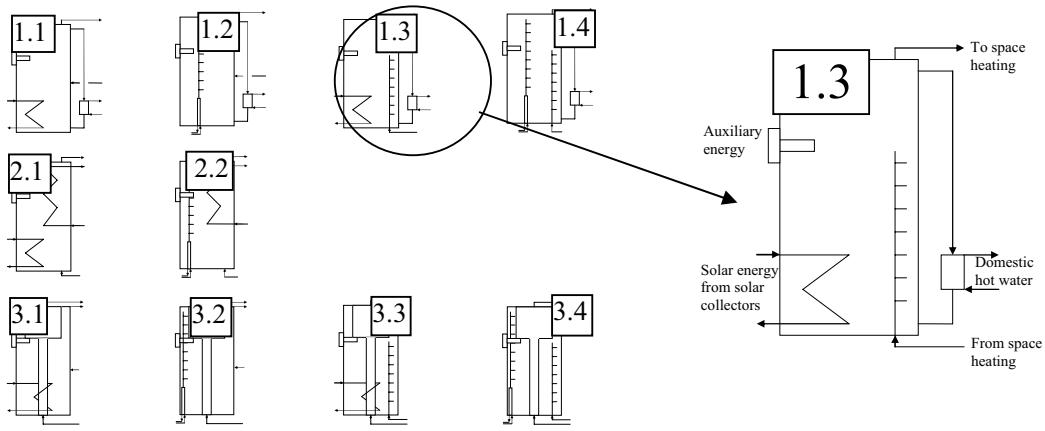

Figure 1: Schematics of the three system models: Model 1 (top), model 2 (middle) and model 3 (bottom), and the successively numbered variations of the system models.

2.1 Assumptions for the calculations

The Danish Design Reference Year, DRY data file, is used as weather data [12]. The daily hot water consumption is either 100 litres (DHW100) or 200 litres (DHW200). Domestic water is heated from 10ºC to 50ºC. Hot water is tapped from the top of the tank at 7 am, noon and 7 pm in three equal portions with a volume flow rate of less than 2 l/min. Neither the size of the external heat exchanger for domestic hot water preparation nor the power of the auxiliary energy supply system is part of the investigation and hence the volume flow rate during domestic hot water draw-off is unimportant. The influence of the draw-off profile was investigated for a solar combi system [13] and it was found that a realistic draw-off profile (statistical derived) decreases the yearly thermal performance 2% mainly because a realistic draw-off profile includes vacation during the summer period. A similar investigation for solar domestic hot water systems [14] showed a yearly thermal performance decrease of 11% – 14% when a realistic draw-off profile was applied. The draw-off profile influences the thermal performance of solar heating systems but the influence is much lower for solar combi systems than for solar domestic hot water systems. Therefore investigations of the hot water consumption pattern are not included in this study.

The temperature in the top of the heat storage is determined by the set point temperature of the auxiliary energy supply system and the temperature supplied from the solar collector during sunny hours. The set point temperature of the auxiliary volume is 57ºC. The efficiency of the boiler is assumed to be 100%.

The required heating power and the flow and return temperatures for the space heating system for three one family houses of 150 m^2 with different degrees of insulation are shown in Figure 2 and Figure 3. The heating demand of the three houses is about 108 MJ/(m^2 year), about 216 MJ/(m^2 year) and about 360 MJ/(m^2 year). The heating demand is referred to as SH108, SH216 and SH360, respectively, corresponding to 17345 MJ/year, 34157 MJ/year and 57132 MJ/year, respectively.

All positions for inlet to the tank and outlet from the tank are given as relative heights defined as: inlet height / total height of the tank, where 0 equals the bottom of the tank and 1 equals the top of the tank.

Table 1 shows data of the solar combi systems used in the calculations. The heat loss coefficient of the sidearm and the external heat exchanger for domestic hot water preparation are measured on a well insulated solar combi system. The heat loss coefficient of the tank is calculated. Investigations of the tank-in-tank heat transfer coefficient based on experiments and Computational Fluid Dynamics calculations showed that the heat transfer coefficient varies with the operation conditions, the design of the inner tank and the temperature level [15]. For simplification, a constant is used.

Table 1: Data used in the calculations.

Solar collector area	20 m^2
Optical efficiency of incident radiation, η_0	0.756
Heat loss coefficients, a_1 / a_2	4.17 W/m^2/K / 0.0095 W/m^2/K^2
Efficiency for all incidence angles, η	$\eta_0 \cdot k_\theta - a_1 \cdot (T_m - T_a)/E - a_2 \cdot (T_m - T_a)^2/E$
Incidence angle modifier for beam radiation, k_θ	$1\text{-}\tan^{4.2}(\theta/2)$
Collector tilt / Orientation	65° / South
Solar collector fluid	40% (weight) propylene glycol/water mixture
Volume flow rate in solar collector loop, high / low	1.2 l/min/m^2 / 0.17 l/min/m^2
Storage volume / auxiliary volume	1000 l (260 l DHW tank) / 190 l
Height/diameter	2 / 0.798 m
Heat loss coefficient, tank / sidearm / domestic hot water heat exchanger	3.82 W/K / 0.39 W/K / 0.37 W/K
Heat transfer coefficient of external heat exchanger when stratifier in solar collector loop is used	100 W/K per m^2 collector
Heat transfer coefficient of: spiral in solar collector loop / spiral in space heating system / tank in tank heat transfer	75 W/K per m^2 collector / 750 W/K / 278 W/K
Volume between temperature sensor that controls the supply of auxiliary energy and the lowest part of the auxiliary volume	50 l
Relative inlet/outlet height of domestic hot water loop	0 / 1
Relative outlet height of space heating system	0.98
Relative inlet/outlet height of heat exchanger spiral in solar collector loop	0.305 / 0.06
Control system – Differential thermostat control with one sensor in the solar collector and one in the tank	

Relative height of temperature sensor: spiral in solar collector loop / stratifier in solar collector loop (Figure 10)	0.14 / 0.01
Maximum/Minimum temperature differential	10 K/0.5 K

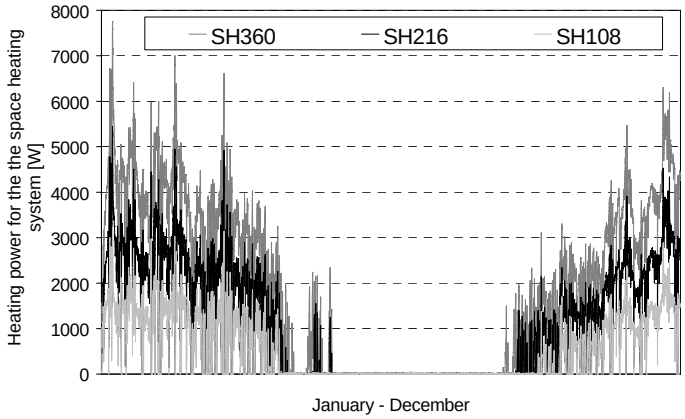

Figure 2: Power for the space heating systems, used in the calculations.

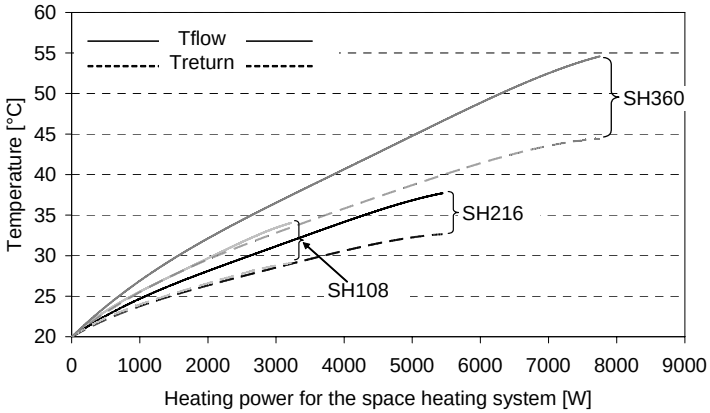

Figure 3: Flow and return temperatures in the space heating systems, used in the calculations.

The net utilized solar energy, the solar fraction and the performance ratio are defined as:

$$Q_{NET} = Q_{DHW} + Q_{SH} - Q_{AUX} \tag{1}$$

$$SF = \frac{Q_{NET}}{Q_{DHW} + Q_{SH}} \cdot 100\% \tag{2}$$

$$PR = \frac{Q_{NET}}{Q_{NET,REF}} \tag{3}$$

2.2 Results

The results are shown as the net utilized solar energy as a function of the parameter varied. Further, the results are shown as the performance ratio as a function of the parameter varied. The parameters varied are: The domestic hot water consumption, the space heating demand and the relative return inlet height from the space heating loop.

Figure 4 shows the calculated yearly net utilized solar energy as a function of the relative return inlet height from the space heating loop for model 1.1 with a heat exchanger spiral in the solar collector loop and fixed return inlet height from the space heating loop. Further, the performance ratio relative to the optimal thermal performance of the system in question is shown. The space heating demand is varied in accordance with Figure 2, and the daily domestic hot water consumption is 100 litres and 200 litres. Also the net utilized solar energy is shown for model 1.3 with a stratifier in the space heating loop. The return water from the space heating loop enters the stratifier at the bottom of the tank and the inlet from the stratifier to the tank varies with the temperature conditions. To highlight the benefit of a stratifier in the space heating loop, the performance with a stratifier is marked at the optimal relative inlet height with a fixed inlet from the space heating loop.

The calculated yearly net utilized solar energy as a function of the relative return inlet height from the space heating loop for models 2 and 3 are not shown. The results are similar to the results for model 1.

The figure shows that the optimal inlet position from the space heating loop varies with the daily domestic hot water consumption and the space heating demand. For low space heating demand, and thereby low return inlet temperatures, the optimal inlet position is low. For increasing space heating demand, and thereby increasing return inlet temperature, the height of the optimal inlet position increases (indicated by the dotted curve connecting the optimum of the curves). Also the optimal return inlet position from the space heating loop increases for increasing domestic hot water consumption. This is due to a larger amount of cold water in the bottom of the tank, which leaves the warmer water that matches the temperature of the return water from the space heating loop at a higher level in the tank.

The yearly net utilized solar energy is reduced by less than 1% if the relative return inlet position from the space heating loop is 0.3 compared to the optimum return inlet position. This is also the case for the system models 2 and 3.

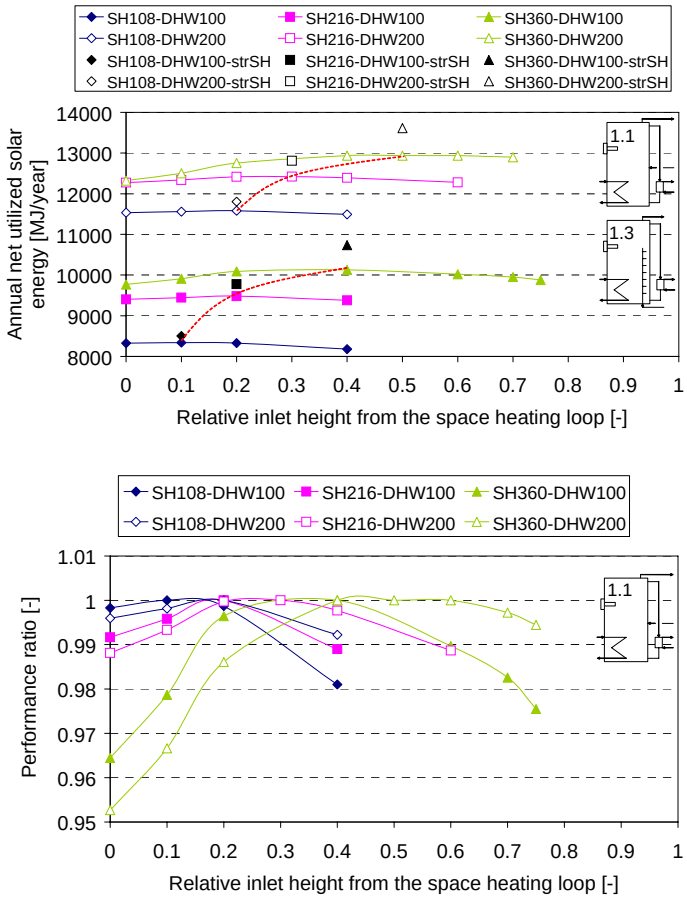

Figure 4: Top: The annual net utilized solar energy as a function of the relative return inlet height from the space heating loop for model 1.1 and model 1.3. Bottom: The performance ratio relative to the optimal thermal performance of the system in question.

Figure 5 shows the net utilized solar energy as a function of the space heating demand and the domestic hot water consumption for model 1 and a step by step improvement of the design. Also the performance ratio relative to the least advanced model 1.1 is shown. In all the calculations with a fixed return inlet height from the space heating loop, the optimal return inlet height shown in Figure 4 is used. The results for system models 2 and 3 are not shown but are similar to the results for system model 1.

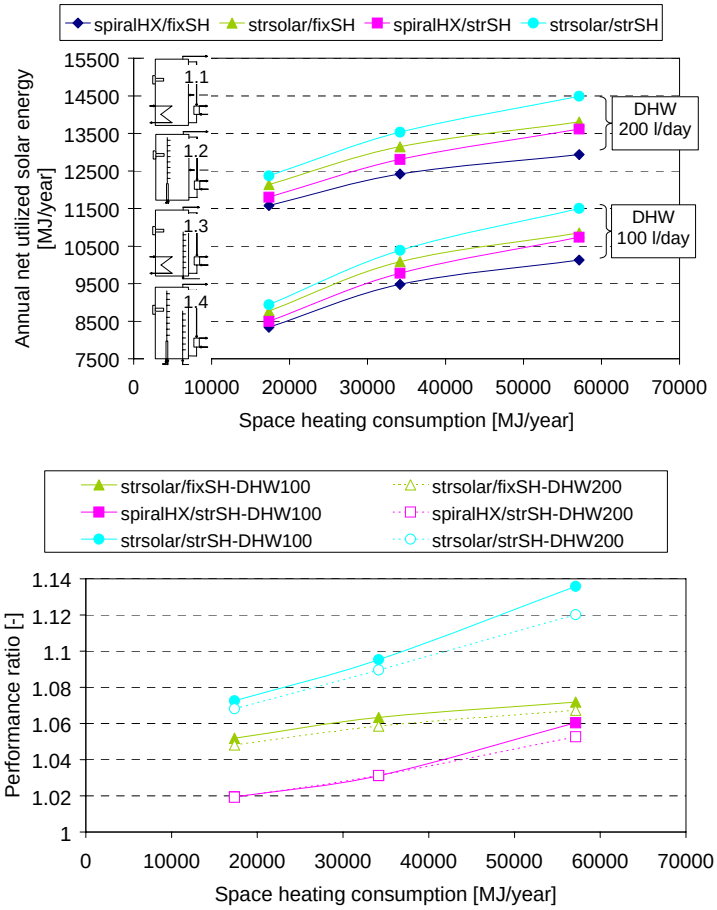

Figure 5: Top: The annual net utilized solar energy as a function of the space heating demand and the domestic hot water consumption for model 1 and the step by step improvement of the models. Bottom: The performance ratio relative to the thermal performance of the least advanced model, model 1.1.

The figure shows that the thermal performance increases for increasing space heating demand and increasing domestic hot water consumption. Also the thermal performance increases when inlet stratifiers are used, and most when an inlet stratifier is used in the solar collector loop. The best performing system has inlet stratifiers both in the solar collector loop and in the space heating loop.

The extra net utilized solar energy by using stratifiers increases for increasing space heating demand. This is because the return temperature from the space heating system is higher for high space heating demand than for low space heating demand. Hence the variation in the return temperature from the space heating system is higher for houses with high space heating demand than for houses with low space heating demand and this leads to a better utilization of a stratifier.

The increase in yearly net utilized solar energy by using a stratifier in the solar collector loop, in the space heating loop, or in both the solar collector loop and the space heating loop is in the range of 5 – 8%, 2 – 6% and 7 – 14%, respectively, for the system models 1, 2 and 3.

It is obvious that the thermal performances of the systems are highly influenced by the total energy consumption and the design of the systems.

2.3 System comparison

Figure 6 shows the annual net utilized solar energy as a function of the space heating demand and a domestic hot water consumption of 100 l/day for system model 1, 2 and 3. The figure also shows the performance ratio where, in all cases, the reference system is the similar system model 1.

Figure 6 shows that model 1 always has the lowest thermal performance compared to the similar models 2 and model 3. Further, it can be seen that model 2 has a higher thermal performance than the similar model 3. The best performing system is the tank-in-tank system model 3.4 with inlet stratifiers in both the solar collector loop and in the space heating loop.

The reason why model 2 is performing better than the similar models 1 and 3 is most likely because the tank is a domestic hot water tank where the incoming cold water is directly utilized to cool the lower part of the tank. In model 1 the water returning from the domestic hot water heat exchanger to the tank is somewhat warmer than the cold water. In model 3 the incoming cold water reaches a higher level in the heat storage after a domestic hot water draw off caused by the shape of the inner tank. The reason why model 3 is performing better than model 1 is most likely due to the higher tank heat loss coefficient of model 1 since the heat loss coefficients of the sidearm and the external domestic hot water heat exchanger are added to the tank heat loss coefficient. A further disadvantage for model 1 is that the set point temperature of the auxiliary volume must be about 10 – 15 K higher than the required hot water temperature to meet the hot water demand. The set point temperature in models 2 and 3 only needs to be slightly higher than the required hot water temperature to meet the same demand. This effect is not investigated by calculations in this paper.

The performance ratio is higher for low space heating demand than for high space heating demand. With domestic hot water consumption of 100 l/day, the performance increase by using model 2 instead of model 1 is in the range of 1.5 – 2.2%, and in the range of 0.8 – 1.5% by using model 3 instead of model 1. The same investigations with domestic hot water consumption of 200 l/day show that the performance increase by using models 2 and 3 instead of model 1 is in the range of 3.4 – 3.9% and 0.4 – 1.9%, respectively.

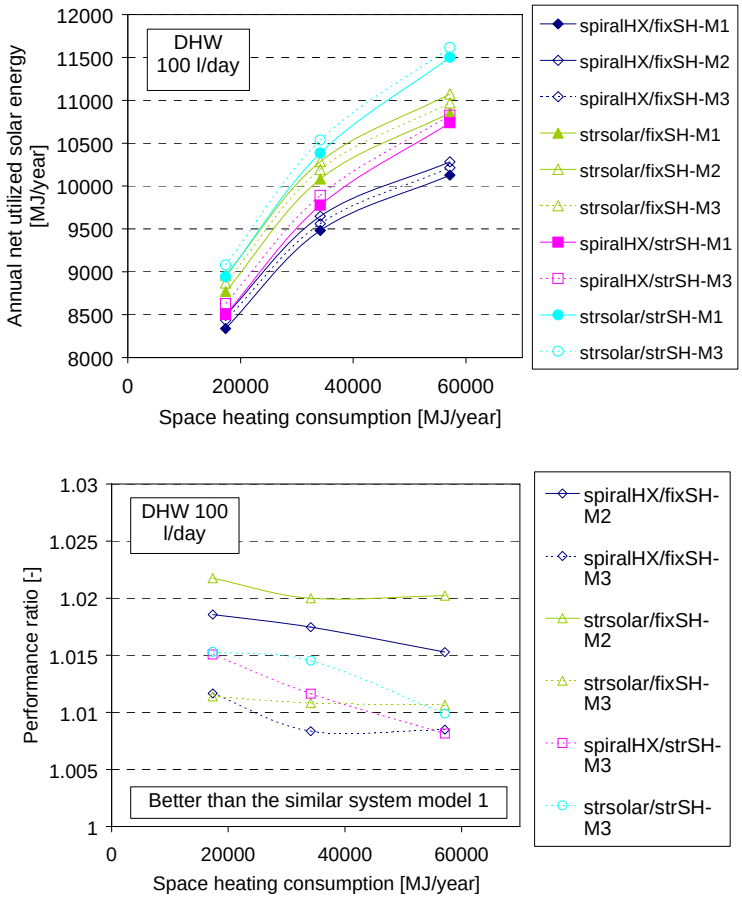

Figure 6: Comparison of model 1, model 2 and model 3. Top: The annual net utilized solar energy as a function of the space heating demand and the domestic hot water consumption and the step by step improvement of the models. Bottom: The performance ratio relative to the thermal performance of the similar system model 1.

3 Further investigations of solar combi systems

It is investigated how the size of the space heating system influences the thermal performance of solar combi systems. Also the influence on the thermal performance of different operation conditions of the control system for the solar collector loop is investigated. The investigation is only carried out for system model 1.

3.1 Space heating system

The size of the space heating system is varied for the house with a heating load of about 216 MJ/(m^2·year). The flow and return temperatures for a small, a standard and a large space heating system as a function of the heating power demand are shown in Figure 7.

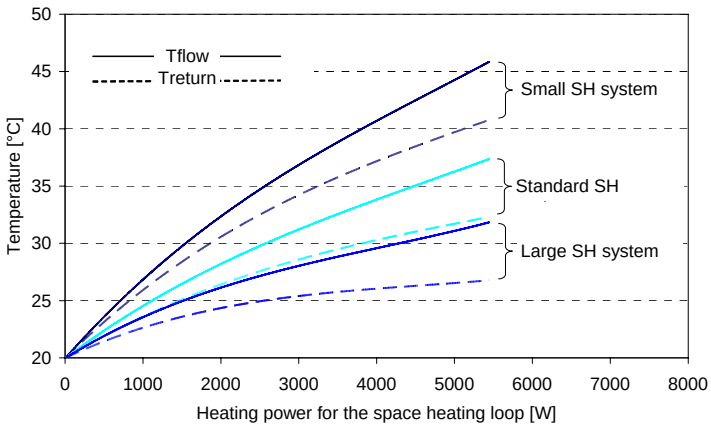

Figure 7: The flow and return temperatures for the space heating systems as a function of the heating power demand.

Figure 8 shows the annual net utilized solar energy as a function of the relative return inlet height from the space heating loop and the performance ratio, relative to the optimal thermal performance, of the system in question. Figure 9 shows the performance ratio, relative to the optimal thermal performance, of the system with the standard space heating system.

Figure 8 shows that the annual net utilized solar energy is strongly influenced by the size of the space heating system. The larger the space heating system, the larger is the thermal performance of the solar heating system. Also the optimal relative return inlet height from the space heating loop is influenced by the size of the space heating system. For small space heating systems, the optimal relative return inlet height increases, while the optimal return inlet height decreases for large space heating systems. Further, the figure shows the benefit of replacing the fixed inlet from the space heating loop with a stratifier, and it can be seen that the largest improvement of the thermal performance is achieved for small space heating systems. This is caused by the fact that the return inlet temperature varies more for houses with small space heating systems than for houses with larger space heating systems.

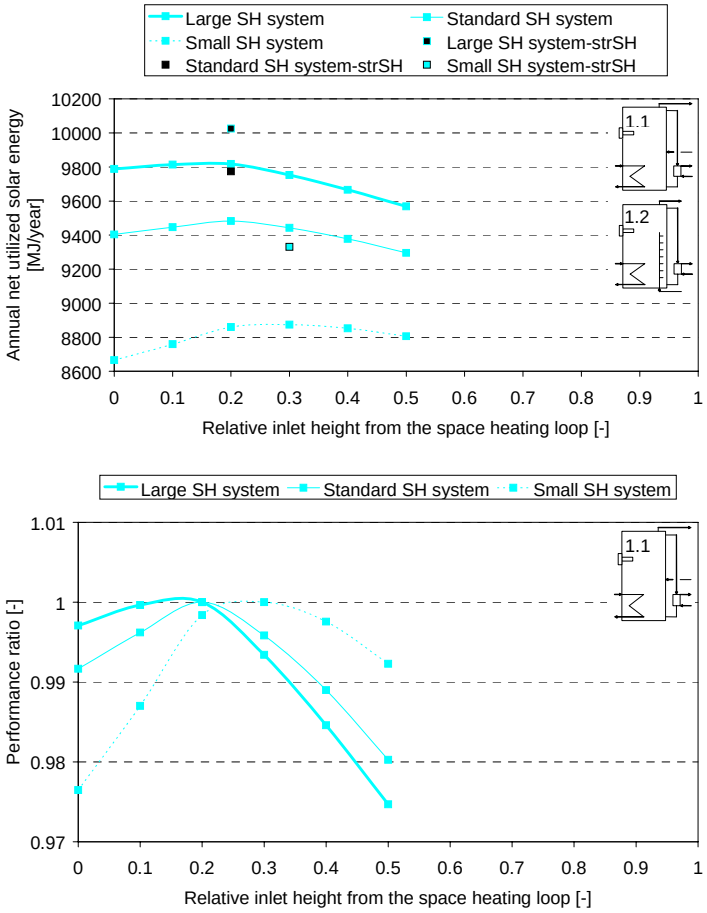

Figure 8: Top: The annual net utilized solar energy as a function of the relative return inlet height from the space heating loop. Bottom: The performance ratio, relative to the optimal thermal performance, of the system in question.

Figure 9 shows that the thermal performance of model 1.1 with the standard space heating system increases about 3% when a stratifier is used in the space heating loop instead of a fixed return inlet height. The thermal performance of models 1.1 and 1.2 with the large space heating system is about 4% and 6% higher than the thermal performance of model 1.1 with the standard space heating system. The thermal performance of models 1.1 and 1.2 with the small space heating system is about 6% and 2% lower than the thermal performance of model 1.1 with the standard space heating system.

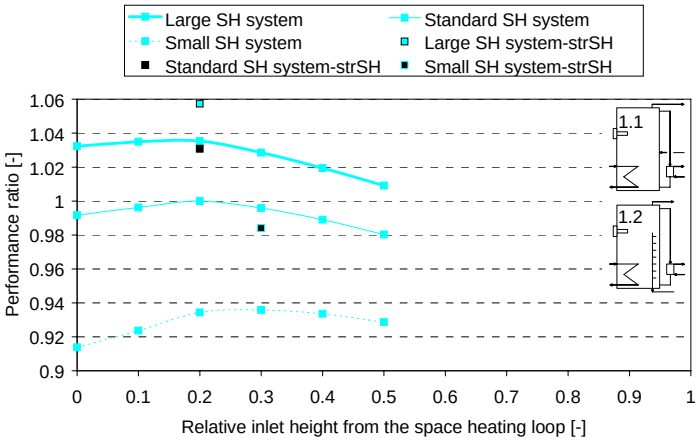

Figure 9: The performance ratio as a function of the relative return inlet height from the space heating loop. The performance is relative to the optimal thermal performance of the system with the standard space heating system.

It is clearly an advantage to use a stratifier instead of a fixed return inlet position from the space heating loop, especially because the size of the space heating system is normally not known in advance when the storage tanks are designed. Therefore the optimum fixed position of the return inlet from the space heating loop is not known.

3.2 Control system in the solar collector loop

The position of the temperature sensor mounted in the tank and the minimum temperature differential that controls the operation of the pump in the solar collector loop are investigated for different operation conditions:

- Space heating demand: 108 MJ/(m^2·year), 216 MJ/(m^2·year) and 360 MJ/(m^2·year).
- Domestic hot water consumption: 100 l/day and 200 l/day.
- Daily domestic hot water consumption patterns: 7 am, noon, 7 pm and 6 am, 7 am, 8 am and 7 pm, 8 pm, 9 pm.
- Fixed inlet heights (optimal position) and stratified inlet from the space heating loop.
- Volume flow rates in the solar collector loop: 1.2 l/(min·m^2), 0.5 l/(min·m^2) and 0.2 l/(min·m^2).
- Lengths of the pipe from/to the solar collector to/from the tank: 5, 10 and 15 m
- Stratifier in solar collector loop.
- Including the energy consumption of one and two pumps in the solar collector loop.

In Figure 10 the different positions of the temperature sensor used in the calculations are shown. The numbers next to the temperature sensors, seen to the right in the figure, correspond to the relative position in the tank. The relative positions 0.3 and 0.065 correspond to the top and the bottom of the heat exchanger, while the relative positions of 0.18, 0.14, 0.085 and 0.075 correspond to 1/2, 1/3, 1/10 and 1/20 of the heat exchanger height calculated from the bottom of the heat exchanger.

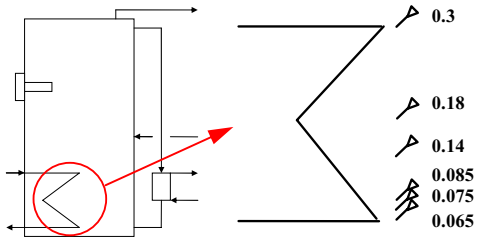

Figure 10: Different positions of the temperature sensor in the tank.

The investigations are carried out with sensor positions according to Figure 10 with minimum temperature differential varied between -1 K and 3 K.

In Figure 11 an example of such an investigation for one set of operation conditions is shown. The figure shows the net utilized solar energy for model 1.3 as a function of the position of the temperature sensor in the tank and the minimum temperature differential for the pump in the solar collector loop and the performance ratio relative to the thermal performance of the system with the highest thermal performance. The space heating demand is 216 MJ/(m^2·year), the domestic hot water consumption is 100 l/day, and domestic hot water is tapped at 7 am, noon and 7 pm. The volume flow rate in the solar collector loop is 1.2 l/(min·m^2).

From Figure 11 it can be seen that the optimal position of the temperature sensor is 1/10 of the heat exchanger height calculated from the bottom of the heat exchanger with a minimum temperature differential of about 0 K. Also it can be seen that for lower stop temperature differences, the optimal position of the temperature sensor is higher than 1/10 of the heat exchanger height, while for higher minimum temperature differentials the optimal position of the temperature sensor is lower than 1/10 of the heat exchanger height.

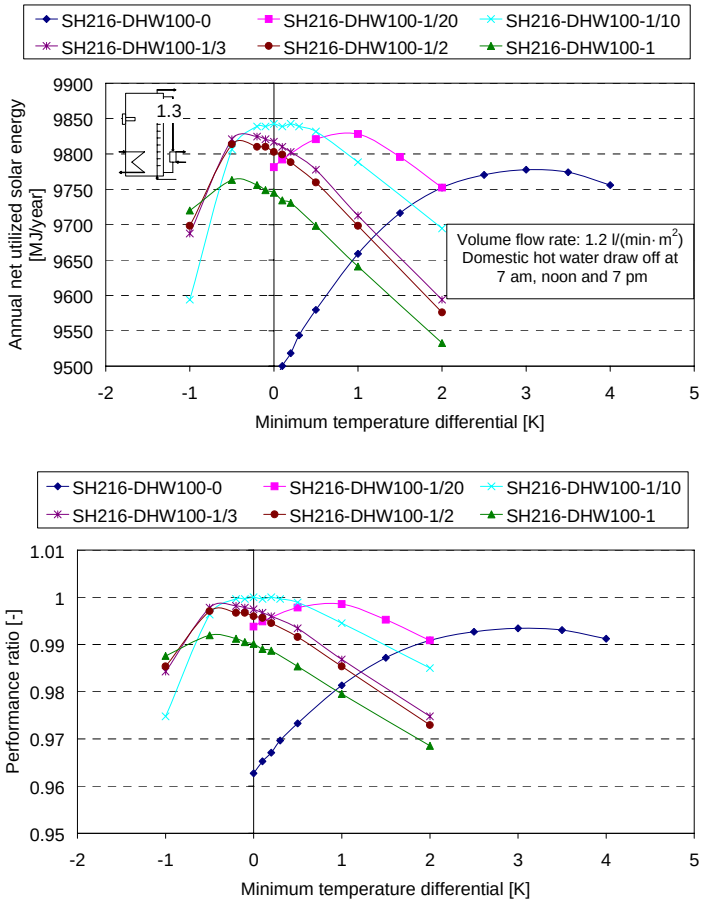

Figure 11: Top: The annual net utilized solar energy as a function of the position of the temperature sensor in the tank and the minimum temperature differential of the pump in the solar collector loop. Bottom: The performance ratio relative to the thermal performance of the system with the highest thermal performance.

The investigation including all the different operation conditions shows that, regardless of the applied operation conditions, the optimal position of the temperature sensor in a tank with a heat exchanger spiral in the solar collector loop is between 1/10 and 1/20 of the heat exchanger height with a minimum temperature differential between 0 K and 1 K. The optimum position of the temperature sensor and the optimum stop temperature difference will not be changed even when the pump energy is included in the calculations. Further, the investigation shows that the optimal position of the temperature sensor in a tank with a stratifier in the solar collector loop is at the very bottom of the tank and that the optimal minimum temperature differential lies in a quite wide range from -1 to 2 K. Consequently, a stratifier makes a system less sensitive regarding correct installations of temperature sensors and settings of the control parameters in the solar collector loop.

4 Investigations of different sized solar combi systems

It is investigated how the size of the solar combi system influences the thermal performance. Table 1 shows the data of one system size and Table 2 shows data of further system sizes used in the calculations. Only data that differ from data given in Table 1 are listed in Table 2.

Table 2: Data of the systems.

Solar collector area	10 m^2 / 30 m^2
Storage volume	500 l / 1500 l
Height of tank	1.5 m / 2.5 m
Diameter of tank	0.652 m / 0.874 m
Heat loss coefficient, tank	2.42 W/K / 5.09 W/K

4.1 Differently sized solar combi systems with varying space heating demand and daily hot water consumption

The investigation is carried out for different sizes of system model 1 and a step by step improvement of the model. The results with the system model with 1000 litre storage tank and 20 m^2 solar collector areas are shown in section 2.2.

Figure 12 shows the annual net utilized solar energy as a function of the relative return inlet height from the space heating loop for different sizes of model 1. Further, the performance ratio relative to the optimal thermal performance of the system in question is shown.

Figure 13 shows the yearly net utilized solar energy as a function of the space heating demand and the domestic hot water consumption for the two different sizes of model 1, and a step by step improvement of the model. Also the performance ratio relative to the performance of the least advanced model 1.1 is shown. In all the calculations with a fixed return inlet height from the space heating loop, the optimal return inlet height shown in Figure 12 is used.

Figure 14 shows the monthly net utilized solar energy for the three differently sized models 1 and the step by step improvement of the models. Also the monthly solar radiation per m^2 solar collector is shown. Finally, Figure 14 shows the extra net utilized solar energy gained by replacing the heat exchanger spiral in the solar collector loop and the fixed return inlet height from the space heating loop with stratifiers. The calculations are made for a space heating demand of about 216 MJ/(m^2 year) and with a domestic hot water consumption of 100 l/day.

Table 3 shows the thermal performance increase by using stratifiers.

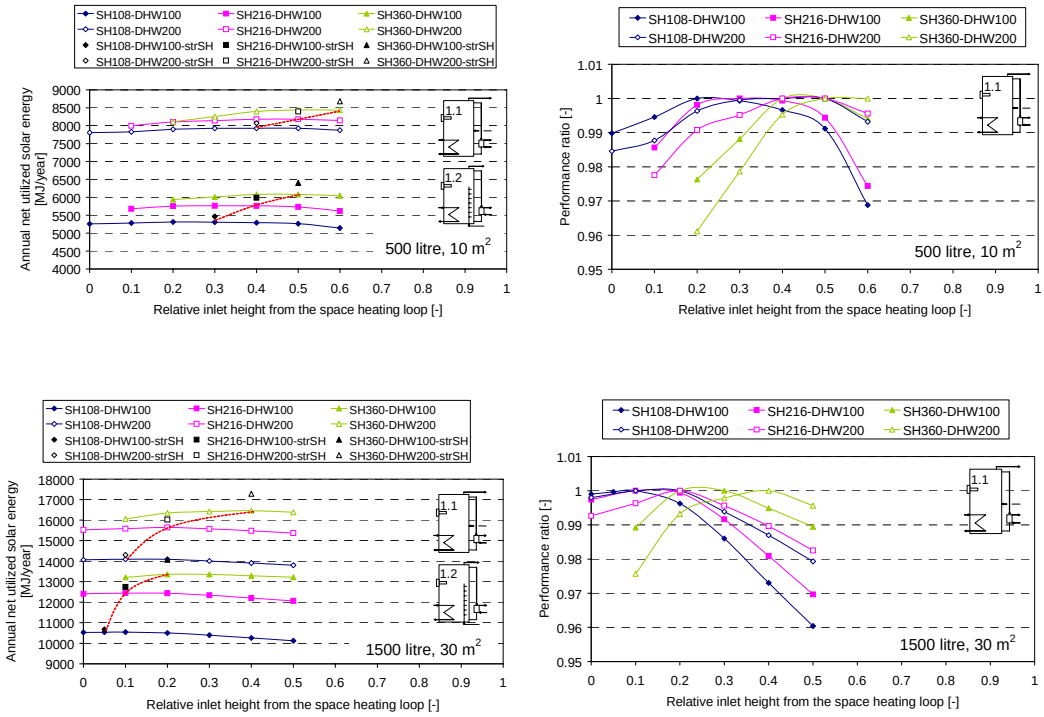

Figure 12: Left: The annual net utilized solar energy as a function of the relative return inlet height from the space heating loop for different sizes of model 1.1 and model 1.2. Right: The performance ratio relative to the optimal thermal performance of the system in question. Top: 10 m^2 collector, Bottom: 30 m^2 collector.

Figure 12 shows that the optimal inlet position from the space heating loop varies with the daily domestic hot water consumption and the space heating demand. For low space heating demand and thereby low return inlet temperatures from the space heating loop, the optimal inlet position is low. For increasing space heating demand and thereby increasing return inlet temperature from the space heating loop, the height of the optimal inlet position increases (indicated by the dotted line connecting the optimum of the curves). Also the optimal return inlet position from the space heating loop increases for increasing domestic hot water consumption. This is due to a larger amount of cold water in the bottom of the tank which leaves the warmer water that matches the temperature of the return water form the space heating loop at a higher level in the tank. The most suitable relative position of the inlet from the space heating loop in the systems with 500 litre tank, 1000 litre tank and 1500 litre tank are 0.4, 0.3 and 0.2, respectively. Regardless of the space heating demand and the hot water consumption, these positions will be close to the optimum positions.

The tendency is that the relative inlet position from the space heating loop is lower for larger systems than for smaller systems. However, the volume below the inlet from the space heating loop is in the same range between 200 litres and 300 litres for all three system sizes.

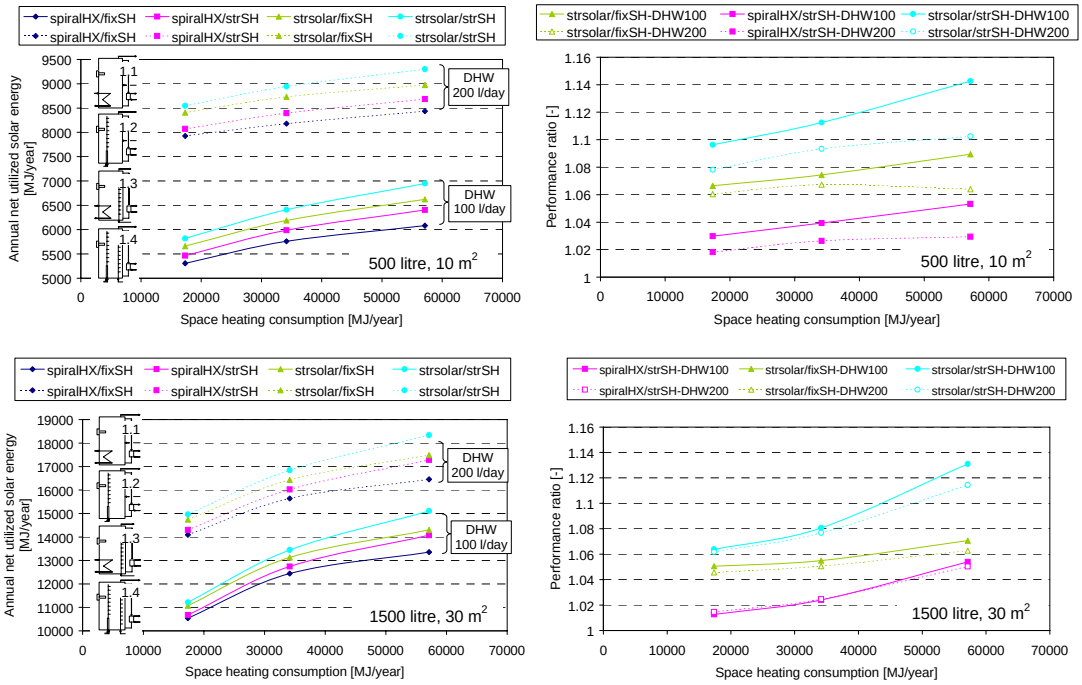

Figure 13: Left: The annual net utilized solar energy as a function of the space heating demand and the domestic hot water consumption for different sizes of model 1, and the step by step improvement of the model. Right: The performance ratio relative to the thermal performance of the least advanced model 1.1. Top: 10 m^2 collector, Bottom: 30 m^2 collector.

Figure 13 shows that the thermal performance increases for increasing space heating demand and increasing domestic hot water consumption. Also, the figure shows that the thermal performance increases when the heat exchanger spiral in the solar collector loop and the fixed return inlet from the space heating loop are replaced with stratifiers and this especially applies to the heat exchanger spiral in the solar collector loop. The performance ratio of the system by using inlet stratifiers is almost the same, regardless of the size of the solar combi system.

The increase in net utilized solar energy by using a stratifier in the solar collector loop, in the space heating loop, and in both the solar collector loop and the space heating loop is in the range of 5 – 9%, 1 – 6% and 6 – 14%, respectively. The additional gained net utilized solar energy by using stratifiers is increasing for increasing space heating demand due to higher temperature variations in the space heating loop and thereby better utilization of a stratifier.

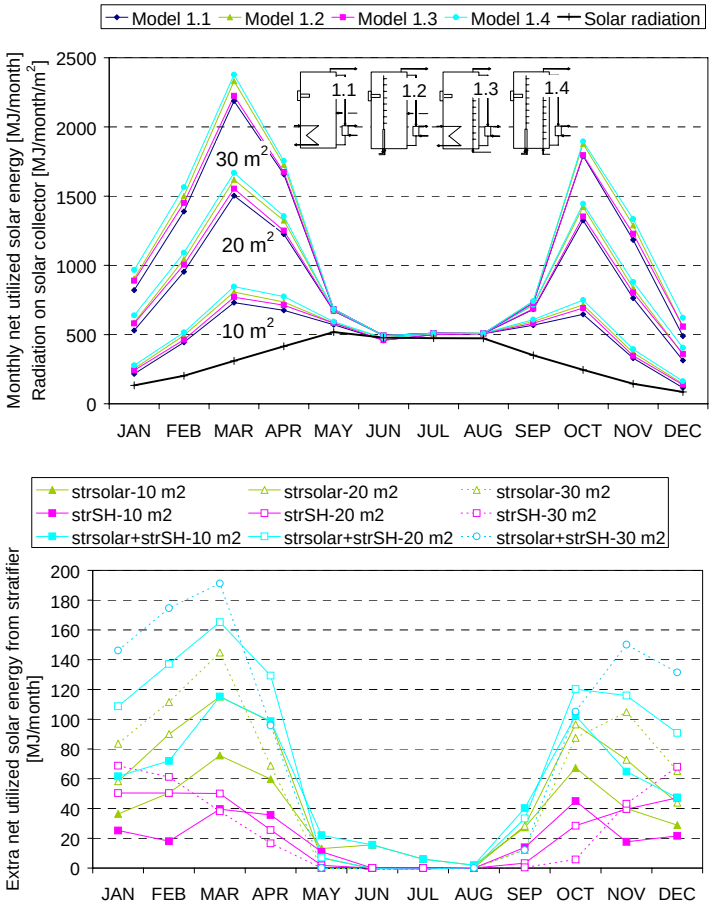

Figure 14: Top: Monthly net utilized solar energy for the three different size models 1.1, 1.2, 1.3 and 1.4 with solar collector areas of 10 m^2, 20 m^2 and 30 m^2. Bottom: Extra net utilized solar energy by using stratifiers.

From Figure 14 it is obvious that the solar fraction is 100% during the summer months. Further, it is obvious that the increased performance of larger solar combi systems is especially due to higher thermal performance during spring and autumn. Also the figure shows that small solar combi systems benefit from stratifiers in the space heating loop during a longer period than larger systems due to the lower solar fraction for small systems. For high solar fractions close to 100%, there is little or no benefit by using stratifiers.

From Table 3 it can be seen that large and medium sized solar combi systems benefit more from stratifiers than a small solar combi system. Finally, it is seen that the extra net utilized solar energy for a system with stratifiers in both the solar collector loop and the space heating loop equals the sum of the extra net utilized solar energy of the system with only one stratifier in the solar collector loop and the system with only one stratifier in the space heating loop.

Table 3: The net utilized solar energy and the extra net utilized solar energy with stratifiers in solar collector loop and in space heating loop and in both the solar collector loop and the space heating loop.

Solar collector area	10 m^2	20 m^2	30 m^2
Net utilized solar energy and solar fraction for model 1.1	5760 MJ/year 14.3%	9482 MJ/year 23.6%	12442 MJ/year 31.0%
Extra net utilized solar energy and solar fraction for model 1.2	421 MJ/year 15.4%	608 MJ/year 25.1%	677 MJ/year 32.6%
Extra net utilized solar energy and solar fraction for model 1.3	227 MJ/year 14.9%	295 MJ/year 24.3%	302 MJ/year 31.7%
Extra net utilized solar energy and solar fraction for model 1.4	648 MJ/year 15.9%	907 MJ/year 25.8%	1004 MJ/year 33.5%

4.2 Differently sized solar combi systems with constant space heating demand and constant daily hot water consumption

The investigation is carried out for different sizes of system model 1 and a step by step improvement of the model. The storage tanks are described in Tables 1 and 2. The solar collector areas vary from 5 m^2 to 60 m^2. The space heating demand is 216 MJ/(m^2·year) and the daily domestic hot water consumption is 100 litres.

Figure 15 shows the annual net utilized solar energy and the extra annual net utilized solar energy from stratifiers as a function of the solar collector area.

Figure 16 shows, at the top, the performance ratio as a function of the solar collector area for the solar combi systems with the operation conditions used in the calculations. At the bottom, the figure shows the performance ratio as a function of the solar fraction. The reference system in the performance ratio is the corresponding system model 1.1 with heat exchanger spiral in the solar collector loop and optimum fixed return inlet position from the space heating loop.

Figure 15 shows that the annual net utilized solar energy increases for increasing solar collector area. Further, the figure shows that, with the applied operation conditions, there is an optimum ratio between storage volume and solar collector area regarding extra thermal performance from a stratifier in the solar collector loop. For the storage tanks of 500 litres and 1000 litres, the ratio is 50 l/m^2 solar collector area, and for the storage tank of 1500 litres the ratio is 30 l/m^2 solar collector area (indicated by the circles in the figure). Consequently, the stratifiers are most advantageous for typical storage volume/collector area ratios. There is no optimum ratio between storage volume and solar collector area regarding extra thermal performance from a stratifier in the space heating loop within the investigated system sizes and operation conditions.

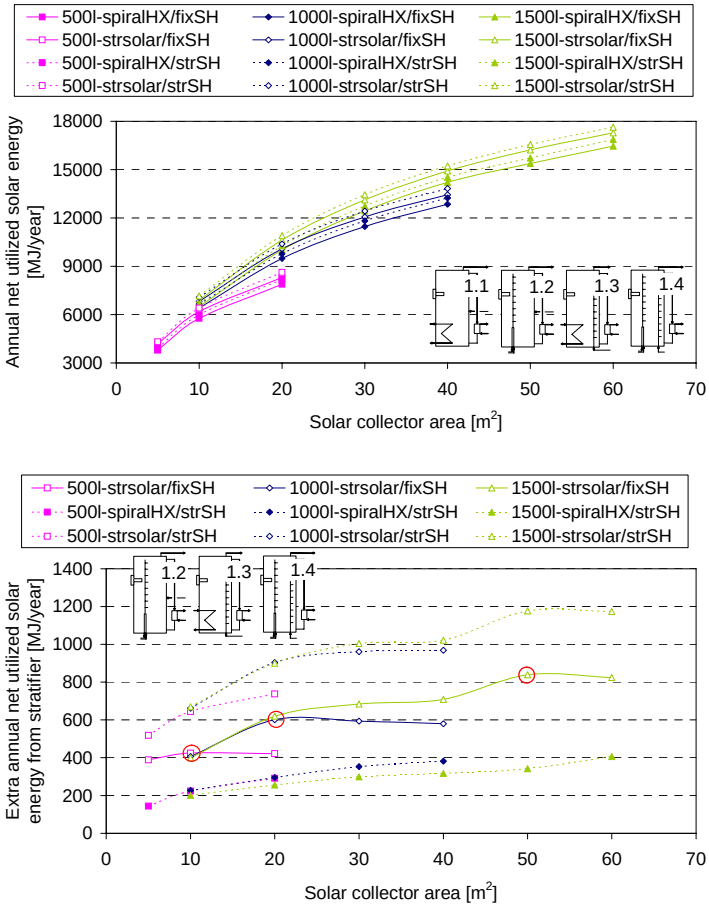

Figure 15: Top: The annual net utilized solar energy as a function of the solar collector area and heat storage volume. Bottom: The extra annual net utilized solar energy from stratifiers as a function of the solar collector area and heat storage volume. The annual thermal performances are shown for system model 1 and a step by step improvement of the system model.

Figure 16 shows that the performance ratio decreases for increasing solar collector area and solar fraction. Further, it can be seen that the curves for the step by step improvements of the solar combi systems lie in continuation of each other for different solar collector areas and different solar fractions. Consequently, the extra percentage thermal performance of the stratifiers is strongly depending on the solar fraction. The higher the solar fraction, the smaller the extra percentage thermal performance of stratifiers.

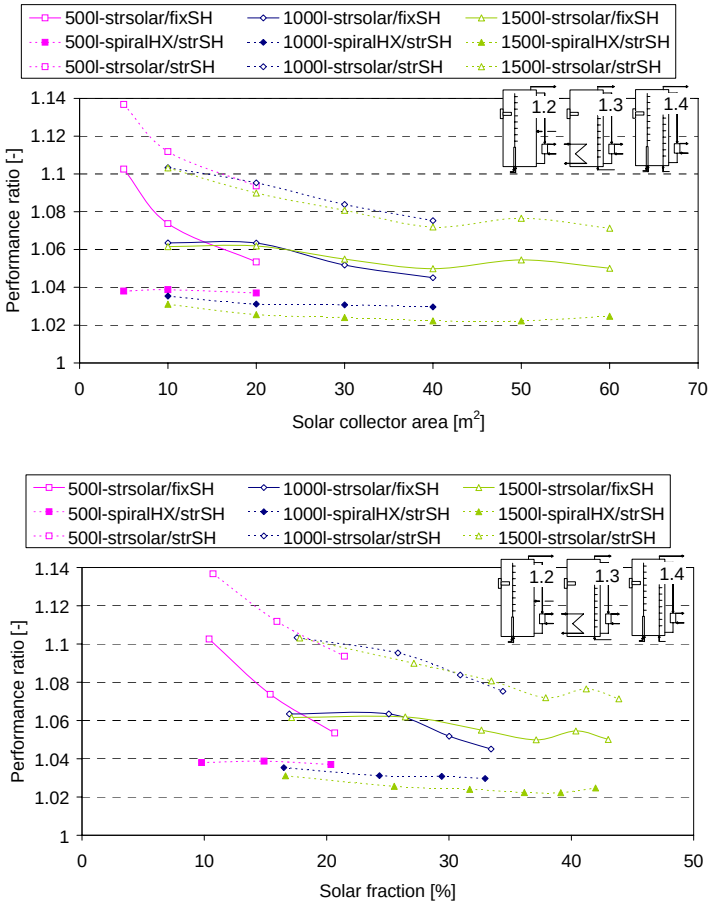

Figure 16: Top: The performance ratio as a function of the solar collector area. Bottom: The performance ratio as a function of the solar fraction. The reference system is the corresponding system model 1.1 with heat exchanger spiral in the solar collector loop and optimum fixed return inlet position from the space heating loop.

5 Conclusion

Three basically differently designed solar combi system models are investigated theoretically. The solar combi systems have a storage volume of 1000 litres with 20 m^2 solar collector area. The investigation includes the influence of thermal stratification, the size of the space heating system, space heating demand, domestic hot water consumption, and the control system in the solar collector loop. Also differently sized solar combi systems with storage tank volumes of 500 litres, 1000 litres and 1500 litres and solar collector areas between 5 m^2 and 60 m^2 are investigated.

Conclusions: **1)** The best performing solar combi system is based on a tank-in-tank storage with stratifiers both in the solar collector loop and the space heating loop. **2)** The thermal performance increases 5 – 10% if stratifiers are used only in the solar collector loop. **3)** The thermal performance increases 2 – 6% if stratifiers are used only in the space heating loop. **4)** The thermal performance increases 7 – 14% if stratifiers are used both in the solar collector loop and the space heating loop. **5)** The

extra net utilized solar energy for a system with stratifiers in both the solar collector loop and the space heating loop equals the sum of the extra net utilized solar energy of the system with stratifier in the solar collector loop and the system with stratifier in the space heating loop. **6)** The thermal performance is strongly increased for increasing size of the space heating system. **7)** The thermal performance increase by using stratifiers is highest for small space heating systems. **8)** The percentage thermal advantage by inlet stratifiers decreases for increasing solar fraction. **9)** Small solar combi systems benefit from stratifiers in the space heating loop during a longer period than larger systems due to a lower solar fraction. **10)** If the system has a direct return inlet from the space heating loop to the storage, the optimal relative inlet position from the space heating loop is lower for larger systems than for smaller systems, while the absolute inlet position as well as the optimum volume below the inlet from the space heating loop is in the same range. The optimal volume below the inlet is between 200 litres and 300 litres. **11)** In a tank with heat exchanger in the solar collector loop (high flow system), the best position of the temperature sensor in the tank for controlling the pump in the solar collector loop is between 1/10 and 1/20 of the heat exchanger height, calculated from the bottom of the heat exchanger with a minimum temperature differential between 0 K and 1 K regardless of the operation conditions. **12)** In a tank with stratifier in the solar collector loop (low flow system), the best position of the temperature sensor in the tank for controlling the pump in the solar collector loop is in the very bottom of the tank with a minimum temperature differential between -1 K and 2 K regardless of the operation conditions.

In practice there is a great advantage by using ideal working stratifiers instead of internal heat exchanger spirals and direct inlets because the optimal design of solar combi systems varies with the consumption and because solar combi systems with stratifiers are less sensitive towards non-optimal operation conditions.

Nomenclature

η_0	Optical efficiency of incident radiation	[-]
η	Solar collector efficiency	[-]
θ	Incidence angle	[-]
k_θ	Incidence angle modifier for beam radiation	[-]
a_1	Heat loss coefficient	[W/m^2/K]
a_2	Heat loss coefficient	[W/m^2/K^2]
T_m	Mean collector fluid temperature	[ºC]
T_a	Ambient temperature	[ºC]
E	Total solar irradiance on collector	[W/m^2]
Q_{AUX}	Auxiliary energy consumption	[J]
Q_{DHW}	Domestic hot water load	[J]
Q_{NET}	Net utilized solar energy	[J]

$Q_{NET,REF}$	Net utilized solar energy of reference system	[J]
Q_{SH}	Space heating load	[J]
SF	Solar fraction	[%]
PR	Performance ratio	[-]

Abbreviations

DHW	Domestic hot water
SH	Space Heating
spiralHX	Heat exchanger spiral in the solar collector loop
fixSH	Fixed return inlet height from the space heating loop
strsolar	Stratifier in the solar collector loop
strSH	Stratified return inlet from space heating loop

References

[1] Weiss et al., Solar Heating Systems for Houses, a Design Handbook for Solar Combisystems. James & James Ltd, London. ISBN 1 902916 46 8, 2003.

[2] Streicher W., Heimrath R., Analysis of System Reports of Task 26 for Sensitivity of Parameters, Technical Report for Subtask C, IEA SHC-Task 26, 2004.

[3] Streicher W., Elements and Examples of "Dream Systems" of Solar Combisystems. A Report of IEA SHC – Task 26, 2004.

[4] Lorenz K., Kombisolvärmesystem – Utvärdering av möjliga systemförbättringar. Ph.D Thesis, Institutionen för Installationsteknik, Chalmers Tekniska Högskola, Göteborg, 2001.

[5] Jordan U., Untersuchungen eines Solarspeichers zur kombinierten Trinkwassererwärmung und Heizungsunterstützung. Dissertation, Universität Marburg, 2001.

[6] Pauschinger, T., Drück, H., Hahne, E., Comparison test of solar heating systems for domestic hot water preparation and space heating, Proceedings of Second International ISES Solar Congress, 1998.

[7] Streicher W., Simple estimation of the solar fraction of combisystems and centralized big solar plants, Proceedings of Second International ISES Solar Congress, 1998.

[8] Drück H., Hahne E., Test and comparison of hot water stores for solar combisystems, Proceedings of Second International ISES Solar Congress, 1998.

[9] Andersen E., Furbo S., Fan J., Investigations of fabric stratifiers for solar tanks, Accepted for publication in Journal of Solar Energy, November 2006.

[10] Klein S.A et al., TRNSYS 15, User Manual. University of Wisconsin Solar Energy Laboratory, 1996.

[11] Drück H., MULTIPORT Store – Model, Type 140 for TrnSys. Institut für Thermodynamik und Wärmetechnik. Universität Stuttgart, 2000.

[12] Skertveit, A., Lund, H., and Olseth, J. A., Design Reference Year, Report no. 1194 Klima, Det Norske Institutt, 1994.

[13] Jordan, U., Vajen, K., Influence of the DHW-load profile on the fractional energy savings: a case study of a solar combi-system with TRNSYS simulations, Proceedings of EuroSun 2000 Congress, Copenhagen, Denmark, 2000.

[14] Knudsen, S., Consumers' influence on the thermal performance of small SDHW systems – theoretical investigations, Solar Energy Vol. 73, No. 1, pp. 33-42, 2002.

[15] Knudsen S., Heat transfer in a „tank-in-tank" combi store. Department of Civil Engineering, Technical University of Denmark, report R-025, ISBN 87-7877-083-1, 2002.

Paper VI

Theoretical and Experimental Investigations of Inlet Stratifiers for Solar Storage Tanks

Applied Thermal Engineering 25, pp. 2086-2099, 2005

Theoretical and Experimental Investigations of Inlet Stratifiers for Solar Storage Tanks

Louise Jivan Shah, Elsa Andersen and Simon Furbo

Department of Civil Engineering Technical University of Denmark

DK-2800 Kgs. Lyngby, Denmark.

Applied Thermal Engineering 25, pp. 2086-209, 2005

Abstract

A rigid stratifier is investigated theoretically with Computational Fluid Dynamics and experimentally with Particle Image Velocimetry and temperature measurements. The stratifier consists of a main tube with three circular openings. The stratifier is mounted inside a 144 l water tank.

During a tank charge test, the investigations show that cold tank water is sucked into the stratifier through the lowest opening. The mixed fluid enters the tank through the top opening.

To illustrate the influence of mounting flaps working as “non-return valves” at the stratifier openings, the experiment is repeated with the stratifier with flaps. The results show that the “non-return valves” reduce the unwanted flows into the lowest opening.

To quantify how well the stratifier with the flaps works for other flow rates more tank charge tests are carried out. Based on a stratifier efficiency it is found that the stratifier is most efficient for flow rates between 5 l/min and 8 l/min.

Keywords Thermal stratification, solar storage, computational fluid dynamics, particle image velocimetry.

1 Introduction

Thermal stratification in sensible energy storages plays an important role on the efficiency of the energy system of which the storage is a part of. For example in hot water tanks heated by gas burners a well stratified storage, where the cold water inlet does not disturb the thermal stratification, leads to better operation of the gas burner (less starts and stops) and thus an increased burner efficiency. Analogous, energy systems with stratified heat storages heated by biomass burners will have a higher efficiency compared to systems with non stratified storages.

Thermal stratification in solar storage tanks has a major influence on the thermal performance of a solar heating system. In solar combisystems, which are solar heating installations providing space heating as well as domestic hot water [1], very often

diffuser manifolds or stratifiers, which should promote stratification, have been adopted.

These stratifiers are used in the solar storage tanks for the return flow from the solar collector, and/or from the space heating system and/or from the return of the domestic hot water preparation. Figure 1 shows a diagram of a solar combisystem with two stratifiers in the solar collector loop and the space heating loop respectively.

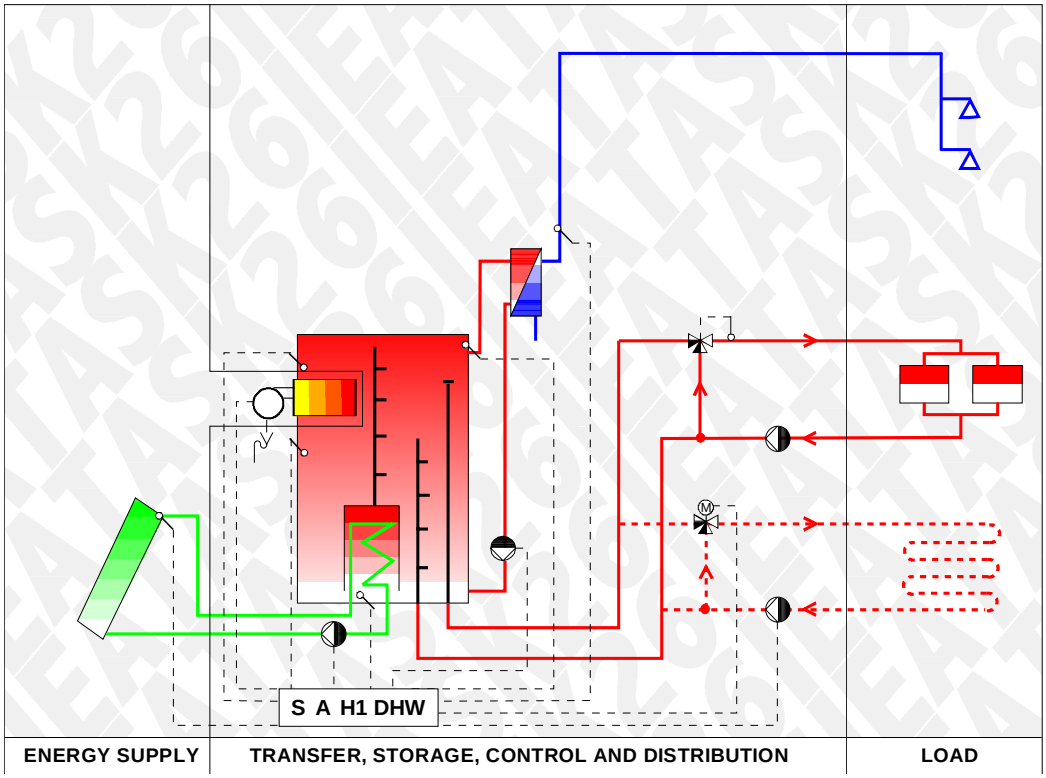

Figure 1: A solar combisystem with two stratifiers in the solar collector loop and the space heating loop respectively. (Figure from [2]).

Generally, stratifiers are developed for variable inlet-temperature and flow, corresponding to the conditions in the solar collector loop and the space heating loop of a solar combisystem. The main purpose for a stratifier is to allow the incoming fluid to enter the tank at the "right" height of thermal equilibrium.

One of the first stratifier designs was suggested by van Koppen et al. [3]. A floating flexible light rubber hose was used, and by buoyancy forces the hose should reach the thermal equilibrium in the tank of the incoming fluid. Due to problems with dirt accumulated in the hose, this solution never worked in practice.

Loehrke et al. [4] investigated two types of stratifiers. One was based on a rigid perforated PVC drain pipe with a diameter of 10 cm and another was based on a flexible 10 cm diameter "sleeve" made of a polyester cloth. It was found that the performance of the flexible stratifier was superior to the rigid stratifier, due to the fact that the "sleeve" diameter changed with the inlet flow rate and the thermal conditions in the tank.

Davidson and Adams [5] worked further on flexible stratifiers. Experimentally, they investigated different fabric materials for the flexible sleeve and they concluded that synthetic fabrics were superior to natural fibres and that effective manifold materials should be rib-knit which stretch easily in one direction. Based on the MIX-number [6] they also found that the flexible stratifier was 4% more effective than a rigid stratifier and 48% more effective than a traditional drop-tube inlet.

Abu-Hamdan et al. [7] investigated a highly perforated tube with a diameter of 35.6 cm and a length of 1.47 m. For variable inlet conditions they found that this configuration offered no advantages over conventional side and top inlets.

On the market today there are several rigid stratifier designs. A design based on a long tube with openings is used. One example of the use of this stratifier design is shown in Figure 2.

Another more advanced stratifier design is shown in Figure 3. Here, at the openings there are mounted flaps, which work as “non-return valves”. The flaps are constructed with a soft material which allows the flap to close and open depending on the temperature and pressure conditions inside and outside the pipe. The stratifier is designed by the German company Solvis GmbH, and according to the company the stratifier is suitable for flows up to 13 l/min.

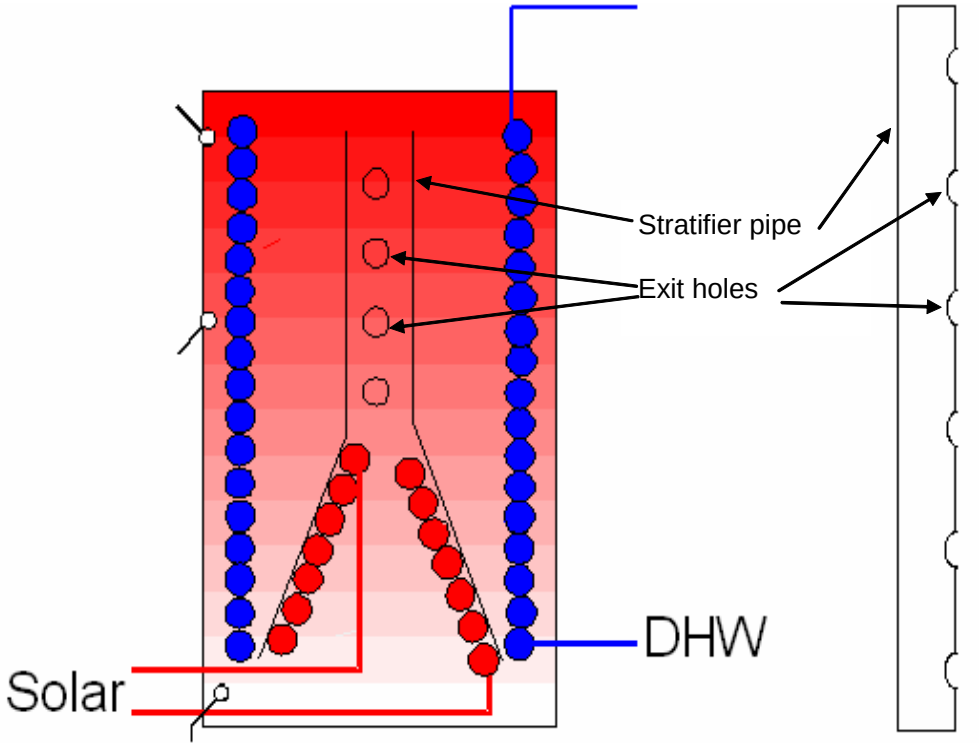

Figure 2: **Left:** Stratifiers for the return flow from the solar collector inside a storage tank. The stratifier is based on a pipe with openings. Inside the stratifier the flow is natural convection driven. **Right:** The stratifier seen from the side.

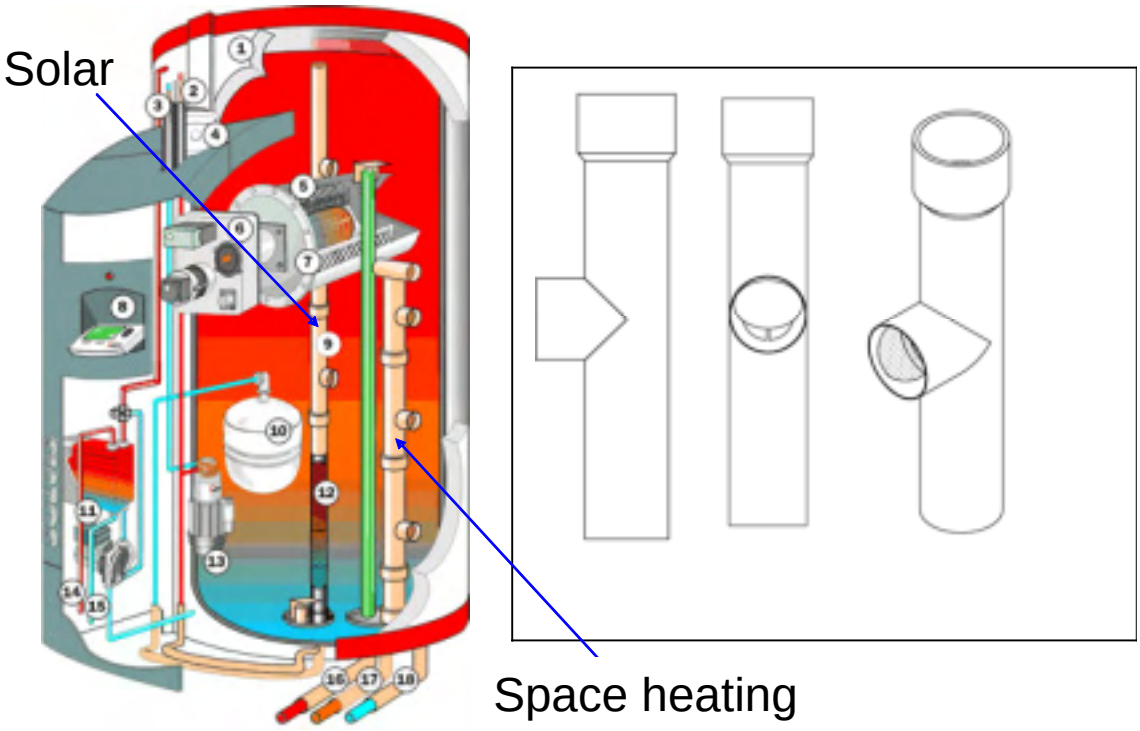

Figure 3: **Left:** The SOLVIS stratifiers for the return flow from the solar collector and from the space heating system inside a storage tank. The stratifier design is based on a pipe with openings where flaps working as "non-return valves" are mounted. **Right:** Schematics of the stratifier.

Essert [8] experimentally investigated this stratifier and found that the stratifier was well working for flows below 10 l/min. For higher flow rates it was found that the performance also strongly depended on the thermal conditions.

Also Andersen et al. [9] experimentally investigated this stratifier design. Several tank charge tests were performed and generally, it was found that thermal stratification was well built up with the stratifier. However, they also concluded that further detailed investigations are needed, before the function of this stratification inlet pipe is fully elucidated.

The aim of the present work is to evaluate by theoretical and experimental means, how a stratifier with unobstructed openings performs. The aim is also to illustrate the influence of mounting flaps at the openings.

2 Theoretical investigations

A water tank with a stratifier is investigated by means of Computational Fluid Dynamics (CFD) calculations. The tank is square with side lengths of 0.4 m and a height of 0.9 m, and thus a volume of approximately 144 litres.

The investigated stratifier is designed as the stratifier shown in Figure 3, however, the flaps are removed. The distance between the bottom of the tank and the centre of the lowest opening is 0.15 m and the distances between the openings are 0.30 m. Each opening diameter is 0.06 m, the pipe is closed at the top and the fluid enters the

stratifier through the bottom. The tank outlet is also placed at the tank bottom. Figure 4 (left) shows a schematic illustration of the investigated stratifier.

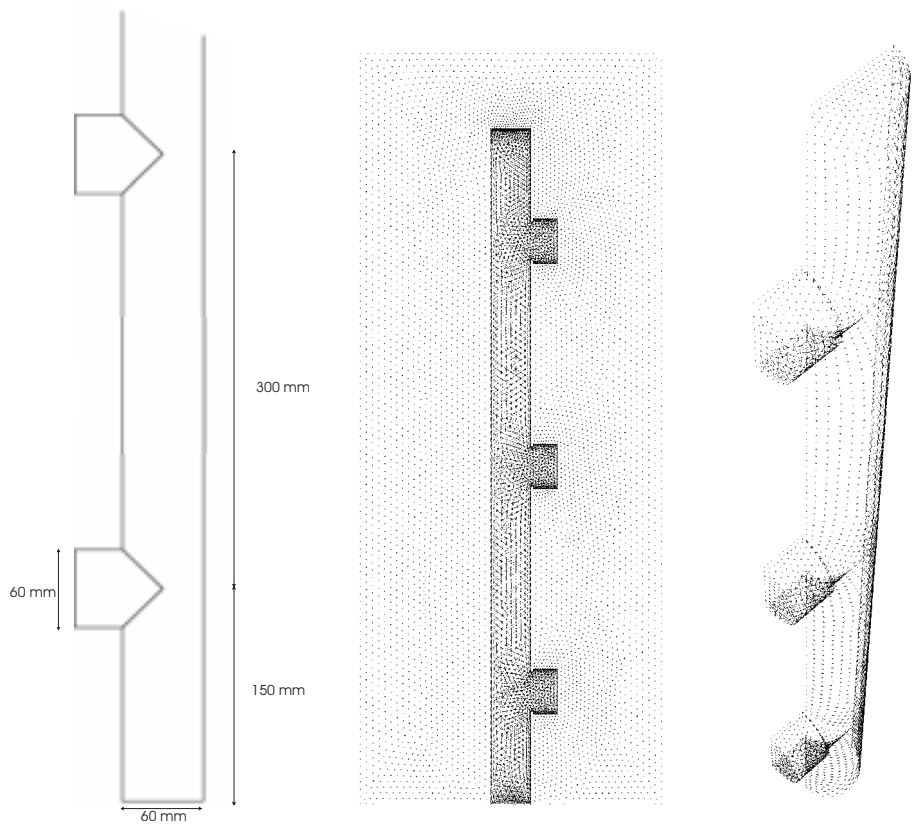

Figure 4: **Left:** Measures of the stratifier. **Middle:** The grid distribution in the symmetry plane. **Right:** The wall grid of the stratifier.

A 50 min. long charge test is modelled. The tank is initially cold (20°C) and through the stratifier, the tank is charged by an inlet flow of about 2 l/min and a temperature of about 43°C, corresponding to the test conditions of the experiments described later.

To solve the flow and energy equations, a simulation model of the flow in the tank is developed using the CFD code Fluent 6.1 [10]. A stratifier with three openings is investigated. The tank outlet is placed at the bottom corner of the tank. The tank walls are not modelled and symmetry is assumed in the centre plane of the tank. Further, the heat loss from the tank is not modelled. This has no significant influence on the results as the simulated tests are of a duration of only 50 min and as the heat loss power through the tank wall is magnitudes lower than the tank charge power. The mesh is built up of 580,149 tetrahedral cells and is thus an unstructured mesh. Figure 4 shows the model outline, the grid distributions in the symmetry plane and the wall grid of the stratifier.

Numerical solutions are obtained for transient laminar flow with the Boussinesq assumption for the buoyancy modelling. The velocity-pressure coupling is treated by using the SIMPLE algorithm and the First Order Upwind scheme is used for the momentum and energy terms. A time step of 0.5 second is used.

Figure 5 shows the temperature distribution in the tank centre plane after 10 min., 30 min. and 50 min. The temperature profiles show how the tank water is sucked into the stratifier especially through the bottom opening. The cold tank water is mixed with the hot inlet flow and this mixed flow enters the tank through the top opening. After 50 min. there is almost no thermal stratification in the tank. The temperature difference between the top and bottom of the tank is only about 5-6 K.

The computations show that under the present operating conditions (2 l/min inlet flow) this type of stratifier actually works more as a “mixing device” than as a stratifying device.

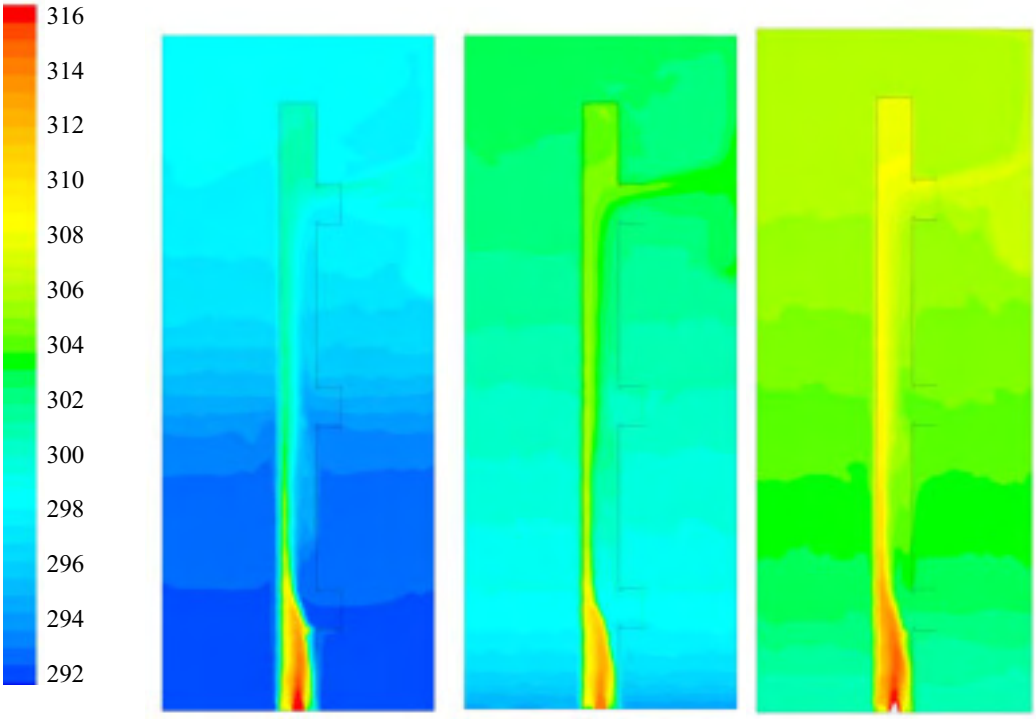

Figure 5: Temperatures in the tank after 10 min., 30 min. and 50 min. The scale at the left shows the temperature level in [K].

3 Experimental investigations

In order to verify the simulated results, the stratifier is experimentally investigated by means of PIV (Particle Image Velocimetry).

The experimental set-up is shown in Figure 6. The set-up consists of a rectangular glass tank with side lengths of 400 x 400 x 900 mm^3, a heating and a cooling unit, and standard PIV equipment (Dantec Dynamics). The PIV equipment consists of a laser, a camera and a processing system for analysing the pictures taken by the camera. More details about the PIV equipment and the heating/cooling unit are given in [9].

With the PIV equipment the two-dimensional flow field near each opening is visualized. The interrogation area near each opening has the size 0.127 x 0.159 m^2 as illustrated in Figure 7. Figure 8 shows photos of the stratifier.

In addition to the PIV measurements, also temperature measurements are carried out. The inlet temperature, the outlet temperature and five temperatures inside the tank are measured. The temperature sensors inside the tank are respectively placed at 145 mm, 345 mm, 545 mm, 705 mm and 865 mm from the bottom of the tank.

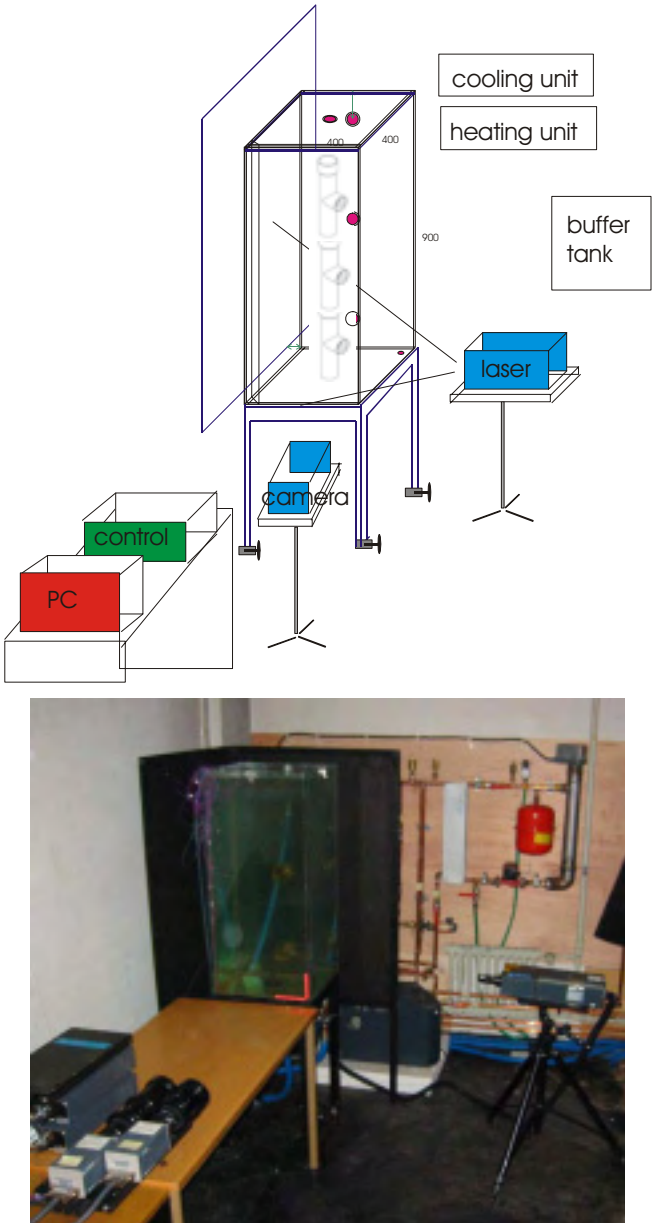

Figure 6: Experimental set-up. (Figure from [9]).

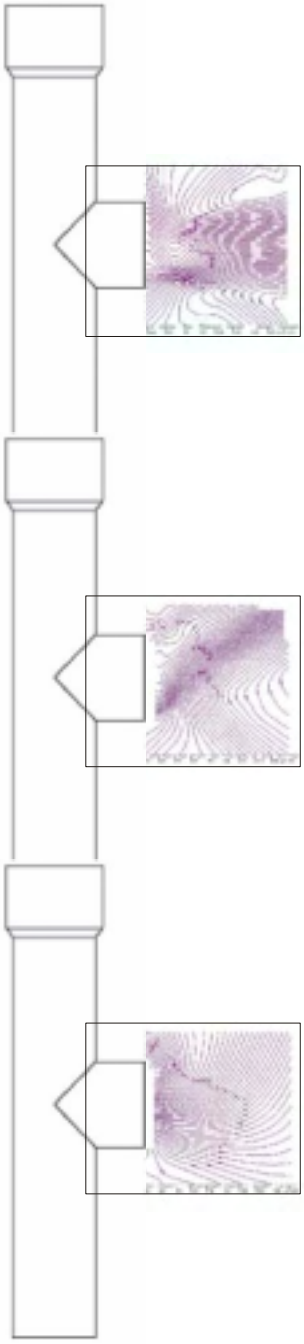

Figure 7: Illustration of the interrogation areas. (Figure from [9]).

Figure 8: Photos of one stratification inlet pipe (right) and the stratifier made of three compound inlet pipes.

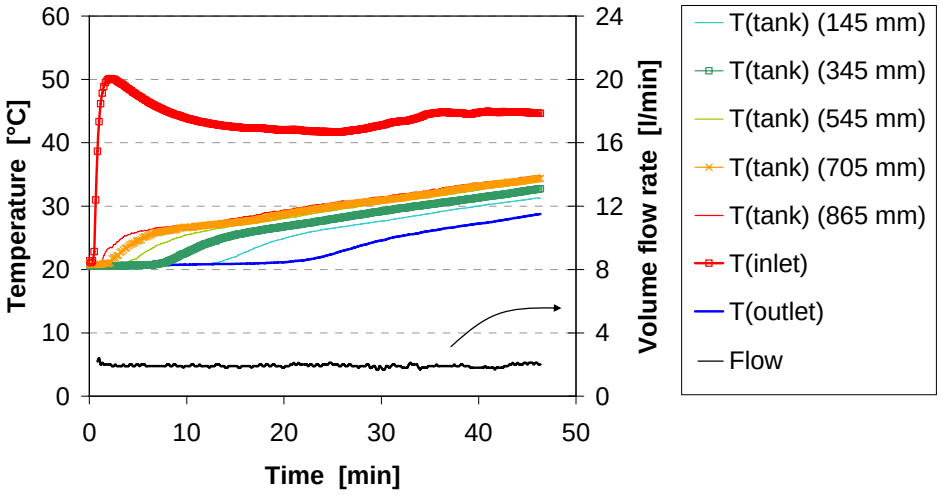

Figure 9: The test conditions and the temperatures in the tank during the experiment.

A 47 min. long charge experiment is carried out. As in the previous computations, the tank is initially cold (20°C) and through the stratifier the tank is charged by an inlet flow of about 2 l/min and a temperature of about 43°C.

Figure 9 shows tank inlet- and outlet temperatures, the flow rate and the temperatures in the tank. It can be seen that the tank outlet temperature rises after only 25 min.,

which is after only a 50 l draw-off. This shows that the thermal stratification is not build up in a good way. If the thermal stratification was build up in an ideal way the bottom outlet temperature should rise after approximately 60 min. as the tank volume below the top opening is approximately 120 l and the flow rate is about 2 l/min.

As an example, Figure 10 shows calculated and measured velocity vectors near the openings after 40 min. The main flow stream in both the experiments and the calculations enters the tank through the top opening of the stratifier. At the middle outlet there is a difference between the measured and calculated flow patterns as the measurements show a small flow entering the bottom of the opening and a significant flow stream leaving at the very top of this opening. The reason for the difference is most likely that the numerical grid is too coarse to solve this complicated flow. Another reason could be that the modelled and the actual stratifier geometry is not completely identical as the stratifier is modelled as a thin non-conducting shell instead of a 3 mm thick wall. However, both in the calculations and in the measurements, a significant flow through the bottom opening into the main stratifier pipe is present.

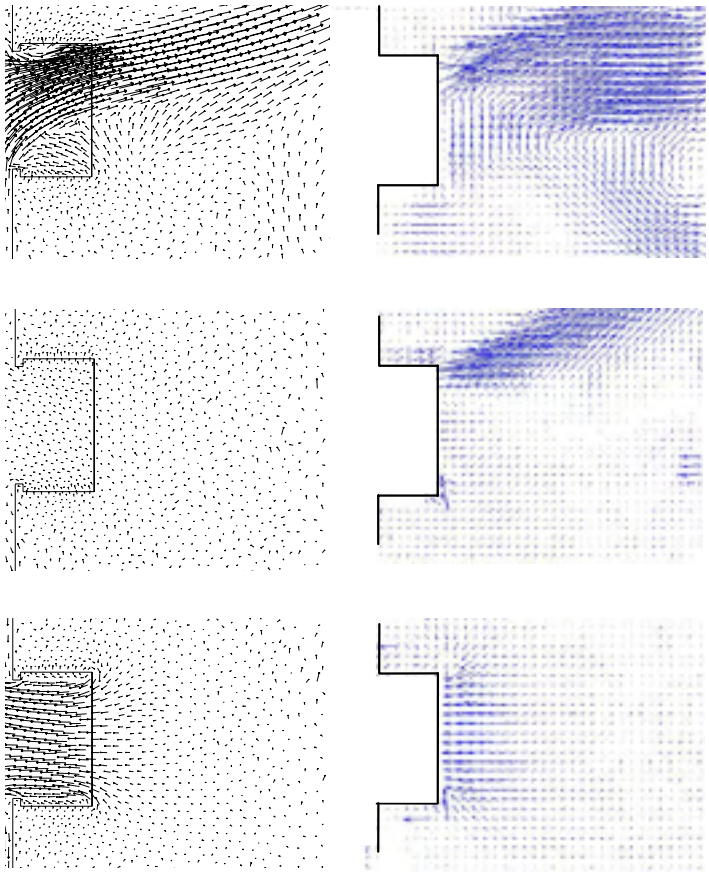

Figure 10: Calculated (left) and measured (right) velocity vectors. Calculated and measured velocity magnitude: 0 m/s – 0.06 m/s.

To illustrate the influence of placing the flaps at the openings, the experiment was repeated now with the stratifier with the flaps. The flaps are made of a soft rubber material and they should work as “non-return valves”. Each flap is mounted on a small hook in the top of each opening. This allows the flap to open when there is a

flow going out and to close when the flow inside the main tube is rising to an upper opening.

Figure 11 shows tank inlet- and outlet temperatures, the flow rate and the temperatures in the tank during this experiment. Now it can be seen that the bottom outlet temperature hardly rises during the test. This means that the thermal stratification is build up in a better way with the stratifier with “non-return valves” compared to the stratifier without “non-return valves”.

The influence of the “non-return valves” is further illustrated in Figure 12. Here, the measured velocity vectors near the openings after 40 min. in the experiment for the stratifiers without and with the “non-return valves” are compared. Here it is quite clear that the “non-return valves” reduces the unwanted flow going into the stratifier at the lowest opening.

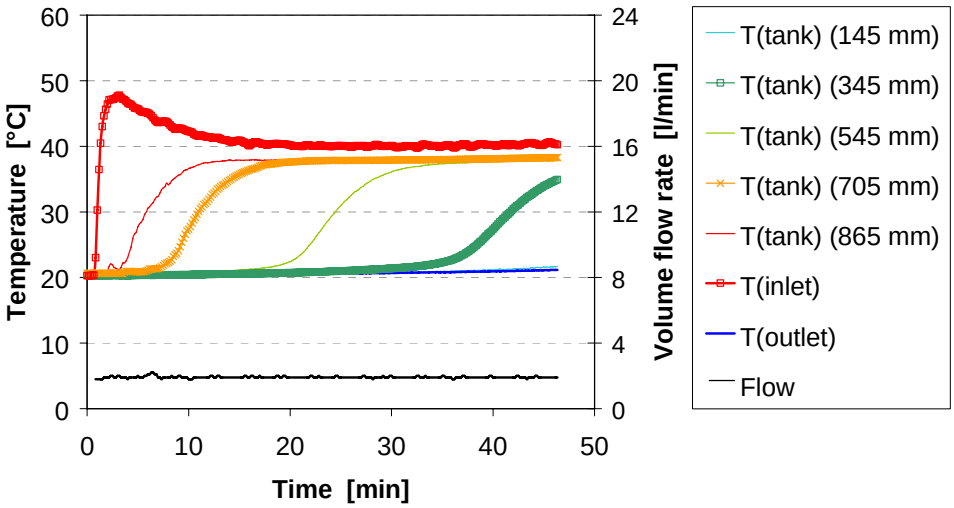

Figure 11: The test conditions and the temperatures in the tank during the experiment with the stratifier with “non-return valves”.

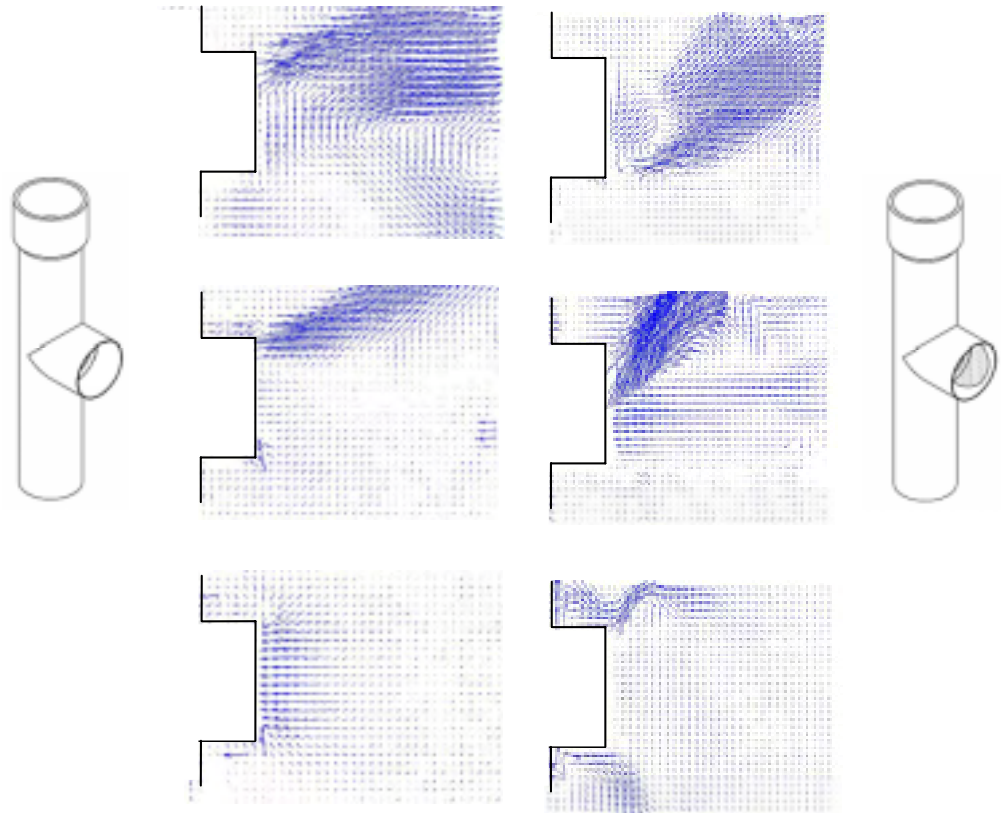

Figure 12: Measured velocity vectors for the stratifier without the “non-return valves” (left) and with the “non-return valves” (right).

For the stratifier with the “non-return valves”, it can also be seen that there are some natural convection flows near the stratifier wall below and above the lower opening. Since there is less fluid being sucked into the stratifier pipe, the fluid temperature in the stratifier with “non-return valves” is higher compared to the stratifier without the “non-return valves”. Furthermore, the tank bottom temperature is colder compared to the bottom temperature in the tank without the “non-return valves”. Consequently, the temperature difference, and thus the natural convection, between the stratifier wall and the fluid in the tank are more significant for the system with “non-return valves” compared to the system without the “non-return valves”.

Figure 12 also shows that the stratifier with the “non-return valves” is not ideally working. As the flow leaving the top opening seeks upwards, the temperature inside the stratifier must be warmer than the tank temperature in the same height. This means that the flow should only leave the top opening. From the figure, however, it is quite clear that there is also fluid streaming out of the middle opening.

The investigations clearly show that the flaps have a significant influence of how well the thermal stratification is being built up in the tank. However, the investigations also show that the stratifier with the flaps is not ideally working.

The results described above are valid for a flow rate of about 2 l/min. To quantify how well the stratifier with flaps works for other flow rates other tank charge tests have been carried out. In total 5 experiments are performed with flow rates of 2 l/min, 4 l/min, 5 l/min, 8 l/min and 10 l/min. These experiments are in detail described in [11].

By means of the measured inlet and outlet temperatures and the flow rate, the actual energy amount supplied to the tank, Q_1, is determined until one tank volume is exchanged.

Further, assuming that no mixing occurs, the maximum possible energy amount supplied to the tank, Q_2, is determined. Q_1 and Q_2 are described by equation (1) and (2):

$$Q_1 = \int_{t_{start}}^{t_{stop}} \dot{V} \cdot \rho \cdot c_p \cdot (T_{inlet} - T_{outlet}) \cdot dt \qquad [J] \qquad (1)$$

$$Q_2 = V \cdot \rho \cdot c_p \cdot (T_{average,inlet} - T_{initial}) \qquad [J] \qquad (2)$$

The efficiency of the stratifier is defined as Q_1/Q_2. Thus, the stratifier is ideally working if Q_1/Q_2 equals 1 when one tank volume has been charged. In order to take into account that the test periods do not have equal lengths, the efficiency results are corrected for the tank heat loss. That is, the calculated efficiencies are based on the measured temperatures, which are corrected to the values they would have obtained if there were no heat losses.

As a function of the volume flow rate the efficiencies are shown in Figure 13. Here it can be seen that the stratifier efficiency is highest for flow rates between 5 l/min and 8 l/min. The reasons are as follows:

For small volume flow rates, the inlet flow rises as expected in the stratifier but the heat transfer through the stratifier wall from the hot inlet fluid to the colder tank will significantly decrease the temperature at the top opening. Consequently, the temperature at the top opening is reduced and thus the efficiency is reduced. Further, during the experiments it was noticed that the lowest flap does not close completely tight as the suction on the lower flaps is quite small due to the relatively small velocity in the stratifier. Therefore, some fluid is sucked in to the stratifier through the lowest hole. This is, however, not clearly seen in Figure 12.

For higher flow rates, the temperature drop inside the stratifier due to heat transfer through the stratifier is less significant. Consequently, compared to the lowest flow rate, the temperature at the top opening is increased and thus the efficiency is increased. Further, under these experiments it was noticed that the lowest flap is completely closed. As the velocity in the stratifier is increased the suction on the lower flaps is higher and the flaps close more tightly.

For the highest flow rate, the velocity in the stratifier is so large that, due to the momentum forces, the fluid exits not only the top opening. Therefore, the efficiency is decreased again.

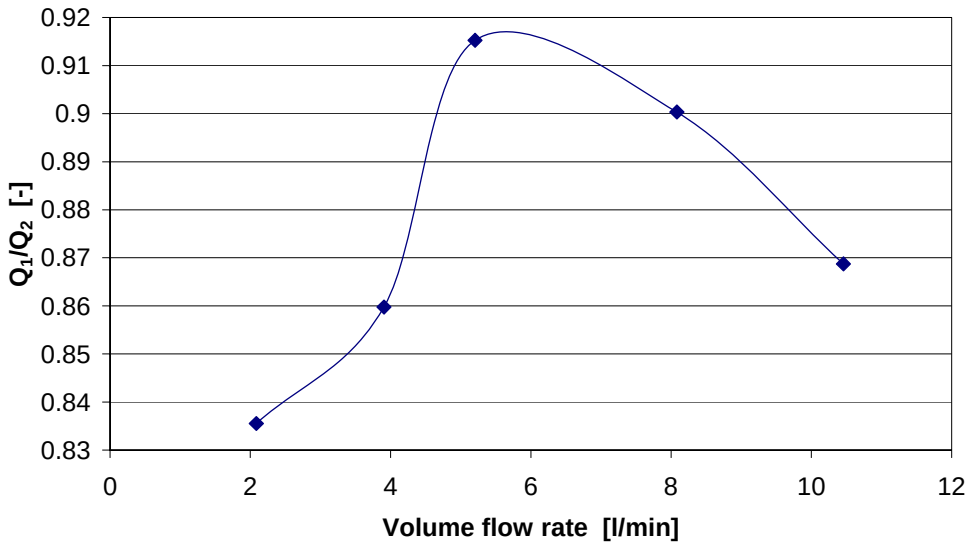

Figure 13: The stratifier efficiency as a function of the volume flow rate.

4 Conclusion

A rigid stratifier is investigated theoretically with Computational Fluid Dynamics and experimentally with Particle Image Velocimetry and temperature measurements. The stratifier is designed as a main tube with three circular openings. The stratifier is mounted inside a 144 l water tank.

A tank charge investigation is performed. The tank was initially cold (20°C) and through the stratifier the tank is charged by an inlet flow of about 2 l/min and a temperature of about 43°C.

Both the experimental and the theoretical investigations show that cold tank water is sucked into the stratifier especially through the lowest opening and the mixed fluid enters the tank through the top opening. Consequently, under the examined operating conditions this type of stratifier actually works more as a “mixing device” than as a stratifying device.

To illustrate the influence of placing “non-return valves” at the stratifier openings, the experiment is repeated with the stratifier with flaps working as “non-return valves”. Here it is clear that the “non-return valves” reduces the unwanted flows at the lowest opening.

To quantify how well the stratifier with the flaps works for other flow rates more tank charge tests are performed. In total 5 experiments are performed with flow rates in the interval from 2 l/min to 10 l/min.

Based on a stratifier efficiency defined as the ratio between the actual energy amount supplied to the tank and the maximum possible energy amount supplied to the tank assuming that no mixing occur, it is found that the stratifier is most efficient for flow rates between 5 l/min and 8 l/min.

As the investigated stratifiers often are used for volume flow rates much less than 5 l/min it is concluded that there still is a need for further development of these stratifier designs.

References

[1] IEA-SHC, Task26 (2003), http://www.iea-shc.org/task26/index.html

[2] Streicher W. (ed.) (2003), Report on Solar Combisystems modelled in Task 26. A report of IEA SHC – Task 26. Solar combisystems, April 2003. http://www.iea-shc.org/outputs/task26/C_Streicher_Sys_Models.pdf

[3] van Koppen C.W.J., Thomas J.P.S. and Veltkamp W.B. (1979), *The Actual Benefits of Thermally Stratified Storage in a Small and Medium Size Solar System*. Proceedings ISES Biennial Meeting, Atlanta. Vol. 2, pp. 576-580.

[4] Loehrke R.I., Holtzer J.C., Gari, H.N. and Sharp M.K. (1979), *Stratification Enhancement in Liquid Thermal Storage Tanks*. Journal of Energy, Vol. 3, No. 3, pp. 129-130

[5] Davidson J.H. and Adams D.A. (1994), *Fabric Stratification Manifolds for Solar Water Heating*. Journal of Solar Energy Engineering, Vol. 130, pp. 130-136.

[6] Davidson J.H., Adams D.A. and Miller J.A. (1994), *A Coefficient to Characterize Mixing in Solar Water Storage Tanks*. Journal of Solar Energy Engineering, Vol. 116, pp. 94-99.

[7] Abu-Hamdan M.G., Zurigat Y.H. and Ghajar A.J. (1992), *An Experimental Study of a Stratified Thermal Storage under Variable Inlet Temperature of different Inlet Designs*. Int. J. of Heat and Mass Transfer, Vol. 35, No. 8, pp. 1927-1934.

[8] Essert H. (1995) *Aufbau und Inbetriebnahme eines Speicherversuchsstandes.* Diploma Thesis, Graz University, Austria.

[9] Andersen E., Jordan U., Shah L.J. and Furbo S. (2004), *Investigations of the Solvis Stratification Inlet Pipe for Solar Tanks.* Proceedings, EuroSun2004, Freiburg, Germany, Vol. 1, pp. 76-85. ISBN. 3-9809656-1-9.

[10] Fluent 6.1 User's Guide (2003). Fluent Inc. Centerra Resource Park 10 Cavendish Court Lebanon, NH 03766

[11] Shah L.J. (2002), *Stratifikationsindløbsrør.* Report SR-02-23. Department of Civil Engineering, Technical University of Denmark. ISSN 1393-402x. (In Danish).

Nomenclature

Q_1	actual energy amount supplied to the tank	[J]
Q_2	maximum possible exchanged energy amount	[J]
V	exchanged tank volume	[m³]
$\dot{V}$	volume flow rate	[m³/s]
Δt	time interval	[s]
$T_{initial}$	initial tank temperature	[°C]
T_{inlet}	inlet temperature	[°C]

T_{outlet}	outlet temperature	[°C]
$T_{average,inlet}$	average inlet temperature during the experiment	[°C]
c_p	water heat capacity	[J/kg·K]
ρ	water density	[kg/m³]

Paper VII

Multilayer Fabric Stratification Pipes for Solar Tanks

Paper accepted for publication in Journal of Solar Energy, January 2007

Multilayer Fabric Stratification Pipes for Solar Tanks

Elsa Andersen, Simon Furbo and Jianhua Fan

Department of Civil Engineering Technical University of Denmark

DK-2800 Kgs. Lyngby, Denmark, e-mail: ean@byg.dtu.dk

Paper accepted for publication in Journal of Solar Energy, January 2007

Abstract

The thermal performance of solar heating systems is strongly influenced by the thermal stratification in the heat storage. The higher the degree of thermal stratification is, the higher the thermal performance of the solar heating systems. Thermal stratification in water storages can for instance be achieved by use of inlet stratifiers combined with low flow operation in the solar collector loop.

In this paper, investigations of a number of different fabric stratification pipes are presented and compared to a non flexible inlet stratifier.

Additional, detailed investigations of the flow structure close to two fabric stratification pipes are presented for one set of operating conditions by means of the optical PIV (Particle Image Velocimetry) method.

1 Introduction

The thermal performance of solar heating systems is strongly influenced by the thermal stratification in the heat storage tank. Investigations by (van Koppen et al., 1979, Hollands and Lightstone, 1989) showed that the thermal performance is increasing for increasing thermal stratification in the heat storage.

Thermal stratification in solar storage tanks is normally established in two ways:

- During charge periods, where heat from the auxiliary energy supply system or from the solar collectors is transferred to the "right" level of the tank. That is, the heat from the auxiliary energy supply system is normally transferred to the top of the tank and the solar heat is transferred to the level in the storage tank, where the tank temperature is close to the temperature of the incoming fluid transferring the solar heat to the tank. Shah and Furbo (1998) and Knudsen and Furbo (2004) showed that for small SDHW systems this is with advantage done by means of a vertical mantle heat exchanger. For large SDHW systems and for solar combisystems this is with advantage done by means of inlet stratifiers as shown by (Weiss, 2003, Furbo et al., 2005).

- During discharge periods where heat is discharged from a fixed level of the tank, for instance domestic hot water from the top of the tank for SDHW systems or hot water for space heating from a level just above the lower level of the auxiliary volume in a

storage tank for solar combisystems. Thermal stratification is best established during discharge if cold water enters the bottom of the tank in SDHW systems during draw-offs, and if the returning water from the space heating system enters the tank through inlet stratifiers in solar combisystems as described by (Weiss, 2003).

Consequently, inlet stratifiers can be used to build up thermal stratification in solar heat storages both during charge and discharge periods.

A wide variety of inlet stratifiers such as rigid tubes with either open holes and perforated vertical plates inside the pipes (Loehrke, 1979, Gari and Loehrke, 1992, Davidson, 1992,) or openings in form of balls (e.g. Leibfried, 2000) or flaps (e.g. described by Essert, 1995, Krause, 2001, Shah, 2002, Andersen et al., 2004) have been investigated in the past. Some of these have entered the market during the recent years. Also flexible stratification pipes (fabric manifolds) have been investigated for example by (Davidson and Adams, 1992, Loehrke, 1979, Gari and Loehrke, 1992, Yee and Lai, 2001). These investigations are carried out with flexible stratification manifolds made of one fabric layer and inlet through the top or the middle of the tank. (Davidson et al., 1994) found that fabrics with limited ability to stretch (i.e. woven fabrics) were unsuitable as stratification inlet pipes when the water enters the stratification inlet pipe through the top of the tank.

No guidelines for choosing the diameter of a fabric pipe in this type of application were found in previous studies. (Davidson et. al, 1994) investigated fabric pipes with diameters of 73 and 89 mm with a volume flow rate of 4.2 l/min. (Loehrke et al., 1979) investigated a fabric pipe with a diameter of 100 mm and a volume flow rate of 23 l/min.

In spite of promising results, fabric stratification pipes have not yet entered the market.

In this paper, stratification manifolds made of one or two fabric layers with diameters between 40 mm and 70 mm and with inlet through the bottom of the tank are investigated. The fabric stratifiers are made of Nylon, filament polyester, spun polyester and acrylic.

By leading water into the tank through a stratification pipe, good thermal stratification can be achieved in the tank. By placing the inlet at the bottom of the tank where the coldest water is situated, thermal bridges with high heat losses can be avoided, (Furbo, 1983). Good thermal stratification increases the thermal performance of solar heating systems.

The advantage of using a flexible fabric pipe as a stratification inlet pipe is that the fabric pipe can expand or contract leading to an equalization of the pressure in the pipe and in the tank in all levels of the tank. In this way the water in the tank will not be driven into the pipe by a higher pressure in the tank than in the pipe. The water in the pipe will first enter the tank when it either reaches the top of the pipe where it is forced to leave the pipe because new water is constantly feed into the pipe or when the temperature in the pipe equals the temperature in the tank leading to a slightly higher pressure in the pipe than in the tank. The pipe will expand in an attempt to equalize the pressure difference, but the expansion is limited by the expansion properties of the fabric and this leads to a flow of liquid from the pipe into the tank in the right temperature level.

Because one layer of fabric is very thin, heat is constantly transferred horizontally between the fabric pipe and the tank. By designing the stratification inlet pipe of more

than one fabric layer with a distance between the fabric layers the unwanted horizontal heat transfer is reduced. Figure 1 shows a picture of a two fabric layers pipe during an experiment where hot water enters a cold tank through the fabric pipe. Also the cross section area of the collapsed (lower right corner) and the expanded (upper right corner) fabric pipe is shown.

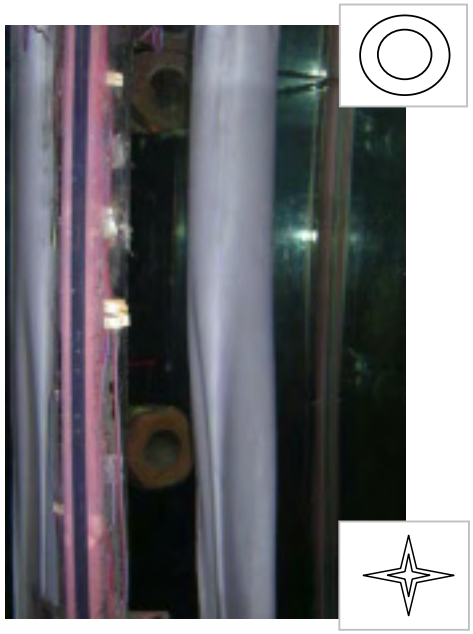

Figure 1: Picture of the two fabric layers pipe during a heating experiment. Upper right corner: cross section of the expanded fabric pipe where hot water leaves the pipe. Lower right corner: cross section of the collapsed pipe.

The heat transferred through each fabric layer leads to an up going flow around each fabric layer. It is assumed that when the distance between the fabric layers is large enough a laminar flow can develop between the two fabric layers and a small amount of heat is transferred from the inlet stratification pipe to the tank. When the distance between the fabric layers is too narrow the flow is disturbed and becomes turbulent and a larger amount of heat is transferred from the inlet stratification pipe to the tank. On the other hand, a larger fabric pipe diameter results in a larger surface area of the pipe increasing the heat transfer between the inlet stratification pipe and the tank. Therefore detailed investigations are needed in order to determine the optimum diameters of the fabric pipes.

2 Experimental investigations

2.1 Experimental set up

The experimental setup shown in Figure 2 consists of a glass tank (400 x 400 x 900 mm), a heating and a cooling unit and standard PIV equipment from Dantec Dynamics. Table 1 shows data for the PIV equipment.

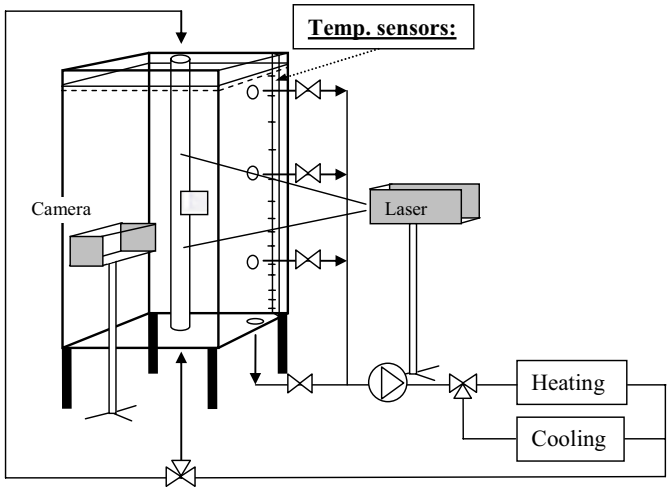

Figure 2: Experimental setup with the glass tank, the laser and the camera.

laser	type	Nd:YAG, NewWave Solo (Neodym-Yttrium-Aluminium-Granat)
	energy/pulses	100 mJ/pulse
	wavelength	532 nm (frequency doubled)
CCD camera	type	HiSense 12 bit
	resolution	1280 x 1024 pixel (64 x 64 pixel interrogation area)
particles		Polyamid, 5µm (PSP-5)
software		Flowmanager, Dantec Dynamics

Table 1: PIV equipment.

The PIV method has previous been used to investigate flow structures in water tanks by for example (Knudsen et al., 2005).

The camera is placed perpendicular to the laser that illuminates a thin slide in the flow. The fabric stratification pipe is mounted in the centre of the glass tank with the possibility to have a forced flow to enter the stratification pipe either from the top or the bottom of the tank. The outlet can take place in four different levels between the top and the bottom of the tank. The thickness of the tank wall is 12 mm and the tank is not insulated. !4 temperature sensors are mounted on a plate of Perspex in one corner of the tank (Figure 2). The temperatures are measured with copper-constantan thermocouples type TT with an accuracy of 0.5 K. The volume flow rate is measured with an electro magnetic inductive flow meter, type HGQ1 from Brunata HG a/s. The flow meter has an accuracy of about ± 1 %.

2.2 Experiments

The thermal performance of the fabric stratifiers are investigated for three sets of operation conditions:

- heating tests where the tank is heated from 20°C to 40°C through one layer fabric stratification pipes with diameters of 60 mm and two layers fabric stratification pipes with diameters of 40 mm and 70 mm. The inlet to the fabric stratification pipe is through the bottom of the tank. The outlet is in the bottom of the tank.
- heating test with an initially stratified tank 50°C/20°C and an inlet temperature of 30°C through two fabric layers stratification pipe with diameters of 40 mm and 70 mm. The inlet to the fabric stratification pipe is through the bottom of the tank. The outlet is in the bottom of the tank.
- cooling test where cold water of 20°C is lead into the tank with a temperature of 50°C through two fabric layers stratification pipe with diameters of 40 mm and 70 mm. The inlet to the fabric stratification pipe is through the bottom of the tank. The outlet is in the top of the tank.

The fabric stratifiers are closed in the top.

The duration of the heating and the cooling tests is 50 minutes. The duration of the stratified test is 35 minutes. The volume flow rate is 2 l/min.

The investigated fabrics are listed in Table 2. The fabrics are obtained from the US company Test Fabric Inc. The fabrics are a mixture of knit and woven fabrics and the ability to stretch that was found important by (Davidson et al., 1994) seems not important at all in the application investigated here where the water is entering the stratification inlet pipe through the bottom of the tank. The important properties are the ability to reduce the cross section area by more or less collapse. Hence, the permeability and the density of the fabrics are found to be more important than the stretch abilities.

Fabric Style
Style 314, Texturized Nylon 6.6 Stretch Fabric, Double Knit
Style 361, Spun Nylon 6.6 DuPont Type 200 Woven Fabric (ISO 105/F03)
Style 703, Texturized Polyester, Woven
Style 769, 100% Spun Dacron Type 54 Knit (Disperse Dyeable)
Style 864, Spun Orlon Type 75 Acrylic Plain Weave
Style 867, Spun Acrilan 16 Acrylic Knit
Style 981, Creslan Acrylic Type 61

Table 2: Investigated fabrics.

Further , the test results obtained with two fabric layers stratification pipes are compared to results of identical tests with a marketed rigid stratification pipe with three holes with “non-return” valves from Solvis GmbH & Co KG (Krause, 2001, Shah, 2002, Andersen et al., 2004). Figure 3 shows a schematic of the rigid stratification pipe.

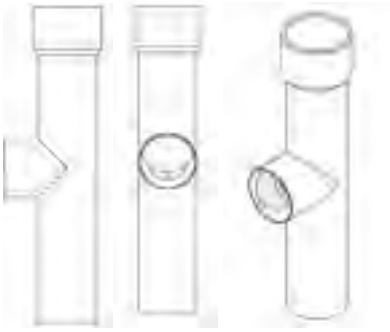

Figure 3: Schematic illustrations of the SOLVIS stratification inlet pipe.

Finally, the flow structure close to the fabric stratification pipes with one and two fabric layers, S361 are investigated during a heating test by means of the PIV method. The method is described in (Andersen et al., 2004).

Recordings of the velocity field are taken in a frame of 65.5 x 80 mm^2 about 450 mm from the bottom of the tan as shown in Figure 2.The duration between two succeeding illuminations of the particle field is 100 ms. Time delay between succeeding velocity vector recordings is about 250 ms.

2.3 Analysis method

There are different ways to evaluate thermal stratification of thermal energy storages. (Rosen, 2001) describes how to perform an exergy analysis of a thermal energy storage. (Adams, 1993; Davidson et al., 1994) describe how to analyse a thermal energy storage with a quantitative "momentum of energy" analysis. Both methods are suitable for comparing differently designed heat storages. The latter is used to analyse the results in this paper.

The tank is divided into N equal sized horizontal layers with the volume V. The temperature is not measured in each volume. Therefore the temperatures of the volumes are determined by linear interpolation between the measured temperatures.

In the analysis of the "momentum of energy", M, the energy of each layer of the tank, $E_i = \rho_i \cdot c_i \cdot V \cdot T_i$ is weighted by the vertical distance from the bottom of the tank to the centre of each layer, y_i. The "momentum of energy" is:

$$M = \sum_{i=1}^{N} y_i \cdot E_i , \tag{1}$$

A mixing number is derived based on the measured temperature profile and the corresponding ideal stratified and fully mixed temperature profiles.

The mix number is:

$$MIX = \frac{M_{str} - M_{\exp}}{M_{str} - M_{mix}} , \tag{2}$$

M_{str}, $M_{\exp}$ and M_{mix} are the "momentum of energy" of a perfectly stratified tank, the experiment and a fully mixed tank respectively. The value of the mix number is between 0 and 1 where 0 corresponds to a perfectly stratified tank and 1 corresponds to a fully mixed tank.

For the experiment where the tank is heated from the surrounding temperature to a higher temperature level the temperature profiles for the perfectly stratified tank and the fully mixed tank are calculated by means of the measured temperatures.

The temperature of the fully mixed tank is calculated as the measured weighted average temperature. The temperature in the perfectly stratified tank consists of a high temperature in the upper part of the tank and a low temperature in the lower part of the tank. In the charging case, the low temperature equals the start temperature of the tank. The lower part of the tank has a volume equal to the total water volume in the tank minus the water volume which has entered the tank during the test. Based on the measured temperatures the temperature in the upper part of the tank with a volume equal to the water volume which has entered the tank during the test is determined in such a way that the energy of the perfectly stratified tank is equal to the measured energy in the tank.

For the experiment where the tank is cooled from a high temperature to a lower temperature the temperature profiles for the perfectly stratified and fully mixed tank are calculated in a similar way. In this way heat losses and the heat capacity of the tank material are accounted for. No mix number is calculated for the stratified experiment. In this case only $M_{\exp}$ is calculated with the ambient temperature as the reference temperature.

3 Results

3.1 Heating tests

Figure 4 and Figure 5 show the temperature stratification in the tank in different heights every 5 minutes during the heating test with stratification manifolds of one and two fabric layers, style 361. For comparison, the temperature stratification profile with the marketed rigid stratification pipe (ref. Figure 3) with three holes with “non-return” valves is shown in Figure 6. In each of the figures the perfectly stratified temperature profile after 20 minutes and after 50 minutes are shown.

From the figures it is clear that the temperature stratification profile is much more desirable when a stratification manifold of two fabric layers instead of one fabric layer is used. With two layers of fabric the temperature curves are more horizontal and the temperature at the top of the tank is increased and the temperature at the bottom of the tank is decreased compared to the test with the one layer fabric stratification pipe. Also it can be seen that the stratification profile with the marketed rigid stratification pipe with three holes with “non-return” valves is very close to the perfectly stratified profile.

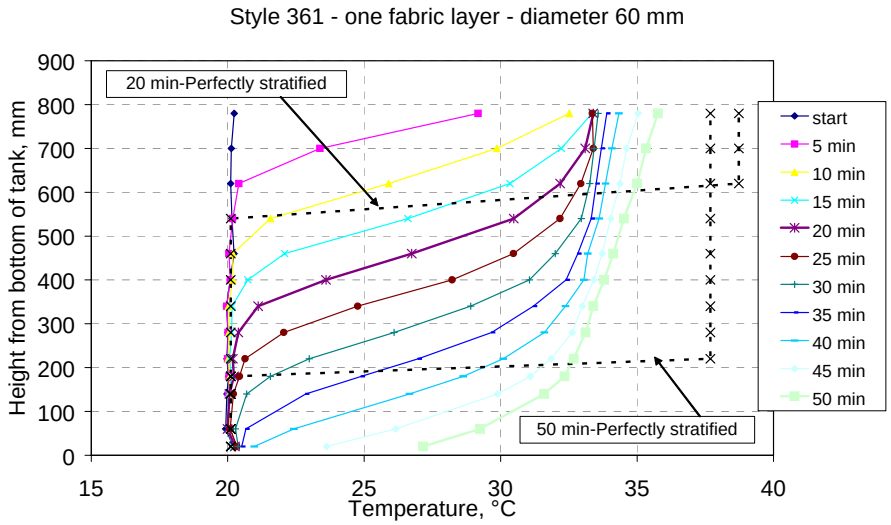

Figure 4: Temperature profile during a heating test with fabric stratification pipes, Style 361 with one fabric layer.

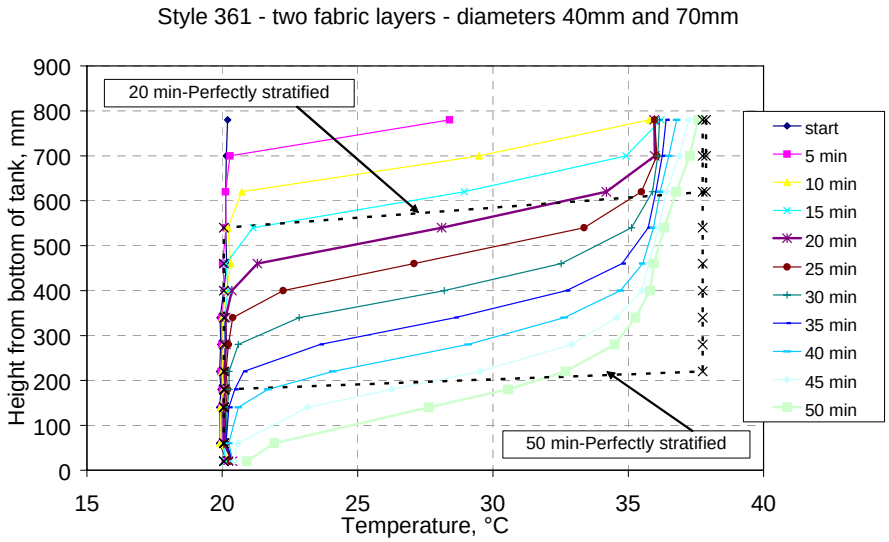

Figure 5: Temperature profile during a heating test with fabric stratification pipes, Style 361 with two fabric layers.

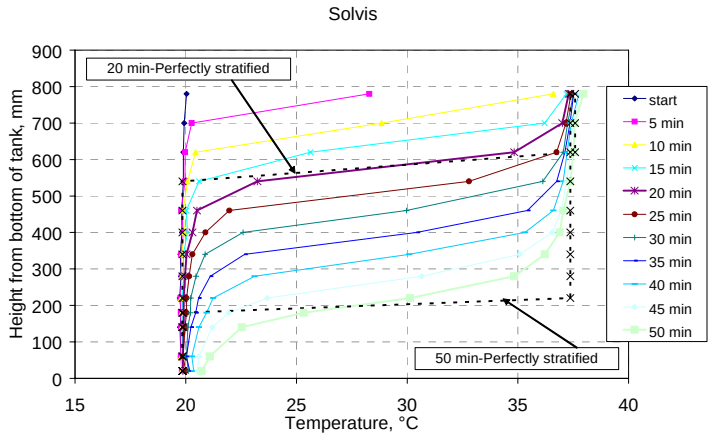

Figure 6: Temperature profile during a heating test with the rigid stratification pipe.

The rigid stratifier performs slightly better than the two fabric layer stratification pipe because the horizontal heat transfer between the hot water in the pipe and the cold water in the tank is lower.

Figure 7 and Figure 8 show the mix numbers during the heating test with one and two fabric layer stratification pipes. In Figure 8 the mix number of the rigid pipe with three holes with “non-return” valves is also shown.

From Figure 7 and Figure 8 it is seen that the mix numbers are dramatically reduced by using two fabric layers with a distance between the layers instead of only one fabric layer. The mix number increases during the experiment because the hot water enters the bottom of the tank and heat is transferred from the fabric pipe to the tank water in the lower part of the tank during the whole heating test. The mix number obtained with the rigid stratification pipe is very low and somewhat lower than the mix numbers obtained with the fabric stratification pipes. This is because the horizontal heat transfer through the wall of the rigid pipe is much lower than the horizontal heat transfer through the fabric wall.

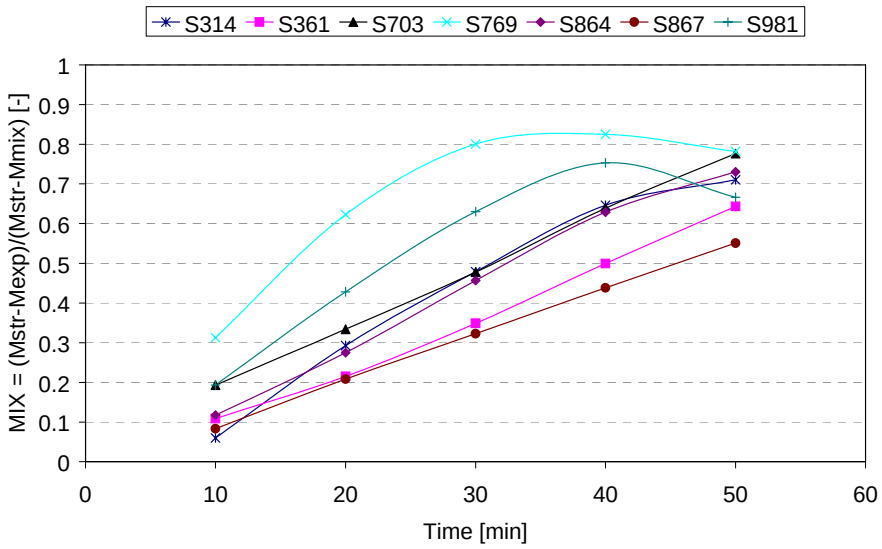

Figure 7: Mix numbers for fabric stratification pipes of one fabric layer.

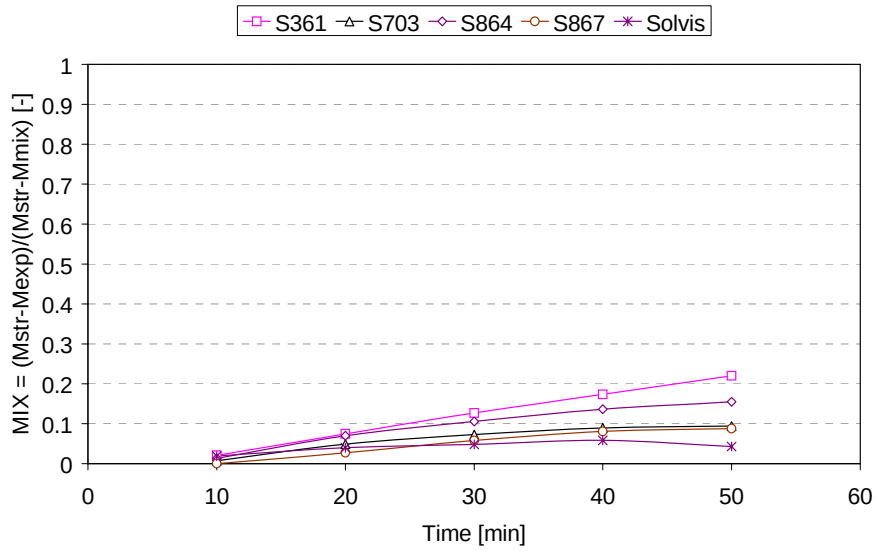

Figure 8: Mix numbers for fabric stratification pipes of two fabric layers and the rigid pipe.

3.2 Stratified heating tests

Figure 9 shows the experimental “momentum of energy” during the stratified heating test with two fabric layer stratification pipes, S361 and the rigid pipe with holes with “non-return” valves.

From the figure it obvious that the fabric stratification pipe with two fabric layers and the rigid pipe with holes with “non-return” valves perform almost equally under the applied test conditions. After about 10 minutes the curve for the rigid pipe switches place with the curve for the fabric pipe. In the start of the test the incoming water has entered the tank through the upper hole in the rigid pipe. After 10 minutes the inlet temperature is too low to enter the upper hole and too high to enter the middle hole.

Hence, the incoming water enters both the upper and the middle hole and the temperature difference between the upper and the middle hole decreases.

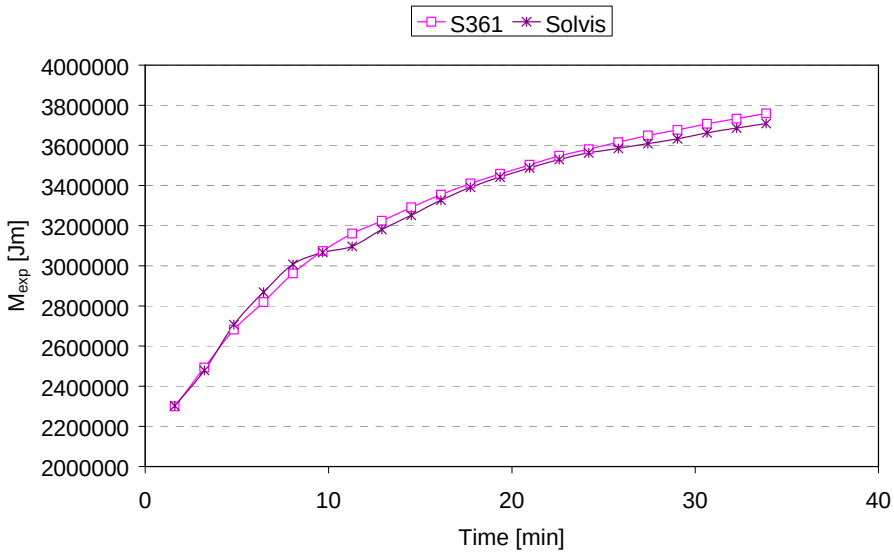

Figure 9: Moment of energy M_{exp} of the experimental data.

3.3 Cooling tests

Figure 10 shows the mix numbers during the cooling test with a two fabric layer stratification pipe, S361 and the rigid pipe with three holes with “non-return” valves.

From the figure it can be seen that the mix number is lower for the fabric stratification pipe than for the rigid pipe with holes with “non-return” valves. This is due to the fact that the incoming cold water only can leave the rigid pipe through the lowest hole whereas the incoming cold water can leave the fabric stratification pipe in any desired level.

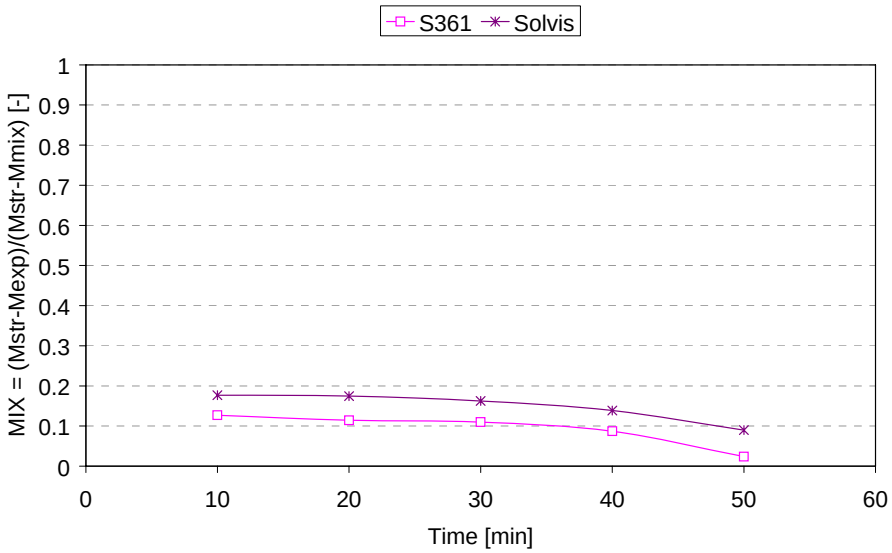

Figure 10: Mix number for fabric stratification pipes with two fabric layers and the rigid pipe with holes with “non-return” valves.

3.4 PIV measurements

Figure 11 and Figure 12 show the velocity vector maps and the corresponding streamlines to the vector maps 10, 20, 26 and 36 minutes after the heating is started. The velocity vector maps are calculated as mean values from 10 instantaneous velocity recordings by adaptive cross correlations and finally range validation procedure is applied. The corresponding temperature profiles are shown in Figure 4 and Figure 5.

From the figures it can be seen that the primary movement of the tank water after 10 minutes is downward towards the outlet in the bottom of the tank. Close to the fabric stratification pipe the direction of the water is upwards due to horizontal heat transfer through the fabric stratification pipe, especially for the one layer pipe. After 20 minutes the upward flow has stopped close to the one layer fabric pipe because thermal stratification has been built up in the level where the pictures are taken. The thermal stratification stops the upward flow. Water is leaving the pipe just above the level of the picture. This is not the case close to the two layer fabric pipe where the picture is the same as after 10 minutes. After 26 minutes water leaves the one layer fabric pipe in the level where the picture is taken. There apparently is a mismatch temperature difference between water entering the tank and the tank water creating eddies. After 36 minutes water starts to leave the two layer fabric pipe. At this time the temperature thermocline has reached the level of the picture. The pictures illustrate very well the advantages of using stratification fabric pipes with two fabric layers instead of one fabric layer.

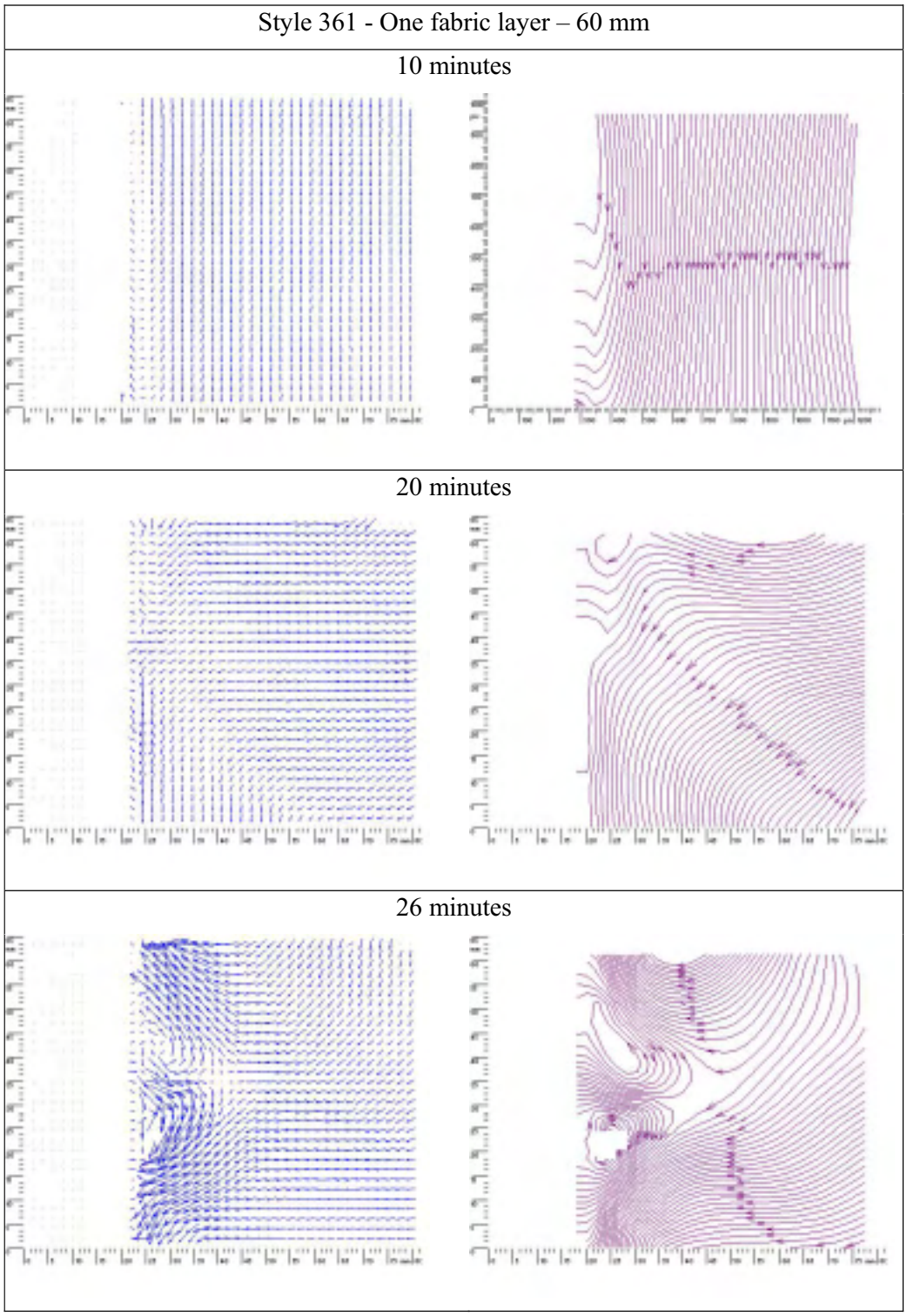

Figure 11: Velocity vector maps and corresponding streamlines around the fabric stratification pipes with one fabric layer.

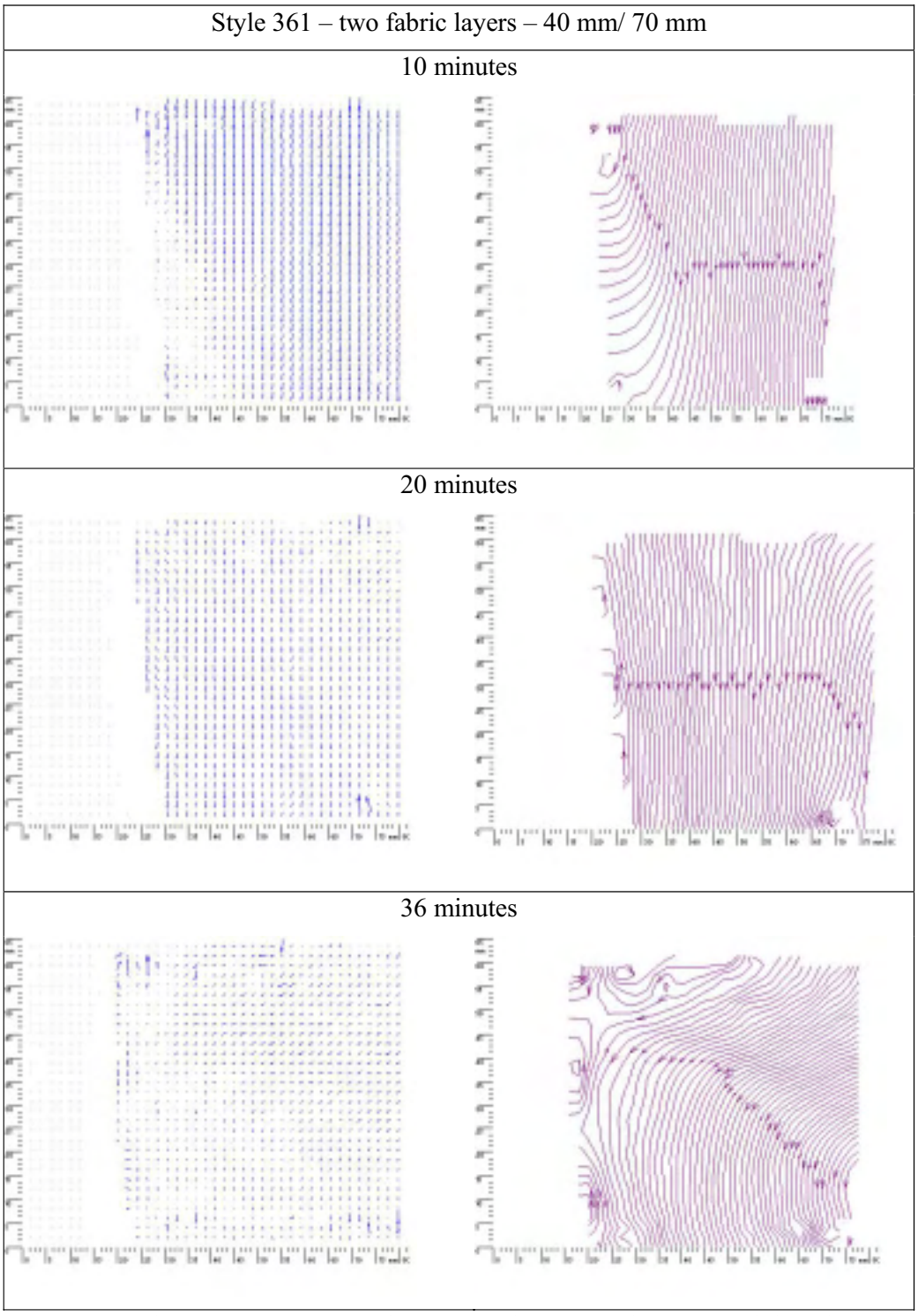

Figure 12: Velocity vector maps and corresponding streamlines around the fabric stratification pipes with two fabric layers.

4 Conclusions

A number of stratifications pipes for hot water tanks made of different fabrics are investigated. The investigation comprises stratification pipes of one and two fabric

layers. The performance of the fabric stratification pipes is investigated during heating, cooling and stratified heating tests. In all the tests, water enters the stratification pipe through the bottom of the tank. Further the performances of the fabric stratification pipes are compared to the performance of a marketed rigid stratification pipe with three holes with "non-return" valves.

The investigation shows that the performance of fabric stratification pipes can be improved significant by using two fabric layers with a distance of about 10 mm between each fabric layer instead of using one fabric layer.

The investigation also shows that the largest disadvantage of the fabric stratification pipes is the high horizontal heat transfer through the very thin fabric. This disadvantage is most significant when hot water enters a cold tank and flows from the bottom to the top of the fabric stratification pipe. In this particular case the rigid stratifier has an advantage because of the low horizontal heat transfer through the pipe wall.

For the cooling test the two fabric layer stratification pipe performs somewhat better than the rigid stratifier, while the two fabric layer stratification pipe and the rigid stratifier perform identical during stratified heating tests.

Nomenclature

M	=	"Momentum of energy" (J·m)
E	=	Energy (J)
y	=	Vertical distance (m)
V	=	Volume (m^3)
c	=	Specific heat capacity (kJ/kg/K)
ρ	=	Density (kg/m^3)
T	=	Temperature (K)
N	=	Number of tank layers

Subscripts

i	=	Tank layer
str	=	Stratified
exp	=	Experimental
mix	=	Mixed

References

Adams D. E. Design of a Flexible Stratification Manifold for Solar Water Heating Systems. Master Thesis, Colorado State University, Fort Collins, CO. 1993.

Andersen E., Jordan U., Shah L.J., Furbo S. Investigation of the Solvis Stratification Inlet Pipe for Solar Tanks. Proceedings of ISES Solar World Congress 2004, Freiburg, Germany, pp. 659-668, 2004.

Davidson J.H., Adams D.A., Miller J.A. A Coefficient to Characterize Mixing in Solar Water Storage Tanks. Journal of Solar Energy Engineering, Vol. 116, pp. 94-99, 1994.

Davidson J.H., Adams D.A. Fabric Stratification Manifolds for Solar Water Heating. Journal of Solar Energy Engineering, Vol. 116, pp. 130-136, 1994.

Essert H. Aufbau und Inbetriebnahme eines Speicherversuchsstandes. Diploma Thesis, Graz University, Austria, 1995.

Furbo S. Test Procedure for Heat Storages for Solar Heating Systems. Int. J. Solar Energy, Vol. 1, 1983.

Furbo, S., Vejen, N.K., Shah, L.J., 2005. Thermal performance of a large low flow solar heating system with a highly thermally stratified tank. Journal of Solar Energy Engineering, Vol. 127, no.1, 15-20.

Gari H.N., Loehrke R.I. A controlled buoyant jet for enhancing stratification in a liquid storage tank. Journal of Fluids Engineering, Vol. 104, pp. 475-481, 1982.

Hollands K.G.T., Lightstone, M.F., 1989. A review of low-flow, stratified-tank solar water heating systems. Solar Energy 43, 97-105.

Knudsen, S., Furbo, S., 2004. Thermal stratification in vertical mantle heat exchangers with application to solar domestic hot water systems. Applied Energy, Vol 78/3, 257-272.

Knudsen, S. Morrison, G.L., Behnia, M., Furbo, S., 2005. Analysis of the flow structure and heat transfer in vertical mantle heat exchanger. Solar Energy 78, 281-289.

Krause Th., Kühl L. Solares Heizen: Konzepte, Auslegung und Praxiserfahrungen, 2001.

Liebfried U. Combitanks with internal thermosyphonically driven heat exchangers for hot water – comparison of existing systems, 2000. Proceedings Terrastock Conference, pp. 315-320.

Loehrke R.I., Holzer J.C., Gari H.N., SharpM.K. Stratification enhancement in liquid thermal storage tanks. Journal of Energy, Vol. 3, No. 3, pp. 129-130, 1979.

Rosen M. A. The Exergy of Stratified Thermal Energy Storages. Solar Energy, Vol. 71, pp. 173-185, 2001.

Shah, L.J., Furbo, S., 1998. Correlation of Experimental and Theoretical Heat Transfer in Mantle Tanks used in Low Flow SDHW Systems". Solar Energy, Vol. 64 (4-6), 245-256.

Shah L.J. Stratifikationsindløbsrør. Department of Civil Engineering, Technical University of Denmark, DTU, 2002.

van Koppen, C.W.J., Thomas, J.P.X., Veltkamp, W.B., 1979. The Actual Benefits of Thermally Stratified Storage in a Small and Medium Size Solar System. In Proceedings of ISES Solar Wor.ld Congress, Atlanta, USA, 579-80.

Weiss, W. (Ed.), 2003. Solar Heating Systems for Houses. A design Handbook for Solar Combisystems. James & James Ltd. Solar Heating and Cooling Executive Committee of International Energy Agency (IEA).

Test Fabric Inc., www.testfabrics.com.

Yee C. K., Lai F. C. Effects of a Porous Manifold on Thermal Stratification in a liquid Storage Tank. Solar Energy, Vol. 71, pp. 241-254, 2001.

Paper VIII

Fabric Inlet Stratifiers for Solar Tanks with different Volume Flow Rates

Paper in proceedings: EuroSun 2006 Congress, Glasgow, Scotland, 2006

Fabric Inlet Stratifiers for Solar Tanks with different Volume Flow Rates

Elsa Andersen and Simon Furbo

Department of Civil Engineering Technical University of Denmark

DK-2800 Kgs. Lyngby, Denmark, e-mail: ean@byg.dtu.dk

Paper in proceedings: EuroSun 2006 Congress, Glasgow, Scotland, 2006

Abstract

In this paper investigations of two different two layer fabric stratification pipes are presented and compared to a rigid stratification pipe with holes with "non-return" valves. The fabric stratification pipes are constructed of filament polyester and acrylic. The fabric pipes are mounted in the centre of a glass tank (400 x 400 x 900 mm). The forced volume flow rate is in the range of 6 – 10 l/min, and water enters the stratification pipe from the bottom of the tank. The thermal behaviour of the stratification pipes is investigated for different realistic operation conditions.

Keywords Solar tanks, thermal stratification, inlet stratification pipes

1 Introduction

Thermal stratification in water storages can be achieved in different ways. For instance, water heated by the solar collectors or water returning from the heating system can enter the water storage through stratification inlet devices in such a way that the water enters the tank at a level, where the tank temperature is the same as the temperature of the entering water.

With a rigid stratification pipe with holes the water will flow through the holes depending on the pressure differences between inside and outside of the stratification pipe. With a well performing fabric stratification pipe, the cross section area is flexible. Hence, the fabric pipe can equalize the pressure difference between the inside of the pipe and the tank by contracting or expanding. During periods at tank levels where the temperature in the fabric pipe is higher than the temperature in the tank a contraction of the fabric pipe will reduce the cross section area of the fabric pipe. This leads to a higher velocity inside the fabric stratification pipe and thereby a higher pressure. The fabric pipe contracts until the pressure difference between the inside of the pipe and the tank is eliminated. Consequently, no water from the tank will enter the fabric pipe. The water in the fabric stratification pipe enters the tank when it either reaches the top of the pipe where it is forced to leave the pipe because new water is constantly feed into the pipe or when the temperature in the pipe equals the temperature in the tank leading to a slightly higher pressure in the fabric pipe than

in the tank. The fabric pipe will at the right tank level expand in an attempt to equalize the pressure difference, but the expansion is limited by the expansion properties of the fabric and this leads to a flow of liquid from the pipe into the tank in the right temperature level.

Previously a number of fabric stratification inlet pipes have been investigated. Different operation conditions were applied and water with a volume flow rate of 2 l/min entered the fabric stratification pipes through the bottom of the tank. The results were compared to similar results with a good marketed rigid stratification pipe with holes with “non-return” valves. The fabric stratification inlet pipes were constructed of one and two fabric layers. The investigation showed that the largest disadvantage of the fabric stratification inlet pipe was the high horizontal heat transfer through the very thin fabric. The horizontal heat transfer was dramatically reduced when the fabric pipe was constructed of two fabric layers instead of one fabric layer. Further, the investigation showed that a two layer fabric stratification pipe performed as well as the rigid stratification pipe with holes with “non-return” valves [1].

2 Experimental investigations

2.1 Experimental setup

Two fabric stratification pipes made of two fabric layers as well as a marketed rigid stratification pipe with three holes with “non-return” valves are investigated experimentally. The aim of the investigations is to determine how well thermal stratification is build up during different realistic operation conditions. Figure 1 shows a schematic of the experimental setup (left), consisting of a glass tank (400 x 400 x 900 mm), a heating and a cooling unit. To the right, the figure shows a schematic of the rigid stratification pipe with a hole with “non-return” valve.

The inlet stratification pipe is mounted in the centre of the glass tank with the possibility to have a forced flow to enter the stratification pipe from bottom of the tank. The outlet can take place in the top and the bottom of the tank. The thickness of the tank wall is 12 mm and the tank is not insulated. The tank temperatures are measured in 13 different uniformly distributed levels in the tank. The temperatures are measured with copper-constantan thermocouples type TT with an accuracy of 0.5 K. The volume flow rate is measured with an electro magnetic inductive flow meter, type HGQ1 from Brunata HG a/s. The flow meter has an accuracy of about ± 1 %.

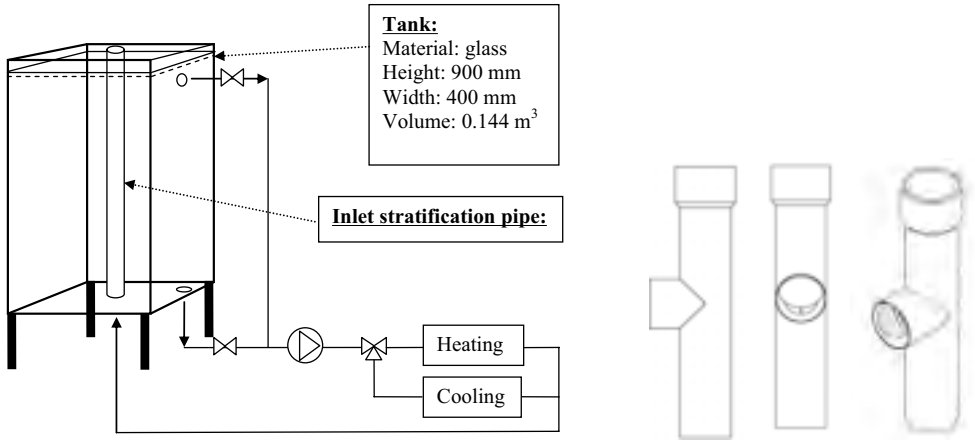

Figure 1: Left, a schematic of the experimental setup with a stratification pipe mounted in the centre of the tank. Right, schematic illustrations of a rigid stratification pipe with a hole with "non-return" valve.

2.2 Stratification pipes

The fabric stratification pipes are constructed of an inner pipe with diameter of 40 mm and an outer pipe with diameter of 70 mm. The fabrics are from the US Company Test Fabric Inc. [4]

The rigid stratification inlet pipe has a height of 328 mm and an inner/outer diameter of 52/60 mm. When the inlet stratification pipes are compound the distance between the centres of each inlet is about 292 mm. The stratification pipe is from the German company Solvis GmbH & Co KG [2,3]

2.3 Experiments

The thermal performance of the inlet stratification pipes are investigated for three sets of operation conditions:

heating tests where the tank is heated from 20°C through the inlet stratification pipe with an inlet temperature of about 32- 40°C. The inlet to the fabric stratification pipe is through the bottom of the tank. The outlet is in the bottom of the tank.

stratified heating test with an initially stratified tank of 50°C/20°C and an inlet temperature higher than 20°C and lower than 50°C through inlet stratification pipe. The inlet to the fabric stratification pipe is through the bottom of the tank. The outlet is in the bottom of the tank.

cooling test with an initially heated tank of 50°C and an inlet temperature of about 25-30°C is lead into the tank through the stratification pipe. The inlet to the fabric stratification pipe is through the bottom of the tank. The outlet is in the top of the tank.

The heating tests simulate the thermal behaviour of a stratification pipe in a solar collector loop while the cooling tests simulate the behaviour of a stratification pipe in a space heating loop.

The forced volume flow rates are 6 l/min, 8 l/min and 10 l/min. In each experiment about 90 litres of water are circulated through the tank.

The upper hole of the rigid stratification pipe is situated about 60 mm below the water level in the tank.

The fabric stratification pipes are closed in the top. This is important in order to make the fabric pipes behave as intended. The water in the fabric pipes flows from the pipes into the tank when the total pressure in the pipes exceeds the total pressure in the tank in the corresponding level and where the resistance against passing the fabric pipe walls is lowest. If the fabric stratification pipes are left open in the top, the lowest resistance might be through the top of the pipes regardless of the temperature conditions in the pipes and the tank. The experiments are carried out with two fabric styles:

- Style 864, Spun Orlon Type 75 Acrylic Plain Weave (non-stretchable)
- Style 700-12, Filament polyester, Poly-Lycra (stretchable)

2.4 Results – heating and cooling experiments

The temperature profiles during the heating and the cooling tests with forced volume flow rates of 6 l/min, 8 l/min and 10 l/min are shown in Figure 2, Figure 3 and Figure 4, respectively. The figures show the normalized temperatures in different levels in the tank. The curves show the temperature profile after 30 litres, 60 litres and 90 litres of water have been circulated through the tank.

During the heating tests with a volume flow rate of 6 l/min, the rigid stratification pipe with holes and “non-return” valves perform better than the fabric stratification pipes, but only slightly better than the fabric stratification pipe style 700-12. The fabric stratification pipes perform better for volume flow rates of 8 l/min and 10 l/min than for a volume flow rate of 6 l/min and much better than the rigid stratification pipe. The reason why the thermal performance of the fabric stratification pipe improves for increasing volume flow rates is most likely that the horizontal heat transfer through the thin fabric pipe to the tank decreases for increasing volume flow rates.

During the cooling tests, the fabric stratification pipes perform better than the rigid stratification pipe for all volume flow rates used in the tests.

Especially the fabric stratification pipe style 700-12 performs very well in all the experiments.

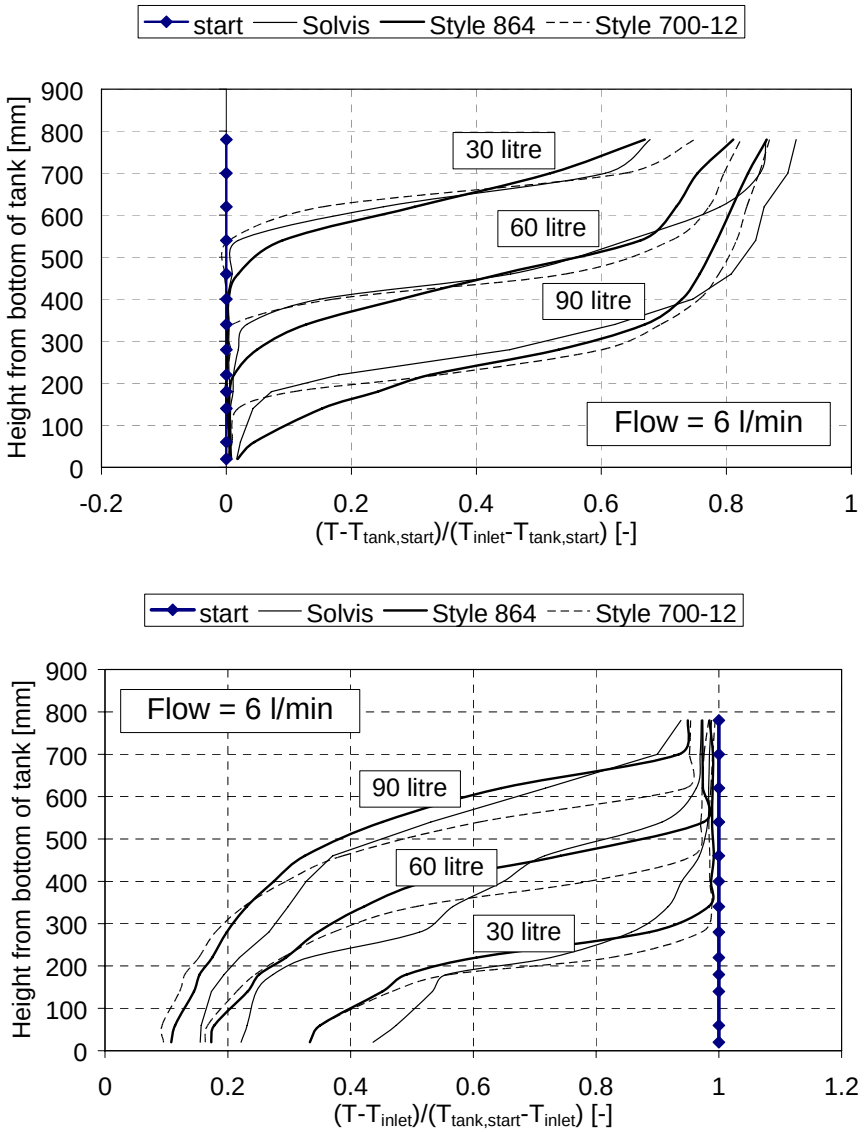

Figure 2: Temperature profiles from heating (top) and cooling tests (bottom) with the rigid inlet stratification pipe with holes with "non-return" valves and fabric inlet stratification pipes style 864 and style 700-12. The forced volume flow rate is 6 l/min.

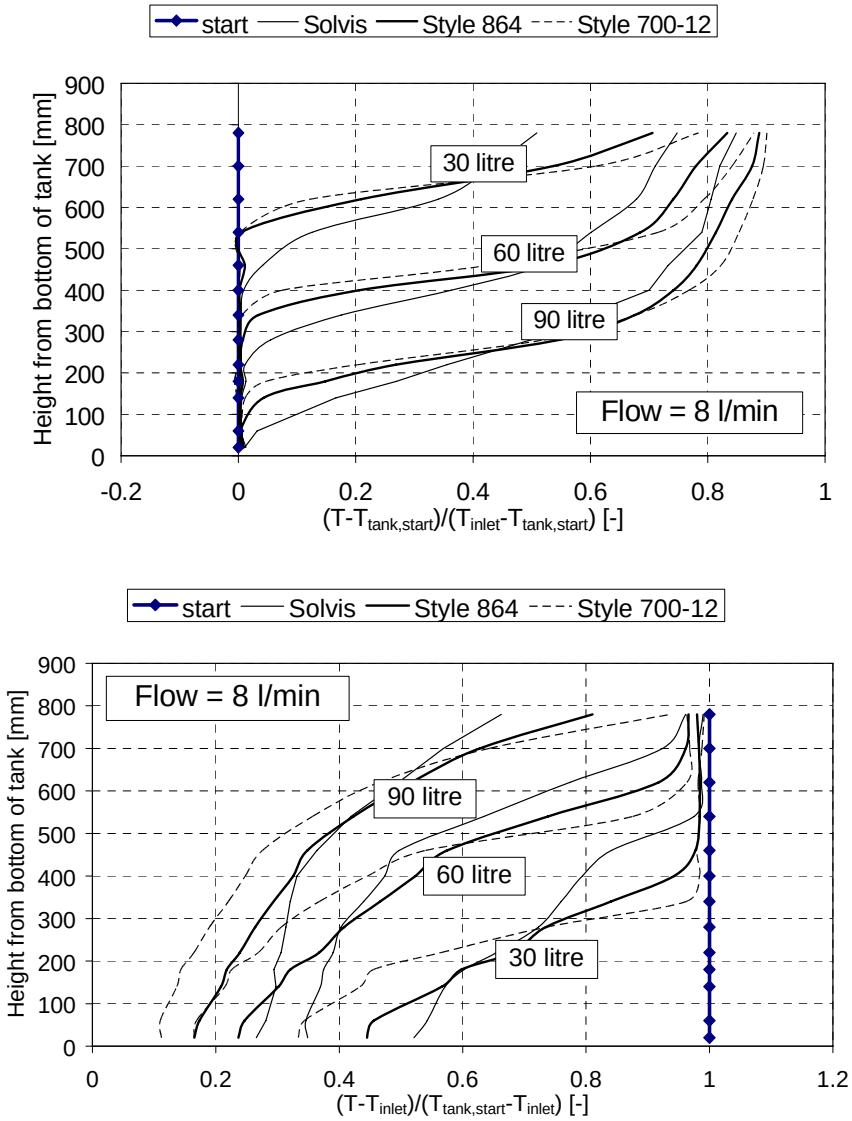

Figure 3: Temperature profiles from heating (top) and cooling tests (bottom) with the rigid inlet stratification pipe with holes with “non-return” valves and fabric inlet stratification pipes style 864 and style 700-12. The forced volume flow rate is 8 l/min.

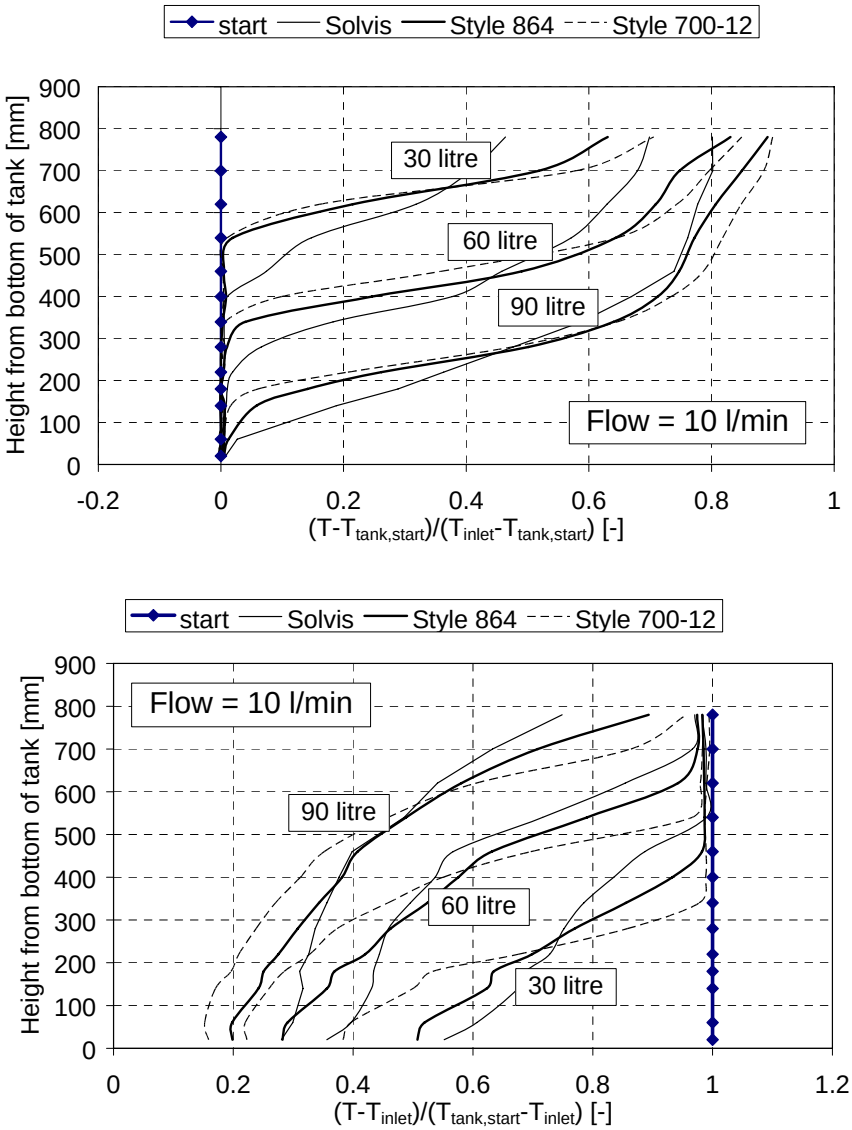

Figure 4: Temperature profiles from heating (top) and cooling tests (bottom) with the rigid inlet stratification pipe with holes with "non-return" valves and fabric inlet stratification pipes style 864 and style 700-12. The forced volume flow rate is 10 l/min.

2.5 Results – stratified heating experiments

The temperature profiles during the stratified heating tests with forced volume flow rates of 6 l/min, 8 l/min and 10 l/min are shown in Figure 5. The figures show the temperatures in different levels in the tank. The curves show the temperature profile after 30 litres, 60 litres and 90 litres of water have been circulated through the tank. The inlet temperatures used in the tests with volume flow rates of 6 l/min, 8 l/min and 10 l/min are about 41°C, 37°C and 33°C respectively. The start temperature at the top of the tank is about 50°C and the aim of the tests is to investigate if the stratification pipes can build up thermal stratification without destroying the already existing thermal stratification.

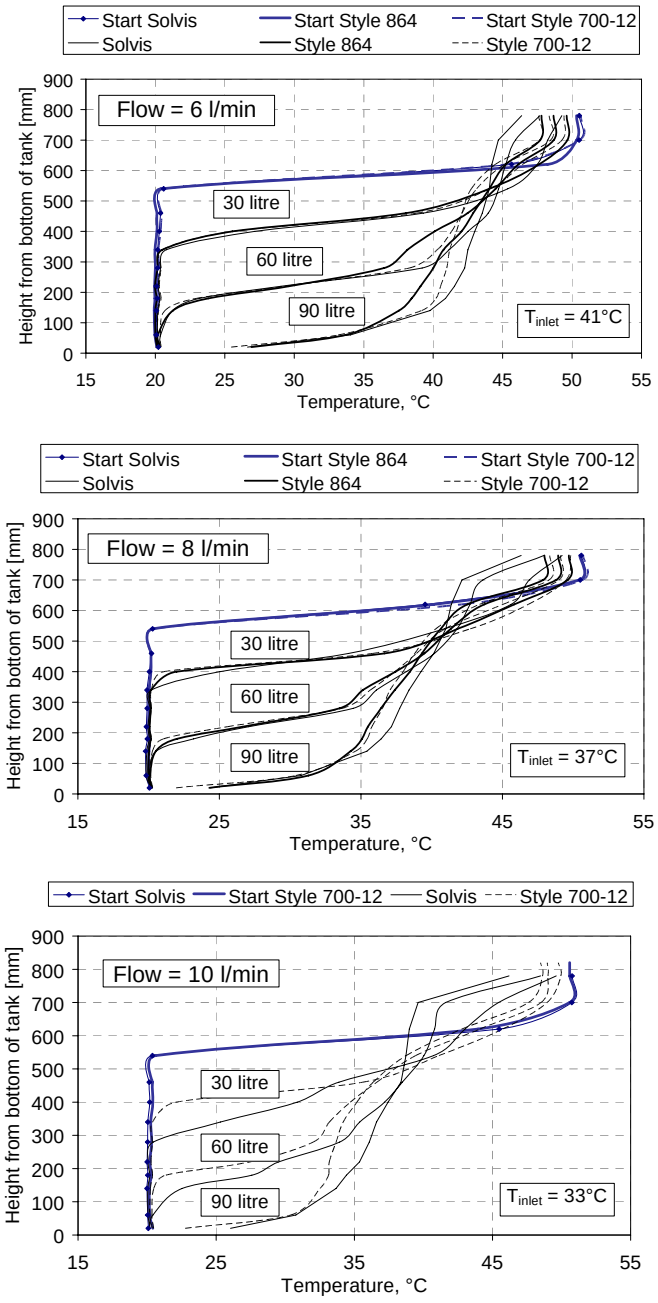

Figure 5: Temperature profiles from stratified heating tests with the rigid inlet stratification pipe with holes with “non-return” valves and fabric inlet stratification pipes style 864 and style 700-12. The forced volume flow rate is 6 l/min, 8 l/min and 10 l/min.

The figure shows that the fabric stratification pipes succeed to heat up the middle part of the tank without destroying the already existing thermal stratification in all the tests with different volume flow rates while the rigid stratification pipe is not able to maintain the already existing thermal stratification. The reason the rigid stratification pipe is not able to maintain the existing thermal stratification in the same good way as the fabric stratification pipe, is that water can only leave the rigid stratification pipe

through one of the three holes and when the right temperature level lies between two holes, the water leaves through both the hole above and the hole below the right temperature level.

3 Summary and outlook

Figure 6 shows the temperature profiles during the heating tests with forced volume flow rates of 6 l/min, 8 l/min and 10 l/min. The figures show the normalized temperatures in different levels in the tank. The curves show the temperature profile after 30 litres, 60 litres and 90 litres of water have been circulated through the tank. The results are shown for the rigid stratification pipe with holes with “non-return” valves and the two layer fabric stratification pipes style 864 and style 700-12.

The figure shows that, for the rigid stratification pipe, the thermal stratification is build up in a very good way with a volume flow rate of 6 l/min and worse for increasing volume flow rates. For the fabric stratification pipes the picture is the opposite. The thermal stratification is build up in a better way for high volume flow rates than for low volume flow rates. With low volume flow rates, the heat loss from the surface of the fabric stratification pipes to the tank destroys the thermal stratification. One way of reducing the heat loss for low volume flow rates is to use fabric stratification pipes with a smaller diameter and thereby a smaller surface area and higher velocity in the pipes. Consequently, it is expected that fabric stratification pipes can work well for all volume flow rates, provided that the pipe diameter is adjusted to the flow rate.

From the investigation, it is obvious, that the fabric stratification pipes work very well under the applied realistic operation conditions. The disadvantage at this point, is that knowledge of the long term durability of fabric stratification pipes has not yet been obtained. Long term durability tests will be carried out at the Technical University of Denmark from the end of year 2006.

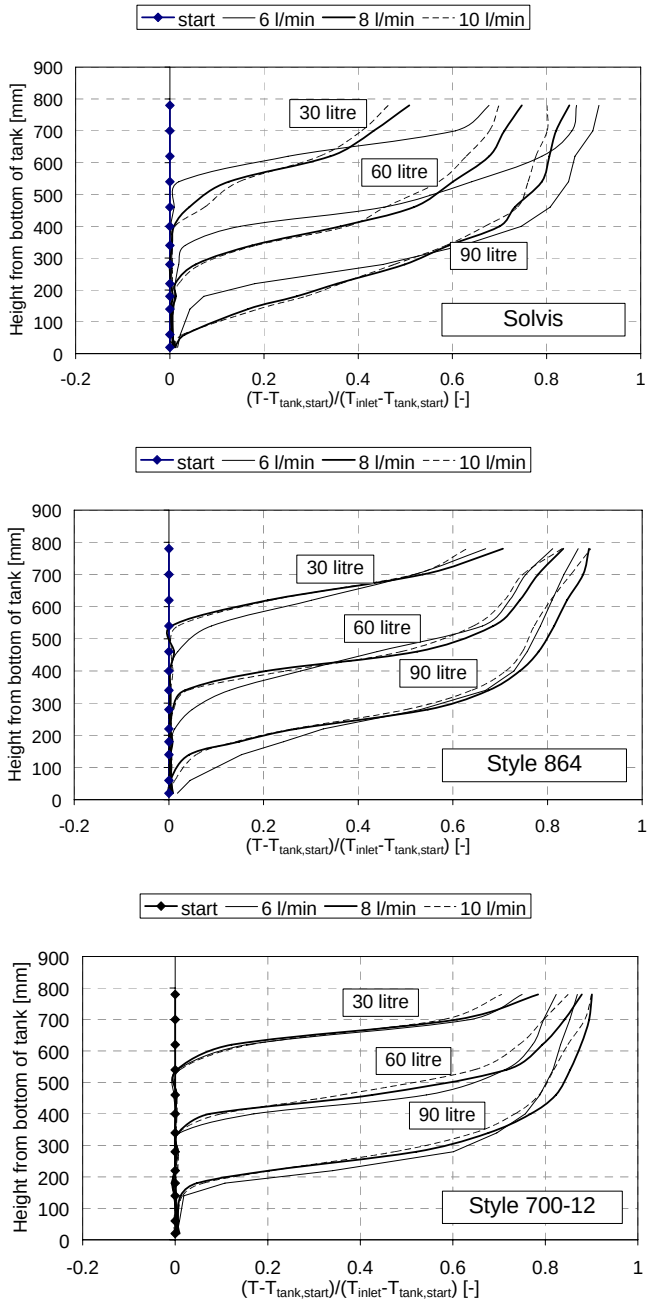

Figure 6: Temperature profiles from heating tests with the rigid stratification pipe and fabric pipes style 864 and style 700-12. The forced volume flow rates are 6 l/min, 8 l/min and 10 l/min.

4 Conclusion

Two inlet stratification pipes made of two fabric layers are investigated at different operation conditions. The results are compared to identical tests with a marketed rigid stratification pipe with three holes with “non-return” valves. The thermal performance

of the stratification pipes is investigated during heating, stratified heating and cooling tests with volume flow rates of 6 l/min, 8 l/min and 10 l/min.

The investigation shows that the thermal stratification is build up in a very good way with the investigated fabric stratification pipes during all the experiments, especially with the stretchable fabric style 700-12. Further, the investigation shows that the thermal stratification is build up in a better way with volume flow rates of 8 and 10 l/min than with a volume flow rate of 6 l/min. It is expected that fabric stratification pipes can work well for all volume flow rates, provided that the pipe diameter is adjusted to the flow rate.

The investigation also shows that the rigid stratification pipe works very well during the heating test with a volume flow rate 6 l/min and that the thermal performance decreases with increasing volume flow rates. Finally, the investigation shows that, during the stratified heating test and the cooling test, the thermal stratification is not maintained in the same good way as with the fabric stratification pipes.

References

[1] Andersen E., Furbo S., Fan J., Investigations of fabric stratifiers for solar tanks, Proceedings of ISES Solar World Congress 2005, Orlando, Florida, USA, 2005.

[2] Krause Th., Kühl L. Solares Heizen: Konzepte, Auslegung und Praxiserfahrungen, 2001.

[3] Shah L.J. Stratifikationsindløbsrør. Department of Civil Engineering, Technical University of Denmark, DTU, 2002.

[4] www.testfabrics.com

Paper IX

Investigations on Stratification Devices for Hot Water Heat Stores

Paper accepted for publication in International Journal of Energy Research, May 2007

Investigations on Stratification Devices for Hot Water Heat Stores

Elsa Andersen and Simon Furbo

Department of Civil Engineering Technical University of Denmark

DK-2800 Kgs. Lyngby, Denmark, e-mail: ean@byg.dtu.dk

M. Hampel, W. Heidemann and H. Müller-Steinhagen

Institute of Thermodynamics and Thermal Engineering (ITW), University of Stuttgart

Pfaffenwaldring 6, D-70550 Stuttgart, Germany

Paper accepted for publication in International Journal of Energy Research, May 2007

Abstract

The significance of the thermal stratification for the energy efficiency of small solar-thermal hot water heat stores is pointed out. Exemplary the thermal stratification build-up with devices already marketed as well as with devices still in development has been investigated experimentally and theoretically, taking into account different realistic operation conditions. The methods (selective temperature measurement, non-invasive field measuring methods PIV and LIF, Computational Fluid Dynamics (CFD)) suitable for the experimental and theoretical analysis of thermal stratification devices are introduced.

Keywords Solar tanks, thermal stratification, inlet stratification pipes, CFD, PIV, LIF

1 Introduction

Since the 1960s the influence of thermal stratification in hot water stores on the thermal performance of solar heating systems has been studied intensively in order to improve the overall performance of solar thermal systems. Experimental and theoretical investigations showed that the overall system performance of a solar heating system for domestic hot water preparation can be increased with an optimal thermal stratification in the solar storage compared to systems without stratified conditions in the storage.

An overview of direct charging and discharging systems which are nowadays available is given by Göppert et al. (2006). Simple systems suitable for small- and large-sized solar storages use slotted pipe diffusers or radial diffusers with baffles to suppress mixing effects due to high inflow velocities (Bahnfleth et al. (2003), (2005)). The diffusers are mounted in fixed heights of the storage. More sophisticated

stratification systems enable an inflow at variable heights of the storage. The choice of the admission height of the charged fluid can take place through mechanical procedures (Neal (1981)) or through gravitationally induced flow whereas vertically installed tubes with free or lockable openings are used. The last-mentioned charging method represents the state-of the-art and is subject of numerous research and development activities: A large number of differently designed rigid and flexible inlet stratification pipes have been studied in the past by van Koppen et al. (1979), Loehrke et al. (1979), Davidson and Adams (1994), Abu-Hamdan (1992), Essert (1995) and Andersen et al. (2004). Among these, the most promising devices are rigid inlet stratifiers equipped with openings and so-called “non-return” valves as well as flexible inlet stratification pipes mounted vertically in the storage tanks.

By means of experimental and theoretical investigations, Shah et al. (2005) showed that a long tube with a number of openings in different levels works more as a mixing device than a stratifying device, because cold water was sucked into the stratifier especially through the lowest opening. Further tests with “non-return” valves mounted in the openings revealed that the unwanted flow at the lowest openings was reduced.

Several fabric stratification inlet pipes were experimentally investigated by Andersen et al. (2005). The authors found that the largest disadvantage of the fabric stratification inlet pipe - namely the high horizontal heat transfer through the very thin fabric - can be dramatically reduced when using fabric pipes consisting of two fabric layers instead of one fabric layer. Further, the investigation showed that a two layer fabric stratification pipe performs as well as a good performing rigid stratification pipe.

In the following sections the thermal behaviour of three different modern stratification devices with fabric and rigid pipes are presented in detail. Next to the well known measurements with thermocouples, which allow measurements at selected points only, non-invasive field measuring methods like Particle Image Velocimetry (PIV) and Laser Induced Fluorescence (LIF) are used for the assessment of the stratification devices considered. The application of numerical calculations (CFD – Computational Fluid Dynamics) allows a theoretical prognosis of the thermo-hydraulic behaviour of the devices.

2 Inlet stratification pipes and testing equipment

Typical inlet stratifiers used for the investigations presented in this paper are shown in Figure 1-3.

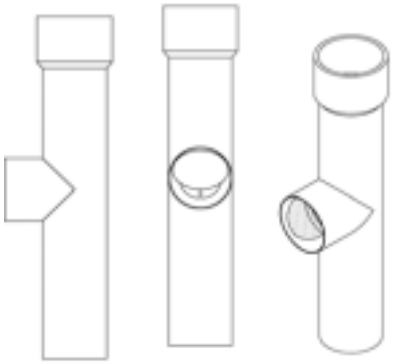

Figure 1: Section of a rigid stratification pipe with lockable openings.

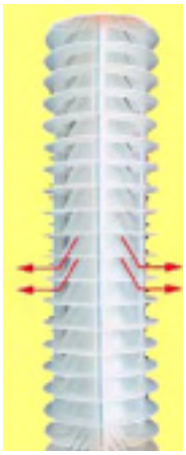

Figure 2: Sketch of a rigid stratification pipe with circular openings.

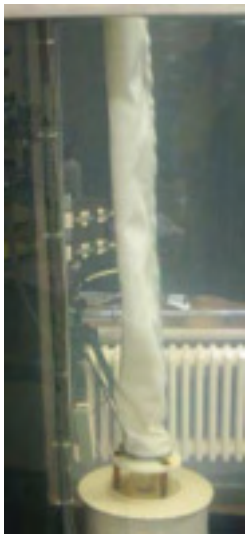

Figure 3: Fabric stratifier.

In Figure 1 a section of a rigid inlet stratification pipe with lockable openings is shown. The pipe is made of polypropylene (PP) with a height of 328 mm, an outer diameter of 60 mm and a thickness of 3 mm (Krause (2001), Shah (2002)). The complete stratification inlet pipe is composed of several pipe sections according to Fig. 1 and has a distance between the centres of each opening of about 292 mm. The pipe is patented and marketed by the German company Solvis GmbH & Co KG and was tested at the Technical University of Denmark, DTU.

In Figure 2 a rigid inlet stratification pipe with circular openings is depicted. The device is made of 2 mm thick synthetic material resistant to temperature and deformation and is built up by a variable number of “hats” connected by 3 thread rods forming an inner flow channel of 24 mm with an outer diameter of 100 mm. Free convection induced fluid flow can leave the stratification pipe through all circular openings which have a height of 18 mm. The device is patented and marketed by the German company Sailer GmbH & Co KG and was tested at ITW of the University of Stuttgart.

A two-layer fabric inlet stratification pipe is shown in Figure 3. The investigated samples consist of pipes with an inner/outer diameter of 40 mm/70 mm and 25 mm/45mm, the pipes are closed at the top. The following two different fabric styles are used: Style 864, Spun Orlon Type 75 Acrylic Plain Weave (non-stretchable fabric) and Style 700-12, Filament polyester, Poly-Lycra (stretchable fabric). The fabric pipe is patented and was mainly tested at DTU.

Due to different experimental equipment available at the Technical University of Denmark, DTU, and the ITW, University of Stuttgart, for the testing of the stratification devices, the following modes of operation are possible:

At DTU experiments are carried out in a glass tank (not insulated) with a volume of 144 litres (400 x 400 x 900 mm) with a wall thickness of the tank of 12 mm. Temperatures within the tank are measured at 13 different uniformly distributed tank levels using copper-constantan thermocouples type T with an accuracy of 0.5 K. The volumetric flow rate is measured using an electro-magnetic inductive flow meter (accuracy 1% of the measured value). Figure 4 shows the setup for experiments with forced volume flow and thermosyphonical flow at DTU.

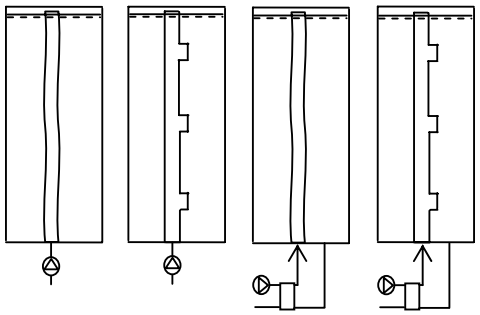

Figure 4: Investigations with forced volume flow and natural buoyancy flow (performed at DTU).

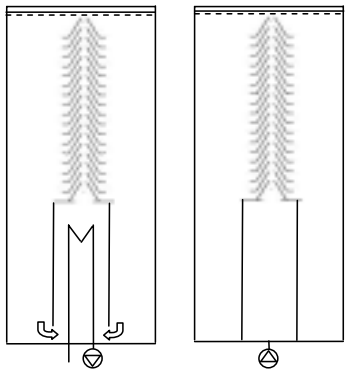

Figure 5: Investigations with natural buoyancy flow and forced volume flow (performed at ITW).

At ITW experiments are carried out in a cylindrical steel tank (volume 550 litres, height 1530 mm, diameter 700 mm). The tank temperatures are measured at up to 10 uniformly distributed levels in the tank with thermocouples (type T, accuracy 0.5 K). Inside the tank mantle view-windows of glass are placed which enable the use of laser-light based PIV/LIF measurement technique for the determination of flow and temperature fields. In Figure 5 and 8 an outline of the experiments at ITW is shown.

3 Experimental investigations

3.1 Test conditions

In order to investigate the thermal performance of the inlet stratification pipes (cf. Figure 1-3) experiments with forced volume flow rates of 2, 6, 8 and 10 l/min are carried out for two sets of operation conditions: (I) heating tests, where the tank water is heated up from 20°C through the inlet stratification pipe with inlet fluid temperatures of (32- 40)°C, (II) stratified heating tests with an initially stratified tank (50°C-20°C) through the inlet stratification pipe with an inlet fluid temperature higher than 20°C and lower than 50°C. In both cases (I, II) the outlet is at the bottom of the tank located as depicted in Figure 4.

Furthermore, experiments with free convection driven flow, generated via an external heat exchanger, are carried out with the test equipment available at DTU (cf. Figure

4). Starting from an initial temperature of 20°C the working fluid water is heated up with a heat flux of 3 kW transferred from the external heat exchanger into the tank.

The heating tests simulate the thermal behaviour of a stratification pipe in a solar collector loop.

3.2 Test results

3.2.1 Forced flow with constant flow rate

In Figure 6 normalized temperatures as a function of the relative height in the tank obtained during heating tests with forced volume flow rates of 6, 8 and 10 l/min are shown. The volume ratio, defined as the ratio between the volume circulated through the tank and the tank volume, is used as a parameter. Curves for 20, 40 and 60% are shown, that is temperatures are shown when 26.9 litres, 53.8 litres and 80.6 litres of water has been circulated through the tank which had a water volume of 134.4 litres.

It can be seen that during the heating tests with a low volume flow rate (6 l/min), the rigid stratification pipe with lockable openings (Solvis) performs better than the fabric stratification pipes (style 864 and style 700-12). The thermal performance of the fabric stratification pipes increases for higher volume flow rates (8 l/min, 10 l/min) and is then better than the performance of the rigid stratification pipe. The reason for that is most likely that the horizontal heat transfer through the thin fabric pipe to the tank decreases for increasing volume flow rates.

In order to examine whether the stratification pipes are able to build up thermal stratification without destroying the already existing thermal stratification so-called stratified heating tests are performed. The resulting temperature profiles for different volume flow rates (2, 6, 8 and 10 l/min) are shown in Figure 7.

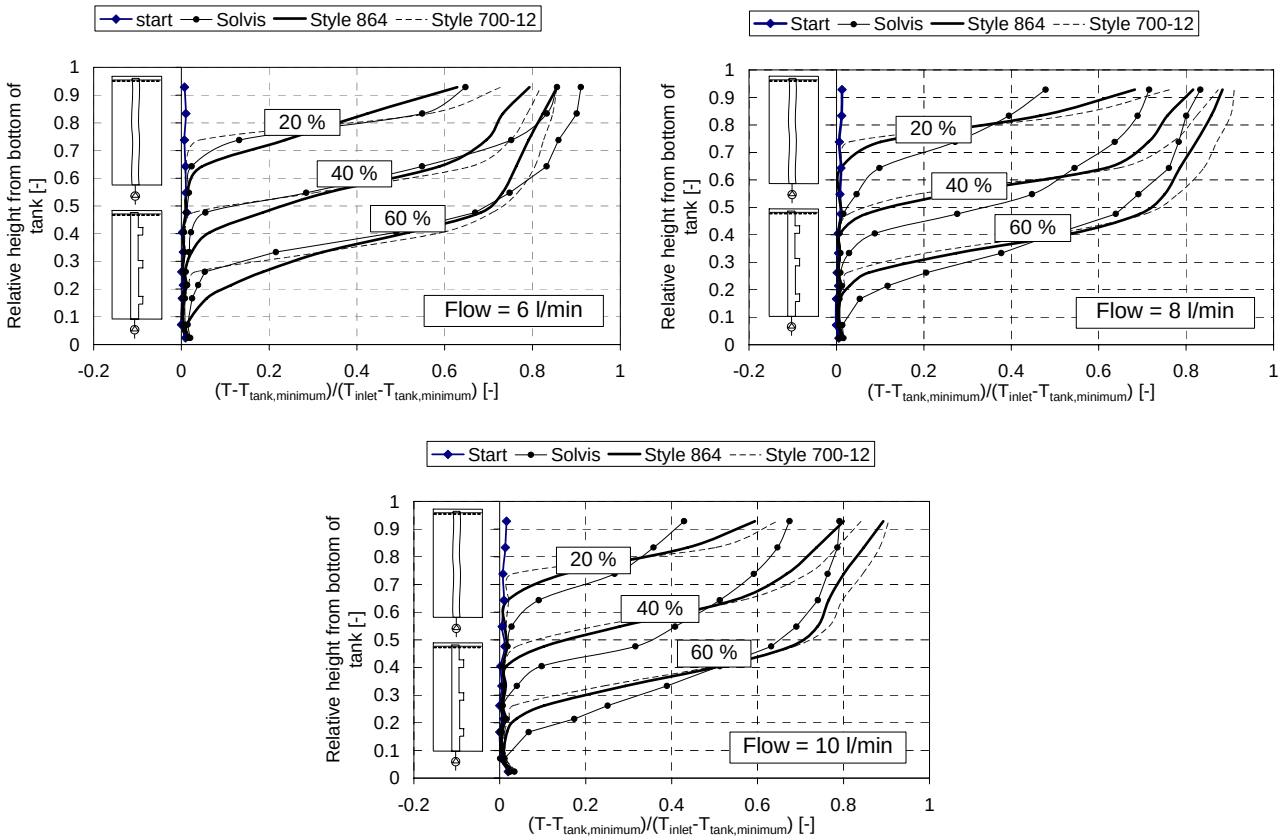

Figure 6: Temperature profiles for rigid inlet stratification pipe with lockable openings (Solvis) and fabric inlet stratification pipes (style 864 and style 700-12) with the diameters 40 mm/70 mm, heating mode.

The initial temperature at the top of the tank is always 50°C except for the volume rate 2 l/min where it is 57°C. In the start of the tests, the inlet temperature is as high as the temperature in the top of the tank. After about 18 % of the water has been circulated through the tank the inlet temperature stabilizes and only the middle part of the tank is heated. However in the test with the stratifier with circular openings, the inlet temperature is constant during the whole experiment.

The fabric stratification pipes succeed to heat up the middle part of the tank without decreasing the already existing high temperature at the top of the tank in all the tests. The rigid stratification pipe with lockable openings is not able to maintain the already existing high temperature at the top of the tank. This is due to the fact that the rigid stratification pipe has only a limited number of openings. When the correct temperature level lies between two openings, the water leaves through both the opening above and below the right temperature level which results in mixing in the tank between the two opening levels.

The rigid stratification pipe with circular openings (Sailer) which was tested only with a volume flow rate of 2 l/min, also succeeds to heat up the middle part of the tank without destroying the already existing thermal stratification. The temperature decrease in the top of the tank is due to heat loss from the not insulated tank.

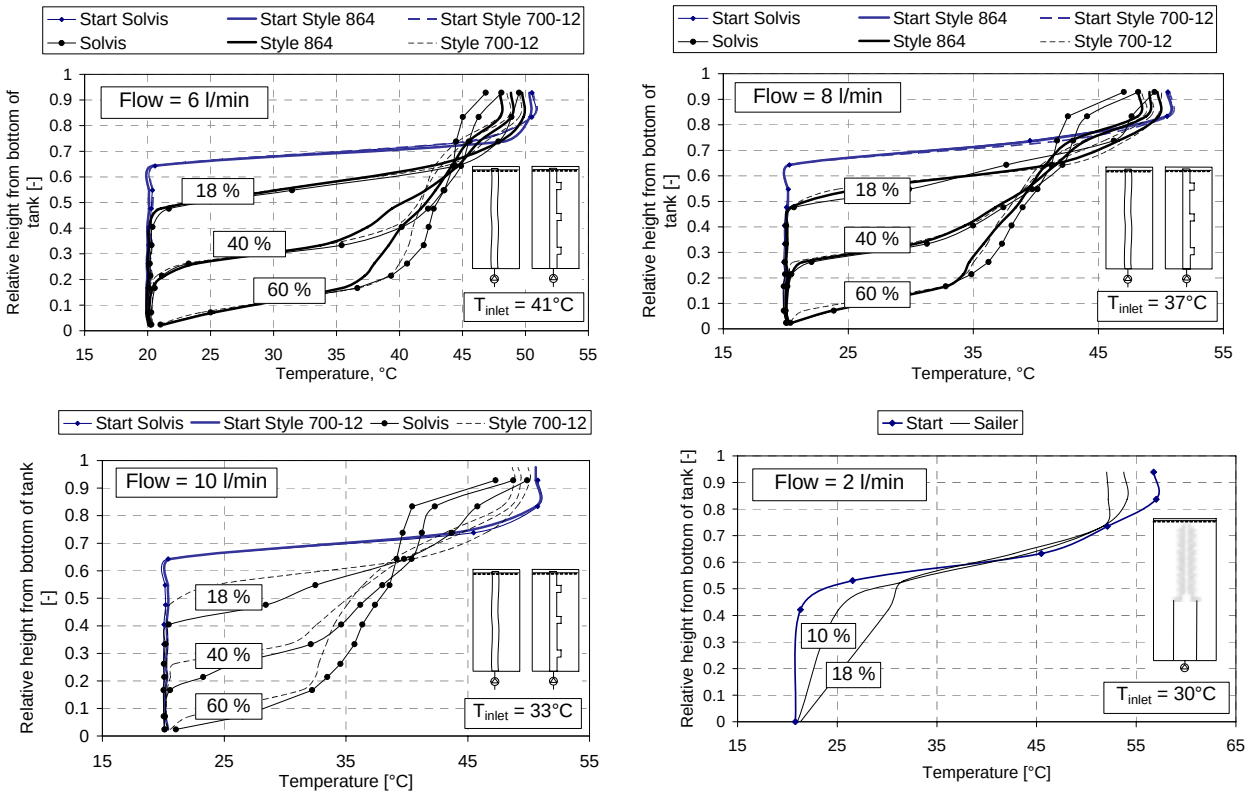

Figure 7: Temperature profiles for the rigid inlet stratification pipe with lockable openings, the fabric inlet stratification pipes with diameters of 40 mm/70 mm and the rigid inlet stratification pipe with circular openings (stratified heating mode).

3.2.2 Experimental validation of numerical calculations

Theoretical investigations for inlet stratifiers can be carried out with CFD-models which allow the prediction of the thermal and hydrodynamic behaviour in detail just by knowing the geometry of the system and the boundary conditions. Reliable numerical models still need to be adapted to physical phenomena like tubulence and should be validated afterwards by comparing calculated and measured values.

With so-called field-measuring-methods like Particle Image Velocimetry (PIV) and Laser Induced Fluorescence (LIF) velocity and temperature measurements for a complete flow and temperature field can be done. The convincing advantage is that data can be gathered without having to insert any testing probes. Tracer particles with the same density as the fluid are added and move with the flow. They reflect the light flashes of a laser and these reflections are recorded by a CCD-camera. The pulsing laser beam is expanded to a very thin light-sheet of approximately 1 mm thickness (see Figure 8). Perpendicular to this, the CCD-camera takes pictures of the reflections of the tracer particles. Some milliseconds later, a second particle picture is taken. A superposition of both pictures gives a double-frame picture which shows the displaced particles. From the distance between the particles and the time between both frames, the velocity and flow direction can be calculated. Adding a fluorescent dye (e.g. Rhodamine B) to the fluid additionally gives the possibility to measure the temperature in the field of observation (LIF-method). After excitation with laser-light

this dye emits fluorescence light, and its intensity is proportional to the temperature. The fluorescence signal is recorded by a camera and processed electronically.

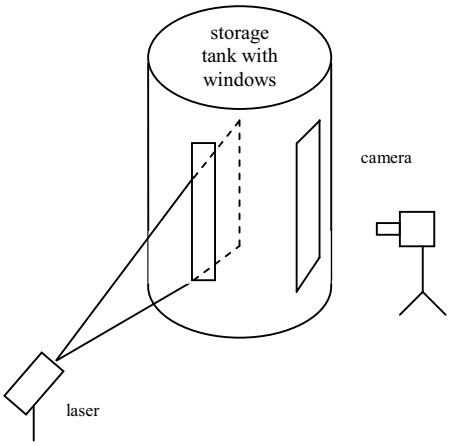

Figure 8: Experimental setup for PIV and LIF measurements.

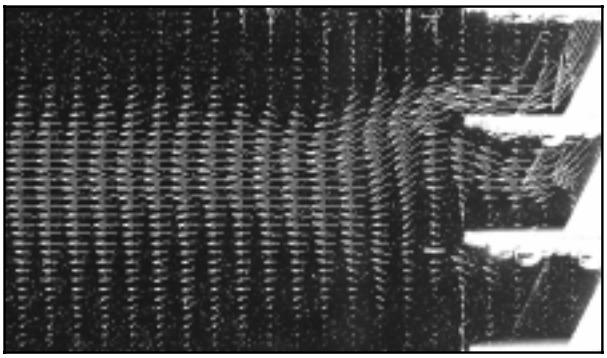

Figure 9: Example of a PIV-measurement: outflow from a stratifier as pictured in Figure 2.

Figure 9 shows, as an example, a cutting from a typical PIV-measurement on a rigid stratifier system with circular openings as depicted in Figure 2. Storage water is heated up by a heat exchanger below a convection chimney. Buoyancy forces transport the water into the chimney. At the same time cold water from the lower part of the storage flows into the heat exchanger area. The warm water leaves the chimney at a height where it has approximately the same temperature (respectively density) as the storage water. PIV-measurements allow the determination of the velocity of the leaving water. For the investigated stratifier system values between 10 to 20 mm/s at the openings and below 10 mm/s further away from the openings occur. When looking at a wider field of view, it is obvious that the flow is not always as straightforward as it appears in this picture, instead a lot of eddies and other flows are made visible.

For the stratification device with circular openings CFD data were compared with thermocouple- and LIF-measurements. The CFD calculations were simulated with a two-dimensional model with axial-symmetry. For the transient simulation of turbulence the realizable k-ε-model was chosen, as laminar simulations produced non-physical results.

Figure 10 shows the direct comparison between LIF measurement and CFD calculations. The measurement was done 32 minutes after the start of the loading process. The start temperature at all levels of the tank is 20°C, the storage is loaded thermosyphonically with a power of 12 kW. It is clearly visible that the biggest temperature change from 22°C to 44°C is within 20 cm in the storage.

In Figure 11 the quantitative comparison between the thermocouples temperature, the LIF measurement and the CFD simulation is shown for the vertical line where the thermocouples are placed, both at t = 22 min and t = 32 min after starting of the loading process. It is obvious that the LIF temperatures at higher temperatures are a little bit lower than the more reliable thermocouple measurements. There can be several reasons for this: mistakes in calibration and dye concentration as well as

fluctuations in laser intensity are possible. Apart from this the CFD calculations reflect the temperature gradient very well. Especially the height of the transition zone from hot to cold water is predicted accurately.

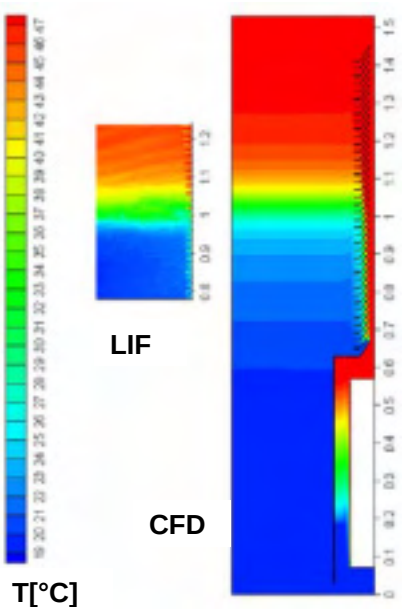

Figure 10: Comparison of CFD and LIF results.

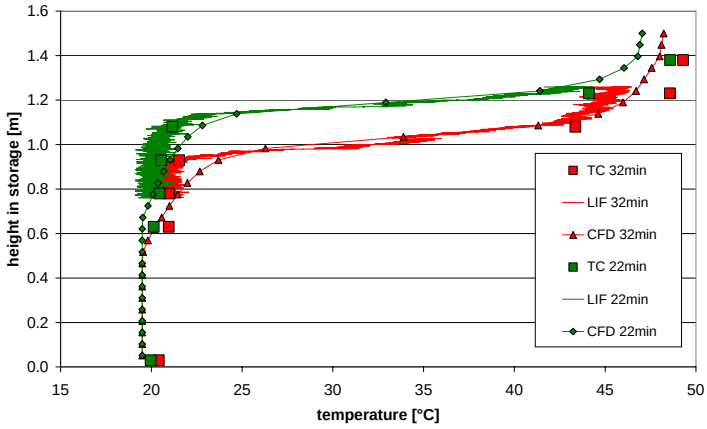

Figure 11: Comparison between measured (thermocouples (TC) and LIF) and calculated (CFD) results.

CFD-calculations allow an insight into flows in areas which are difficult to measure (cf. Figure 12). For the stratifier with the circular openings it is difficult to determine, how much water is sucked in at the bottom of the chimney due to the pressure differences between the water in the tank and the fast flowing water in the chimney. Thermocouple measurements do not provide a satisfying answer to this as well. The inflow through the circular openings will reduce the temperature of the hot upward moving fluid in the centre of the stratifier. The design of the stratifier with circular openings can not fully eliminate the inflow as it is the case for the fabric stratifier and the stratifier with lockable openings (Andersen et al. (2004)). However, a CFD analysis shows that the inflow into the stratifier is about 5.25 l/min, whereas the inflow through the first 4 circular openings from the tank into the chimney is only 0.31 l/min (6%). The simulation also shows that in the upper openings of Fig. 12 eddies are created between the warm water in the chimney and the cold tank water.

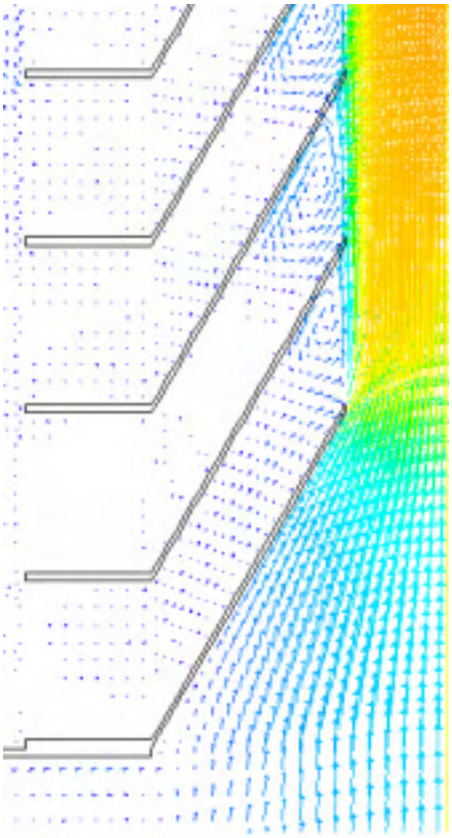

Figure 12: Velocity vectors at the entrance and the first circular openings (bottom-up) of the stratifier system according to Figure 2.

3.2.3 Buoyancy forced flow

Temperature profiles occurring during heating tests with buoyancy-driven flow for different stratifier systems are shown in Fig. 13. Depicted are normalized temperatures as a function of the relative heights in the tank for the rigid pipe with lockable openings (Solvis), fabric pipes style 864 and style 700-12 with inner/outer diameters of 40/70 mm as well as fabric pipes style 864 and style 700-12 with inner/outer diameters of 25/45 mm. The volume ratio of the water which has been circulated through the tank is used as parameter.

During the heating tests with a volume flow rate in the thermosyphon loop of about 1 l/min, the rigid stratification pipe with lockable openings perform better than the fabric stratification pipes with the large diameters. A reason for this is most likely the higher pressure drop in the fabric pipes. It was observed that the calculated thermosyphonical flow rate is slightly lower during the tests with the fabric pipes. Also, the horizontal heat transfer through the thin fabric pipe to the tank is larger than the heat transfer through the rigid pipe.

By reducing the inner and outer diameter of the fabric pipes, the horizontal heat transfer in reduced. From the right diagram of Figure 13 it can be seen, that a smaller inner/outer diameter of the fabric pipe leads to better thermal stratification in the tank. The stretchable fabric stratification pipe style 700-12 that performed very well with

high forced volume flow rates (cf. chapter 3.2.1) performs worse than the rigid pipe with lockable openings and the non-stretchable fabric pipe style 864 with low volume flow rates.

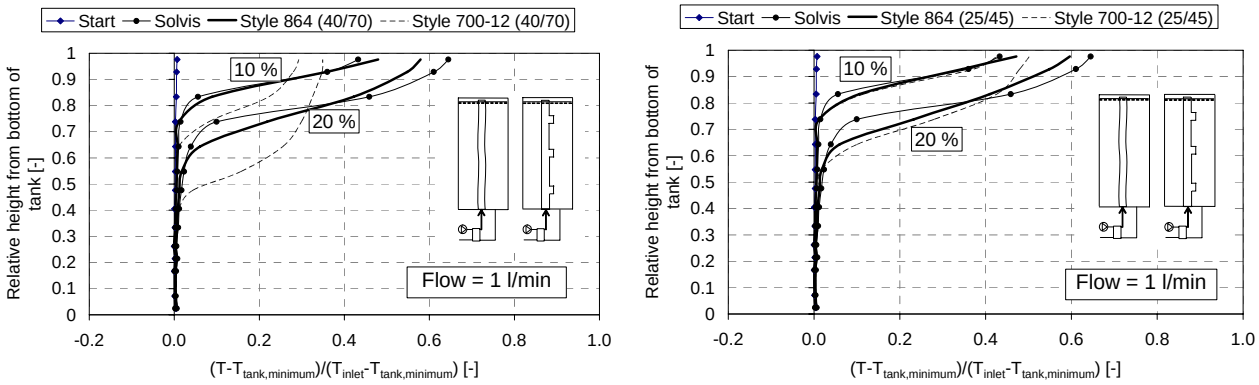

Figure 13: Temperature as a function of the tank height for different stratifier systems, heating mode, thermosyphonical flow.

4 Summary and Conclusion

Two commercially available rigid inlet stratification pipes and two not yet available two-layer fabric inlet stratification pipes are investigated. The stratification pipes are tested with both forced volume flow rates and thermosyphonical flow rates. The investigation shows advantages and disadvantages of the stratification pipes under the applied operation conditions.

Furthermore, the advantages of numerical simulations (CFD) methods are discussed, which can help to achieve new developments for solar storage tanks. In order to create confidence in CFD methods, they still need to be validated. An example of validation with the use of thermocouples and by new measuring methods called PIV and LIF is shown.

The investigation only deals with inlet stratification pipes in laboratory tests with a limited number of operating conditions appearing in solar collector loops. Further investigations should include inlet stratification pipes with operation conditions similar to those in a space heating loop. Also tests in practice should be carried out in order to evaluate inlet stratification pipes under real fluctuating operation conditions. Validated numerical models describing the thermal behaviour of inlet stratification pipes seem to be the most promising tool for future cost- and time-effective R&D activities.

References

C.W.J. van Koppen, J.P.S. Thomas, W.B. Veltkamp. 1979. The actual benefits of thermally stratified storage in small and medium size solar systems. In Proceedings ISES Biennial Meeting, Vol. 2, Atlanta, pp. 576-580.

R.I. Loehrke, J.C. Holtzer, H.N. Gari, M.K. Sharp. 1979. Stratification enhancement in liquid thermal storage tanks. Journal of Energy 3 (3), pp. 129-130.

W.E.J. Neal. 1981. Thermal energy storage. Phys. Technol. 12 (1981), 5, pp. 213-226

J.H. Davidson, D.A. Adams. 1994. Fabric stratification manifolds for solar water heating. Journal of Solar Energy Engineering130, pp. 130-136.

M.G. Abu-Hamdan, Y.H. Zurigat, A.J. Ghajar. 1992. An experimental study of a stratified thermal storage under variable inlet temperature of different inlet designs. International Journal of Heat and Mass Transfer 35 (8), pp. 1927-1934.

W.P. Bahnfleth, J. Song, J.M. Cimbala. 2003. Measured and modelled charging of a stratified chilled water thermal storage tank with slotted pipe diffusors. HVAC&R Res. 9, 4, pp 467-491.

W.P. Bahnfleth, J. Song. 2005. Constant flow rate charging characteristics of a full-scale stratified chilled water storage tank with double-ring slotted pipe diffusers. Appl. Therm. Eng. 25, 17-18, pp. 3067 – 3082.

H. Essert. 1995. Aufbau und Inbetriebnahme eines Speicherversuchsstandes. Diploma Thesis, Graz University, Austria.

E. Andersen, U. Jordan, L.J. Shah, S. Furbo. 2004. Investigations of the Solvis stratification inlet pipe for solar tanks. Proceedings Eurosun 2004, vol. 1, Freiburg, Germany, pp. 76-85. ISBN. 3-9809656-1-9.

E. Andersen, S. Furbo, J. Fan. 2005. Investigations of fabric inlet stratifiers for solar tanks. Proceedings of ISES Solar World Congress, Orlando, Florida, USA.

T. Krause, L. Kühl. 2001. Solares Heizen Konzepte, Auslegung und Praxiserfahrungen.

L.J. Shah. 2002. Stratifikationsindløbsrør. Department of Civil Engineering, Technical University of Denmark, DTU.

L.J. Shah, E. Andersen, S. Furbo. 2005. Theoretical and experimental investigations of inlet stratifiers for solar storage tanks. Applied Thermal Engineering 25, pp. 2086-2099.

M. Hampel, W. Heidemann, H. Drück, H. Müller-Steinhagen 2006. Nicht invasive Messung von Temperaturfeldern in Flüssigkeiten mit LIF. Proceedings for the 16th symposium on solar thermal energy, OTTI, Regensburg, 2006

S. Göppert, T. Urbaneck, U. Schirmer, R. Lohse, B. Platzer 2006. Be- und Entlade-systeme zur thermischen Schichtung. Proceedings for the 16th symposium on solar thermal energy, OTTI, Regensburg.

Paper X

Heat losses from pipes connected to hot water storage tanks

Paper will be submitted to the International Solar World Congress ISES 2007

Heat losses from pipes connected to hot water storage tanks

Elsa Andersen, Jianhua Fan and Simon Furbo

Department of Civil Engineering Technical University of Denmark

DK-2800 Kgs. Lyngby, Denmark, e-mail: ean@byg.dtu.dk

Paper will be submitted to the International Solar World Congress ISES 2007

Abstract

The heat loss from pipe connections at the top of hot water storage tanks with and without a heat trap is investigated theoretically and compared to similar experimental investigations. Computational Fluid Dynamics (CFD) is used for the theoretical analysis. The investigations show that the heat loss from an ideally insulated pipe connected to the top of a hot water tank is mainly due to heat loss to the surroundings through the boundaries and that heat is transferred to the pipe due to a natural convection flow in the pipe. Further, the investigations show that the heat loss coefficient of pipes connected to the top of a hot water tank is high, and that a heat trap can reduce the heat loss coefficient significantly. Further, calculations show that the yearly thermal performance of solar domestic hot water systems is strongly reduced if the hot water tank has a thermal bridge located at the top of the tank.

Keywords Hot water stores, pipe connection, thermal bridge, heat loss, heat trap, measurements, CFD-calculations

1 Introduction

To charge or discharge hot water stores, pipe connections to the store are necessary. It is well known that perforation of the insulation material encapsulating a hot water store, leads to a thermal bridge at the perforation. Especially pipe connections can result in large thermal bridges resulting in a low thermal performance of the solar heating systems. Changing the position of pipe connections from the hot part to the cold part of the store, e.g. at the bottom of the store, reduce strongly both the heat loss coefficient and the heat loss of the pipe connections. This results in a strongly increased thermal performance of the solar heating system (Furbo, 1983). It is therefore strongly recommended to locate pipe connections at the lower part of the hot water tank. These recommendations have been known for almost 30 years (Furbo, 1980). However, for different practical reasons, pipe connections are often situated in the upper hot part of the store. The heat losses of pipe connections depend not only on the geometry, the position and the insulation level of the pipe, but also on the temperature level at which the system is operated.

The real heat losses from stores are generally much larger than the theoretical once, mainly due to convection of the air in the insulation material, air leakages and thermal bridges (Vajen, 1996).

A strong hot air flow from an uninsulated circular slit between a vertical pipe connection at the top of a hot water tank and the surrounding insulation material was discovered (Weber et al., 1983), (Suter, 2003). A hot air flow of 0.5 m/s was recorded. Further it was observed how water cooled in the pipe connected to the side of the tank flows into the tank like a "water-fall" and is replaced by hot water from the tank. It was concluded that careful insulation at pipe connections eliminate heat losses resulting from hot air flows and that the "water-fall" can be avoided by mounting the pipe in a downwards position.

Schäpfer and Wellinger (1984) investigated differently designed hot water stores with a well insulated (30 mm insulation) hot water tapping pipe connected to the top of the hot water store. They found that the heat loss coefficient of the hot water tapping pipe was 0.6 W/K.

Schabbach et al. (1999) investigated the convective brake "Convectrol" from the German company Wagner Co by means of a 2D simulation programme. The storage and the ambient temperatures were 60ºC and 15ºC respectively. The pipe was connected to the side of the hot water tank. The heat loss coefficient of the pipe without the convection brake was calculated to 0.34 W/K and 0.25 W/K with the convective brake.

Furbo (1989) investigated experimentally the impact of a heat trap on the heat losses from hot water tapping pipes connected to the top of a tank. Well insulated copper pipes with outer/inner diameter of 22/20 mm were used for the experiments. He found that a heat trap mounted on a vertical hot water tapping pipe as well as on a horizontal hot water tapping pipe reduced the total heat loss coefficient with 0.2 W/K. The heat loss coefficients of a 5 meter horizontally mounted pipe without and with heat trap were found to 0.5 W/K and 0.3 W/K respectively.

The general recommendations for the design of a heat trap is that the height of the heat trap should be ten times the diameter of the pipe (Hadorn, 2005)

In the following sections the thermal behaviour of differently designed hot water tapping pipes are presented in detail. The application of numerical calculations (CFD – Computational Fluid Dynamics) allows a theoretical prognosis of the thermo-hydraulic behaviour of the pipes. Further the influence of differently sized thermal bridges on the yearly thermal performance of a solar domestic hot water system is estimated.

2 Investigated pipe designs

A hot water tapping pipe is investigated by means of Computational Fluid Dynamics (CFD) calculations. CFD-calculations can provide information on flow and temperature distribution in locations where it is difficult to measure. Further, parametric studies can be performed relatively fast and in an inexpensive way compared to parametric studies based on experiments. Regarding reliability, numerical models need to be validated by comparing calculated and measured values. The CFD calculations are compared to the experimental investigations by Furbo (1989).

The hot water tapping pipe is made of copper with outer/inner diameter of 22/20 mm. The pipe (WICU-EXTRA) is pre insulated with 12 mm insulation material with a thermal conductivity of 0.026 W/(m·K). The heat loss coefficient is calculated to 0.18 W/(m·K). The pipe is 5 meters long in horizontal direction and connected to the top of a hot water tank through a 90º bending. The vertical part of the pipe is 0.21 m.

The tank temperature is held constant at 73.5ºC in accordance with the experimental investigations by Furbo (1989).

Also, the influence of a heat trap build in to the horizontal part of the hot water tapping pipe is investigated. The heat trap is 0.21 m deep, corresponding to about ten times the diameter of the pipe, with a width of 0.1 m. Here, the tank temperature is held constant at 75.5ºC in accordance with the experimental investigations by Furbo (1989). In both cases, the ambient temperature is 20ºC. Figure 1 shows the design of the pipes schematically.

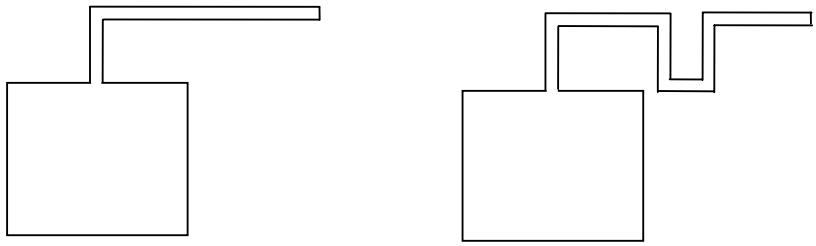

Figure 1: Outline of the tank and pipe geometry used in the investigations. Left: Hot water tapping pipe without heat trap. Right: Hot water tapping pipe with heat trap build into the horizontal pipe.

3 CFD calculations

To solve the flow and energy equations, a simulation model of the flow in the hot water tapping pipe and in the tank volume close to the pipe connection is developed using the CFD code Fluent 6.1 (2003). The side and bottom tank walls are not modelled. Further, the heat loss from the tank is not modelled since the tank temperature is held constant and the flow in the tank is unimportant.

The top 3 mm steel tank wall is modelled in order to allow thermal conduction between the tank wall and the pipe wall.

The mesh is build with hexahedral elements by the cooper scheme both in the solid region (pipe wall and top tank wall) and the fluid region (pipe water and tank water) and is thus an unstructured mesh. Figure 2 shows the model outline, the grid distributions and the grid in a cross section of the pipe (I-I) and in a cross section of the tank (II-II). In order to investigate the grid independency, two different grids are used: One fine grid and one coarse grid. The coarse grid is used to verify the calculations with the fine grid.

3D numerical solutions are obtained for steady-state laminar flow (Reynolds number < 2300) with the Boussinesq assumption for the buoyancy modelling. The temperature dependent viscosity is modelled with a power law function. The velocity-

pressure coupling is treated by using the SIMPLE algorithm and the Second Order Upwind scheme is used for the momentum and energy terms.

All the surfaces of the pipe walls are considered to be wall boundaries in Fluent with only convective heat losses considered. The convective heat loss from the pipe surface in the CFD calculations are determined by the heat loss coefficient from the tested pipes. In Table 1 data of material properties used are showed.

Table 1: Material properties.

Material	Density [kg/m^3]	Specific heat capacity [J/(kg·K)]	Thermal conductivity [W/(m·K)]
Steel	8750	460	60
Copper	8978	381	388
Plastic (PE)	950	2300	0.35

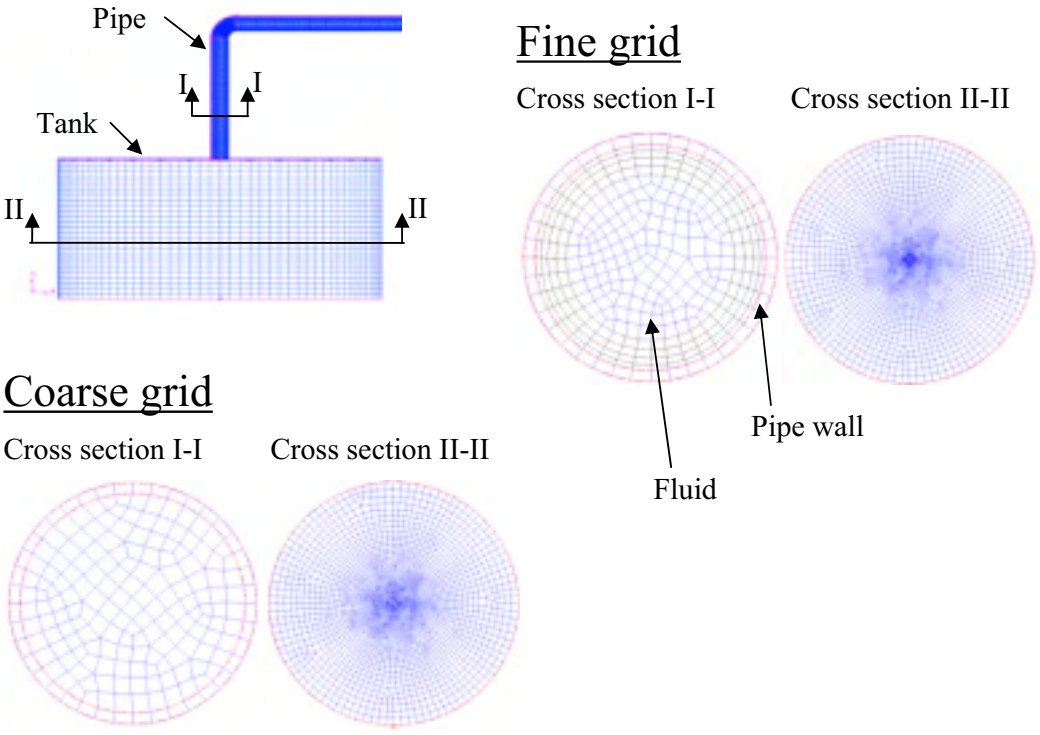

Figure 2: The grid distribution of the fine and the coarse grid used in the calculations.

4 Results

4.1 Without heat trap

The calculations are carried out for two different cases:

- Well insulated copper pipe, fine grid.

- Well insulated copper pipe, coarse grid.

The heat loss coefficients of the insulated copper pipe calculated with the fine and the coarse grid are 0.27 W/K and 0.28 W/K respectively. Hence it is concluded that the calculated results are grid independent and that the fine grid can be used with a good accuracy.

Figure 3 shows for the calculations with the fine grid and the well insulated copper pipe the calculated temperature and flow distribution in the pipe when steady-state is reached. It is seen that about 3 meter of the 5 meter long pipe is kept hot by the hot water from the tank. The calculations show that the natural convection flow in the vertical part of the hot water tapping pipe is a disturbed flow while the fluid in the horizontal part of the pipe flows into the upper part of the pipe and returns at a lower temperature level in the lower part of the pipe, indicated with arrows.

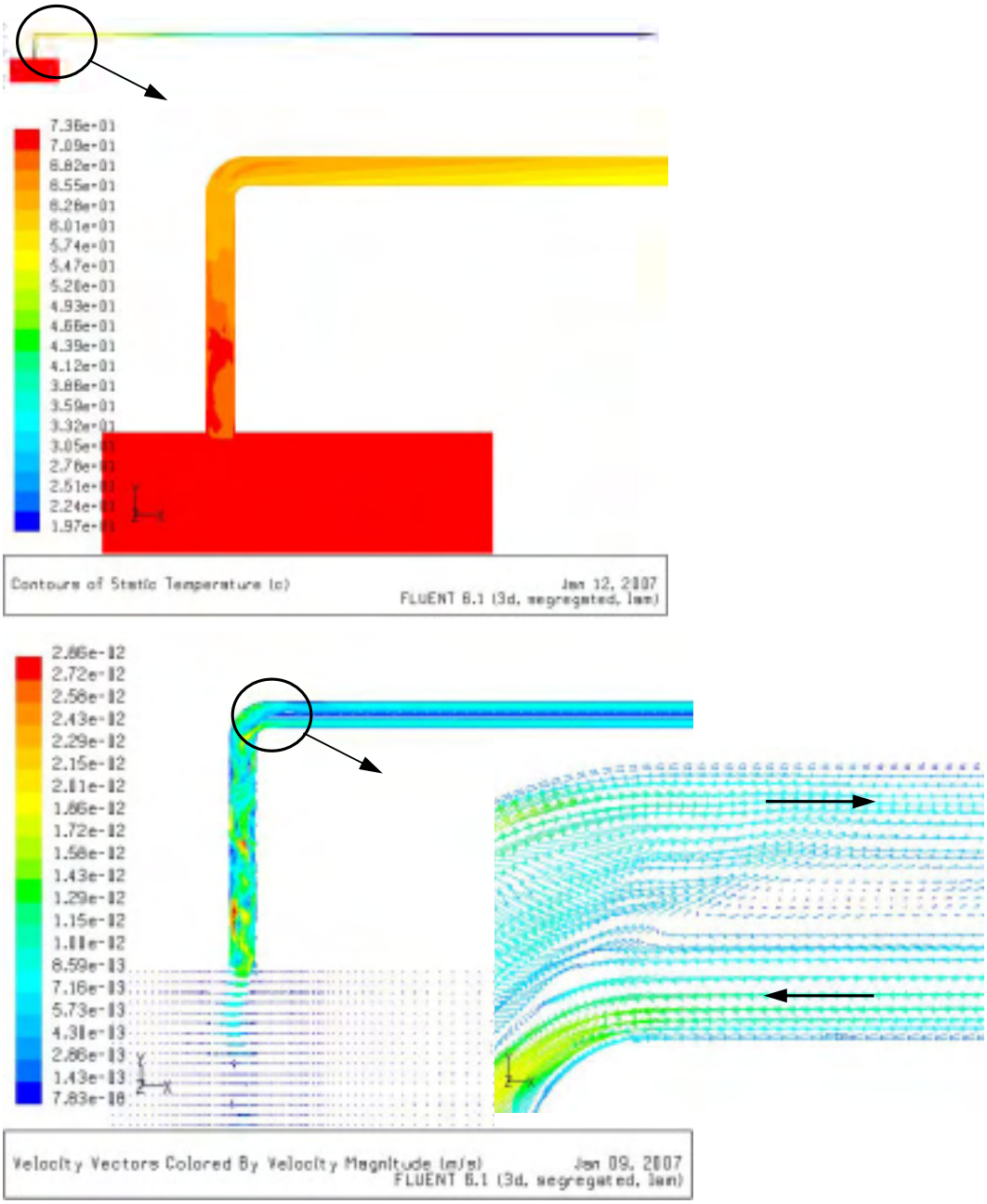

Figure 3: Calculated temperature field [ºC] and flow field [m/s] in the 5 m long hot water tapping pipe. The pipe material is copper and the pipe is well insulated.

4.2 With heat trap

The calculations are carried out for three different cases:

- Well insulated copper pipe, fine grid.
- Well insulated plastic pipe, fine grid.
- Well insulated copper pipe with a thermal bridge of 0.2 W/K on the horizontal part of the pipe before the heat trap, fine grid.

The calculated heat loss coefficients of the insulated pipe made of copper and plastic are 0.15 W/K and 0.08 W/K respectively. The significant difference between the copper pipe and the plastic pipe is the thermal conductivity which is much lower for plastic than for copper. Obviously the low thermal conductivity of the plastic prevents the heat from spreading.

The calculated heat loss coefficients of the insulated copper pipe with a thermal bridge of 0.2 W/K on the horizontal part of the pipe before the heat trap is 0.31 W/K. The size of the thermal bridge does not contribute fully to the increase of the heat loss coefficient of the pipe.

Figure 4 shows the calculated temperature and flow distribution in the pipe when steady-state is reached in the well insulated copper pipe. The figure shows that heat is passing the heat trap.

Figure 5 shows the calculated temperature and flow distribution in the pipe when steady-state is reached in the well insulated plastic pipe. The figure shows that heat does not pass the heat trap.

Figure 6 shows the calculated temperature and flow distribution in the insulated copper pipe with an additional thermal bridge of 0.2 W/K when steady-state is reached. The figure shows that the temperature in the horizontal part of the pipe before the heat trap is reduced due to the thermal bridge.

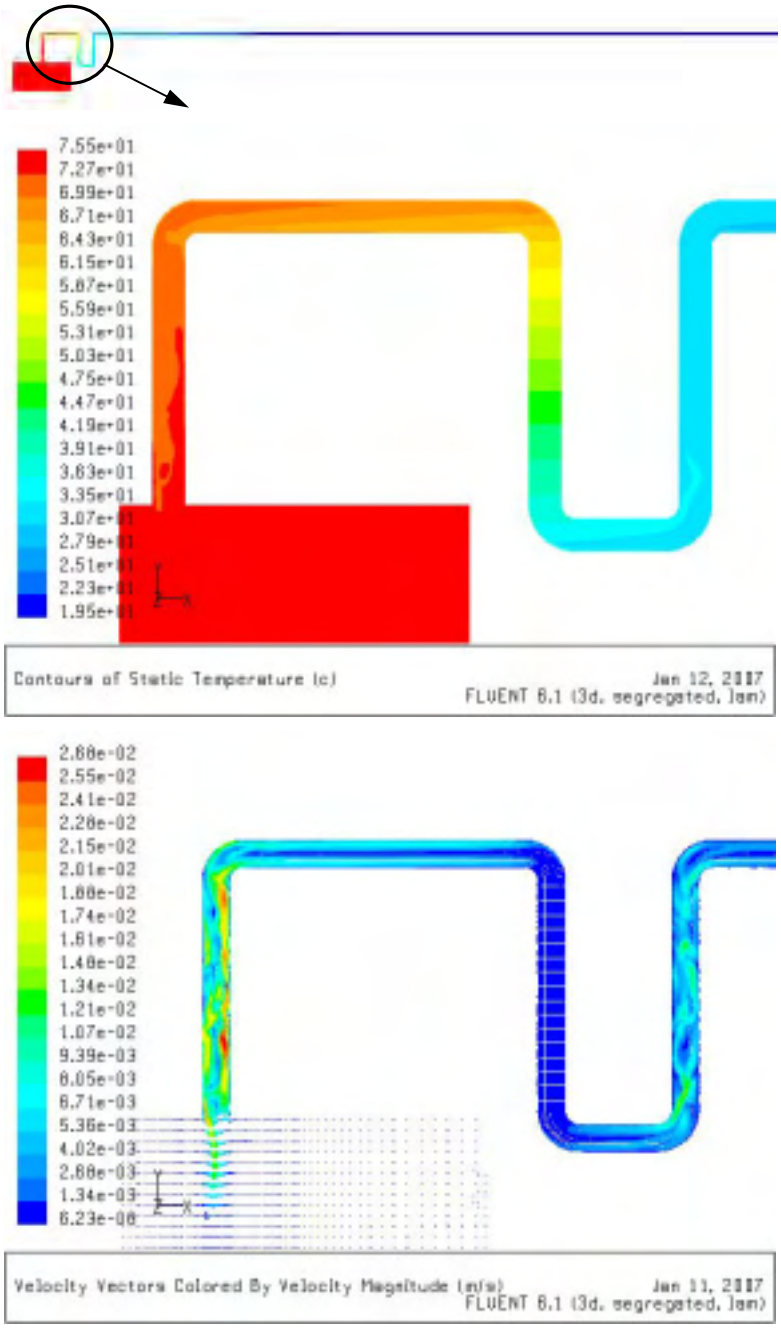

Figure 4: Calculated temperature field [ºC] and flow field [m/s] in the 5 m long hot water tapping copper pipe with a heat trap. The pipe is well insulated.

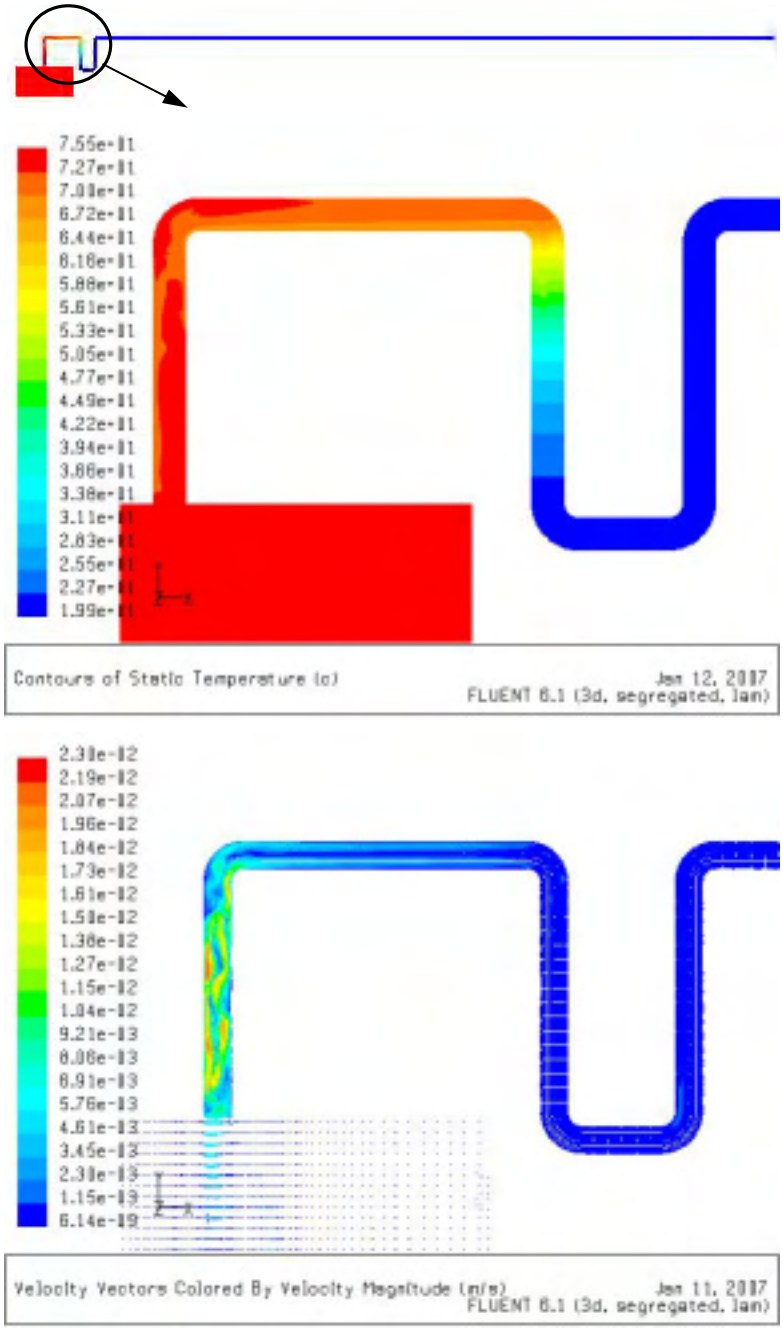

Figure 5: Calculated temperature field [ºC] and flow field [m/s] in the 5 m long hot water tapping plastic (PE) pipe with a heat trap. The pipe is well insulated.

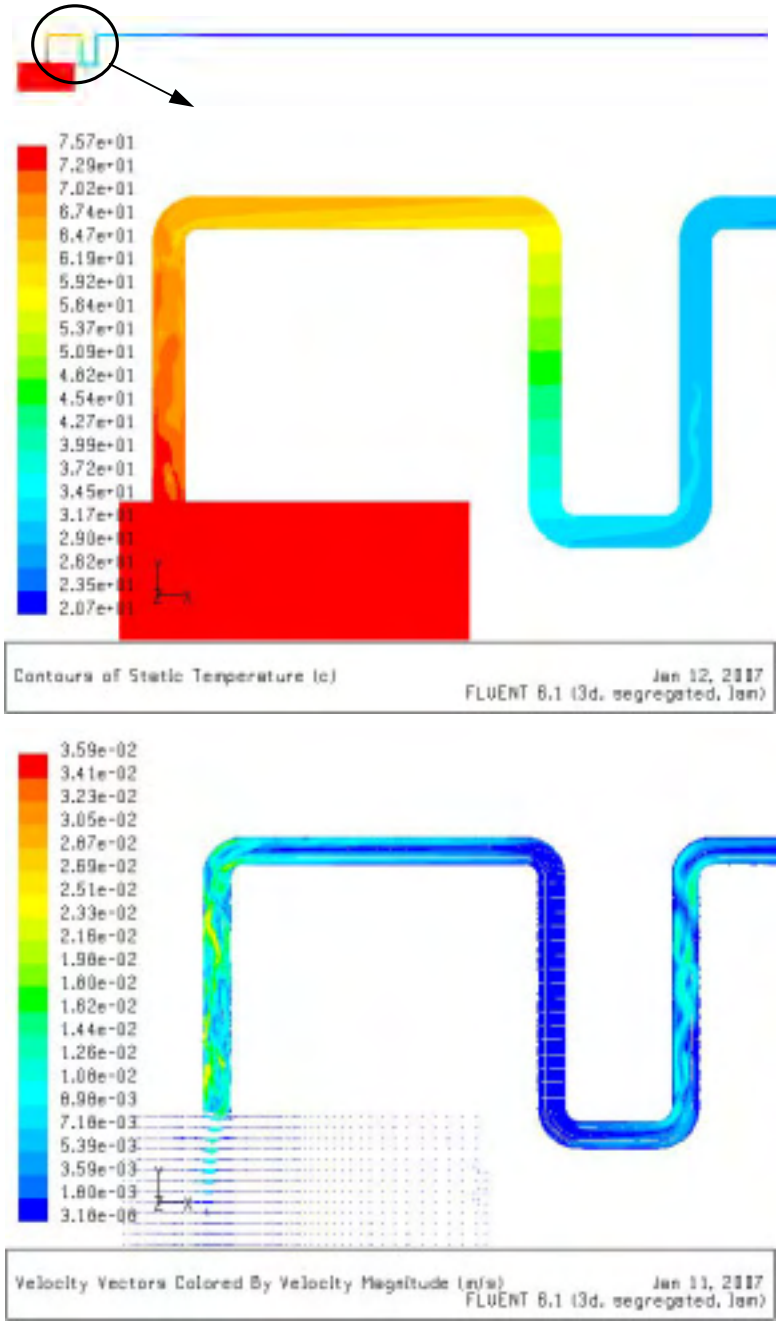

Figure 6: Calculated temperature field [ºC] and flow field [m/s] in the 5 m long hot water tapping copper pipe with a heat trap and a thermal bridge of 0.2 W/K.

4.3 Summary of the CFD calculations

Table 2 shows an overview of the calculated and measured heat loss coefficients. The calculated values are given with two significant digits in order to be able to distinguish between the results. The accuracy of the measured results is calculated to ± 0.1 W/K.

Table 2 shows that the calculated heat loss coefficients are lower than the measured heat loss coefficients. In the calculations the insulation is assumed to be ideal with no thermal bridges. Also the properties of the insulation material are like stated by the manufacturer. In reality, it is difficult to insulate ideally, especially at junctions, e.g. where a pipe is connected to a tank or where a pipe is bend.

Table 2: Overview of calculated and measured heat loss coefficients.

System	Calculated heat loss coefficient [W/K]	Measured heat loss coefficient [W/K]
5 m insulated copper pipe.	0.27	0.5 (± 0.1)
5 m insulated copper pipe with heat trap.	0.15	0.3 (± 0.1)
5 m insulated plastic pipe with heat trap.	0.08	-
5 m insulated copper pipe with heat trap and a thermal bridge of 0.2 W/K.	0.31	0.3 (± 0.1)

The investigations show that:

- A heat trap can reduce the heat loss coefficient by 44%
- A heat trap with a pipe material with low thermal conductivity works better than a heat trap with a pipe material with a high thermal conductivity.

5 The influence of a thermal bridge on the yearly thermal performance of a solar domestic hot water system

5.1 Simulation model

The influence of a thermal bridge in the top of a hot water storage tank of a low flow solar domestic hot water system based on a marketed mantle tank is investigated by means of the simulation program Mantlsim developed at the Technical University of Denmark (Furbo and Berg, 1990, Shah and Furbo, 1998, Knudsen and Furbo, 2004, Furbo and Knudsen, 2004). Weather data is the Danish Test Reference Year developed by Statens Byggeforskningsinstitut (1982).

The daily hot water consumption is 4.6 kWh, corresponding to 100 litres water heated from 10ºC to 50 ºC tapped in three equal portions at 7 am, noon and 7 pm.

Table 3 shows data of the solar domestic hot water system used in the calculations.

Table 3: Data for the solar domestic hot water system used in the calculations.

Tank design – Nilan A/S	
Hot-water tank volume, [m³]	0.189
Inner height / inner diameter [m]	0.986 / 0.494
Tank wall thickness, [m]	0.003
Auxiliary volume, [m³]	0.075
Power of electric heating element, [W]	1200
Mantle volume, [m³]	0.006
Mantle height / mantle gap, [m]	0.389 / 0.0095
Thermal conductivity of insulation material, [W/m·K]	0.037
Insulation top, [m] / Insulation bottom, [m]	0.075 / 0.03
Insulation side above/below mantle, [m]	0.05
Insulation side mantle, [m]	0.0375
Solar collector – Type: BA22, Batec Solvarme A/S	
Area, [m²]	2.19
Start efficiency, [-]	0.761
1st order heat loss coefficient, [W/m²·K]	5.18
Incident angle modifier coefficient (tangens equation)	3.6
Heat capacity, [J/m²·K]	5297
Tilt, [º] / Orientation	45 / South
Solar collector loop	
Flow rate, [l/min/m^2]	0.15
Pipe heat loss coefficient, [W/m·K]	0.24
Length of pipe from storage to collector, indoor, [m]	3.5
Length of pipe from storage to collector, outdoor, [m]	1.5
Length of pipe from collector to storage, indoor, [m]	3.5
Length of pipe from collector to storage, outdoor, [m]	1.5
Start / stop temperature difference for control system, [K]	10 / 2

5.2 Simulation results

The net utilized solar energy is defined as: Energy tapped from the system - Auxiliary energy supplied to the system. The performance ratio is defined as: Net utilized solar energy of the system in question / Net utilized solar energy of reference system. The reference system is the system without a thermal bridge in the top of the tank.

Figure 7 shows the annual net utilized solar energy and the performance ratio as function of the thermal bridge in the top of the tank. The auxiliary volume is constantly heated to 50.5ºC.

Figure 8 shows the annual net utilized solar energy and the performance ratio as function of the thermal bridge in the top of the tank for a pre-heating system that is a system where the solar tank only can be heated by the solar collectors.

From the two figures it can be seen that the influence of a thermal bridge in the top of the hot water tank can be significant for tanks where the auxiliary volume is kept at a constant high temperature while the influence is much smaller in a pre-heating tank without an auxiliary heated volume.

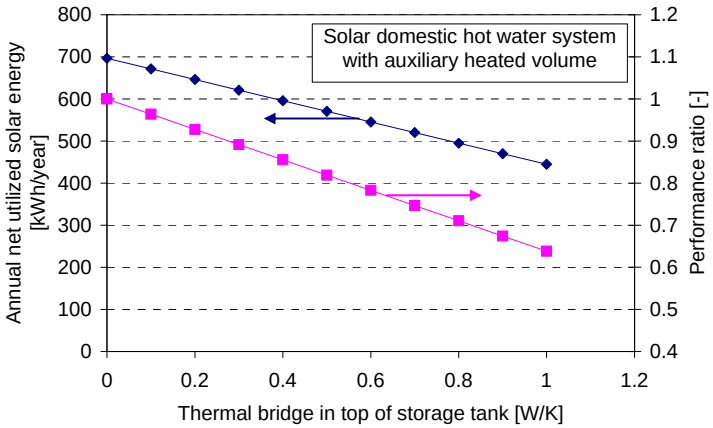

Figure 7: Annual net utilized solar energy and performance ratio as function of the thermal bridge in the top of the tank. The auxiliary volume is heated to 50.5ºC.

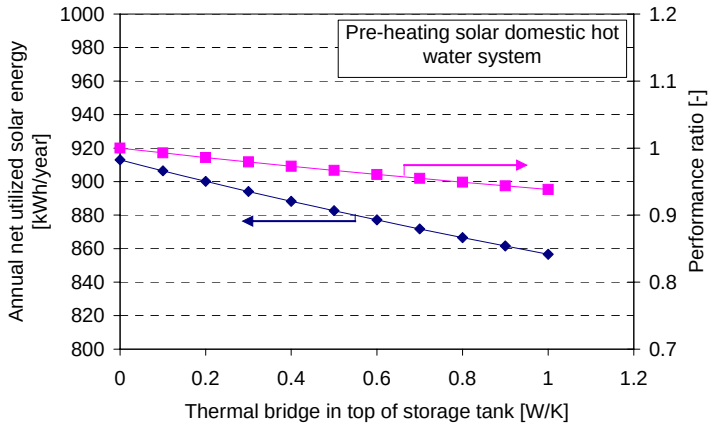

Figure 8: Annual net utilized solar energy and performance ratio as function of the thermal bridge in the top of the tank. The tank has no auxiliary heated volume.

6 Conclusion

The investigations show that the heat loss from an ideally insulated pipe connected to the top of a hot water tank is due to heat loss to the surroundings through the boundaries and that heat is transferred to the pipe due to a natural convection flow in the pipe. The investigations also show that the natural convection flow in the vertical part of the hot water tapping pipe is a disturbed flow while the fluid in the horizontal part of the pipe is flowing into the upper part of the pipe and returning with a lower temperature in the lower part of the pipe.

Calculations show that the heat loss coefficient of pipes connected to the top of a hot water tank is high, and that a heat trap can reduce the heat loss coefficient significantly. Further, calculations show that the yearly thermal performance of solar domestic hot water systems is strongly reduced if the hot water tank has a thermal bridge located at the top of the tank

Finally the investigations show that the calculated heat loss coefficients of ideally insulated hot water tapping pipes are lower than the measured heat loss coefficients.

References

Furbo, S., 1980. Prøvning af varmelagerunits til solvarmeanlæg. Thermal Insulation Laboratory, Technical University of Denmark. Report 97.

Furbo, S., 1983. Test Procedures for Heat Storages for Solar Heating Systems. Int. J. Solar Energy, Vol. 1.

Furbo, S, 1989. Thermal bridges. EU Solar Storage Testing Group Final Report, Vol. II, Part B, 15, pp. 309-318.

Furbo, S., Berg, P., 1990. Calculation of the thermal performance of small hot water solar heating systems using low flow operation. In: North Sun'90 Proceedings, Reading, England.

Furbo, S., Knudsen, S., 2006. Improved design of mantle tanks for small low flow SDHW systems. International Journal of Energy Research, Vol: 30, Issue 12, pp. 955-965.

Fluent 6.1 User's Guide, 2003. Fluent Inc. Centerra Resource Park 10 Cavendish Court Lebanon, NH 03766.

Hadorn, J-C., et al., 2005. Thermal energy storage for solar and low energy buildings, State of the art by IEA Solar Heating and Cooling Task 32. Typeset by Servei de Publicacions (UdL). ISBN 84-8409-877-X.

Knudsen, S., Furbo, S., 2004. Thermal stratification in vertical mantle heat exchangers with application to solar domestic hot water systems. Applied Energy, Vol 78/3, 257-272.

Schabbach, T., Mandel, H., Drück, H., 1999. ***CON***VEC***TROL*** - Neuentwicklung zur Verminderung der Wärmeverluste an den Rohranschlüssen von Solarspeichern. In: Proceedings of 9. Symposium Thermische Solarenergie, Kloster Banz, Bad Staffelstein.

Schläpfer, B., Wleeinger, K., 1984. Waermeverluste von 6 wassererwaermern unterschiedlicher form und groesse. c/o E. Schweizer AG, Metallbau, 8908 Hedingen.

Shah, L.J., Furbo, S., 1998. Correlation of Experimental and Theoretical Heat Transfer in Mantle Tanks used in Low Flow SDHW Systems". Solar Energy, Vol. 64 (4-6), 245-256.

Statens Byggeforskningsinstitut, 1982. Vejrdata for VVS og Energi. Dansk referenceår TRY.

Suter, J.-M., 2003. Heat losses from storage tanks: Up to 5 times higher than calculated. Suter Consulting, P. O. Box 130, CH-3000 Bern 16, Switzerland.

Vajen, K., 1996. Systemuntersuchungen und Modellierung solarunterstützter Warmwasserbereitungssysteme in Freibädern, Dissertation, Universität Marburg.

Weber, H., Brack, M., Suter, J.-M., 1983. Ein Wildbach unter Wasser / Zur freien Konvektion in Warmwassertanks. In: Proceedings of 4. Symposium Forschung und Entwicklung von Sonnenenergie in der Schweiz.

Report no R-156
ISSN 1601-2917
ISBN 978-87-7877-228-2